CHARACTERIZATION OF THE TOPOLOGY, TARGETING AND BINDING PROPERTIES OF SUN PROTEINS AND THEIR INVOLVEMENT IN LAMINOPATHIES

Thesis submitted for the degree of

Doctor of Philosophy

at the University of Leicester

by

Farhana Haque MSc (Leicester) MBBS (Dhaka)

Department of Genetics

University of Leicester

September 2010

Characterization of the topology, targeting and binding properties of SUN proteins at the nuclear envelope and their involvement in laminopathies

Farhana Haque

Abstract

The nuclear envelope (NE) is a double membrane structure enclosing the chromatin and forms the interface between cytoplasm and nucleus. The NE harbours numerous integral membrane proteins, mostly located at the inner nuclear membrane (INM) and is underlined by the nuclear lamina, which along with its interacting proteins gives mechanical strength to the NE. Mutation in lamins and their interacting NE proteins give rise to laminopathy diseases. SUN1 and SUN2 are novel mammalian NE proteins, sharing a conserved C-terminal SUN domain. Their *C. elegans* homologue, UNC-84, is hypothesized to have roles in nuclear migration and positioning by forming a bridge across the NE through interaction with ANC-1 in the outer nuclear membrane (ONM), which in turn binds cytoplasmic actin.

Previously, SUN1 was identified in the lab as a lamin A-binding protein in a yeast two-hybrid screen. Here, I have confirmed SUN1 as an INM protein, comprising a nucleoplasmic N-terminus that interacts with lamin A and a lumenal C-terminus that interacts with mammalian ANC-1 homologues, nesprins. I further identified novel nucleoplasmic interactions of the SUN proteins with emerin and nucleoplasmic isoforms of nesprins, thus demonstrating multi-protein interactions of SUN proteins at the NE.

Notably, lamin A/C, emerin and nesprins are mutated in the laminopathy Emery-Dreifuss muscular dystrophy (EDMD). Here, I have demonstrated SUN protein involvement with laminopathies for the first time. SUN1 and SUN2 interaction with L530P and L527P EDMD lamin A mutants and with G608G and T623S progeria lamin A mutants were dramatically reduced. Although SUN proteins were not mislocalized from the NE in EDMD patient fibroblasts examined, increased recruitment of SUN1, but not SUN2, was observed in progeria patient fibroblasts, possibly due to increased expression of prelamin A. Subtle disruptions in the interactions between SUN proteins and their binding partners may therefore contribute to laminopathy disease phenotypes.

ACKNOWLEDGEMENTS

My first and foremost gratitude to my supervisor, Dr. S. Shackleton, for giving me the opportunity to work with her as a research student and for all the support and guidance she has given me not only to do my research but also in every aspect of my life. I cannot thank enough my family and friends, specially my husband, my mother, my mother-in-law and my daughter, for their patience and help throughout this work. I am also very thankful to all my past and present colleagues for their constant support and friendship.

I would also like to take the opportunity to thank Prof. A. Fry and Dr. Kayoko Tanaka for their valuable suggestions. I am very grateful to Dr. J. Ellis, Prof. C. Shanahan, Dr. E. Schirmer and Dr. D. M. Hodzic for providing us with valuable constructs.

The thesis is dedicated to the memory of my father.

CONTENTS

LIST OF ABBREVIATIONS

°C	Degrees centrigrade
A	Appendix
A	Adenine
aa	Amino acids
ABD	Actin binding domain
ABI	Applied Biosystems
AD-EDMD	Autosomal-dominant Emery-Dreifuss muscular dystrophy
ANC-1	Nuclear anchorage defect gene
APS	Ammonium persulphate
ATCC	American Type Culture Collection
ATP	Adenosine triphosphate
BAF	Barrier of autointegration factor
BMP	Bone morphogenic protein
Bp	Base pair
Bqt	Bouquet
BSA	Bovine serum albumin
Btf	BCL2-associated transcription factor
C	Cytosine
CAAX	Cys-aliphatic-aliphatic-any residue
CC	Coiled-coil
cDNA	Cloned DNA
Cdk1	Cyclin dependent kinsae 1
C. elegans	*Caenorhabditis elegans*
Ce	*Caenorhabditis elegans*
CH	Calponin homology
cm	Centimeter
CMT	Charcot-Marie-Tooth disease
cNLS	Classical NLS
CNBr	Cyanogen bromide
Co-IP	Co-immunoprecipitation
CTD	C-terminal domain
CSK	Cytoskeletal

DAPI	4',6-Diamidino-2-phenylindole
DCM	Dilated cardiomyopathy
Del	Deletion
dH$_2$O	Distilled water
ddH$_2$O	Double distilled water
DKO	Double knock out
DMSO	Dimethyl sulfoxide
DMEM	Dulbecco's Modified Eagle Medium
Dm	*Drosophila melangoster*
DNA	Deoxyribonucleic acid
dNTP	deoxy-nucleoside triphosphate
DTT	Dithiothreitol
E. coli	*Escherichia coli*
ECL	Enhanced chemiluminescence
EDTA	Ethylenediamine teta-acetic acid
EDMD	Emery-Dreifuss muscular dystrophy
e.g.	exempli gratia
EM	Electron Microscopy
ER	Endoplasmic reticulum
et al	et alia (and others)
FACE1	Farnesylated proteins-converting enzyme 1
FCS	Fetal calf serum
Fig	Figure
FL	Full-length
FPLD	Familial partial lipodystrophy
FRAP	Fluorescence recovery after photobleaching
FRET	Fluorescence resonance energy transfer
FTase	Farnesyltransferase
FTI	Farnesyltransferase inhibitors
g	Gram
g	Gravity force
G	Guanine
G1	Gap phase
GCL	Germ cell less

GFP	Green fluorescent protein
GST	Glutathione-S-transferase
GTP	Guanosine triphosphate
H1	Histone1
H(1-4)	Hydrophobic sequences (1-4)
HA	Hemagglutinin
hALP	Human acetyl-transferase-like protein
HCl	Hydrochloric acid
HeLa	Henrietta Lacks cells
HGPS	Hutchinson-Gilford progeria
HP1	Heterochromatin protein 1
HEPES	4-(2-hydroxyethyl)-1-piperazineethanesulfonic acid
hFF	Human for skin fibrblasts
hr	Hour
HRP	Horse radish peroxidise
hSUN1	Human SUN1
hSUN2	Human SUN2
Hyp7	Hypodermal syncitium
ICMT	Isoprenylcysteine carboxyl methyltransferase
IF	Intermediate filament
IF	Immunofluorescence
Ig	Immunoglobulin
IgG	Immunoglobulin G
INM	Inner nuclear membrane
IP	Immunoprecipitation
IPTG	Isopropyl-β-D-thiogalactosidase
IVT	In vitro translation
Kb	Kilobase
kDa	KiloDalton
Kapα/β1	Karyopherin α/β1
KASH	Klarsicht ANC-1 Syne-1 homology
KLS	Klarisicht like domain
L	Litre
LA	Lamin A

LAP	Lamina-associated polypeptides
LBR	Lamin B receptor
LB	Luria Bertani
LEM	LAP/emerin/MAN1
LINC	Linker of nucleoskeleton and cytoskeleton
LIPA	Lamin interacting protein from adipocytes
LGMD	Limb girdle muscular dystrophy
LMNA	human lamin A/C gene
LMNB1	lamin B1 gene
LMNB2	lamin B2 gene
M	Molar
MAD	Mandibulo-acral dysplasia
MBP	Maltose binding protein
MEF	Mouse embryonic fibroblast
mA	Milli Amplitude
mg	Milligram
min	Minutes
ml	Milliliter
mm	Millimeter
mM	Milli Molar
MMs	Microsomal membranes
Mps3	Monopolar spindle 3
Msp-300	Muscle-specific protein 300 kDa
mSUN1	Murine SUN1
mSUN2	Murine SUN2
MT	Microtubule
MTOC	Microtubule organization center
MWCO	Molecular-weight cutoff
MyoD	Myogenic differentiation protein
Myne	Myocyte nuclear envelope
NaOH	Sodium hydroxide
NE	Nuclear envelope
NEBD	Nuclear envelope break down
NES	Nuclear export signal

Nesprin	Nuclear envelope spectrin repeat protein
NETN	Nonidet P-40/EDTA/Tris-HCL/NaCl
NETs	Nuclear envelope transmembrane proteins
ng	Nanogram
NL	Nuclear lamina
ΔNLA	Lamin A mutant lacking its amino-terminal domain
NLS	Nuclear localization signal
nm	Nanometer
NMR	Nuclear magnetic resonance spectroscopy
NPCs	Nuclear pore complexes
NRK	Normal rat kidney cells
NIH 3T3	National Institute of Health (3-day transfer, inoculum 3 x 10^5 cells) mouse fibroblast cell line
NTD	N-terminal domain
NUANCE	Nucleus and actin connecting element
OD	Optical density
ONM	Outer nuclear membrane
OPTI-MEM	Reduced Serum Media
ORF	Open reading frame
PAGE	Polyacrylamide gel electrophoresis
PBS	Phosphate buffered saline
P-cell	Epithelial blast cells
PCNA	Proliferating cell nuclear antigen
PCR	Polymerase chain reaction
PEG	Polyethylene glycol
P*fu*	*Pyrococcus furiosus* DNA polymerase
pH	Potential of Hydrogen
PIPES	Piperazine-N,N′-bis(2-ethanesulfonic acid)
PPARγ	Peroxisome proliferator activated receptor gamma
PMSF	Phenylmethylsulphonyl fluoride
POM	Pore membrane
Rb	Retinoblastoma protein
RCE1	Ras-converting enzyme 1
RD	Restrictive dermopathy

RFC	Replication factor complex
rpm	Revolutions per minute
RNA	Ribonucleic acid
RNAi	RNA interference
RT	Room temperature
^{35}S	^{35}Sulphur
SPB	Spindle pole body
Sad1	Spindle architecture disrupted/ Spindle pole associated protein
S. cerevisiae	*Saccharomyces cerevisiae*
sec	Second
SDS	Sodium dodecyl sulphate
SPAG4	Sperm associated antigen 4
S. pombe	*Schizosaccharomyces pombe*
SSHR1	A polyclonal antibody to the CTD of mouse SUN1
SR	Spectrin repeats
SREBP1	Sterol regulatory element binding protein 1
SUN	Sad1-UNC-84 related protein
Syne	Synaptic nuclear envelope
T	Thymine
T4	Bacteriophage
TAE	Tris acetic acid EDTA buffer
TBE	Tris borate EDTA buffer
TB	Transformation buffer
TE	Tris EDTA
TEMED	Tetramethyl-ethylenediamine
TGF-β	Transforming growth factor-β
TM	Transmembrane
TMD	Transmembrane domain
TMpred	Prediction of transmembrane regions and orientation
TNT$^{®}$	Transcription and translation
μl	Microlitre
U	Unit
UNC	Uncoordinated
U2OS	Human osteosarcoma cells

UV	Ultra-violet
v/v	Volume to volume
WT	Wild type
w/v	Weight to volume
V	Voltage
X-EDMD	X-linked Emery-Dreifuss muscular dystrophy
X-Gal	5-Bromo-4-chloro-3-indoxyl-beta-D-galactopyranoside
ZMPSTE24	Zinc metalloprotease related to yeast Ste24p
ZYG	Zygote defective

TABLES AND FIGURES

Tables:

Figures:

xx

CHAPTER 1

INTRODUCTION

1.1 NUCLEAR ENVELOPE

In eukaryotic organisms, the genetic material is enclosed within the nucleus of the cell. The nucleus is surrounded by a double membrane structure, the nuclear envelope (NE). The NE forms a selective barrier, thereby controlling traffic of macromolecules between the nucleus and the cytoplasm. Apart from acting as a physical barrier and providing structural support for the nucleus, the NE is also responsible for various other cell-specific functions which are only now emerging. These include chromatin organization, regulation of tissue-specific gene expression, nuclear positioning and migration in cells (reviewed in Dechat et al., 2008).

The NE is composed of an outer nuclear membrane (ONM), an inner nuclear membrane (INM) and nuclear pore complexes (NPCs) (Fig. 1.1). The INM is underlined by the nuclear lamina (Fig. 1.1; section 1.1.2). The NE can be considered as a specialized domain of the endoplasmic reticulum (ER), as it is very similar structurally and functionally to the rough ER membrane. The ONM has ribosomes attached to its outer surface and is continuous with the ER. The peri-plasmic lumen between the ONM and the INM is also continuous with the lumen of the ER. In contrast, the INM has distinct structural features to the ONM and lacks ribosomes. The NE harbours numerous integral membrane proteins that are unique and maintain extensive interaction with the nuclear lamina and chromatin (Schirmer et al., 2003; reviewed in Burke and Stewart, 2002; Burke and Stewart, 2006,).

1.1.1 Nuclear pore complexes

The NE of each cell is penetrated by several thousand NPCs. NPCs are massive complexes each with a molecular mass of about 125 million Daltons and NPCs consist of multiple copies of 50-100 different proteins, known as nucleoporins. NPCs are basket-like structures with eight-fold symmetry arranged around a central channel (Fig. 1.2). Each NPC has eight spikes connected by rings at the nuclear and cytoplasmic surfaces and anchored at the NE by three INM proteins, POM121, gp210 and Ndc1 (D'Angelo and Hetzer, 2008). The gated channels of NPCs allow small molecules and proteins less than 40 kDa to pass freely between the cytosol and nucleoplasm, but larger
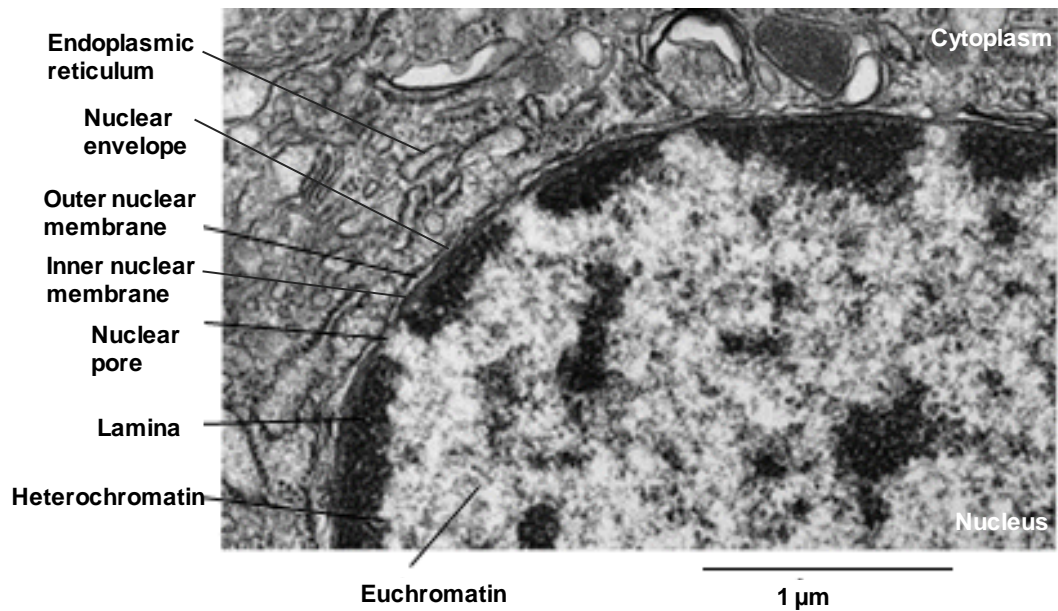
Fig. 1.1. Electron micrograph of a mammalian cell nucleus. The nuclear envelope consists of an outer nuclear membrane and an inner nuclear membrane. It is penetrated by nuclear pore complexes and is continuous with the endoplasmic reticulum. The nuclear lamina underlies the inner nuclear membrane. Heterochromatin is preferentially located at the nuclear periphery. Reproduced from Alberts et al. (1994).

3
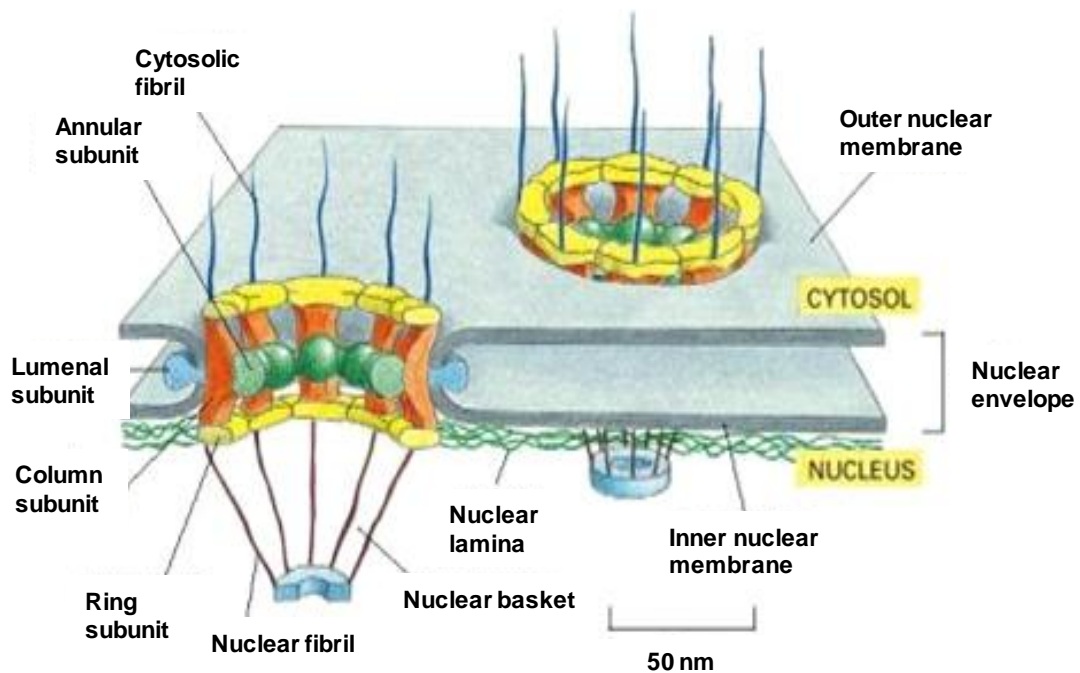
Fig. 1.2. Schematic representation of nuclear pore complexes embedded in the nuclear envelope. A nuclear pore complex has four structural subunits: column subunit that forms the pore wall; annular subunit; lumenal subunit that contains transmembrane proteins for anchoring in NE; and ring subunit that forms the cytosolic and nuclear faces of the complex. Fibrils protrude from both the cytosolic and the nuclear sides. On the nuclear side, the fibrils converge and form basket-like structures. Reproduced from Alberts et al. (1994).

proteins and RNAs are selectively transported by active mechanisms (Cooper et al., 2000). At the periphery of the NPCs, the ONM is joined to the INM by the pore membrane (POM). The lateral channel between POM and NPCs allows membrane proteins with a cytoplasmic or nucleoplasmic domain less than 60 kDa to pass freely between the ONM and INM (reviewed in Holmer and Worman, 2001).

1.1.1.1 Nucleocytoplasmic transport

Large macromolecules are transported into and out of the nucleus through the NPCs by an energy dependent RanGTPase system. Carriers that are involved in import and export are called 'importins' and 'exportins', respectively, and are collectively known as karyopherins. Generally, proteins contain certain sorting signal for transport, known as nuclear localization signal (NLS) for import and nuclear export signal (NES) for export. The classical NLS (cNLS) consists of either one (monopartite) or two (bipartite) stretches of basic amino acids (lysine or arginines). Typically, the NLS in a cargo is recognised by importin α, that in turn binds with importin β. The complex then interacts with nucleoporins, lining the aqueous channel of the pore and is translocated through the NPCs. Within the nucleus, binding of RanGTP to importin β releases the cargo-importin α complex. RanGTP recycles with importin β back to the cytoplasm and is hydrolysed to RanGDP (Fig. 1.10). A similar mechanism exists in the opposite direction for nuclear export (Alberts et al., 2007; reviewed in Lange et al., 2007).

1.1.2 The nuclear lamina

The nuclear lamina is a 20-50 nm thick proteinaceous layer that underlies the inner face of the INM in metazoan cells (Fawcett 1966) (Fig. 1.1). It is composed of nuclear lamins and lamin-binding proteins. The nuclear lamina gives structural support and strength to the NE and helps maintain the shape and size of the interphase nucleus. The nuclear lamina is attached to the NE by its interaction with the various INM proteins (Section 1.1.3). It also provides anchoring sites for NPCs and transcriptionally repressed heterochromatin (Section 1.2; reviewed in Gruenbaum et al., 2005).

Initially, the nuclear lamina was found as an amorphous material underlying the INM in biochemical fractionation studies, and as salt- and detergent-resistant nuclear

components in association with NPCs (Aaronson and Blobel, 1975; Gerace et al., 1978). The nuclear lamina isolated from the rat liver showed three prominent bands which were later named according to their size as lamin A (70 kDa), lamin B (67 kDa) and lamin C (60 kDa) (Gerace and Blobel, 1980). The types of lamins are described below. There has been extensive study on lamins ever since. Lamins were shown to be type V intermediate filament (IF) proteins and are thought to be the progenitors of the intermediate filament family of proteins that includes cytoplasmic IFs such as keratins, vimentin, desmin and neurofilaments (Aebi et al., 1986; Goldman et al., 1986; McKeon et al., 1986; Doring and Stick, 1990).

1.1.2.1   Lamin structure

Lamin proteins range in size from 60 to 70 kDa and, like other IF proteins, possess an N-terminal head domain, followed by a central α-helical rod domain and a C-terminal tail domain. The central rod domain has four coiled-coil domains (1A, 1B, 2A, 2B), connected by linker regions (L1, L2, L3) (Fig. 1.3A). The α-helical rod domain contains characteristic heptad amino acids repeats, thus allowing the lamin monomers to self-interact by parallel interactions to form coiled-coil homodimers. The head and tail domains of lamin homodimers assemble to form head to tail polymers, which in turn are thought to organize by lateral interaction, into a thin filamentous lattice-work (Fig. 1.3 B,C) (reviewed in Stuurman et al., 1998). However, in vitro, the lamin filaments associate to form fibres and large paracrystalline arrays (Goldman et al., 1986). The endogenous latticework of lamins has been visualized by electron microscopy only in *Xenopus lavis* oocytes (Fig. 1.4), and it is presumed that higher animals also have similar organization of the nuclear lamina (Aebi et al., 1986). It is not known whether different lamin isoforms form homopolymers or heteropolymers in higher organisms (Stuurman et al., 1998).

The globular tail domain of lamins contains an immunoglobulin (Ig)-like domain (residues 430-545 in lamin A/C) (Ig-fold) (Dhe-Paganon et al., 2002; Krimm et al., 2002) and a nuclear localization signal between the central rod and Ig-fold for transport of lamins into the nucleus (Fisher et al., 1986; Loewinger and McKeon 1988) (Fig. 1.3A).

A

Linker region

Head domain

L1   L2   L3

| 1A | 1B | 2A | 2B |

Tail domain

α-helical coiled–coil domain

NLS   Ig-fold   CAAX

B

0.1 μm

C

NH₂ ... COOH

I   α-helical region in monomer

NH₂ ... COOH

II   coiled-coil dimer

NH₂ ... COOH

48 nm

NH₂   COOH   COOH   NH₂

III

NH₂   COOH   COOH   NH₂

staggered tetramer of two coiled-coil dimers

IV   two tetramers packed together

V   eight tetramers twisted into a ropelike filament

10 nm
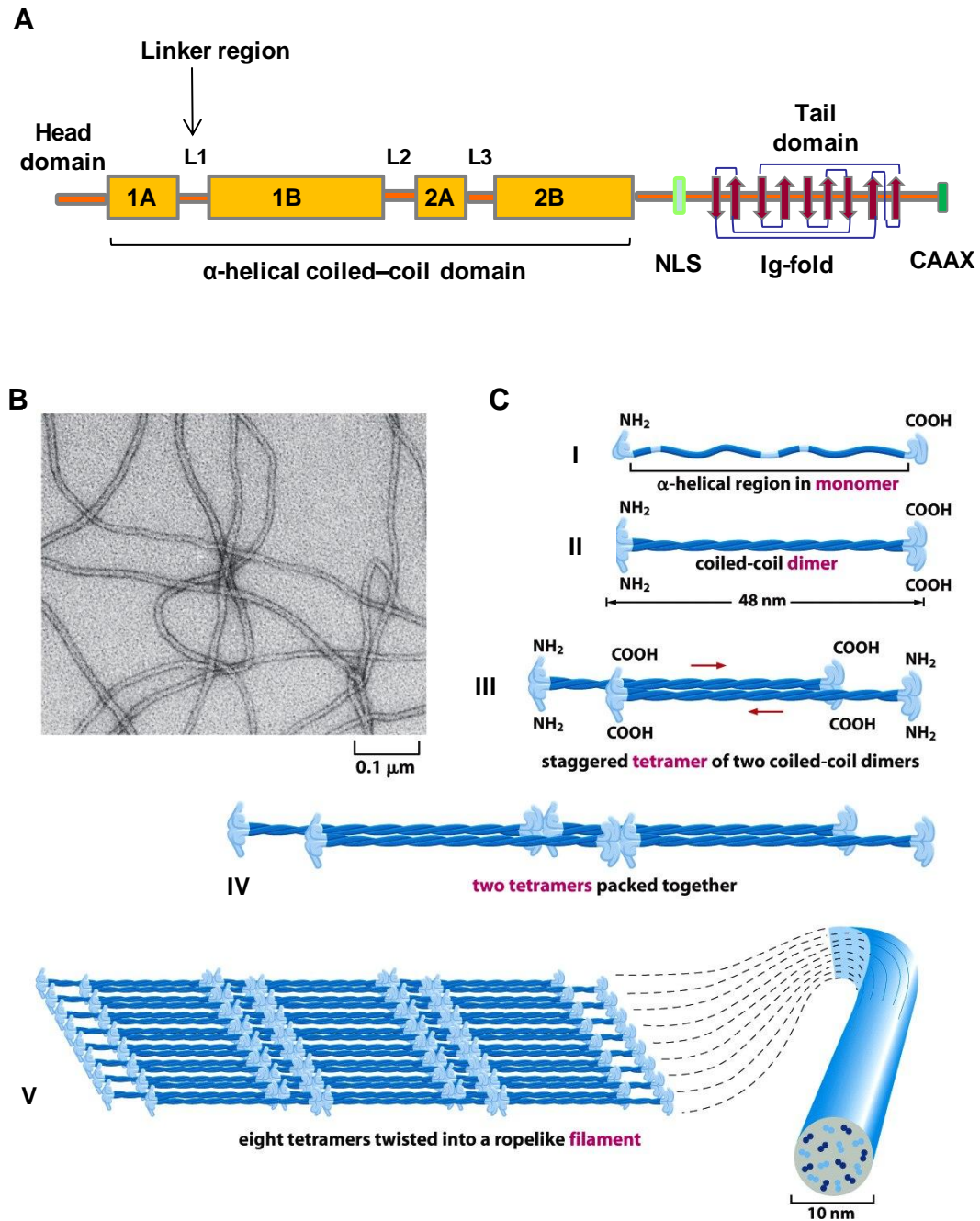
Fig. 1.3.   Nuclear lamin structure and association. A) Generalized schematic structure of nuclear lamins. Lamin proteins have a conserved structure that consists of a variable globular head domain, a central α-helical domain with four coiled-coils that facilitates dimerization, linker domains and a variable globular tail domain. The coiled-coil domains are termed 1A, 1B, 2A and 2B, respectively. The globular tail domain contains a nuclear localization signal sequence (NLS), immunoglobulin (Ig)-like fold and CAAX motif. **B)** Model photograph showing intermediate filaments obtained by transmission electron microscopy. **C)** Model of lamin assembly. A monomer (I) forms a dimer (II), two dimers then line up in a head-to-tail fashion to form tetramers (III), tetramers then associate (IV) eventually forming rope-like filaments (V). Reproduced from Albert et al. (2007).
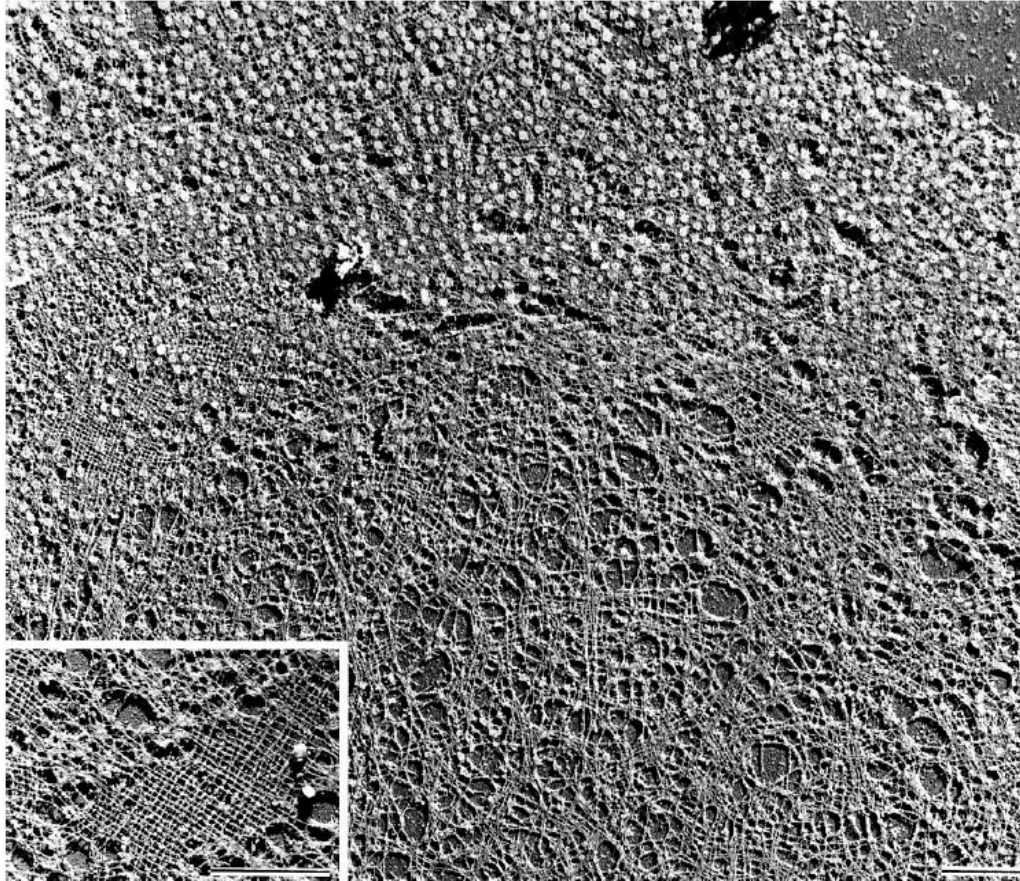
Fig. 1.4. *Xenopus laevis* **oocyte nuclear lamina.** Photograph showing the inner face of the nuclear envelope of *Xenopus* oocytes after extraction with Triton X-100 and visualized by scanning electron microscopy. This overview of the nuclear envelope shows the nuclear lamin meshwork and associated nuclear pore complexes (circular structures). Inset shows higher-magnification view of lamina latticework. Bars, 1 μm. Reprinted by permission from Macmillan Publishers Ltd: Nature (Aebi. et al.), copyright (1986).

1.1.2.2   Lamin isoforms and their expression

Lamins are found in all metazoan organisms, but they are absent from plants and unicellular organisms. Most invertebrates have single lamin genes, for example, *Caenorhabditis elegans* has only one lamin gene termed *Ce-lamin* or *lmn-1* that most closely resembles the mammalian B-type lamin (see below). However, *Drosophila melangoster* has two lamin genes (*Dm0* and *C*) (Osman et al., 1990; Meier 2001; Melcer et al., 2007). The number and complexity of lamins have increased with metazoan evolution. Vertebrates have two major types of lamins: A- and B-type (Fig. 1.5), which differ biochemically, structurally and in their behaviour during mitosis (reviewed in Stuurman et al., 1998, Gerace and Blobel, 1980). A-type lamins consist of major isoforms, lamin A and C, and two minor isoforms, $A_{\Delta 10}$ and C2, which are all alternative splice variants of a single *LMNA* gene (Fisher et al., 1986, Machiels et al., 1996; Furukawa et al., 1994). Lamin A and lamin C are identical for the first 566 residues, and then they differ as lamin C lacks exon 11 and 12. The lamin C transcript reads through to end of exon 10, which contains a stop codon and polyadenylation signal to terminate the process. In contrast, lamin A is produced by use of an alternative splice site upstream of the exon 10 stop codon and then reads through exon 11 and 12 to a stop codon in exon 12 (Fig. 1.5A). Therefore, at the C-terminus, lamin A possesses 98 unique residues and, on the other hand, lamin C has six unique residues encoded within exon 10. Both proteins are found in equal amounts at the nuclear lamina (Fisher et al., 1986; Lin and Worman, 1993). Lamin $A_{\Delta 10}$ has a 30 amino acid deletion at the C-terminus encoded by exon 10 and is found in low abundance in normal cells (Machiels et al., 1996). Lamin C2 is similar to lamin C except that 86 residues at the N-terminus are replaced by six unique residues, generated by differential splicing of *LMNA* gene (Furukawa et al., 1994). On the other hand, B-type lamins, lamin B1 and B2, are encoded by the *LMNB1* and *LMNB2* genes, respectively and lamin B3 is a small splice variant of lamin B2 (Peter et al., 1989; Lin and Worman, 1995; Hoger et al., 1988; Hoger et al., 1990; Zewe et al., 1991; Furukawa and Hotta, 1993).

In higher eukaryotes, B-type lamins (either B1 or B2 or both) are ubiquitously expressed in all somatic cells and are essential for cell viability, but the expression of A-type lamins is developmentally regulated and tissue specific (Stewart and Burke, 1987; Rober et al., 1989). A-type lamins are absent in early embryonic cells, haemopoietic
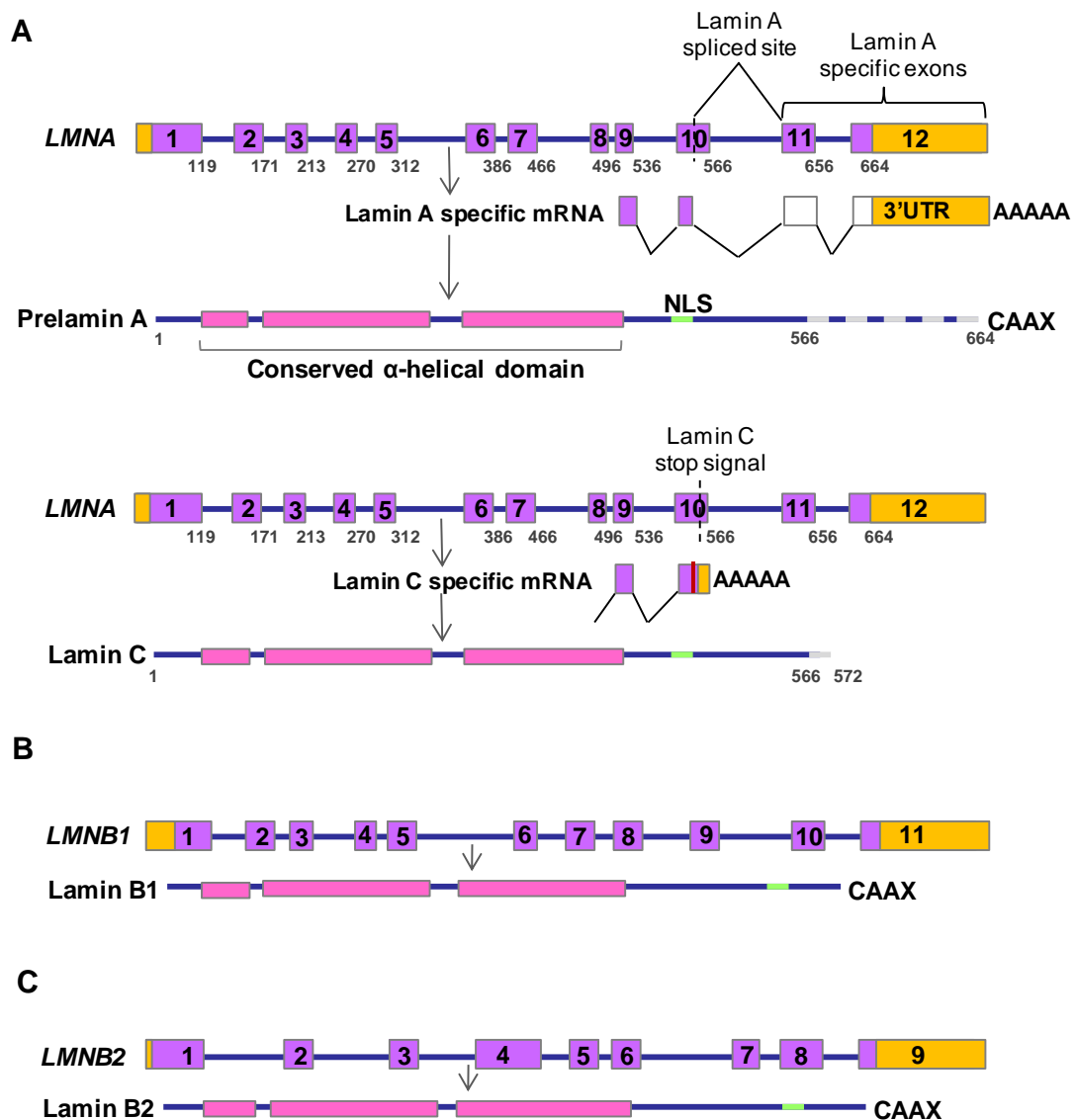
Fig. 1.5. Different types of lamins. Three genes encode nuclear lamins in mammals. **A)** *LMNA* on chromosome 1q21.2, has 12 exons (boxes) that encode the A-type lamins. The last residue encoded by each exon of lamin A is numbered. Lamin A and lamin C are generated by alternative RNA splicing in exon 10. Lamin A and lamin C mRNAs generated from exon 9, 10, 11, and 12 are schematically drawn. Bent lines indicate RNA splicing between exons. The mRNA region coding for lamin C-specific amino acids is shaded red and regions coding for prelamin A-specific amino acids are white. The 5'-3'-untranslated sequences are indicated by yellow boxes. Poly A tails are indicated. Prelamin A protein has 98 unique amino acids and lamin C has 6 unique amino acids at the carboxyl terminus (grey striping). **B)** *LMNB1* on chromosome 5q23.3–q31.1 encodes lamin B1, and **C)** *LMNB2* on chromosome 19p13.3 encodes lamin B2. Genes are indicated in purple and corresponding proteins are indicated in pink. The nuclear localization signals (green) are located in the tail domain of lamins. All lamins except lamin C have C-terminal CAAX motifs. Adapted from Worman et al. (2009).

10

cells and stem cells and are expressed mainly in differentiated cells (Stewart and Burke, 1987; Rober et al., 1989; Rober et al., 1990). A-type lamins are thought to play a role in chromatin organization and tissue-specific gene expression, maintaining a differentiated state of cells (section 1.2). During development lamin B2 is expressed relatively constantly in all cell types (except hepatocytes), while lamin B1 is mainly expressed during proliferation, early in the developmental stage. B-type lamins are sufficient to constitute a functional nuclear lamina (Broers et al., 1997; reviewed in Stuurman et al., 1998). Lamin C2 and lamin B3 are expressed in germ cells only (Furukawa and Hotta, 1993; Furukawa et al., 1994). From now on only lamin A, C, B1 and B2 will be considered as they are the major A and B type lamins that are expressed in most tissues.

1.1.2.3   Lamin processing

Each major lamin isoform is processed differently after synthesis. All except lamin C have a C-terminal CAAX (Cys-aliphatic-aliphatic-any residue) motif that undergoes a series of post-translational modifications (Fig. 1.6) (reviewed in Rusinol and Sinensky, 2006). The cysteine residue in the CAAX motif undergoes farnesylation by farnesyltransferase (FTase), which adds a lipid group (isoprene) that facilitates membrane association and protein-protein interactions (Zhang and Casey, 1996; Farnsworth et al., 1989). Subsequently, the AAX sequence is removed by enzyme ZMPSTE24 (Zinc metalloprotease related to yeast Ste24p)/ FACE1 (Farnesylated proteins-converting enzyme 1) for lamin A or by RCE1 (Ras-converting enzyme 1) for lamin B (Zhang and Casey, 1996; Corrigan et al., 2005; Leung et al., 2001). Afterwards the farnesylated cysteine is carboxymethylated by isoprenylcysteine carboxyl methyltransferase (ICMT) (Winter-Van and Casey, 2005). These modifications are required to render lamins more hydrophobic and thus facilitate their attachment to the INM and also influence protein-protein interactions (Holtz et al., 1989; Krohne et al., 1989; Kitten and Nigg, 1991; reviewed in Davies et al., 2009).

In contrast to lamin B, which remains permanently farnesylated, lamin A undergoes a further cleavage. Lamin A whose initial precursor is known as prelamin A, is further processed by removal of the modified cysteine residue and an additional 14 residues (residues 647-661) by ZMPSTE24 enzyme, to produce mature lamin A. Prelamin A is the only known substrate for ZMPSTE24 in mammals (Corrigan et al., 2005). The
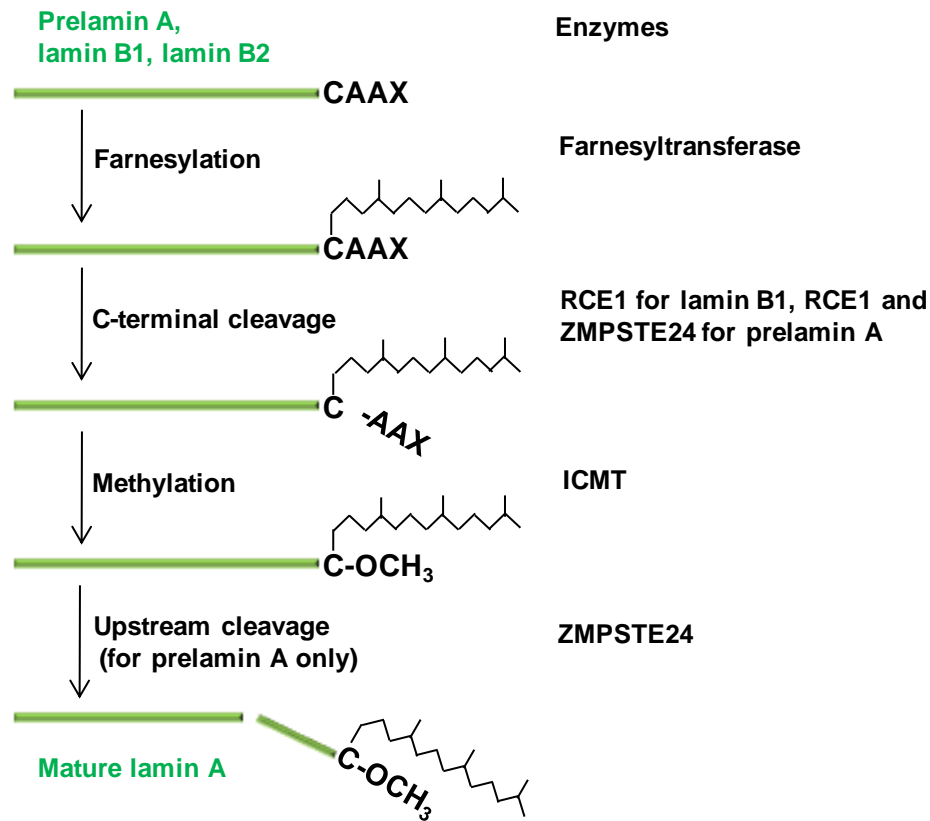
Fig. 1.6. Post-translational modification of prelamin A, lamin B1, and lamin B2. Initially, a farnesyl group is attached to the cysteine residue of the C-terminal −CAAX motif of lamins by a farnesyltransferase; then the last three residues (−AAX) are cleaved off by an endopeptidase (RCE1 or ZMPSTE24); then the carboxylic acid group (−COOH) of the C-terminal cysteine residue is methylated by a carboxyl methyltransferase (ICMT). These lead to formation of mature lamin B1 and B2. In the case of prelamin A, an additional 15 C-terminal residues, including the farnesylated/carboxymethylated cysteine, are cleaved off by ZMPSTE24. Lamins B1 and B2 remain farnesylated and carboxymethylated, while lamins A and C are not. Adapted from Worman et al. (2009).

recognition site is a highly conserved hexapeptide domain (RSYLLG) (Weber et al., 1989; Hennekes and Nigg, 1994; Kilic et al., 1997). This cleavage event occurs after association of lamin A with the nuclear lamina. Overall, 18 residues are removed from prelamin A to produce mature lamin A (Weber et al., 1989; reviewed in Moir et al., 1995; Corrigan et al., 2005). Lamin C does not have a CAAX motif and is not farnesylated, therefore requires lamin A for its assembly into the nuclear lamina (Vaughan et al., 2001). These various modifications are responsible for the different properties of the lamin isoforms, for example, during mitosis, when the NE dissembles, only lamin B remains farnesylated and attached to the ER membrane, whereas A-type lamins are more soluble and become dispersed in the cytosol (Gerace and Blobel, 1980; Burke and Gerace 1986). A-type lamins are transported into the nucleus mainly after NE reformation (reviewed Dechat et al., 2010; section 1.2.3).

Of note, the exact location of posttranslational processing of lamins is not known. The lamin processing enzymes FTase is found in the cytosol and ZMPSTE24 and ICMT are found in both the INM and ER (Barrowman et al., 2008). However, it is thought that the processing of all lamins is intranuclear, as lamins are transported into the nucleus soon after its synthesis in the cytoplasm (reviewed in Dechat et al., 2010; Barrowman et al., 2008; Lutz et al., 1992; Lehner et al., 1986).

1.1.2.4   *Nucleoplasmic lamins*

In addition to their location at the nuclear periphery, nuclear lamins are also found in the nuclear interior, or nucleoplasm. They are present as intranuclear foci, veils or channels forming stable complexes (an internal lamina) (Bridger et al., 1993; Goldman et al., 1992; Moir et al., 1994). The organization of these complexes is not fully understood. Lamin A/C that is present in the nucleoplasm is dynamic and plays a role in transcription, DNA replication and RNA splicing. Nucleoplasmic lamin B is more stable and is associated with DNA replication sites (Spann et al., 1997; Jagatheesan et al., 1999; reviewed in Broers et al., 2006; Reviewed in Dechat et al., 2008). Fluorescence recovery after photobleaching (FRAP) and solubility studies show that lamin B is highly immobile, possibly due to presence of the farnesyl group, while lamin A although immobile has a fraction that is more soluble and mobile, possibly due to

absence of a farnesyl group and presumably representing the nucleoplasmic pool (Broers et al., 1999; Moir et al., 2000a). Functions of nuclear lamins are described in detail in section 1.2.

1.1.3 Integral membrane proteins of the nuclear envelope

The NE harbours numerous integral membrane proteins. Currently it is thought that there are at least 80 integral nuclear membrane proteins present (Schirmer et al., 2003, reviewed in Wilson and Foisner, 2010). Most integral membrane proteins are associated with the INM. Lamin B receptor (LBR) was the first INM protein identified in 1988 (Worman et al., 1988, Worman et al., 1990). Among other NE integral proteins are lamina associated protein 1 (LAP1), LAP2, emerin, MAN1, nurim, LUMA, nesprins and SUN proteins (Table 1.1) (Fig. 1.7). Three membrane proteins, gp210, POM121 and Ndc1 are associated with the NPCs, their role being to anchor the NPCs in the NE (D'Angelo and Hetzer, 2008). Nearly all INM proteins are type II transmembrane proteins with the N-terminus located in the nucleoplasm and the C-terminus in the NE lumen. Most INM proteins have a large nucleoplasmic domain that interacts with lamins and/or chromatin, a single membrane spanning region and a small lumenal C-terminal domain. Lamins bind *in vitro* to most of the INM proteins found to date, except nurim (reviewed in Burke and Stewart, 2002).

By, 2002 approximately 18 INM proteins had been identified. However, a proteomic approach to comprehensively identify all the NE proteins present in rat liver found 67 novel nuclear envelope transmembrane proteins, termed NETs (Schirmer et al., 2003). In this comparative and subtractive proteomic study, NEs and microsomal membranes (MMs) were isolated from rodent liver and were extracted with sodium hydroxide to obtain transmembrane proteins. Another NE fraction was extracted with salt and detergent to identify integral membrane proteins associated with the lamins. Proteins from all three fractions were subjected to mass spectrometry for analysis. The MM protein fractions, representing the ER, were subtracted from the NE fractions to obtain NE-specific proteins. Among the NE proteins common to both NE extractions, 67 were potential NE proteins, with predicted transmembrane domains or demonstrated lamin association (Schirmer et al., 2003). The precise functions of most of the NE proteins are still not known (Burke and Stewart, 2006). Most INM proteins interact with lamins and
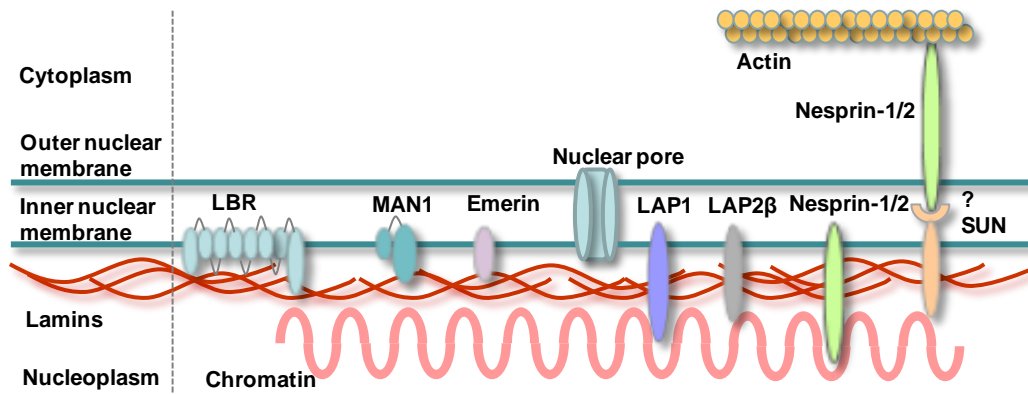
Fig. 1.7. Schematic drawing of the nuclear envelope with integral nuclear membrane proteins. The nuclear lamina (shown in red) underlies the inner nuclear membrane (INM). The lamins interact with several inner nuclear membrane proteins, including lamin B receptor (LBR), MAN1, emerin, lamina-associated polypeptide 1 (LAP1), LAP2β and small nesprin-1 isoforms. Large nesprin-1 and nesprin-2 isoforms interact with actin and are located at the outer nuclear membrane, thought to be tethered by SUN proteins located at the INM. "?" denotes possible interaction. Adapted from Worman et al. (2009).

Name	Molecular weight	Lamin binding	Chromatin binding partners	Comments
LAP1A	75 kDa	A/B-type lamins		It has two splice variants (below), which share the same transmembrane and lumenal domain. Lumenal domain binds Torsin A.
LAP1B	68 kDa	A/B-type lamins		Splice variant of LAP1A
LAP1C	57 kDa	A/B-type lamins		Splice variant of LAP1A
LAP2β	50 kDa	B-type lamins	BAF, HA95	Large nuceoplasmic domain; LEM domain.
LAP2ε,δ,γ	38-46 kDa	Most likely A/B-type lamins	BAF	Splice variants of LAP2β. Another splice variant LAP2α is soluble protein.
LBR	70 kDa	B-type lamins	HP1, HA95	Multi-spanning proteins with sterolreductase activity. Defects associated with Pelger-Huet anomaly
Emerin	29 kDa	A/B-type lamin	BAF	LEM domain; defects linked to Emery-Dreifuss muscular dystrophy
Nurim	29 kDa			Multi-spanning hydrophobic membrane protein, unknown function
MAN1	82 kDa	A/B-type lamin	BAF	LEM domain; binds SMAD proteins to inhibit TGF-β signalling pathway

(Continued overleaf) |

Table 1.1 Properties of mammalian integral nuclear envelope proteins. (Adapted from Burke and Stewart, 2006)

Name	Molecular weight	Lamin binding	Chromatin binding partners	Comments
LUMA	45 kDa			Multi-spanning membrane protein, unknown function
RFPB (RING finger-binding protein)	126 kDa		RING finger motif of RUSH transcription factor	Muti-spanning ATPase
SUN1	102 kDa			C-terminal SUN domain, poteintial function to tether KASH domain proteins at the ONM
SUN2	80 kDa			C-terminal SUN domain, poteintial function to tether KASH domain proteins at the ONM
Nesprin-1	100-1000 kDa	A-type lamins		Membrane protein with C-terminal KASH domain, multiple spectrin repeats, multiple isoforms. Some isoforms have N-terminal actin binding domain
Nesprin-2	50-800 kDa	A-type lamins		C-terminal KASH domain, multiple spectrin repeats, multiple isoforms. Some isoforms have N-terminal actin binding domain

Table 1.1 (continued) Properties of mammalian integral nuclear envelope proteins. (Adapted from Burke and Stewart, 2006)

anchor the lamina at the INM. In addition, many INM proteins bind to chromatin or chromatin binding proteins, therefore contribute to chromatin organization and regulation of gene expression (section 1.2). Recent advancements show that there may be significant differences in the NE proteome in different tissues, with preferential expression of unique subsets of NETs in different cell types. This therefore emphasizes the important role of the nuclear lamina in tissue-specific gene expression patterns (Schirmer and Gerace, 2005).

1.1.3.1   *Lamin B receptor (LBR)*

LBR, the first integral membrane protein to be identified, was isolated as a lamin B1 binding protein of 70 kDa (Worman et al., 1988). LBR has a nucleoplasmic amino-terminal domain and a carboxy-terminal with 8 putative transmembrane domains (Fig. 1.7). In addition to binding B-type lamins, the LBR N-terminus also interacts directly with double-stranded DNA, chromatin-associated proteins and heterochromatin protein 1 (HP1) (Ye and Worman, 1994; Ye and Worman, 1996; Ye et al., 1997). LBR is thought to mediate chromatin organization by anchoring heterochromatin to the INM through these interactions (Holmer and Worman, 2001). LBR is the only INM protein so far identified with an enzymatic activity. The membrane embedded-domain of LBR has structural similarity to sterol-reductase involved in cholesterol metabolism and it catalyzes conversion of cholesta-8,14-dien-3β-ol to cholesterol (Worman et al., 1990; Holmer et al., 1998; Waterham et al., 2003). Heterozygous mutations in *LBR* cause Pelger-Huet anomaly, an abnormality of nuclear shape and chromatin organization in blood neutrophils (Hoffmann et al., 2002). On the other hand, homozygous mutations of *LBR* that disrupt its sterol reductase activity are associated with Greenberg skeletal dysplasia, an in utero lethal disorder with hydrops-ectopic calcification (Waterham et al., 2003; Hoffmann et al., 2007) (Table 1.2).

1.1.3.2   *LEM domain proteins*

Integral membrane proteins <u>L</u>AP2, <u>E</u>merin and <u>M</u>AN1 share a conserved 43 residue motif near the N-terminus, located in the nucleoplasm, called the LEM domain. Most LEM domain proteins are located at the INM and interact with either A- or B-type lamins or both (reviewed in Gruenbaum et al., 2005). The LEM domain has been found

to interact with a transcriptional repressor protein known as barrier to autointegration factor (BAF), a highly conserved chromatin-associated protein essential for cell viability (Segura-Totten and Wilson, 2004). Apart from the founding members, other LEM domain proteins more recently identified are Lem2, Lem3, Lem4 and Lem5 (Lee and Wilson, 2004).

Lamina-associated polypeptide 2 (LAP2) is one of the most studied INM protein families. LAP2 has six alternatively spliced isoforms ($\alpha,\beta,\gamma,\delta,\epsilon$ and ϕ) transcribed from the *LAP2* gene, also known as thymopoietin. Five of the LAP2 isoforms are INM proteins with a common N-terminal nucleoplasmic domain and single C-terminal transmembrane domain (Harris et al., 1995; Berger et al., 1996). LAP2α, on other hand, lacks a membrane spanning region and is found in the nuclear interior, where it binds to A-type lamins (Dechat et al., 2000). LAP2β binds specifically to B-type lamins and chromatin (Foisner and Gerace, 1993; Furukawa et al., 1997; Furukawa and Kondo, 1998). Mitosis-specific phosphorylation of LAP2β inhibits its binding to lamin B and chromatin and promotes nuclear breakdown and reassembly in mitosis (Foisner and Gerace, 1993; Gant et al., 1999), as described in section 1.2.3. In addition to the LEM domain that interacts with BAF (Shumaker et al., 2001), LAP2β also binds transcription regulator germ cell-less (GCL), which in turn represses E2F-mediated gene transcription (Nili et al., 2001).

Rather than being located at the INM, LAP2α is found throughout the nucleoplasm, in complex with the nucleoplasmic pool of lamin A/C. The role of this complex is to bind the retinoblastoma (Rb) protein, a cell cycle regulator and tumour-suppressor. Rb regulates the activity of E2F transcription factors that control the expression of cell cycle regulatory genes. In its hypophosphorylated state Rb is active as a transcriptional repressor. Over-expression of LAP2α inhibits E2F-Rb-dependent gene activity and reduces cell proliferation, whereas LAP2α RNA interference increases cell proliferation. LAP2α–lamin A/C complexes are thought to bind hypophosphorylated Rb, thereby delay its deactivation and maintain E2F in a repressed state (Dorner et al. 2006). In LAP2α knock-out mice, loss of LAP2α causes nucleoplasmic A-type lamins to relocalize to the NE and also impairs Rb function, which in turn leads to hyperplasia of certain tissues (Naetar et al., 2008). Expression of LAP2α has also been shown to initiate differentiation of pre-adipocytes into adipocytes by accumulation of

hypophosphorylated Rb (Dorner et al. 2006). Therefore, the nucleoplasmic A-type lamin-LAP2α complexes are predicted to control cell proliferation and also differentiation through the Rb pathway in early progenitor cells (Naetar et al., 2008). Mutations in LAP2α have been found in some cases of dilated cardiomyopathy (Taylor et al., 2005), although this disease is more commonly associated with mutations in the *LMNA* gene (see section 1.4).

Emerin is a 29 kDa INM protein, first identified as being encoded by a gene *EMD/STA* on the X chromosome, which when mutated causes X-linked Emery-Dreifuss muscular dystrophy (EDMD) (Bione et al., 1994). Emerin is located at the INM, with a nucleoplasmic N-terminus, containing the LEM domain and a C-terminal membrane spanning domain (Bione et al., 1994; Manilal et al., 1996; Wolff et al., 2001). There is evidence of emerin being at the ONM as well (Salpingiduo et al., 2007). The structure of the LEM domain of emerin has been solved by NMR and contains a small N-terminal helix and two large parallel α-helices similar to the LAP2-LEM domain (Wolff et al., 2001). The rest of the protein is disordered, suggesting interaction with multiple proteins. Emerin binds directly with all types of lamins, but preferentially interacts with lamin C (Vaughan et al., 2001). The precise function of emerin is unknown. However, it binds to transcription regulators BAF and GCL. BAF and GCL compete for binding with emerin at the same site and form complexes separately by binding to lamin A, and thereby suppress transcription (Lee et al., 2001; Holaska et al., 2003). BAF is required for assembly of emerin at the NE after mitosis (Haraguchi et al., 2001). To further demonstrate its regulatory role in transcription, emerin also interacts with a death promoting factor, BCL2-associated transcription factor (Btf) and splicing associated factor, YT521-B (Haraguchi et al, 2004; Wilkinson et al., 2003). Emerin may have a role in organization of NE architecture as well, through its interaction with several structural proteins, such as nuclear actin, lamins, nesprin-1 and nesprin-2 (Lattanzi et al., 2003; Mislow et al., 2002; Zhang et al., 2005; Bengtsson and Wilson, 2004). Emerin can stabilize nuclear actin and promote its polymerization and formation of a cortical network beneath the NE (Holaska et al., 2004).

Emerin is associated with X-EDMD (described in section 1.4). However, emerin deficient mice do not overtly show muscular dystrophy (Ozawa et al., 2006). Nevertheless, mouse embryonic fibroblasts (MEFs) lacking emerin show altered nuclear

20

shape and gene regulation, leading to apoptosis upon mechanical stimulation, demonstrating its potential role in altering mechano-sensitive transcriptional regulation in EDMD (Lammerding et al., 2005).

MAN1 is the third founding member of the LEM domain protein family, also known as LEMD3 (LEM domain containing protein 3) (Lin et al., 2000). MAN1 was initially identified as a NE protein detected by antibodies from a patient with collagen vascular disease (Paulin-Levasseur et al., 1996). MAN1 has two transmembrane domains that result in a topology where both the N- and the C-termini reside in the nucleoplasm (Wu et al., 2002). MAN1 interacts with lamin A/B1 and emerin at the INM (Mansharamani and Wilson, 2005). MAN1 and emerin have been demonstrated to have overlapping functions, in *C. elegans*, where RNAi mediated depletion of Ce-MAN1 alone is only lethal to 15% of embryos, however combined depletion of both Ce-MAN1 and Ce-emerin is lethal to all embryos, resulting in defects in chromosome segregation and cell division (Liu et al., 2003). MAN1 also binds transcriptional regulators GCL, BAF and Btf (Mansharamani and Wilson, 2005). MAN1 is the first INM protein found to have a role in signal transduction. In mammals and *Xenopus*, the C-terminal domain of MAN1 interacts with receptor–regulated SMAD (R-SMAD) and inhibits SMAD mediated transcriptional activity of transforming growth factor-β (TGF-β) and bone morphogenic protein (BMP), possibly by sequestering SMADs at the NE (Osada et al., 2003; Lin et al., 2005; Pan et al., 2005). Loss of function heterozygous mutations in MAN1 cause osteopoikilosis in humans, with hyperostotic bone and skin abnormality, and shows enhanced by TGF-β and BMP regulated gene expression (Hellemans et al., 2004). MAN1 deficient mice die during embryogenesis due to abnormal yolk-sac vascularisation, which is also linked to enhanced TGF-β activity (Ishimura et al., 2006; Cohen et al., 2007).

1.1.3.3   Other important NETs

Among other NETs are LAP1, nesprins and SUN proteins. Three isoforms of lamina associated polypeptide 1 (LAP1) have been described so far; LAP1A, LAP1B and LAP1C. LAP1 proteins remained poorly characterized but interact with all three types of lamins, with possible roles in anchoring the nuclear lamina to the NE (Foisner and Gerace, 1993). Nesprins and SUN proteins are described in section 1.5.

1.2 FUNCTIONS OF THE NUCLEAR LAMINA

The nuclear lamina, that includes both lamins and lamin-binding INM proteins, performs a multitude of functions within the nucleus. The fundamental function of the nuclear lamina is to give structural support to the nucleus. The lamina also maintains the size and shape of the nucleus, helps anchoring and spacing of NPCs and anchors INM proteins at the NE. In addition, recent research reveals further important roles of the lamina in anchoring and segregation of chromatin, NE assembly/disassembly at mitosis, DNA replication, mRNA transcription, apoptosis, maintaining cell polarity, nuclear positioning and migration during development (reviewed in Dechat et al., 2008). This wide variety of functions is possible due to the ability of lamins and their associated INM proteins to interact with a great number of nuclear proteins, thereby influencing most nuclear processes (Fig. 1.8).

1.2.1 Lamina maintains nuclear size and shape

The nuclear lamina is important in determining nuclear size and shape. For example, mouse spermatocytes have hook-shaped nuclei, due to expression of spermatocyte-specific lamin B3. Studies show that introduction of lamin B3 in somatic cells induces a change in the morphology of the nucleus to a hook shape (Furukawa and Hotta, 1993). Another study on *Lmna* knock-out mice revealed that nuclei of lamin A/C null mouse embryonic fibroblasts (MEFs) are morphologically compromised with elongated, irregular shapes and herniation of the NE (Sullivan et al., 1999). These findings stress the importance of the lamina in determining nuclear shape.

Lamins also control the size of the nucleus. Immunodepletion of lamins in cell-free nuclear assembly extracts derived from *Xenopus* eggs, results in formation of small fragile nuclei (Newport et al., 1990). Lamins therefore give strength to the NE and help resist deformation of the NE and are hypothesized to act as a geodesic dome, a cage-like structure protecting the chromatin (Hutchison, 2004).

1.2.2 Organization of the nuclear envelope

The lamina anchors NPCs at regular intervals at the NE. In *Drosophila*, reduction of lamin *Dm0* expression and, in *C. elegans*, RNAi mediated knock down of lmn-1 (both
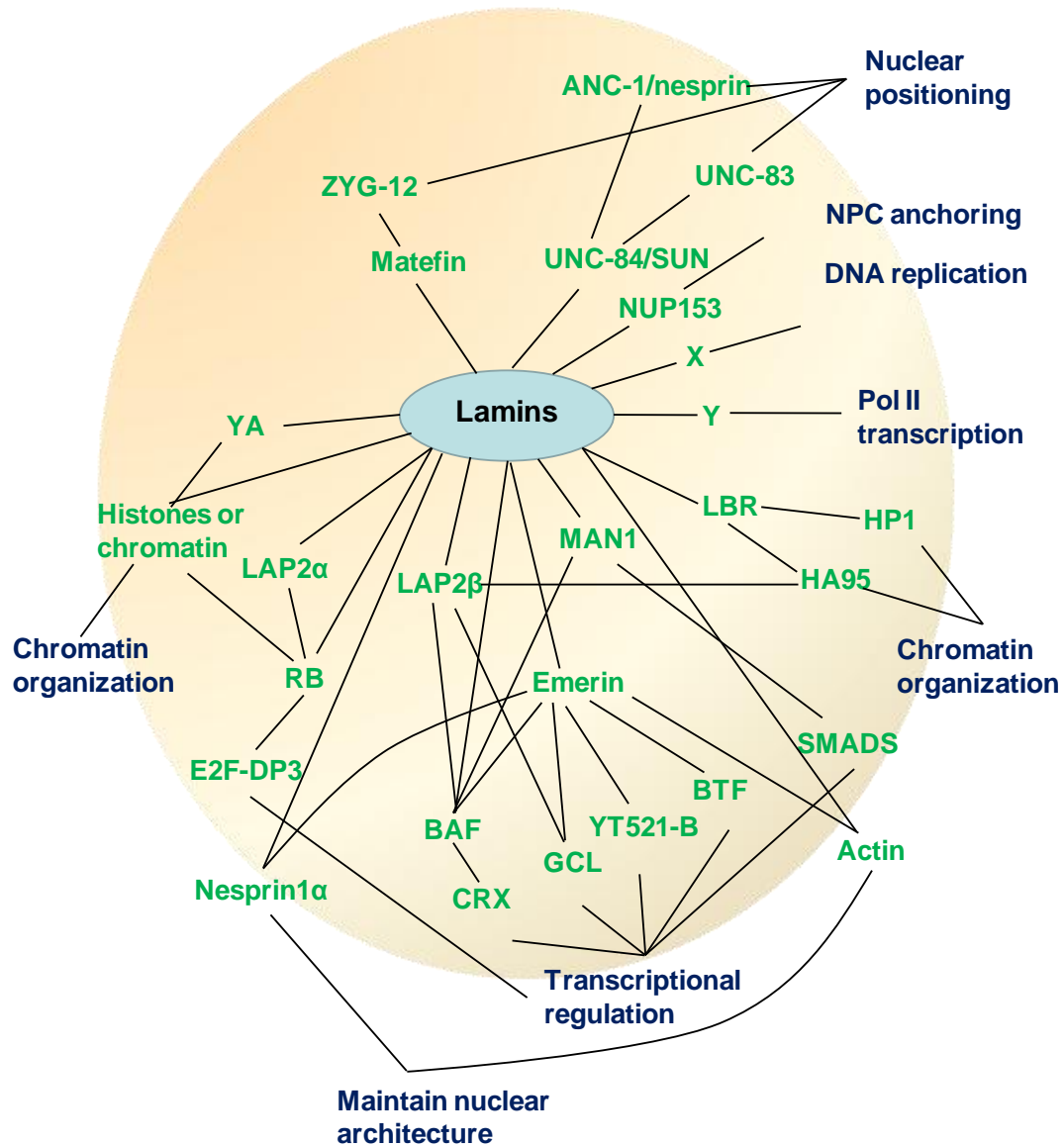
Fig. 1.8. Interactions between proteins of the nuclear lamina. Connecting lines indicate pairs of proteins that interact directly or indicate activities such as DNA replication that depend on lamins. X and Y represent unknown proteins. BAF, barrier-to-autointegration factor; BTF, BCL2-associated transcription factor; CRX, cone-rod homeobox; GCL, Germ cell-less; HP1, heterochromatin protein-1; Pol II, RNA polymerase II; RB, retinoblastoma protein; YA, young arrest. Adapted from Gruenbaum et al. (2005).

equivalent to vertebrate B-type lamin) causes the NPCs to float freely and cluster together within NE (Lenz-Bohme et al., 1997; Liu et al., 2000). In *Xenopus* egg extracts, lamin B3 has been shown to interact with nuclear pore complex protein Nup153 and thereby anchors and spaces the NPCs (Smythe et al., 2000). The lamina also recruits and anchors NETs at the INM, such as emerin. In lamin A null MEFs, emerin is mislocalized to the ER due to lack of anchoring function of the lamina (Sullivan et al., 1999). How the INM proteins are targeted to the INM is explained in more detail in section 1.3.

1.2.3 NE breakdown and assembly in mitosis

Nuclear lamins and INM proteins are involved in NE breakdown (NEBD) and reassembly during mitosis, but the exact mechanism is not known (reviewed in Margalit et al., 2005). In general, NEBD is triggered by phosphorylation events. Here, the principal mitotic kinase, cyclin dependent kinase 1 (Cdk1), phosphorylates lamins at the onset of mitosis, which prevents their interaction with each other and with chromatin, leading to depolymerization of the lamina (Peter et al., 1990, Heald and McKeon, 1990) and dispersal of lamins in the mitotic cells (Stick et al., 1988). Lamin B remains attached to the membrane vesicles during mitosis as it is permanently farnesylated, while lamin A/C become soluble in the cytosol (Gerace and Blobel, 1980). Several INM proteins, such as LBR and LAP1/2, are also phosphorylated by Cdk1 at the onset of mitosis, which in turn inhibits LAP2 binding to lamins (Courvalin et al., 1992; Foisner and Gerace, 1993). These phosphorylation events are thought to weaken the NE and lead to NEBD by vesicle formation (Alberts, 1994). More recently, in conjunction with this, mechanical tearing of the nuclear lamina through dyenin-mediated microtubule attachments to the NE is thought to aid in NEBD at mitosis (Beaudouin et al., 2002; Salina et al., 2001). It is hypothesized that after NEBD the NE membrane either vesicularizes to form vesicles that are distinct from the ER, or resorbs into the ER. Evidence of both these phenomena exists (reviewed in Margalit et al., 2005).

The NE and associated structures reassemble around chromosomes during anaphase and telophase, when the phosphorylated NE proteins become dephosphorylated. Time lapse microscopy of GFP-tagged INM proteins in HeLa cells revealed that INM proteins such as LAP2β, LBR and emerin localize to distinct regions of the condensed chromosomes

in anaphase, but by the end of telophase are uniformly distributed at the chromatin periphery. LBR and a small fraction emerin are identified before LAP2β at the chromosomal surface (Buendia et al., 2001; Chaudhary and Courvalin, 1993; Buendia and Courvalin, 1997; Haraguchi et al., 2000, Dechat et al., 2004). Shortly after LAP2β, lamin B is recruited on chromosomes during the anaphase-telophase transition, while lamin A is incorporated at the NE in early G1, after NE reformation by import through NPCs (Moir et al., 2000c). As B-type lamins bind membranes, they are targeted to chromosome with membranes. Also INM proteins located either in the membrane vesicles or the ER, bind chromatin. The NE membrane vesicles are thus assembled around chromosomes at the end of mitosis. Lamins are dephosphorylated at this stage and it is thought that lamin-lamin (presumably B-type) interactions form bridges that connect nuclear membrane vesicles to chromatin and thus mediate reassembly of the NE by membrane fusion (Lopez-Soler et al., 2001; reviewed in Goldman et al., 2002, Margalit et al., 2005). Studies show that in *Drosophila*, lamin mutation *Dm0* blocks NE assembly and produces annulate lamellae instead (Lenz-Bohme et al., 1997). Also, immuno-depletion of lamins prevents nuclear membrane formation, chromosome de-condensation and NPC assembly after mitosis (Burke and Gerace, 1986; Ulitzur et al., 1992); but a small amount of lamin protein, not the lamin network is enough to initiate NE formation (Lourim and Krohne, 1993). Therefore lamina breakdown and reassembly are important parts of NE breakdown and reformation during mitosis.

1.2.4 Chromatin organization and transcription

A considerable amount of chromatin in cells is transcriptionally repressed and is highly condensed. A large proportion of this heterochromatin, including centromeres and sometimes telomeres and the gene poor chromosomal regions, lies in close proximity to the nuclear lamina (Qumsiyeh, 1999). Studies have shown that positioning of chromatin in cells is not random but highly organized. For example, the inactive X chromosome lies near the NE but the active X chromosome is present in the nuclear interior (Kay and Johnston, 1973). Other studies, using fluorescence in situ hybridization, reveal that gene-rich chromosome 19 is situated in the interior of the cells while gene-poor chromosome 18 lies at the periphery of cells (Croft et al., 1999). Lamins can directly bind with DNA, histones and DNA crosslinking protein BAF (Stierle et al., 2003; Taniura et al., 1995; Holaska et al., 2003). Thus, the nuclear lamina is thought to be

involved in higher-order chromatin organization. Furthermore, cells lacking in A-type lamins show thinning or loss of heterochromatin at the nuclear periphery (Sullivan et al., 1999). Lamin interacting protein LBR interacts with HP1, LAP2β interacts with BAF and chromatin, emerin and MAN1 also interact with BAF (Ye et al., 1997; Furukawa, 1999; Furukawa et al., 1997; Lee et al., 2001; Mansharamani and Wilson, 2005) (section 1.1.3). It is thought that these direct or indirect interactions of lamins and associated proteins can anchor chromatin at the nuclear periphery and affect chromatin organization during interphase and therefore regulate gene activity (reviewed in Cohen et al., 2001; Goldman et al. 2002, Dechat et al., 2008).

Alteration in lamin expression level is correlated with changes in gene expression. For example, in *Xenopus*, lamin B1 expression is increased during the mid-blastula transition and lamin B2 expression is induced during gastrulation (Stick and Hausen, 1985; Benavente et al., 1985). In contrast, developmental studies in mice show that A-type lamins become expressed only during tissue differentiation (Rober et al., 1989). The precise function of lamins in transcription is not known. An increasing number of transcription factors have been found to localize at the nuclear periphery. For example, oct-1, a collagenase gene repressor, colocalizes with lamin B and acts as a transcriptional repressor only when located at the NE. Dissociation of oct-1 from the nuclear periphery causes an increase in collagenase expression (Imai et al., 1997). Transcriptional repression activity of Rb also correlates with its binding with laminA/C (Mancini et al., 1994; Ozaki et al., 1994). Lamin associated proteins such as LAP2β also interact with transcription factor GCL protein that is required for germ cell formation and over-expression of LAP2β alone or along with GCL represses E2F-DP regulated genes (Nili et al., 2001). Among other transcription factors that bind to lamins are sterol regulatory element binding protein 1 (SREBP1) involved in adipocyte differentiation (Lloyd et al., 2002) and zinc finger transcription factor MOK2 (Dreuillet et al., 2002).

Additional studies show that a dominant-negative mutant lamin, lacking the N-terminal domain, causes disruption of nuclear lamina organization and alters the distribution of basal transcription factors and thus inhibits synthesis of RNA polymerase II-dependent transcripts, in both mammalian cells and *Xenopus laevi*s embryonic nuclei (Spann et al., 2002). Therefore, it is postulated that lamins might act as a scaffold by interacting with transcription machineries for assembly or stabilization of transcription factors or, act as

a repository for transcription factors (reviewed in Goldman et al., 2002, Dechat et al., 2008).

1.2.5 DNA replication

Normal lamin organization is required for DNA replication. Studies show that lamin-depleted nuclei in *Xenopus* do not replicate their DNA, and mutant lamins lacking the N-terminal domain disrupt lamin organization and can block DNA synthesis, in both *Xenopus* nuclear extract and in mammalian cells (Newport et al., 1990; Spann et al., 1997; Ellis et al., 1997). Studies on *Xenopus* nuclear extracts suggest that lamins are required for initial formation of the DNA replication centres. It is thought that, by supporting the NE, a properly assembled lamina allows efficient transport and retention of replication factors and aids in DNA synthesis. However, maintenance and function of the replication centre is not dependent on lamins (Meier et al., 1991; Walter et al., 1998; Ellis et al., 1997).

Studies also demonstrate that, in mammalian cells, lamin A co-localizes with sites of nucleotide incorporation and lamin B co-localizes with proliferating cell nuclear antigen (PCNA) that is required for the elongation phase of DNA replication (Moir et al., 1994; Moir et al., 1995; Spann et al., 1997; Kennedy et al., 2000). Lamin mutant, ΔNLA, lacking the amino-terminal domain, when added in *Xenopus* nuclear extracts, can disrupt distribution of lamins to form nucleoplasmic aggregates. This also alters normal localization of PCNA and replication factor complex (RFC), which are found in the lamin aggregates. Moreover, lamin-disruption in *Xenopus* nuclear extracts also produces short replication products. Together, these demonstrate that lamins are required for the elongation phase of DNA replication (Spann et al., 1997; Moir et al., 2000a). It is thought that normal organization of the nuclear lamina is required to form part of a nucleoplasmic scaffold, which assembles the elongation factors involved in DNA synthesis (Moir et al., 2000b; reviewed in Goldman et al., 2002).

1.2.6 Apoptosis

The lamina also has a role in apoptosis. During apoptosis, or programmed cell death, nuclei go through morphological changes such as break down of the nuclear lamina through proteolytic cleavage, clustering of NPCs, detachment of chromatin from the NE and DNA cleavage (Thompson, 1998). These features are also reproduced in the nuclei

of lamin deficient cells. In *Drosophila*, lamin *Dm0* reduction causes clustering of NPCs and in *C. elegans*, reduction in *lamin-1*, results in altered nuclear shape, position of NPCs, and also chromatin detachment and condensation (Lenz-Bohme et al., 1997; Liu et al., 2000). Disruption of the nuclear lamina is an important step in the initiation and execution of apoptosis (Lazebnik et al., 1993; Steen and Collas, 2001). Both A- and B-type lamins are early targets that are cleaved by caspases during apoptosis, which leads to disassembly of the lamina and thereby inhibits vital nuclear functions (Lazebnik et al., 1993; Lazebnik et al., 1995; Takahashi et al., 1996). Expression of un-cleavable lamin mutants leads to failure of chromatin condensation, delays in DNA cleavage and thus slows the progression of apoptosis (Rao et al., 1996). Therefore, lamin degradation is critical for shutting down nuclear functions during apoptosis and the lamina might also provide the site of attachment for apoptotic signalling machineries (reviewed in Cohen et al., 2001, Goldman et al., 2002).

1.3   NUCLEAR ENVELOPE TARGETING OF PROTEINS

Integral membrane proteins are initially synthesized on ER-bound ribosomes and inserted into the ER membrane. They must then reach the INM and the model proposed to describe how this is achieved is known as the 'diffusion-retention model'. The proteins are thought to diffuse in the plane of the ER membrane to the ONM, then pass through the 'pore membrane domain' (POM) that connects the ONM and INM at the periphery of NPCs, to reach the INM (reviewed in Holmer and Worman, 2001) (Fig 1.9). It is thought that proteins are then retained in the INM by interaction with nuclear ligands, such as the lamina and/or chromatin or other nuclear proteins (Holmer and Worman, 2001). In support of this, experiments on the mobility of the GFP-fused LBR (LBR-GFP), by fluorescence recovery after photobleaching (FRAP), showed that most of the protein is immobilized at the NE; but a subpopulation of the LBR-GFP that remained in the ER, could diffuse freely (Ellenberg et al., 1997). However, studies revealed that only membrane proteins with a nucleoplasmic domain under 60 kDa can reach the INM by diffusing through the channel between POM and NPCs. Experiments demonstrate that while a chimera containing two copies of the LBR N-terminal domain (22.5 kDa) is able to localize to the INM, attaching a third copy of the amino terminus prevents accumulation at the INM (Soullam and Worman, 1995). This is likely to be

28
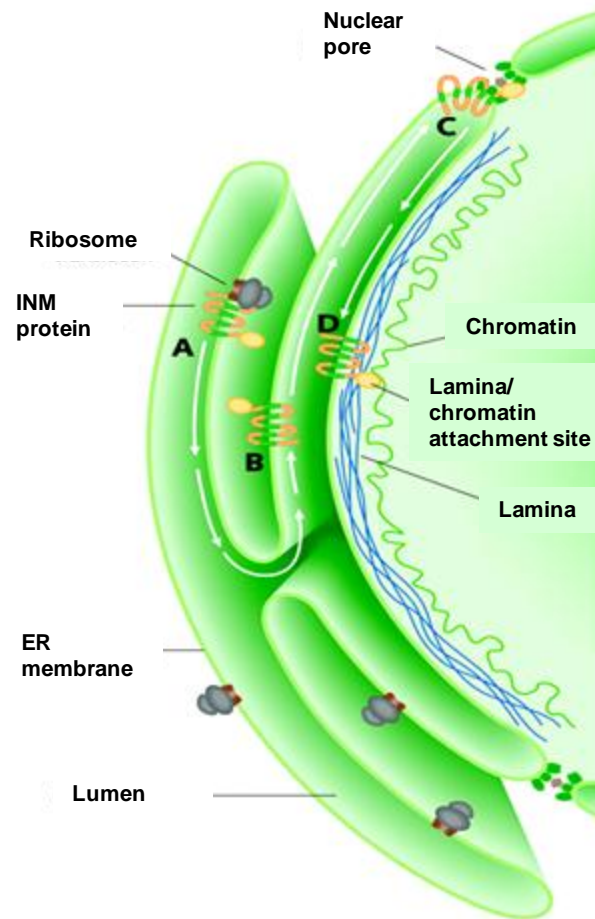
Fig. 1.9. Targeting and retention of inner nuclear membrane (INM) proteins at the NE. INM proteins are synthesized in the ER then translocated in the ER membrane (A) and thereafter reach the ONM (B) by diffusion. They then traverse the pore membrane (C) to reach the INM and are retained there by interacting with lamins or chromatin (D). Reproduced from Voeltz et al. (2002).

due to the increased size of the nucleoplasmic domain, but the exact size limit for passage from the ONM to the INM is not known.

Although it is thought that INM proteins contain a NE targeting signal, a consensus sequence has not been identified. Most integral proteins of the INM contain retention and targeting signals in their nucleoplasmic domain and in some cases the transmembrane domain (TMD) or C-terminal domain can target the protein to the INM (Soullam and Worman, 1995; Smith and Blobel, 1993; Holmer and Worman, 2001). Examples of NE targeting of INM proteins are described below.

LBR has two independent non-overlapping targeting signals for proper NE targeting to and retention at the INM, one at the N-terminus (1-191 aa) and one within the first TMD (201-246 aa) (Soullam and Worman, 1995; Smith and Blobel, 1993). The N-terminal domain of LBR is approximately 22.5 kDa and can concentrate in the nucleoplasm by binding with ligands in absence of TMDs. The N-terminus of LBR can also function as a nuclear localization signal (NLS) (it contains two stretches of amino acids that resemble the bipartite NLS of nucleoplasmin) that can actively target a 70 kDa soluble cytosolic protein to the nucleus. Interestingly, both the N-terminus and the first TMD of LBR can separately act as an inner nuclear membrane targeting signal, when attached to a type II integral protein of the plasma membrane. On the other hand, the NLS of other nuclear proteins such as nucleoplasmin or histone H1, cannot target type II integral proteins to the INM. These findings suggest that signals targeting a soluble protein to the nucleus differ from the signals that target membrane proteins to the INM (Soullam and Worman, 1993; Soullam and Worman, 1995).

The nucleoplasmic domain of LAP2 (aa 244-398, lacking the transmembrane segment) is sufficient for its targeting to the NE. LAP2 might also contain two independent regions in the nucleoplasmic domain for targeting to the NE (Furukawa et al., 1995). The NTD of emerin can concentrate within the nucleus, but unlike LBR, it cannot target soluble cytosolic proteins (>60kD) to the nucleus, which means it does not have a functional NLS. However, the NTD of emerin (aa 1-170) is sufficient to target a type II integral membrane to the INM (Ostlund et al., 1999), suggesting a different signal than the NLS for NE targeting of INM proteins. The entire N-terminus of MAN1 (aa 1-476) is necessary for efficient INM retention and can also target a chimeric type II integral

protein to this location. However, the transmembrane segment and the C-terminus of MAN1 by themselves do not mediate targeting to the INM (Wu et al. 2002).

Recent advances suggest a bimodal passage for INM proteins to the INM. In addition to the diffusion-retention model, active signal-mediated, energy-dependent targeting of INM proteins across the POM has been proposed by Ohba et al. (2004). The majority of INM proteins, including LBR, LAP1, LAP2β, emerin, MAN1 and LEM2, contain basic sequence motifs resembling a NLS-like sequence (Lusk et al., 2007). King et al. have shown that an NLS is important for passage of Heh2, an INM protein in *Saccharomyces cerevisiae*, across the POM. Heh2 is paralogue of mammalian MAN1 and LEM2. A Heh2 mutant lacking the NLS failed to accumulate at the INM (King et al., 2006). It is suggested that, like soluble nuclear proteins, INM proteins with an NLS-like sequence can be actively transported to the INM by the NPC. In this model, INM proteins share active transport machinery with soluble nuclear proteins (section 1.1.1.1). Here, the INM-cargo is recognized by a karyopherin or importin (Kapα/β1 pathway) and then this complex moves through the NPC by interacting with nucleoporins near the POM. Once inside the nucleus, the cargo is released by the Ran GTPase system (Lusk et al., 2007) (Fig 1.10). Studies on Heh proteins in yeast show that mutations in Kapα or Kapβ1 and the Ran GTPase system disrupt Heh protein targeting to the INM (King et al., 2006; Kutay and Muhlhausser, 2006).

As a result of these studies Lusk et al. proposed some "rules of the road" (Fig. 1.11). From current evidence they suggest that INM proteins with a nucleoplasmic domain less than 25 kDa follow the 'diffusion-retention' model to target to the NE. Conversely, INM proteins with a nucleoplasmic domain between 25-75 kDa may require an NLS-like sequence and are targeted to the NE by an active mechanism which requires changes in the nuceloporin interactions. In the case of proteins with a nucleoplasmic domain larger than 75 kDa, NE association of the protein would be required before post-mitotic NE assembly (reviewed in Lusk et al., 2007). Despite these advances, better understanding of the targeting of individual INM proteins is required to broaden our knowledge on the overall mechanism of NE targeting of INM proteins.
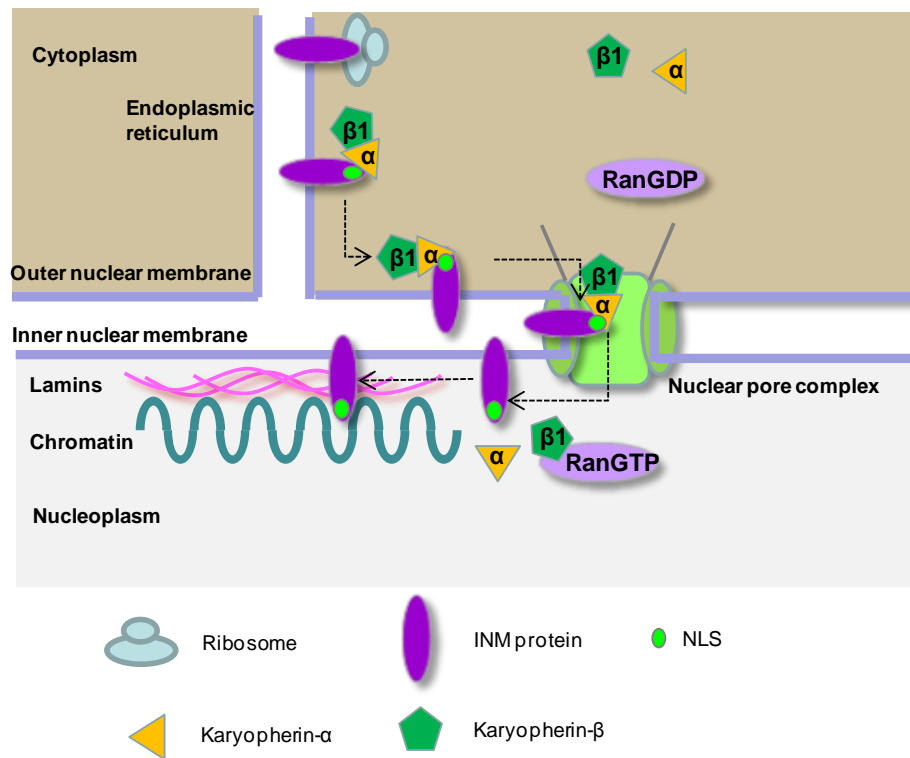
Fig. 1.10.   Receptor-mediated transport of proteins to the inner nuclear membrane. INM proteins are first inserted into the ER membrane. INM proteins containing a nuclear localization signal (green circle) (NLS) interact with a complex of two karyopherin proteins. Karyopherin-α (yellow triangle) recognizes the nuclear localization signal and afterwards, binding of karyopherin-β1 (green pentagon) with the nuclear pore complex actively mediates translocation of the INM protein to the nuclear side of the nuclear envelope. Within the nucleus, binding of Ran-GTP to karyopherin-β1 leads to the dissociation of the complex. The membrane proteins are then retained at the INM by interactions with chromatin or the nuclear lamina. Reviewed in Kutay and Muhlhausser (2006).
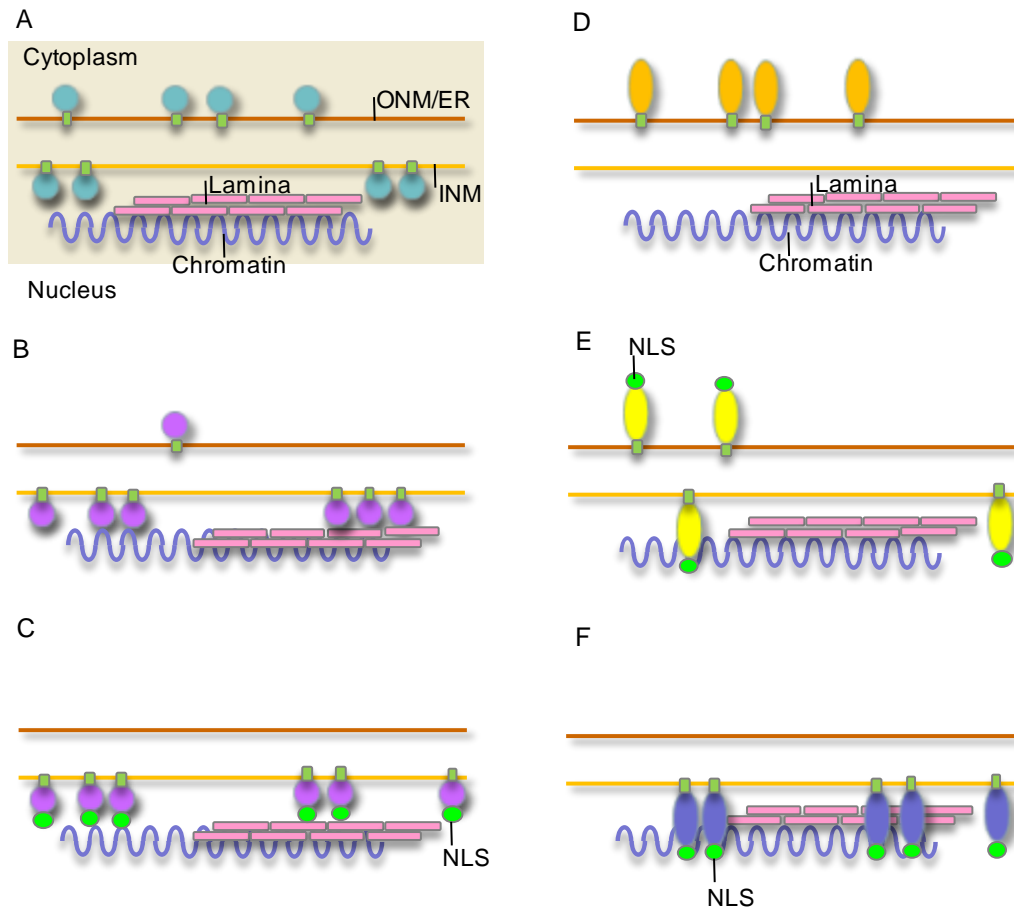
Fig. 1.11. Rules for nuclear envelope membrane proteins targeting.

Rule **A, Diffusion**: Membrane proteins containing extralumenal domains of <~25 kD can diffuse throughout endoplasmic reticulum (ER), and can localize to both the inner nuclear membrane (INM) and the outer nuclear membrane (ONM)/ER.

Rule **B, INM retention**: Membrane proteins containing extralumenal domains of <~25 kDa can access the INM by diffusion. However, at the INM, they are retained by interactions with the nuclear matrix (Diffusion-retention model).

Rule **C, Nuclear-localization signal (NLS)**: Membrane proteins containing extralumenal domains <~25 kDa, with a NLS can access the INM by diffusion. They can also be actively imported by the karyopherin mediated pathway through the nuclear pore complex and subsequently concentrate at the INM.

Rule **D, Extralumenal domain >~25 kDa.** Membrane proteins containing extralumenal domains of >~25 kDa cannot diffuse across the pore membrane properly, and therefore localize to the ONM/ER.

Rule **E, Extralumenal domain ~25–75 kDa with low affinity NLS.** Membrane proteins with extralumenal domains between ~25–75 kDa having low-affinity NLS can use the karyopherin mediated pathway across the POM. However, the protein might access the INM, but is not localized only to the INM, but also found in the ONM/ER.

Rule **F, Extralumenal domain ~25–75 kDa with a high-affinity NLS and/or retention.** Due to high affinity for karyopherin-α the NLS of this type membrane protein is sufficient to mediate exclusive INM localization. Also, a membrane protein with a low-affinity NLS could be retained at the INM by interacting with different the nuclear architecture, such as lamina or chromatin. Reviewed in Lusk et al., 2007.

1.4   LAMINOPATHIES AND NUCLEAR ENVELOPATHIES

Diseases associated with components of the nuclear lamina are known as laminopathies, but the term nuclear envelopathies has arisen due to more recent identification of mutations in other NE proteins. Around 24 diseases are linked to mutation of lamina and NE proteins and half of these laminopathies arise due to mutation of the *LMNA* gene alone (Fig. 1.12 and Table 1.2). Laminopathies affect mainly mesenchymal tissues and can be grouped as following: diseases of striated muscle, lipodystrophy syndromes, peripheral neuropathy and accelerated aging disorders. The laminopathies have been the subject of many review articles, but good general reviews include those of Burke and Stewart (2006) and Worman and Bonne (2007).

1.4.1 Laminopathies affecting striated muscle

Over 200 mutations in *LMNA* have been found to cause laminopathies affecting striated muscle (Burke and Stewart, 2006; http://www.umd.be). The first mutations in *LMNA* gene were identified in autosomal dominant Emery-Dreifuss muscular dystrophy (AD-EDMD) (Bonne et al., 1999). *LMNA* mutations are also responsible for rare cases of autosomal recessive EDMD (Raffaele Di Barletta et al. 2000). X-linked EDMD is associated with emerin mutations, which was the first disease found to be associated with an integral membrane protein of the NE (Bione et al., 1994; Manilal et al., 1996). The association of both lamin A/C and emerin with the EDMD pathology suggests that these proteins work in similar pathway in this disease and are important in muscle.

EDMD is characterized by early contracture of elbows, ankles and posterior neck, slowly progressive skeletal muscle weakness and wasting in a scapulohumero-peroneal distribution, and dilated cardiomyopathy with cardiac conduction defects. The symptoms start in early childhood (<15 years) and there is cardiac involvement by age 30. Patients die due to sudden heart block and progressive heart failure in X-EDMD, the sudden cardiac death can be prevented with insertion of a pacemaker (Emery, 1989; Emery, 2000). In case of AD-EDMD the muscle involvement and contracture is similar to X-EDMD, but more prominent (Wehnert and Muntoni, 1999). AD-EDMD can present variably as late onset mild disease or with more severe early presentation (Helbling-Leclerc et al., 2002). AD-EDMD patients often have more severe cardiac
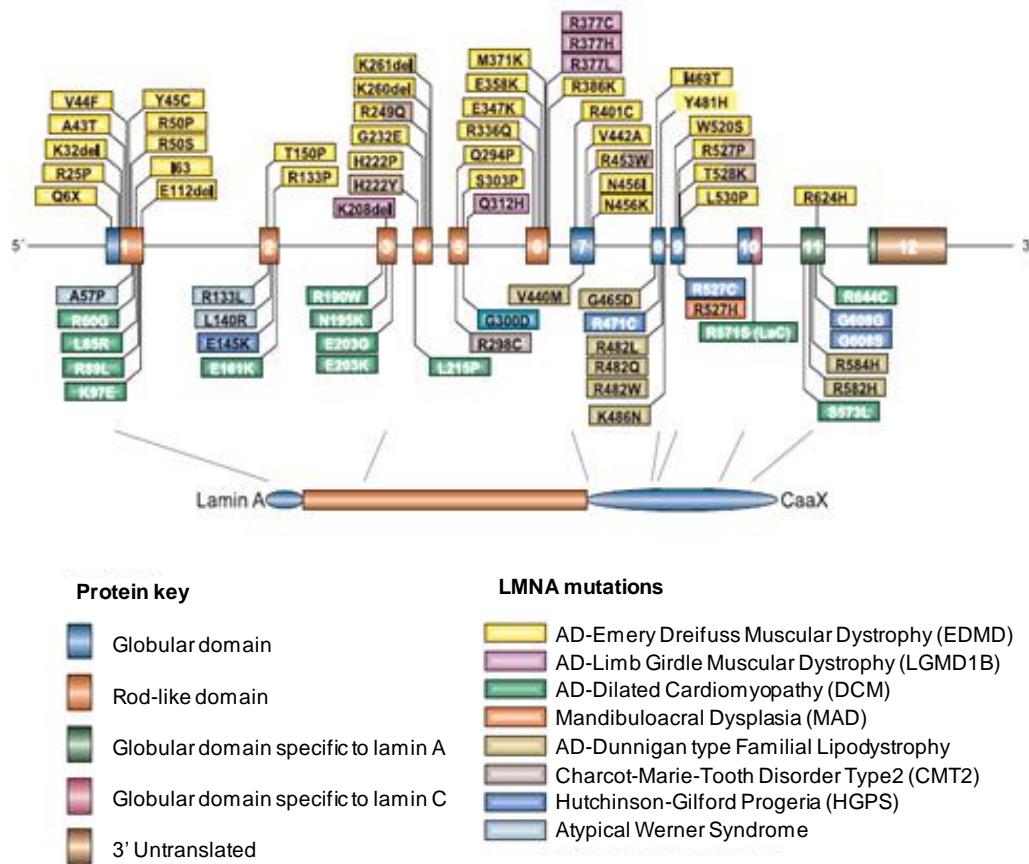
Fig. 1.12. Specific mutations in *LMNA* are associated with different diseases.
Schematic diagram of the *LMNA* gene showing positions of identified mutations and the
disease with which they are associated. Mutations affecting striated muscle are
generally distributed throughout the gene. The majority of the mutations that result in
mandibuloacral dysplasia, Dunnigan-type familial partial lipodystrophy and
Hutchinson-Gilford progeria syndrome are found in exons encoding the C-terminal
domain of *LMNA* gene. Adapted from Burke and Stewart (2006).

phenotype than X-EDMD and manifest as cardiomyopathy with ventricular dysfunction which is improved with insertion of a defibrillator (Meune et al., 2006).

LMNA mutations are also found in dilated cardiomyopathy conduction defect type 1 (DCM-CD1) (Fatkin et al., 1999) and limb girdle muscular dystrophy type 1B (LGMD 1B) (Muchir et al., 2000). Patients with DCM-CD1 have a cardiac conduction defect similar to that seen in EDMD but have little, if any, skeletal muscle involvement. On the other hand, patients with LGMD-1B have less cardiac involvement and tendon contracture and different pattern of muscle wasting. Hence, these diseases are considered as variants of same disease with cardiomyopathy and variable skeletal muscle involvement (reviewed in Worman et al., 2009). Even members of same family with the same *LMNA* mutation have been reported to have different manifestation of the disease, either DCM alone or together with EDMD-like symptoms or LGMD-like symptoms (Brodsky et al., 2000; Bonne et al., 2000).

Intriguingly, *Lmna*$^{-/-}$ mice also exhibit muscular dystrophy and cardiomyopathy. These mice appear normal until birth and then, within 2-3 weeks, the growth rate slows and the mice die prematurely at 6-7 weeks after birth due to muscular dystrophy and cardiomyopathy (Sullivan et al., 1999). This shows that A-type lamins are not essential for embryogenesis but are necessary for maintaining specific tissues in adults. To date, around 60% of the laminopathies are comprised of diseases affecting striated muscle. However, only 50% of patients with EDMD have mutation in either *LMNA* or *EMD* genes. Therefore, in about half of the patients, other genes are likely to be involved and any lamin or emerin binding proteins are likely candidates in this instance (reviewed in Burke and Stewart, 2006). Nesprin-1 and -2 mutations have also been found to be associated with EDMD in a few individuals (Zhang et al., 2007b).

1.4.2 Laminopathies affecting adipose tissues

Mutations in *LMNA* have been identified in Dunnigan-type familial partial lipodystrophy type 2 (FPLD2). A missense mutation of arginine 482 to tryptophan is the most common mutation causing FPLD2 (Shackleton et al., 2000; Cao and Hegele, 2000). Approximately 90% of the mutations causing FPLD are located in exon 8 that encodes part of the immunoglobulin (Ig)-fold structure in the lamin A CTD (Fig. 1.12) (reviewed in Worman et al., 2009). FPLD is an autosomal dominant disorder and is

more common in females. Patients have normal fat distribution at birth, but around puberty they develop loss of subcutaneous white adipose tissue from the extremities and accumulation of fat in the face and neck, with possible hormonal influence (Dunnigan et al, 1974). These patients also have insulin resistance that frequently leads to type II diabetes and hyperlipidemia (Hegele 2001).

1.4.3 Laminopathies affecting axonal myelination

An autosomal recessive *LMNA* missense mutation, R298C, has been found in patients with Charcot-Marie-Tooth disease type 2b, a peripheral neuropathy (De Sandre-Giovannoli et al., 2002). These patients have areflexia in the lower limbs, weakness and wasting of the distal lower limb muscles due to loss of enervation, motor deficit and loss of large myelinated nerves (Chaouch et al., 2003). Interestingly, in the *Lmna* null mice, neurons of the sciatic nerve also manifest demyelination (De Sandre-Giovannoli et al., 2002).

1.4.4 Progeria

Progeria was first described by Hutchinson and Gilford (Hutchinson, 1886; Gilford and Shepherd, 1904). Hutchinson-Gilford progeria syndrome (HGPS) is a very rare form of multi-system disorder, mainly caused by mutation in the *LMNA* gene. Rare cases of HGPS can also result from mutations of *ZMPSTE24,* involved in post-translational modification of the C-terminus of lamin A (section 1.1.2.3) (reviewed in Worman and Bonne, 2007). Children with HGPS show features of premature ageing. They exhibit retarded growth, reduced subcutaneous fat, alopecia, micrognathia and osteoporosis. Most affected patients die at age 12 to 15 years due to atherosclerosis, resulting in myocardial infarction or stroke (Sarker and Shinton, 2001). The most common mutation causing HGPS is a dominant point mutation, G608G, which creates an abnormal splice donor site within exon 11 of the lamin A mRNA resulting in an in-frame internal deletion of 50 amino acids close to the C-terminus of prelamin A. However, lamin C is unaffected (Eriksson et al., 2003; De Sandre-Giovannoli et al., 2003). The mutant prelamin A, called progerin or lamin A Δ50, undergoes normal farnesylation and carboxymethylation at the C-terminus (section 1.1.2.3). However, the final cleavage of prelamin A to mature lamin A, catalyzed by ZMPSTE24, does not occur (Fig. 1.6), as the site of cleavage is deleted by the mutation. Thus, progerin remains permanently

farnesylated and accumulates at the NE with toxic effects on the cells (Goldman et al., 2004; Dechat et al., 2007). *LMNA* mutation V607V results in frequent use of the exon 11 splice donor site (similar to typical HGPS patient) and causes severe progeria, with higher levels of progerin than wild type lamin A (Moulson et al., 2007). Compound heterozygous mutations in lamin A (T528M and M540T) can also cause progeroid syndromes. However, accumulation of prelamin A at the NE is not a feature in these subjects (Verstraeten et al., 2006). Dominant mutations S143F, E578V and E145K cause milder forms of progeria and also are not thought to result in farnesylated lamin A accumulation (Eriksson et al., 2003, Kirschner et al., 2005; Csoka et al., 2004). Therefore, permanent farnesylation of lamin A may not be the only cause of progeria.

Similar to striated muscle disease, different mutations result in a spectrum of progeroid disease phenoptype, with severe restrictive dermopathy at one end and milder mandibulo-acral dysplasia at the other end (reviewed in Smallwood and Shackleton, 2010). Mutations in either *ZMPSTE24* or *LMNA* can cause restrictive dermopathy (RD), a perinatal-lethal progeroid syndrome. These patients have tight skin, loss of fat, prominent superficial vessels, sparse hair and joint contracture (Navarro et al., 2004; Navarro et al., 2005; Moulson et al., 2005; Shackleton et al., 2005; Moulson et al., 2007). Loss of ZMPSTE24 causes accumulation of farnesylated prelamin A, as shown in ZMPSTE24 deficient mice. It is the most severe form of progeria due to complete absence of mature lamin A (Bergo et al., 2002; Pendas et al., 2002).

A rare autosomal recessive disorder mandibulo-acral dysplasia (MAD) is caused by missense mutations in the C-terminal domain of lamin A/C (Novelli et al., 2002). The homozygous mutation R527H accounts for 94% cases of MAD. These patients have fat redistribution and metabolic alteration similar to lipodystrophy. Moreover, they show skeletal defects in craniofacial region, terminal digits and clavicles reminiscent of those exhibited by patients with premature ageing disorders (Simha et al., 2003). MAD can also be caused by ZMPSTE24 mutations that are thought to result in the milder phenotype due to residual ZMPSTE24 activity (Agarwal et al., 2003).

1.4.5 Other nuclear envelopathies

Apart from lamin A, few other NE components had also been found to be associated with disease. In addition to emerin and nesprins described above, *LBR* mutations cause

Greenberg skeletal dysplasia, *MAN1* mutations cause osteopikilosis and *LMNB2* mutations cause acquired partial lipodystrophy (reviewed in Worman et al., 2009) (Table 1.2).

1.4.6 Laminopathy disease mechanisms

Since the emergence of the family of laminopathy diseases, scientists have been curious to understand how ubiquitously expressed lamin A/C give rise to such distinct tissue-specific diseases. Laminopathies are postulated to result from three different mechanisms. First, is the 'structural/mechanical stress' hypothesis, where mutant laminA/C and NE proteins weaken the mechanical stability of the nuclear envelope thereby leading to cell damage and death. Second, is the 'gene expression' hypothesis, where mutations in laminA/C or other specific NE proteins alter the specific attachment sites for various gene regulatory proteins, thus causing defects in gene expression patterns. The toxic effect of farnesylated lamin A in progeria is a third more specific mechanism (reviewed in Mounkes et al., 2003; Wilson et al., 2001; Cohen et al., 2001; Hutchison and Worman, 2004, Worman et al., 2010).

1.4.6.1 Mechanical stress hypothesis

According to the mechanical stress hypothesis, mutations in lamin A/C, emerin and nesprins affect the structural integrity of the nucleus, which results in physical weakness of the NE and reduced ability to withstand mechanical force. This mechanism is likely to account for mainly diseases of striated muscles due to the forces experienced by muscle cells upon muscle contraction. Mutations causing muscular dystrophy and DCM are located throughout the *LMNA* gene and many of these mutations that are mainly located in the coiled-coil domain are proposed to disrupt assembly and incorporation of lamin A/C into the lamina (reviewed in Cohen et al., 2008). Studies with EDMD *LMNA* mutants (N195K, E358K, M371K, R386K,) demonstrate formation of intranuclear foci, accompanied mislocalization of some of the endogenous lamins and decreased localization of the mutant lamins to the nuclear periphery (Ostlund et al., 2001; Holt et al., 2003). Similarly, another study showed that *LMNA* mutants L85R and L530P modify the assembly of the lamina (Raharjo et al., 2001). Some of these mutations (for example N195K, E358K, M371K and mainly lamin A CTD mutants R386K, R453W, R527P, W520S and L530P) cause redistribution of NE proteins, such as emerin, to the

Disease	Mode of inheritance	*LMNA* or other defects	Effects on protein	Clinical phenotype
Striated Muscle diseases				
Emery-Dreifuss muscular dystrophy	Autosomal dominant	*LMNA* mutations detected in every exon except 12, most are missense	Misfolding or failure to assemble lamina, leading to partial or complete loss of function	Slowly progressive contractures and muscle weakness, wasting of skeletal muscle and cardiomyopathy with conduction defects
Emery-Dreifuss muscular dystrophy	Autosomal recessive	One reported case, *LMNA* mutation H222Y	Unknown	Slowly progressive contractures and muscle weakness, wasting of skeletal muscle and cardiomyopathy with conduction defects
Dilated cardiomyopathy type 1A	Autosomal dominant	More than 20 *LMNA* mutations described, usually missense mutations in exon 1 to 3	Unknown; head and rod domains usually affected –likely to affect polymerization	Ventricular dilatation, impaired systolic contractility, arrythmias, conduction defects, minimal or no skeletal muscle involvement
Limb-girdle muscular dystrophy type 1B	Autosomal dominant	Six *LMNA* mutations described, three of which are missense	Unknown	Slowly progressive shoulder and pelvic muscle weakness and wasting; later development of contracture and cardiac disturbances
X-linked EDMD	X-linked	Several missense and nonsense mutation in *EMD*	Loss or reduction of function of emerin	Muscle weakness and wasting in scapulo-humeral peroneal distribution; early contracture and dilated cardiomyopathy
Peripheral neuropathy				
Charcot-Marie-Tooth disorder type 2B1	Autosomal recessive	Homozygous R298C missense *LMNA* mutation	Rod domain affected; could affect lamin binding interactions	Lower limb motor deficits, walking difficulty, lower limb areflexia

Table 1.2 Laminopathy genetics and phenotypes. (Adapted from Capell and Collins, 2006 and Worman et al., 2009)

Disease	Mode of inheritance	*LMNA* or other defects	Effects on protein	Clinical phenotype
Partial lipodystrophy syndromes				
Familial partial lipodystrophy, Dunnigan type	Autosomal dominant	*LMNA* missense mutations cluster in exon 8 and 11, most are in codon 482 of exon 8	Globular domain affected; no effect on three dimensional structure, but protein interactions could be altered	Loss of adipose tissue in the trunk and limbs with concomitant accumulation in the neck and face; insulin resistance diabetes, hypertriglyeridemia and increased susceptibility to atherosclerosis
Acquired partial lipodystrophy	Sporadic	*LMNB2*	unknown	Progressive lipodystrophy with phenotype similar to FPLD
Progeria				
Hutchinson-Gilford progeria syndrome	*De novo* mutations, dominant or recessive	90% cases due to C to T change at codon 608 in exon 11 of *LMNA,* activating a cryptic splice site	Creates permanently farnesylated 'progerin' protein with 50 internally deleted amino acids near the C-terminus	Premature aging including alopecia, loss of subcutaneous fat and premature atherosclerosis; death in early teens
Atypical Werner syndrome or mild progeria	Autosomal dominant	*LMNA* missense mutations, three reported A57P, R133L and L140R	Unknown; interactions with other proteins may alter	Premature aging in the second decade, cataract, premature atherosclerosis, hair greying
Mandibulo-acral dysplasia	Autosomal recessive usually; one compound heterozygous reported	*LMNA*, R527H most common mutation, K542N, A529V and heterozygous R527H/R471C also reported	Unknown; mutation affect surface of the C-terminal domain of lamin A/C; protein interactions could be affected	Delayed closure of cranial sutures, dental crowding, short stature, lipodystrophy, joint contractures, hypoplasia of mandible and clavicle, acro-osteolysis, alopecia and insulin resistance

Table 1.2 Laminopathy genetics and phenotypes (continued). (Adapted from Capell and Collins, 2006 and Worman et al., 2009)

Disease	Mode of inheritance	*LMNA* or other defects	Effects on protein	Clinical phenotype
Progeria				
Restrictive dermopathy	*De novo* mutation in *LMNA* or recessive null mutation in *ZMPSTE24*	Splicing mutations leading to partial or complete loss of exon 11 in *LMNA*; homozygous or heterozygous mutations in *ZMPSTE24*	*LMNA* mutation results in prelamin A with deletion*; ZMPSTE24* mutations lead accumulation of prelamin A	Intra uterine growth retardation, tight skin, loss of fat, prominent superficial vasculature, joint contracture, dysplastic clavicle, sparse hair, perinatal lethal
Other diseases				
Pelger-Huet anomaly/HEM-Greenberg skeletal dysplasia	Autosomal dominant/recessive	*LBR* mutations		Pelger-Huet anomaly: benign blood disorder of hypo segmented nuclei; HEM: lethal in utero with fetal hydrops, short limb skeletal dysplasia
Adult-onset autosomal dominant leukodystrophy	Autosomal dominant	Mutation in *LMNB1*		Myelin loss from central nervous system, phenotype similar to chronic progressive multiple sclerosis
Osteopikilosis, Buschke-Ollendorff syndrome, Melorheostosis	Autosomal dominant	Mutations in *MAN1*	Loss of function of MAN1	Hyperostosis of cortical bone; sclerosis of adjacent soft tissue, dermatofibrosis
Autosomal recessive cerebellar ataxia	Autosomal recessive	Mutations in *Nesprin1/SYNE 1*	Unknown	Dysarthria and ataxia; brisk lower extremity tendon reflexes

Table 1.2 Laminopathy genetics and phenotypes (continued). (Adapted from Capell and Collins, 2006 and Worman et al., 2009)

ER (Ostlund et al., 2001; Raharjo et al., 2001; Holt et al., 2003). Together these lamin A mutants can result in weakening of the NE. Notably, *Lmna* deficient mice develop EDMD phenotype and lamin A/C null nuclei also exhibit a similarly compromised NE (Sullivan et al., 1999). Also, knock-in *Lmna* H222P homozygous mice develop EDMD similar to the human disease (Arimura et al., 2005). Therefore, partial loss of A-type lamins or expression of dominant negative variants results in a structurally compromised NE. Since contractile skeletal and cardiac muscle and vascular smooth muscle are subjected to mechanical stress, NE fragility in these tissues may lead to cell damage and muscle disease pathology.

Studies with MEFs obtained from *Lmna* deficient mice demonstrates decreased nuclear stiffness, lowered bursting force and isotropic deformation of nuclei upon application of force, indicative of impaired nuclear and cytoskeletal connection (Broers et al., 2004). *Lmna* deficiency in *Lmna*$^{-/-}$ MEFs also disrupts cellular migration and nuclear positioning (Lee et al., 2007; Houben et al., 2009). Other studies revealed that *Lmna* deficient MEFs exhibit defective mechanotransduction or mechanically activated gene transcription and impaired viability under mechanical strain. These cells die due to increased apoptosis and necrosis following mechanical stress (Lammerding et al., 2004). Together, these findings suggest that abnormalities in the nuclear lamina may perturb cytoskeletal functions, with possible mechanical vulnerability of the whole cell. However, although lamin A/C mutations physically weaken the NE, it does not explain the muscle pathologies completely. Emerin null mice do not exhibit nuclear fragility; however, they are prone to apoptosis following mechanical strain (Lammerding et al., 2005). Therefore, multiple mechanisms may account for these pathologies, including defects in mechanical signal transduction.

1.4.6.2 Gene expression hypothesis

The second explanation for laminopathy mechanisms is the gene expression hypothesis. Lamins interact either directly or indirectly, with many chromatin associated proteins, transcription factors and transcription regulatory factors. Therefore, lamins are thought to contribute to regulation of gene expression and it is possible that alteration in gene expression could account for the phenotypes observed in some laminopathies (reviewed in Mounkes et al., 2003; Cohen et al., 2008). In support to this, emerin, responsible for

X-EDMD, also interacts with various transcription factors, such as BAF, Btf, GCL and YT521-B (Holaska and Wilson, 2006). Emerin can regulate import of transcriptional co-activator, β-catenin, into the nucleus and β-catenin has been found to accumulate in the nucleus in fibroblasts from patients with *EMD* mutation, which might affect downstream gene expression (Markiewicz et al., 2006).

Emerin is redistributed to the ER in cells lacking lamin A/C and also in cells expressing some lamin A/C mutants, such as L530P (Sullivan et al., 1999, Ostlund et al., 2001; Raharjo et al., 2001), whereas most emerin mutations in X-EDMD are effectively null. Therefore reduction of emerin level at the NE could contribute to both AD-EDMD and X-EDMD. In regenerating muscle of *EMD* deficient mice and human EDMD muscle, upregulation of pRb-MyoD pathway components and delay in induction of myogenic genes have been observed. Therefore, disruption of laminA/C and emerin localization may destabilize pRb complexes, which result in upregulation of pRb and MyoD target genes and, cause defects in muscle regeneration in muscular dystrophies (Melcon et al., 2006; Bakay et al., 2006).

Other studies in different laminopathies also support the gene expression hypothesis. General loss of peripheral hetechromatin is a feature of MAD, FPLD, HGPS and *Lmna*$^{-/-}$ MEFs (Filesi et al., 2005; Capanni et al., 2003; Goldman et al., 2004; Sullivan et al., 1999). In addition, in HGPS, mislocalization of NPCs is observed, which might impair trafficking of mRNA and proteins (Goldman et al., 2004). Alterations in epigenetic modification (such as histone methylation) regulating the heterochromatin, is also observed in HGPS and MAD (Scaffidi and Misteli, 2005; Filesi et al., 2005). Therefore, according the gene expression hypothesis, all these abnormalities may lead to various transcriptional irregularities in cells (reviewed in Capell and Collins, 2006).

Effect of *LMNA* mutations on gene regulation may also depend on their position on the gene, and the specific protein binding that are affected. The adipocyte transcription factor SREBP1 binds to the C-terminus of A-type lamin, where the most common FPLD mutation lies. SREBP1 interaction with lamin A/C is reduced by FPLD, R482W mutation (Lloyd et al., 2002). Expression studies show that R482W mutation does not disrupt lamina assembly (Raharjo et al., 2001). However, in FPLD, prelamin A is found to be accumulated in cells. Prelamin A located at the NE, binds and is co-localized with

SREBP1. It is thought that prelamin A sequesters SREBP1 at the NE, which decreases the pool of active SREBP1 and this in turn reduces expression of peroxisome proliferator activated receptor gamma 2 (PPARγ2) and results in impaired pre-adipocyte differentiation (Capanni et al., 2005). Therefore, the lamina affects gene regulation in many different ways and its perturbation may give rise to different laminopathies.

1.4.6.3 Progeria disease mechanisms and potential therapies

Since *ZMPSTE24* deficient mice have progeria (ZMPSTE24 enzyme responsible for processing prelamin A, section 1.1.2.3), it is hypothesized that accumulation of farnesylated prelamin A or progerin at the NE, may be the culprit in progeria (Fong et al., 2004). Farnesylated prelamin A or progerin have been shown to produce toxicity in cells, leading to abnormal nuclear morphology. This includes misshapen nuclei and blebbing that results in loss of lamin A/C from the nucleoplasm, which could affect the scaffolding functions of lamins (Goldman et al., 2004). The nuclear lamina is thickened in HGPS cells (Goldman et al., 2004), which also displays increased nuclear stiffness and reduced deformability (Dahl et al., 2006; Verstraeten et al., 2008). Farnesyltransferase inhibitors (FTIs) have been proposed for use in treating progeria, as they have been shown to reverse some of the defects in HGPS cells, including nuclear deformation (Yang et al., 2005; Toth et al., 2005; Capell et al., 2005; Verstraeten et al., 2008). FTIs treatments also improved phenotype of mouse models of progeria with either *ZMSPTE24* deficiency or targeted HGPS mutation. Animals treated with FTIs showed improved survival, body weight, reduced rib fracture as well (Fong et al., 2006; Yang et al., 2006). Therefore, FTIs are currently been tested in trials in children with HGPS (Kieran et al., 2007).

However, accumulation of farnesylated prelamin A in progeria does not entirely explain the disease pathogenesis. Expression of a nonfarnesylated variant of progerin can still cause a progeroid syndrome in mice (Yang et al., 2008). Therefore, alteration of A-type lamins, possibly the internal deletion of amino acids or the presence of extreme C-terminal residues, rather than the accumulation of farnesylated form of prelamin A can also lead to progeroid phenotype (reviewed in Smallwood and Shackleton, 2010). Reduced cell proliferation and premature cell senescence are the major features of HGPS phenotype (Goldman et al., 2004). Several other studies also suggest that defects

in DNA repair, accumulation of DNA damage and altered gene expression, thus genome instability may be the cause of progeria (Hasty et al., 2003; Liu et al., 2005; Liu et al., 2006). The exact cause of genome instability in progeria is not clear, but is possibly due to increased sensitivity of HGPS cells to DNA damage (Liu et al., 2005). Of note, FTI treatment does not reduce defects in DNA damage repair (Liu et al., 2006). In addition, disorganization of peripheral heterochromatin, increased telomere shortening and mitotic defects are also observed in progeria (Goldman et al., 2004; Huang et al., 2008; Cao et al., 2007). Therefore, multiple mechanisms are involved in the pathogenesis of progeria. More studies are still needed in our understanding of these disease mechanisms and their treatments.

1.5   NUCLEAR POSITIONING AND NUCLEO-CYTOPLASMIC BRIDGING PROTEINS

The nucleus and cytoplasm need to communicate with each other for various cellular functions to proceed, most notably nuclear positioning and migration. Over many years, various observations have led to the conclusion that the NE and cytoskeleton are linked. Therefore, NE proteins may play major roles in providing this structural communication and interplay with the cytoskeletal proteins to control nuclear positioning and migration.

1.5.1 Cytoskeletal Proteins

Cytoskeletal (CSK) proteins are structural proteins that help in maintaining cell shape in various cell stages and play a crucial role in the intracellular movement of organelles and proteins. There are three types of CSK filaments: intermediate filaments (IF), microtubules (MT) and actin filaments (Alberts et al., 2007). Cytoplasmic intermediate filaments form an extensive network in the cytosol around the nucleus. There are six different types of intermediate filaments with cell-type specific expressions, among them are vimentin, keratin, desmin, neurofilament and nuclear lamins. As already discussed, nuclear lamins are found in all nucleated cell types. The remaining IFs are located within the cytoplasm. These filaments act mainly to resist mechanical stress in cells. Cytoplasmic IFs are further strengthen by crosslinking proteins such as plectin. Plectin crosslinks IFs to each other and also to MTs and actin filaments (Alberts et al., 2007).

Microtubules (MTs) are polymers of tubulin. Tubulin units are formed by heterodimers of α- and β-tubulin. Tubulin dimers stack together to form protofilaments and 13 of these protofilaments are arranged to form a hollow cylindrical MT. The MTs have polar ends that grow and shrink in response to various stimuli. Therefore, MTs can rapidly assemble and disassemble within the cell. The plus end grows by adding tubulin monomers and the minus end loses tubulin. The minus end is embedded in the centrosome from where the MTs nucleate. MTs can also be stabilized by binding to capping proteins or cell structures. These properties help MTs to organize organelles within the cells (Alberts et al, 2007). MTs can move and position organelles within the cytoplasm. There are two motor protein families that work by binding to MTs. The kinesins are plus end-directed motors that move cargoes along the microtubules towards the cell periphery, whereas the dyneins move cargoes towards the centrosome (Reinsch and Gonczy, 1998).

Actin filaments are polymers of globular actin. Like MTs, actin filaments have polar ends and grow by addition of actin monomers to the plus end. Actin filaments are cross-linked to form arrays of actin bundles. Actin bundles extend from the plasma membrane to the nucleus and are found as a gel-like meshwork in the cell cortex, beneath the plasma membrane, thus acting as a major determinant of cell shape. Actin, along with its motor protein myosin forms the basic contractile element in the muscle (Alberts et al, 2007).

Actin filaments can be rearranged to form different structures upon activation by different extracellular stimuli. In this way actin filaments are involved in cell migration. All cell movement requires an initial polarization to a particular direction which involves activation of cell surface receptors in response to stimulus. The cell then pushes out protrusions at its leading edge, by forming thin sheet-like lamellipodia, and thin finger-like filopodia, containing a dense meshwork of actin filaments, generated by rapid local growth of actin filaments. These protrusions then adhere to the local surface by means of focal adhesions, with the help of integrins (transmembrane proteins in the plasma membrane), which in turn anchors actin filaments for cells to crawl. The rest of the cell then reorients along with centrosome and nucleus and drags itself forward by traction on these focal anchorage points (Alberts et al, 2007; Lodish et al., 2000).

47

1.5.1.1 Linked response to mechanical stress

The process by which cells sense and respond to external mechanical stimuli is termed mechanotransduction. It is hypothesized that extracellular matrix receptors, cytoskeletal filaments and nuclear scaffolds (lamins) are 'hard-wired' together so that a mechanical pull on the cell surface can result in co-coordinated re-alignment of structural elements of this interconnected molecular network. This mechanical stress is transferred to nucleus by both actin and intermediate filaments, leading to changes in gene expression (Maniotis et al., 1997). Studies on lamin A knock out MEFs, show decreased mechanical stiffness and altered deformation pattern due to loss of physical connection of nuclear structure with the surrounding cytoskeleton (Broers et al., 2004). In addition, Lee et al. demonstrate that lamin A/C deficiency in *Lmna*^{-/-} MEFs leads to defects in cell polarization, causes separation of the microtubule organizing centre (MTOC) from the nuclear envelope and decreases cell migration at the edge of a wound. Lamin A/C deficiency also reduces the elasticity and viscosity of the cytoplasm in *Lmna*^{-/-} MEFs (Lee et al., 2007). Therefore, this suggests the existence of a mechanical connection between the nucleus and the cytoskeleton and the integrity of the nuclear lamina is required for the cytoskeleton-based processes, such as cell movement, coupled centrosome and nuclear movement and cell polarization (Lee et al., 2007). Of note, emerin deficient MEFs also show abnormal nuclear shape, but have normal nuclear mechanics showing less nuclear deformity under strain than lamin A/C deficient nuclei (Lammerding et al., 2005). However, detachment of centrosome has been observed in emerin null fibroblasts, and emerin that is located at the ONM is thought to interact with tubulin to maintain this connection with centrosome (Salpingiduo et al., 2007). Thus, lamins, NE proteins and the cytoskeleton are linked to act in concert upon activation by extracellular stimuli. Proteins that are responsible for this link are described below in section 1.5.3.

1.5.2 Nuclear migration and positioning

The nucleus, like other organelles, can move within the cell and is very dynamic. Nuclear migration and positioning are necessary for the proper growth and development of eukaryotic organisms. Cytoskeletal proteins play an important role in this process as

it has been shown that both actin and microtubule networks are required for proper positioning and movement of nuclei within the cell (reviewed in Starr and Han, 2003).

Nuclear movement is important for many fundamental cellular and developmental processes, and for subsequent positioning of the nucleus within the cytoplasm after mitosis and meiosis. In *Saccharomyces cerevisiae,* the nucleus moves to the bud neck during mitosis. This movement is required for proper segregation of genetic material to the daughter cells (Stearns 1997). Nuclear migration is also observed during fertilization and embryogenesis in higher eukaryotes. In many species, after fertilization, male and female pronuclei migrate towards each other in a MT dependent manner, a process that is essential for zygote formation (Wilson, 1928; Reinsch and Gonczy, 1998). In some organisms, for example, in rodent spermatocytes, the nucleus rotates and oscillates during meiotic prophase (Yao and Ellingson, 1969). In *Schizosaccharomyces pombe*, during meiotic prophase the whole nucleus is elongated and moves back and forth between the two poles of the cell, which along with telomere clustering, facilitates the homologous pairing of chromosomes (Chikashige et al., 1994; Ding et al., 1998).Therefore, nuclear movement is an essential cellular process that is required for multiple stages in cell development.

The mechanism of nuclear migration is not fully understood. In most cases, nuclear migration involves the microtubules, centrosome or microtubule organization centre (MTOC) and associated motor proteins (Fig. 1.13) (reviewed in Reinsch and Gonczy, 1998). In MTOC-dependent nuclear positioning, the nucleus is associated with the MTOC and is positioned near the centre by forces acting on MTs radiating from the MTOC. One type of force is generated by polymerization of MTs that push the MTOC from the cell cortex or a fixed object in the cytoplasm. In *S. cerevisiae,* during interphase it was found that when growing astral MTs (MTs arising from MTOC in all directions during mitosis) touch the cell cortex, the spindle pole body (SPB) and nucleus moves away from the cortex (Shaw et al., 1997). The nucleus can also move in an MTOC-independent manner, where nucleus lacks associated centrosomes. Experiments revealed that in *Xenopus* egg extracts where nuclei were assembled so that they lack associated centrosomes, the nuclei could still move on microtubules. Here, as for other organelles, nuclei can track along the MTs with help of cytoplasmic dynein

49
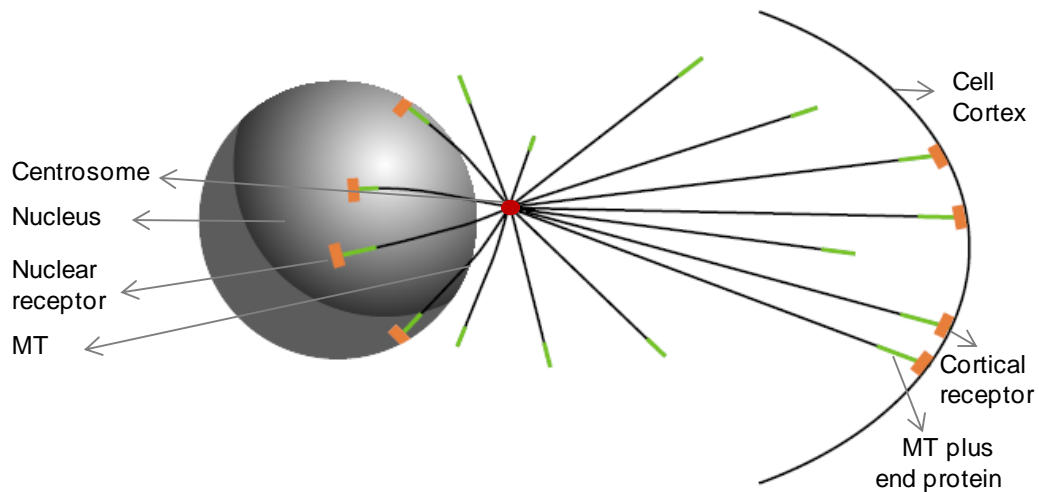
Fig. 1.13. MTOC-dependent nuclear migration. Nuclear movement is generated by the force produced by interaction between nuclear envelope proteins and the centrosome, along with the microtubules (MTs) and the cell cortex. The minus ends of MTs originate from the centrosome (in red). The plus end of MTs are situated near the cell cortex and are dynamic. Proteins (green) that are at the plus ends of MTs interact with receptors (orange) on the cell cortex. MTs from the centrosome also interact with nuclear receptors, which couple the centrosome to the nucleus and position the centrosome. The dynamics of MTs generate the force to move the coupled nucleus. Adapted from Morris (2003).

50

(Reinsch and Karsenti, 1997). But how dynein or other motor proteins are attached to the nuclear membrane is still under investigation.

The actin cytoskeleton also plays important roles in positioning of nuclei in some instances. Actin can either anchor nuclei or provide active force to move nuclei (reviewed in Starr and Han, 2003). Mutations in actin-monomer-binding or actin-filament-binding proteins, disrupt actin filaments and lead to free-floating nuclei with anchorage defects (Robinson and Cooley, 1997). The actin network depolymerizes around migrating nuclei during embryonic development of *Drosophila* and is hypothesized to contribute to the force required for nuclear movement (von Dassow and Schubiger, 1994). In *Arabidopsis* root hairs, actin depolymerising drugs can abolish intracellular nuclear migration completely whereas drugs disrupting microtubules have no effect (Chytilova et al., 2000). In budding yeast, both actin filaments and microtubules are necessary for proper localization of the nucleus and spindle at the bud neck to ensure normal cell division (Palmer et al., 1992; Bloom, 2001).

As recently as ten years ago, little was known about how actin, MTs or the centrosome are connected to the nuclear membrane. However, studies on *S. pombe* and *C. elegans* mutants identified families of NE proteins known as SUN and KASH domain proteins that would be shown to play a major role in nucleo-cytoskeletal connection.

1.5.3 *C. elegans* UNC-84 and ANC-1 NE bridging model

In order to study the relationship between genes and development, Horvitz and Sulston produced cell-lineage mutants by exposing *C. elegans* to different mutagenising agents and then analysed for defects in specific developmental processes (Horvitz and Sulston, 1980). Analysis of genes involved in nuclear migration and anchorage in *C. elegans* revealed two different genes, which are *unc-84 and unc-83*. Mutations in *unc-84* and *unc-83* lead to <u>unc</u>oordinated (unc) movement and vulval and ventral cord developmental defects in nematodes (Horvitz and Sulston, 1980; Sulston and Horvitz, 1981). Hedgecock and Thompson found that mutations in *anc-1* are also involved in nuclear positioning and cause a nuclear <u>anc</u>horage defect (Hedgecock and Thompson, 1982). Subsequent studies demonstrated that UNC-84 is a SUN domain-containing

protein and whilst UNC-83 and ANC-1 are KASH domain proteins. SUN domain and KASH domain proteins are described in detail in sections 1.5.4 and 1.5.5, respectively.

Mutations in *unc-84* affect two sets of nuclear migration events during the developmental stages of *C. elegans* (Malone et al., 1999). The first migration involves formation of dorsal hypodermal syncytium, where precursor hyp7 cells elongate to reach a contralateral position extending over the dorsal midline and the nucleus follows to migrate to the contralateral position within the cytoplasm. After these events the hyp7 cells fuse to form a syncytium. In *unc-84* mutants, the nuclei of hyp7 cells fail to migrate normally. They move slowly and reach only to the dorsal midline (Fig. 1.14). However, the abnormal position of these nuclei does not cause any obvious developmental defects. The second migration involves ventrolateral P-cell (epithelial blast cell) development in *C. elegans* larvae. During the mid-L1 larval stage, six P cell nuclei migrate, followed by the cell body from each side, to form the ventral cord. In *unc-84* mutants, the P cell nuclei fail to migrate and these cells die. This leads to uncoordinated movement and an egg laying defect due to missing neurons and vulval precursor cells that are normally generated from the P cells (Malone et al., 1999) (Fig. 1.15).

In *unc-84* mutants, nuclei also show a nuclear anchoring defect. In wild type embryos, hyp7 syncytium nuclei normally remain anchored in the contralateral position. However, in *unc-84* mutants nuclei are often mispositioned, unanchored and move freely within the cell (Malone et al., 1999). Mutations in *anc-1* also cause a nuclear anchorage defect in the hypodermal syncytium similar to that seen in *unc-84* mutants, hence the name derived ANC-1. However, unlike the *unc-84* mutants, *anc-1* mutants do not show any nuclear migration defects (Hedgecock and Thomson, 1982).

UNC-84 protein consists of 1111 residues, with a conserved C-terminal SUN domain (Fig. 1.16). It is first detected at the 26-cell larval stage of *C. elegans* and subsequently is present at nuclear envelope of most adult cells. Typical of INM proteins, UNC-84 requires the single *C. elegans* lamin protein, Ce-lamin, for its localization at the NE as it is displaced from the NE in lamin deficient embryos (Lee et al., 2002). However, a direct interaction between the two proteins has not yet been demonstrated.
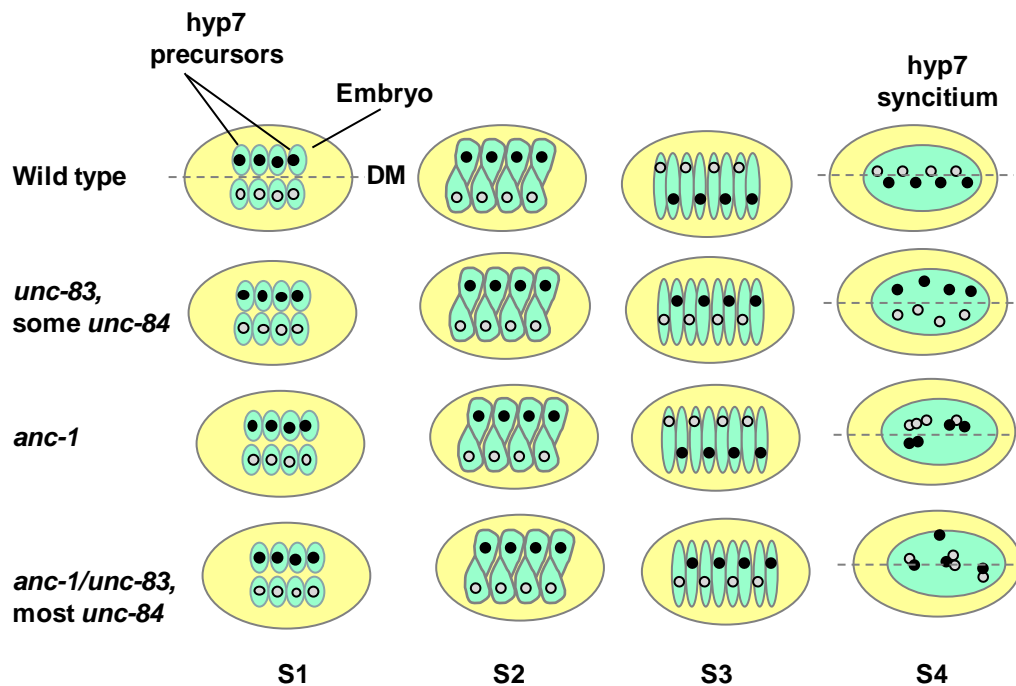
Fig. 1.14. Dorsal view of hyp7 cell phenotypes observed in *C. elegans anc-1, unc-83 and unc-84* mutants. In wild type *C. elegans,* hyp7 precursor cells on the dorsal side of the developing embryo (stage1 or S1), elongate and intercalate. The nuclei (grey and black circles) then move to the opposite sides of the embryo (S3). Thereafter, the hyp7 precursors cells fuse to form the large multi-nucleated syncytium, where the nuclei are evenly anchored near the dorsal midline (DM) (S4). In *unc-83* and some *unc-84* mutants, the nuclei fail to migrate past the DM (S3) and the nuclei are malpositioned in the syncytium (S4). In the *anc-1* mutants, the nuclei migrate normally (S3) but remain unanchored and form clumps in the syncytium (S4). In most of the *unc-84* mutants, and all *unc-83/anc-1* and *unc-84* double mutants, nuclei have defects in positioning and anchorage in the syncytium (S4). Reviewed in Wilhelmsen et al. (2006).
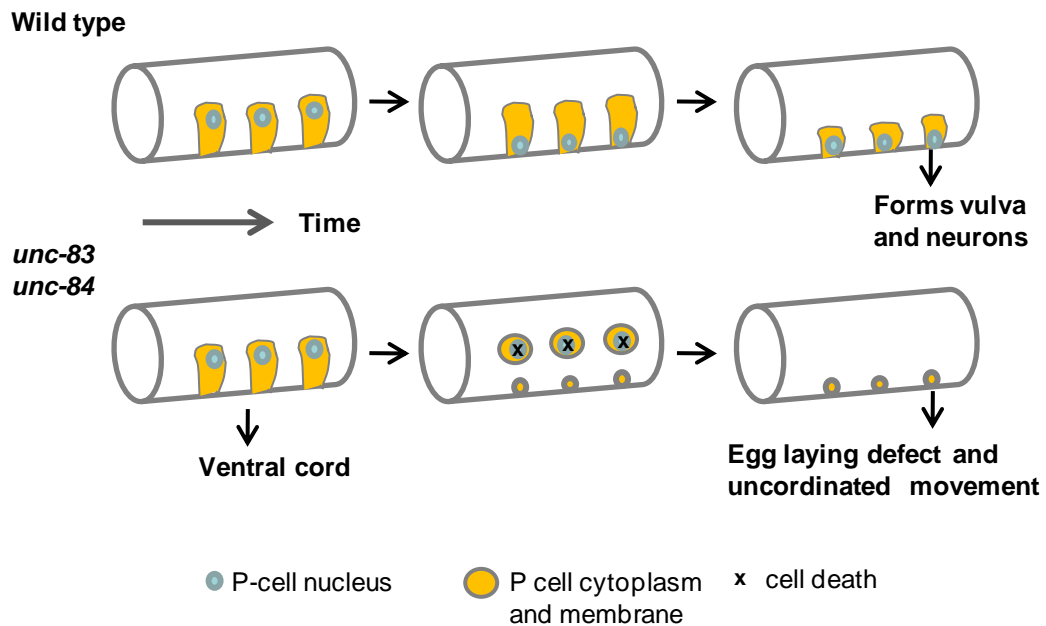
Fig. 1.15. Lateral view of P-cell migration phentotypes of *C. elegans unc-84/unc-83* **mutants**. A newly hatched *C. elegans* larva has a ventrolateral row of six P cell nuclei on each side (three representative cells shown). During mid-larval stage, P-cell nuclei migrate from each side, followed by the cell body, to form the ventral cord. In *unc-83/unc-84* mutants the P cell nuclei fail to migrate and follow the cytoplasm, therefore the cells die. The worm shows uncoordinated movement and a vulval defect. Adapted from Starr and Han (2005).
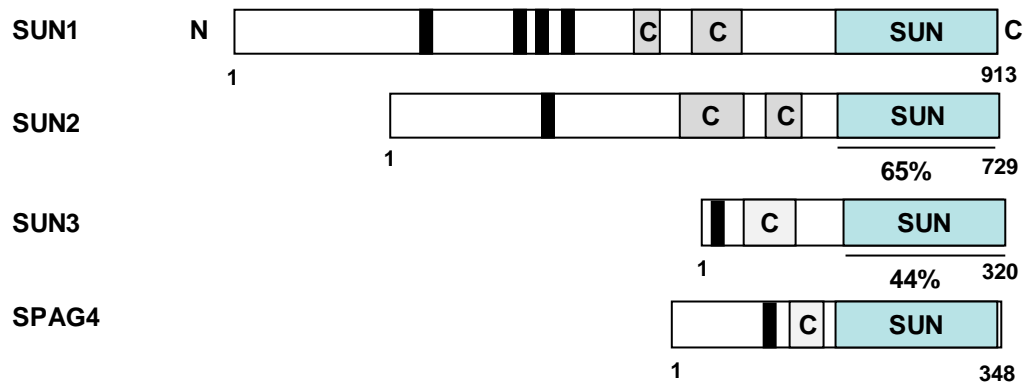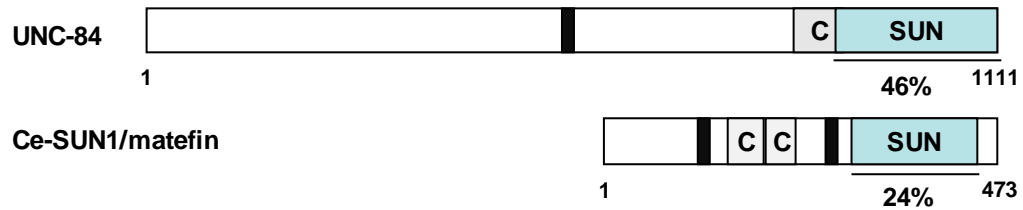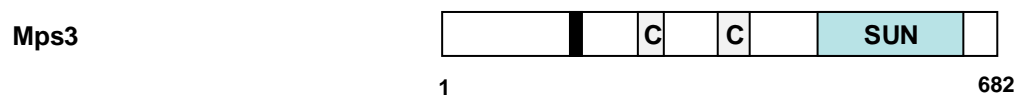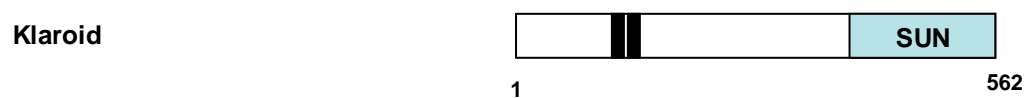
Fig. 1.16. SUN proteins family sequence alignments and predicted structures.
Schematic representation of SUN protein structures showing potential transmembrane domains (black bars) predicted by TMpred, putative coiled-coils (C), and conserved SUN domain (blue box). Percent homology with mouse SUN1 over the relevant region (underlined) is shown for most studied homologues.

ANC-1 is an 8546-residue giant protein with a C-terminal KASH domain, an extensive coiled-coil region and an N-terminal actin-binding domain (Fig 1.17). It is located at the nuclear periphery of most cells and requires UNC-84 for its nuclear envelope localization (Starr and Han, 2002). Both *unc-84* and *anc-1* mutants show disruption of nuclear positioning in the syncytial hypoderm and ANC-1 protein is found mislocalized from the NE in *unc-84* mutants. Therefore, it was proposed that the SUN domain of UNC-84 interacts with the KASH domain of ANC-1 and recruits the protein to the NE, most likely at the ONM. ANC-1 contains an N-terminal calponin homology domain that has been shown to bind actin, leading to the hypothesis that the bridging of UNC-84 and ANC-1 maintains the position of the nucleus within the cell through attachment of the nucleus to the actin cytoskeleton (Starr and Han, 2002; Starr and Han, 2003; Starr and Han, 2004) (Fig. 1.18). However, a direct interaction between ANC-1 and UNC-84 has not been demonstrated.

1.5.4 SUN domain proteins

SUN proteins are a family of integral membrane proteins of the NE that share a conserved C-terminal SUN domain. The SUN domain is approximately 200 residues in length and is conserved from yeast to mammals. The name derives from the very first members of the family to be identified: Sad1 and UNC-84 (found in *S. pombe* and *C. elegans,* respectively) and was first defined by Malone et al. (Malone et al., 1999). Most of these proteins have an N-terminal domain, single central TMD followed by a coiled-coil region and a conserved C-terminal SUN domain (Fig. 1.16) (Starr and Han, 2003).

1.5.4.1 S. pombe Sad1

Sad1 (Spindle architecture disrupted) is a spindle pole body protein that was identified through analysis of *Schizosaccharomyces pombe* mutants (Hagan and Yanagida, 1995). Sad1 is 58 kDa and, like most SUN domain proteins, is comprised of an acidic N-terminus, a membrane spanning domain, a coiled-coil domain and a C-terminal SUN domain. The spindle pole body (SPB) is the major yeast MTOC, which becomes embedded in the nuclear envelope during mitosis and is responsible for spindle microtubule formation (Ding et al., 1997). Sad1 associates with the SPB throughout mitosis and meiosis in cells. It is the first protein found to localize exclusively to the
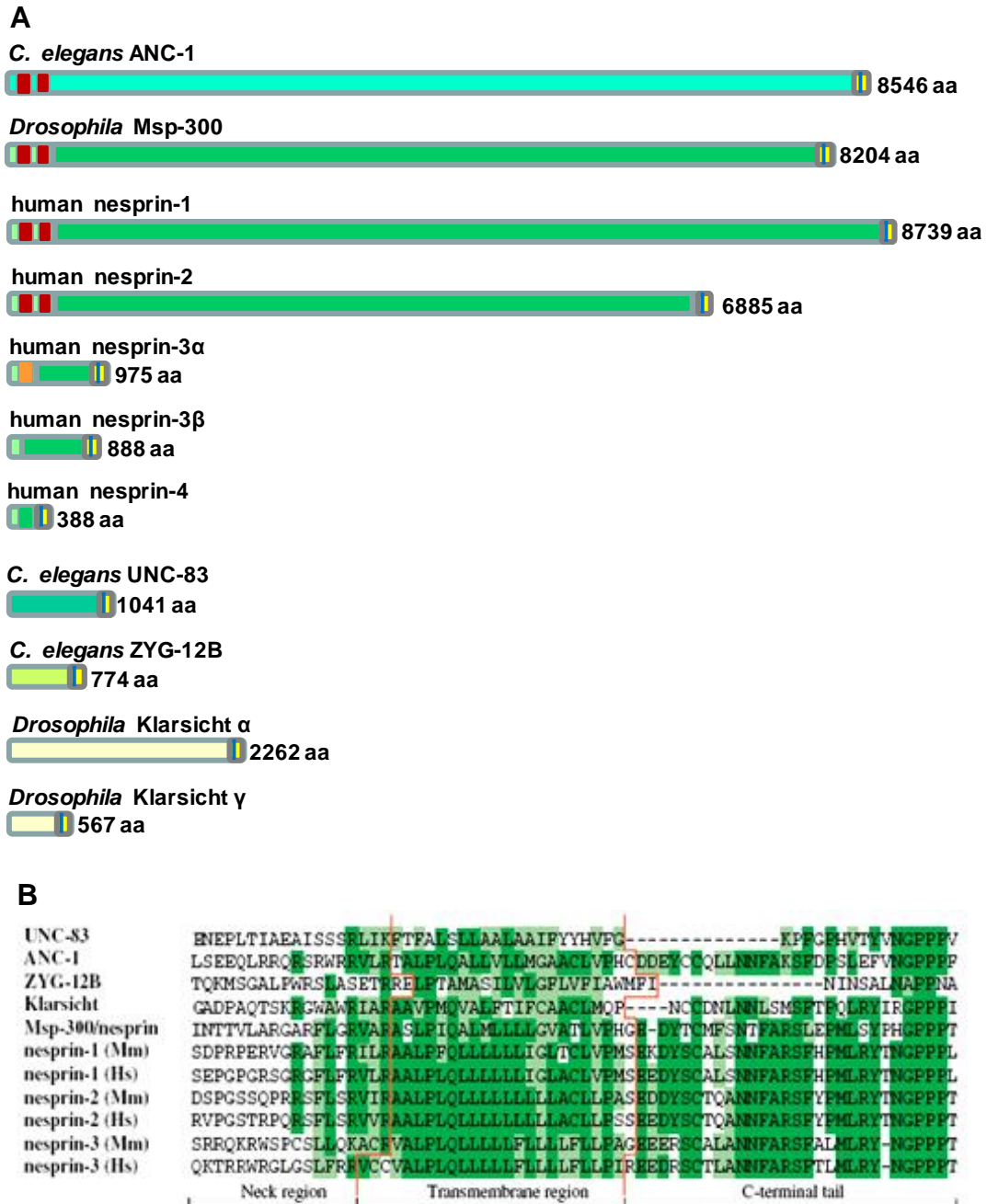
Fig. 1.17. Different KASH domain proteins in various species. A) Schematic representation of various KASH domain of proteins identified in different species. The last 40-60 residues are the KASH domain (in yellow) with a transmembrane domain (in blue). The N-termini of ANC-1, Msp-300 and nesprin-1 and -2 contain two calponin-like domains (red). Nesprin-3 contains a plectin binding domain (orange).The central rod region (light green) of ANC-1consists mainly of novel repetitive stretches. In contrast, the central rod domain of Msp-300 and nesprins consists of mostly spectrin-repeats (dark green). *C. elegans* UNC-83, ZYG-12 and *Drosophila* Klarsicht N-terminal regions lack spectrin repeats and do not have sequence similarity with other KASH domain proteins. B) Alignment of KASH domains of various proteins in different species. The amino acid residues enclosed by red lines represent the transmembrane regions. Dark green represents conserved amino acids, light green represents residues with similar chemical properties. Mm, *Mus musculus; Hs, Homo sapiens*. Adapted from Wilhelmsen et al. (2006).
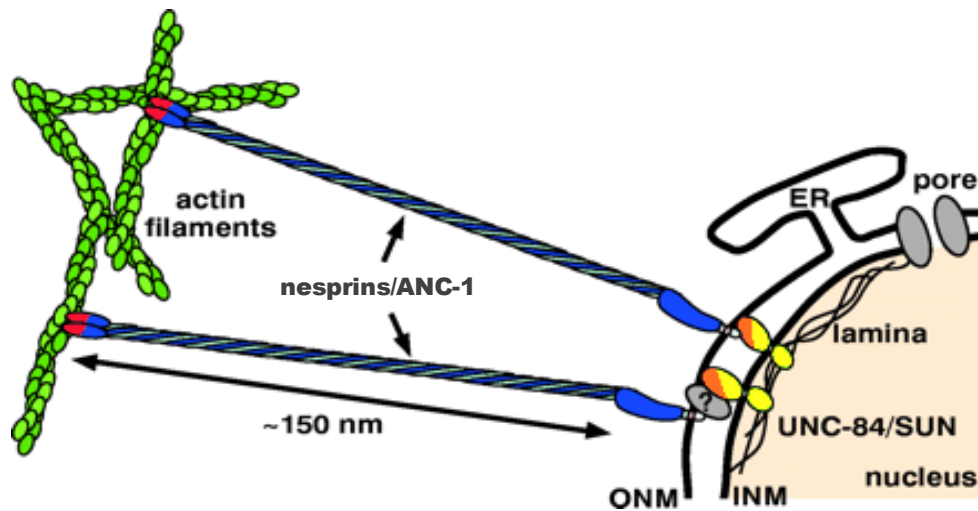
Fig. 1.18. A model for nuclear anchorage and migration. The KASH domain (blue) is retained in the ONM through an interaction with the SUN domain (orange) of UNC-84 (yellow) or through an intermediating protein or complex (grey). This model proposes that ANC-1, UNC-84, the nuclear lamina, and other unknown proteins create a bridge across the nuclear envelope. The calponin domains of ANC-1 (red) attach to actin microfilaments (green) to anchor nuclei in the cytoplasm. Reproduced from Starr and Han (2003).

SPB. When over-expressed, Sad1 accumulates at the nuclear envelope. *Sad1.1* temperature sensitive conditional mutation, results in defects in mitotic spindle formation and function, and deletion of the *sad1* gene is lethal. From these findings it was postulated that Sad1 is a NE protein that have role in association of the SPB with the NE and may also provide an anchor for the attachment of microtubule motor proteins (Hagan and Yanagida, 1995).

During meiosis, telomeres play a role in anchoring chromosomes to the INM. Telomeres are embedded in the INM and they then polarize and cluster together near the MTOC, allowing the chromosomes to form a bouquet structure, which promotes pairing and recombination of homologous chromosomes (Siderakis and Tarsounas, 2007). Recent studies in *S. pombe* found that Sad1 is involved in bouquet formation in meiosis. Sad1 binds Bqt1, which in turn interacts with Bqt2, and this complex binds to telomere associated protein Rap1. Then telomeres are recruited to the SPB to form a bouquet structure (Chikashige et al., 2006; Tomita and Cooper, 2006). Mps3 (monopolar spindle) is the SUN domain protein in *S. cerevisiae*, which also functions in anchoring and telomeres at the NE in both mitotis and in meiotic cells and also mediates the bouquet formation (Jaspersen et al., 2006; Antoniacci et al., 2007; Bupp et al., 2007; Conrad et al., 2007).

1.5.4.2 C. elegans SUN domain proteins

There are two SUN domain proteins described in *C. elegans,* the first is UNC-84, one of the founding members of SUN domain proteins, as described in section 1.5.3. The second SUN domain protein in *C. elegans* is matefin, also known as SUN-1. Matefin is an INM protein, which co-localizes with Ce-lamin. However, unlike UNC-84, it is not dependent on Ce-lamin for its NE localization. Matefin has two putative transmembrane domains and a C-terminal SUN domain (Fig. 1.16). Matefin is expressed in all embryonic cells until mid-embryogenesis and is then present only in germ cell lines in adults. It is the first nuclear membrane protein known to have germline specificity. Matefin is essential for embryogenesis and germ cell proliferation or survival (Fridkin et al., 2004). Matefin binds to a hook protein, ZYG-12, which is required for attachment of the centrosome to the nucleus. ZYG-12 localizes to both the centrosome and the NE and its NE localization is dependent on matefin. In turn, ZYG-12 binds to dynein, thereby linking the nucleus to the microtubule network (Fig. 1.19) (Malone et al., 2003).
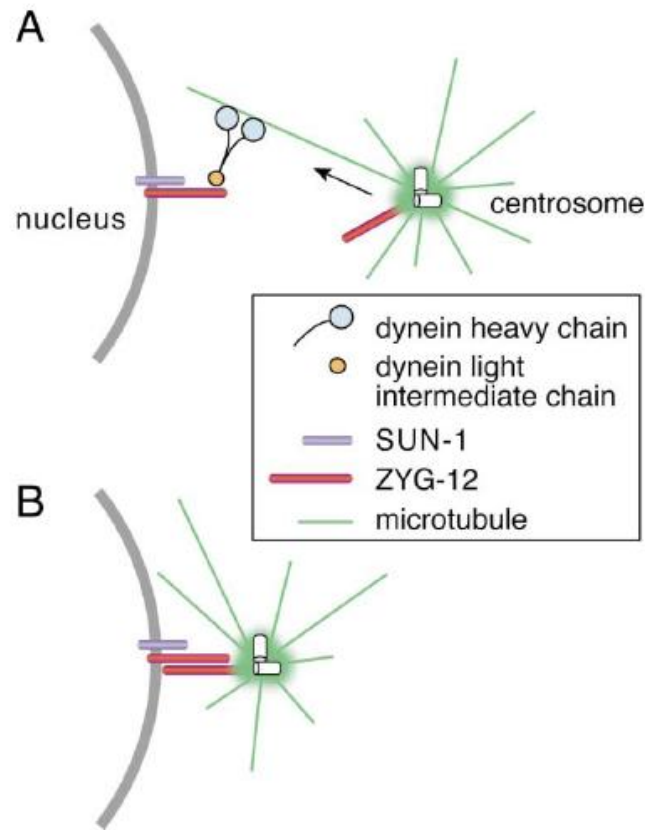
Fig. 1.19. Model for centrosome attachment to the nucleus. A) ZYG-12 at the NE recruits dyenin, which bring nucleus and centrosome closer by minus end oriented dynein mediated movement along the microtubules. **B)** ZYG-12 are localized at the NE in SUN-1-dependent manner and are also localized to the centrosome in a microtuble-dependent mechanism. Homodimerization of ZYG-12 mediate attachment of the nucleus and the centrosome. Reproduced from Malone et al. (2003).

1.5.4.3 Drosophila SUN domain proteins

In *Drosophila* there are two SUN domain homologue identified, known as giacomo (uncharacterized) and klaroid (*koi*). Klaroid tethers klarsicht, a KASH domain protein described in section 1.5.5.2. *Klaroid-klarsicht* double mutants exhibit rough eyes morphology and play a role in nuclear migration in differentiating cells of the *Drosophoila* eye and neurons (Kracklauer et al., 2007).

1.5.4.4 Mammalian SUN domain proteins

Four mammalian SUN domain proteins have been predicted to date, which are: SUN1, SUN2, SUN3 and SPAG4 (sperm associated antigen 4) (Malone et al., 2003). SUN3 and SPAG4 expression are expressed only in germline. SUN1 and SUN2 are components of the NE that were initially identified in NE proteomic studies (Dreger et al., 2001, Schirmer et al., 2003). More detailed studies confirmed SUN2 as an 85 kDa INM protein (Hodzic et al., 2004). Similar to other SUN domain proteins described, SUN2 has an N-terminal domain, a central transmembrane domain, followed two predicted coiled-coil regions and a SUN domain at the C-terminus (Fig. 1.16). The amino-terminus of SUN2, including the transmembrane domain (amino acids 26-339), is sufficient for its NE localization. The N-terminal domain is located within the nucleoplasm, while the SUN domain is located in the periplasmic lumen between the ONM and the INM (Hodzic et al., 2004; section 3.2.5.3). Other mammalian SUN domain proteins had not been characterized at the beginning of this project, and were the focus of this study (Section 1.6).

1.5.5 KASH domain proteins

The second family of nuclear envelope bridging proteins are the conserved KASH domain proteins (Fig. 1.17). The name KASH (<u>K</u>larsicht, <u>A</u>NC-1, <u>S</u>yne <u>h</u>omology) derives from a short stretch of homology found at the extreme C-terminus of proteins found in *Drosophila*, *C. elegans* and human, respectively. The KASH domain consists of approximately 60 residues, including a transmembrane domain, followed by 30-40 residues at the C-terminus of the proteins (Starr and Han, 2002) and so far KASH domain proteins are the first ONM proteins identified. Several of these proteins have a very large N-terminus with two calponin homology domains that bind actin (Zhen et al.,

2002), whilst others have been shown to link to the MT or IF networks. Their function is therefore thought to involve linking the nucleus to the cytoskeleton (Razafsky and Hodzic, 2009). KASH domain is comparatively well conserved but often the N-terminus is very divergent, suggesting either that they have different functions or that the sequence itself is not important, but just act as an extended linker (Razafsky and Hodzic, 2009).

1.5.5.1 C. elegans KASH domain proteins

Three KASH domain proteins have been identified in *C. elegans,* which are ANC-1, UNC-83 and ZYG-12. Other than the KASH domain they do not share sequence similarities with each other. The first defined KASH domain protein was ANC-1, described in section 1.5.3. UNC-83 is of size 117 kDa and its N-terminus does not show any sequence similarity to any known protein (McGee et al., 2006). The mutation of *unc-83* causes nuclear migration defects similar to those seen in *unc-84* mutants (section 1.5.3). UNC-83 is found at the ONM in a limited number of cell types (including P, hyp7, intestinal, pharyngeal and uterine cells) (Starr et al., 2001). Like ANC-1, UNC-83 interacts with UNC-84 and requires UNC-84 for its nuclear envelope localization (McGee et al., 2006). It was predicted that UNC-84 interacts with the KASH domain of UNC-83 as in bridging model to tether nucleus to the centrosomes. However, normal association between the centrosomes and nuclei is observed in *unc-83* and *unc-84* mutants with nuclear migration defects (Lee et al., 2002; Starr et al., 2001). Recently, it was found that UNC-83 acts as a kinesin-1 docking site at the outer nuclear membrane and thus plays a role in MT-dependent nuclear migration (Meyerzon et al., 2009).

ZYG-12 (zygote defective) is a hook family protein of 83 kDa. It has three splice variants: A, B and C. Isoforms B and C have KASH domains, whereas isoform A is not membrane associated. ZYG-12 is expressed in germline and in early embryonic cells. ZYG-12A localizes only to the centrosome, but ZYG-12B and C localizes to the centrosome and the NE. The NE localization of ZYG-12 is dependent on the SUN domain protein matefin. ZYG-12 also interacts with dynein, therefore connects the nucleus to the microtubule cytoskeleton as postulated in the bridging model and plays a role in attachment of centrosomes to the nuclear envelope (Malone et al., 2003) (Fig.

1.19). ZYG-12 and dynein interaction is required for maintenance of gonad architecture in *C. elegans* (Zhou et al., 2009).

1.5.5.2 Drosophila KASH domain proteins

There are two KASH proteins in *Drosophila*, Klarsicht (also known as Marbles) and Msp-300 (<u>m</u>uscle-<u>s</u>pecific <u>p</u>rotein 300 kDa). Msp-300 has a long spectrin-like rod domain connecting the N-terminal actin binding domain (ABD) to the KASH domain. The *Msp-300* gene can encode a giant molecule of 1300 kDa (Zhang et al., 2002). Msp-300 is expressed in somatic, visceral and heart embryonic muscles and has role in myogenesis (Volk, 1992; Rosenberg-Hasson et al., 1996). *Msp-300^{SZ-75}* mutation is lethal and the contractile ability of the embryonic somatic muscle cells is severely compromised. The larvae die as they do not hatch from the chorion due to defect in muscle attachment and contraction (Rosenberg-Hasson et al., 1996). Msp-300 is localized at the NE and is required for correct positioning of the nuclei in the nurse cells and the oocyte. Flies carrying the *Msp-300$_{SZ-75}$* allele only in the germ line exhibit defects in cytoplasmic dumping of nurse cells to the egg chambers during *Drosophila* oogenesis and mislocalization of the nuclei of nurse cells and the oocyte (Yu et al., 2006).

Klarsicht is a microtubule-binding KASH domain protein. The N-terminal region of Klarsicht lacks spectrin repeats, and like UNC-83 in *C. elegans,* does not show sequence similarity to other known proteins (Fischer et al., 2004). Klarsicht has three isoforms α, β and γ. Klarsicht α (251 kDa) and γ (62 kDa) are located at the NE, while Klarsicht β does not have a KASH domain (Guo et al., 2005). Klarsicht associates with dynein, thus connects nucleus to the MTOC (Fischer et al., 2004; Patterson et al., 2004). Klarsicht has been shown to play a role in nuclear migration during *Drosophila* eye development. Mutation of the *klarsicht* gene causes oddly shaped photoreceptors, where most nuclei remain at the basal side, due to failure of the nuclei to migrate to the apex of the developing eye imaginal disc (Fischer-Vize and Mosley, 1994).

1.5.5.3 *Mammalian KASH domain proteins*

Nesprins (<u>n</u>uclear <u>e</u>nvelope <u>sp</u>ectrin <u>r</u>epeat prote<u>ins</u>) are ubiquitously expressed integral membrane proteins containing a C-terminal KASH domain. Nesprins are also known as Syne or Myne (see below). There are four mammalian nesprin genes so far reported: nesprin-1, nesprin-2, nesprin-3 and nesprin-4 (Zhang et al., 2001; Wilhelmsen et al., 2005; Roux et al., 2009). Nesprin-1 and -2 are comprised of over 100 exons and they exhibit a high level of alternative splicing that result in many isoforms, varying in size from around 50 to 1000 kDa, which is not observed in non-mammalian species. In general, nesprins consist of a long N-terminal cytoplasmic domain with multiple, clustered spectrin repeats (globular domains homologous to those found in cytoskeletal spectrins and dystrophin,) and a conserved C-terminal KASH domain (Fig. 1.17). The spectrin repeats are thought to act as huge spacers, separating the N and C-termini. The KASH domain is responsible for localization of nesprins to the NE. At the N-terminus, the giant nesprin-1 and -2 isoforms have calponin homology (CH) domains that constitute an actin binding domain (ABD) (Zhang et al., 2001; Zhen et al., 2002; Zhang et al., 2005). Nesprins are present mainly in the ONM, but are also found at other subcellular locations in certain cell types (Padmakumar et al., 2004). It is thought that there is a specialized cytoskeleton present at the cytoplasmic interface of the NE and also that there are several NE-cytoskeleton-attachment devices (Schneider et al., 2008). KASH-domain proteins are hypothesized to serve as cytoskeletal adaptors at the ONM of cells, which mediate interactions with various cytoskeletal structures including the centrosome, actin, IFs, MTs and MT-motor proteins (Schneider et al., 2008). However, it was not known at this stage how nesprins are anchored at the ONM, although they were predicted to interact with SUN proteins in a manner analogous to the UNC-84-ANC-1 model in *C. elegans*. Of note, cytoplasmic dystrophin in an analogous manner is anchored at the plasmamembrane and bind to actin cytoskeleton by CH domains. Dystrophin show tissue specific expression of different isoforms and the gene is mutated in Duchenne muscular dystrophy and Becker muscular dystrophy (Jin et al., 2007; McNally 2007).

1.5.5.3.1 Nesprin-1

Nesprin-1 was initially identified as a binding partner of a tyrosine kinase of the post synaptic membrane in muscle in a yeast two-hybrid screen and was named as synaptic nuclear envelope 1 (Syne-1) (Apel et al., 2000). It was also independently identified as myocyte nuclear envelope 1(Myne-1) (Mislow et al., 2002a). Thus, various isoforms were identified by different groups and were named differently. However, the name nesprin was later adopted and is now generally accepted (Zhang et al., 2001). The full length nesprin-1 is a giant isoform of the protein (also known as enaptin). Giant nesprin-1 is 976 kDa, with an N-terminal ABD, a rod domain containing 50 spectrin repeats, which comprises the bulk of the protein, and the C-terminal transmembrane KASH domain (Padmakumar et al., 2004; Zhang et al., 2002).

Nesprin-1 also has short C-terminal isoforms that vary in length mainly due to variable truncation of the N-terminus. Some isoforms even appear to lack the C-terminal KASH domain (Fig. 1.20) (Zhang et al., 2001; Zhang et al., 2002; Simpson and Roberts, 2008). Presence of multiple isoforms has rendered studies of nesprins problematic as it is difficult to use isoform-specific antibodies. Nesprin-1 is ubiquitously expressed, but tissue specific expression of nesprin-1 isoforms has been observed (Zhang et al., 2001). The Giant nesprin-1 isoform is expressed dominantly in dermal fibroblasts and it is also present in muscles. However, the main isoforms that are found in skeletal muscles are nesprin-1α and nesprin-1β (Randles et al., 2010). Of note, recent bioinformatic analysis show less support for nesprin-1β1 and nesprin-1α1 isoforms (Simpson and Roberts, 2008).

Nesprin-1 is localized mainly at the NE in a KASH domain-dependent manner (Zhang et al., 2001). However, recent studies by Puckelwartz et al. have demonstrated that KASH domain is dispensable for localization of nesprin-1α to the nuclear periphery (Puckelwartz et al., 2009). In addition to the NE localization, nesprin-1 is also present within the nucleus and found in the sarcomeres of cardiac and skeletal muscle (Zhang et al., 2002).
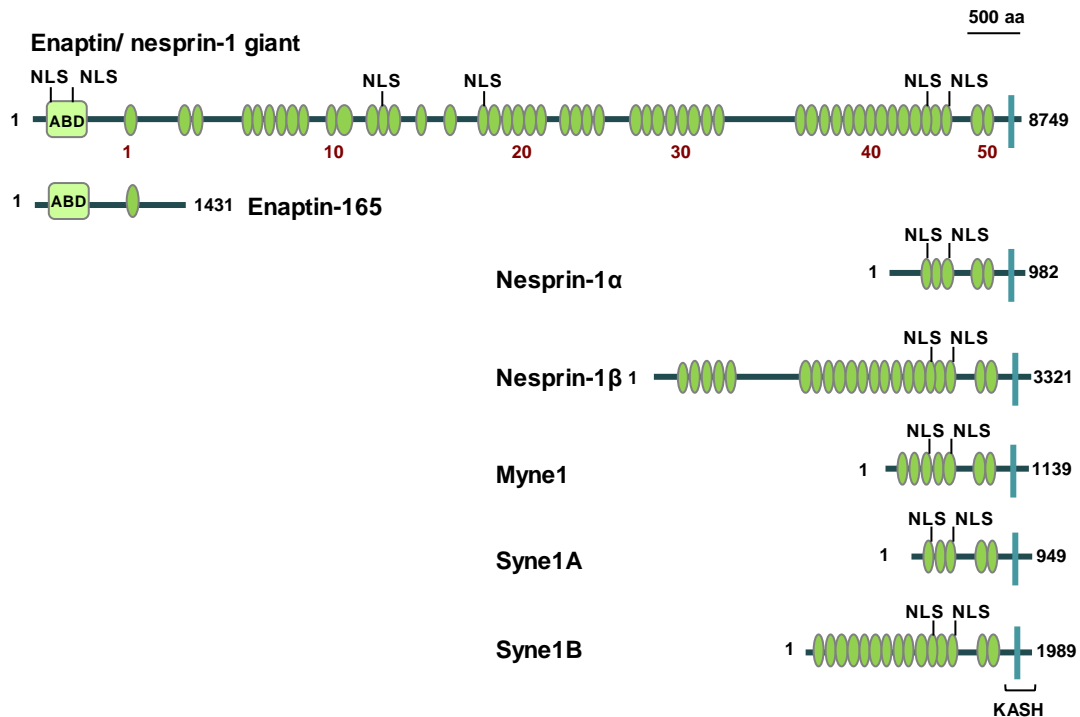
Fig. 1.20. Schematic representation of nesprin-1 with its multiple isoforms. Length of the various isoforms is indicated on the right. Nesprin-1 giant contains an N-terminal actin binding domain (ABD). Green ovals represent spectrin repeats and are numbered below (in red). The C-terminal KASH domain contains a transmembrane domain (vertical blue bar). Position of nuclear localization signals (NLS) are shown. Adapted from Padmakumar et al. (2004).

66

Nesprin-1α interacts with lamin A/C, emerin and can also self associate to form dimers. Therefore it is predicted to reside at the INM to provide a structural scaffold (Mislow et al., 2002b). However, the giant nesprin-1 isoform interacts with F-actin and the amino terminal ABD co-localizes to actin-rich lammellipodia and stress fibres in COS7 cells (Padmakumar et al., 2004). Therefore, giant nesprin-1 is thought to tether nuclei to the actin cytoskeleton, as hypothesized in the bridging model of KASH-SUN domain (Starr and Han, 2003; Padmakumar et al., 2004). To support this, nesprin-1 transgenic mice which overexpress the nesprin-1 KASH domain, fail to form nuclear aggregates in synaptic nuclei at the neuro-muscular junction. Here, endogenous nesprin-1 at the NE is displaced by the KASH domain which cannot interact with actin cytoskeleton (Grady et al., 2005).

Notably, Zhang et al. developed nesprin-1 knockout mice that lack in all isoform of nesprin-1 containing the C-terminal spectrin repeat with or without KASH domain. They also have defect in nuclear positioning and anchorage in skeletal muscle and decreased strain transmission to nuclei from perinuclear regions. These mice show decreased survival rates and growth retardation (Zhang et al., 2007a). On the other hand, another group has demonstrated that mice lacking the nesprin-1 KASH domain only have perinatal lethality as well. However, the surviving mice develop progressive muscle disorder with cardiac conduction defects as in EDMD. The nuclei in muscles also show abnormal localization (Puckelwartz et al., 2009).

Recent advances further demonstrate the disease association of nesprin-1. Nesprin-1 mutations are associated with autosomal recessive cerebellar ataxia and cardiomyopathy (Gros-Louis et al., 2007; Puckelwartz et al., 2010). Additionally, three missense mutations in nesprin-1 have also been detected in EDMD patients, demonstrating functional importance of nesprins in muscular dystrophies (Zhang et al., 2007b).

1.5.5.3.2 Nesprin-2

Nesprin-2 was initially identified in database searches for sequences related to nesprin-1 or the α-actinin ABD (Apel et al., 2000; Zhang et al., 2001). It is also known as Syne-2 (Apel et al., 2000). The full length isoform, nesprin-2 giant, was also separately identified as NUANCE (<u>nu</u>cleus and <u>a</u>cti<u>n</u> <u>c</u>onnecting <u>e</u>lement) (Zhen et al., 2002).

Nesprin-2 giant is a 796 kDa protein with an N-terminal ABD, multiple spectrin repeats and C-terminal KASH domain (Zhen at al., 2002). Similar to nesprin-1, nesprin-2 also has a number of isoforms which are mostly truncated at the N-terminus, but some isoforms also lack the KASH domain (Fig. 1.21) (Zhang et al., 2001; Zhang et al., 2005). Nesprin-2 is also ubiquitously expressed with tissue-specific expression of different isoforms. The principal isoforms observed in muscles are nesprin-2α, nesprin-2β and nesprin-2γ. However, in skin fibroblasts the nesprin-2 giant isoform is prominently expressed (Zhang et al., 2005; Randles et al., 2010). Of note, recent bioinformatic analyses show less support for biological relevance of nesprin-2β1, nesprin-2γ and isoforms lacking the KASH domain for nesprin-2 than nesprin-1 (Simpson and Roberts, 2008).

Nesprin-2 is localized mainly at the NE in a KASH domain-dependent manner, with the giant isoform residing predominantly at the ONM (Zhen et al., 2002). The smaller nesprin isoforms are predicted to locate at the INM (Warren et al., 2005; Morris and Randles, 2010). However, nesprin-2 giant has been shown also to locate inside the nucleus by digitonin extraction methods (Zhen et al., 2002) and both at the ONM and the INM by immunogold electron microscopy in HaCat cells using nesprin-2 antibodies (Libotte et al., 2005). Nesprin-2 is found within the nucleus as small scattered foci and around nucleoli and is also found diffusely in the cytoplasm, at lamellipodia and focal adhesions. In skeletal muscles, nesprin-2 is found at the Z-line and sarcoplasmic reticulum (Zhang et al., 2005). In wound healing assays performed on COS7 cells, nesprin-2 giant was detected at the leading edge of migrating cells, co-localizing with actin. Nesprin-2 giant can also bind F-actin, as observed in actin co-sedimentation assays. Therefore, as hypothesized in the bridging model, nesprin-2 can also link the actin cytoskeleton to the nucleus (Zhen et al., 2002).

Nesprin-2 KASH mice, overexpressing the KASH domain of nesprin-2, exhibit reduced expression of nesprin-1 at the NE and show a myonuclear anchorage defect, therefore nesprin-1 and nesprin-2 may share the same docking site at the NE. Nesprin-1 and nesprin-2 KASH domain double knockout mice die after birth due to respiratory arrest, therefore at least one copy of *nesprin-1* or *nesprin-2* is essential to function after birth
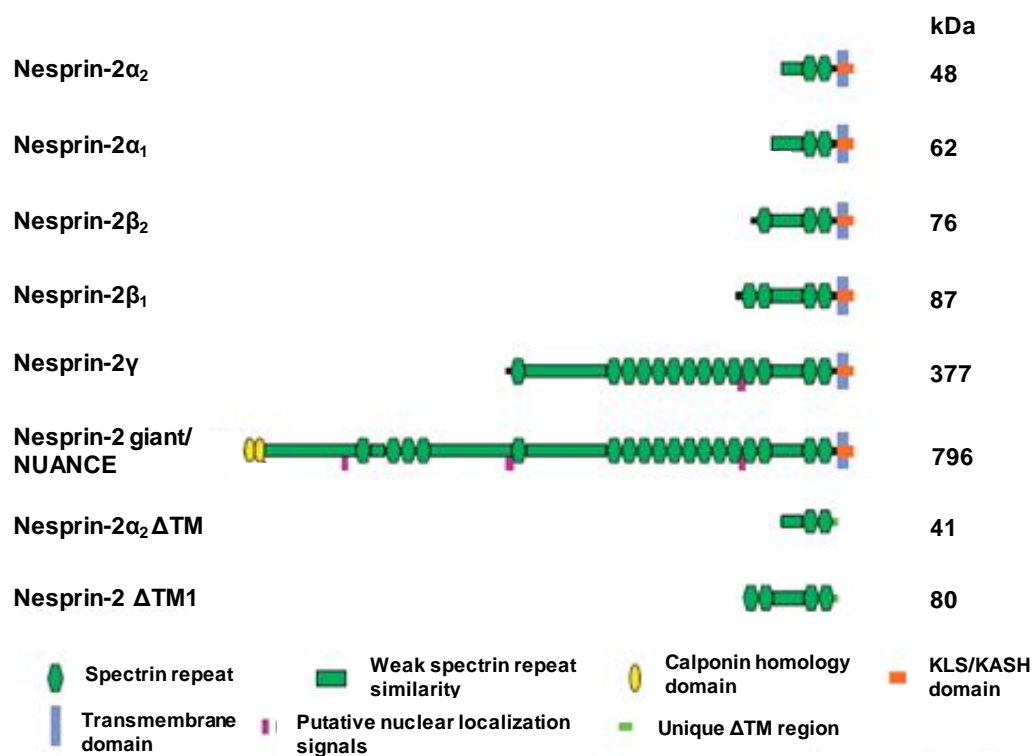
Fig. 1.21. Schematic structure of nesprin-2 with its major isoforms. Isoforms lacking the KASH domain are denoted as ΔTM. Molecular mass (kDa) of each isoform is shown. Green spectrin repeats form a continuous rod domain. Adapted from Zhang et al. (2005).

(Zhang et al., 2007a). Recently, disease association of nesprin-2 has been demonstrated as well, since one nesprin-2 missense mutation has been reported in EDMD (Zhang et al., 2007b). Like nesprin-1α, nesprin-2α and nesprin-2β can bind emerin and lamin A/C (Zhang et al., 2005; Libotte et al., 2005). Therefore, disruption of nesprin/lamin/emerin interactions may have a role in the pathology of EDMD (Zhang et al., 2007b). Additionally, Wheeler et al., reported that emerin mutations associated with X-linked EDMD, disrupt emerin binding to both nesprin-1α and -2β isoforms (Wheeler et al., 2007).

1.5.5.3.3 Nesprin-3

Nesprin-3 is the third member of the KASH domain family (Fig. 1.17) and the product of a separate gene, which was identified in a yeast two-hybrid screen as a plectin-1 binding protein. Plectins are cytoskeletal proteins that cross link the actin to IFs. Similar to other nesprins, nesprin-3 has C-terminal KASH domain and multiple spectrin repeats. However, it lacks the N-terminal ABD; instead it binds to plectin-1A and -1C. Nesprin-3 is ubiquitously expressed and has two isoforms nesprin-3α and -3β. Nesprin-3α is the major isoform of size 110 kDa. Nesprin-3 localizes to the ONM, where it can recruit plectin. Plectin in turn binds IFs, thus linking the nucleus to the IF cytoskeleton. Since plectin binds integrin α6β4 at the cell surface and nesprin-3 at the nucleus, it is therefore suggested to form a continuous link between the nucleus and extracellular matrix (Wilhelmsen et al., 2005).

1.5.5.3.4 Nesprin-4

Recently, the fourth KASH domain protein family member, nesprin-4 (Fig. 1.17), has been identified in database searches for mammalian KASH domain-containing proteins (Roux et al., 2009). Nesprin-4 is of 42 kDa and, similar to other nesprins, it contains a spectrin repeat domain. It is located at the ONM and the NE anchoring is dependent on the KASH domain. Nesprin-4 is expressed mainly in secretory epithelia, salivary gland, exocrine pancreas, bulbourethral gland and mammary tissues. No alternate splice variant of nesprin-4 has been found. Yeast two-hybrid and co-immunopreciptation studies show that nesprin-4 interacts with kinesin-1, a plus-end directed microtubule motor protein. Secretory epithelia maintain cell polarity, where microtubules are non-

centrosomal, the nucleus is mainly located in basal position and Golgi body lies between the nucleus and the apical surface. It is suggested that nesprin-4 has role in microtubule dependent nuclear positioning in secretory epithelia and may also drive positioning of the centrosome and Golgi apparatus in these cells (Roux et al., 2009).

1.6 WORK LEADING UP TO THIS PROJECT

Previously in the lab, murine SUN1 (mSUN1) was found as a lamin A binding protein in a yeast two-hybrid screen. mSUN1 is a 101 kDa protein with 913 amino acids. Software algorithms predicted mSUN1 to have N- and C-terminal domains, separated by 3 clustered putative membrane spanning domains and a fourth putative transmembrane domain around 100 residues upstream of this cluster (Fig. 1.22A and Fig. 3.1A). The N-terminus has a serine-rich region and a potential zinc finger domain; on the other hand the C-terminus contains two potential coiled-coil regions and the C-terminal SUN domain (Haque et al., 2006).

A polyclonal antibody (SSHR1) was raised in rabbit against the CTD of mouse SUN1(amino acids 450-913), which recognized a doublet of the expected size of 100 kDa. SUN1 was found enriched in insoluble nuclear fractions of NIH 3T3 cells and immunofluorescence studies showed NE staining that co-localizes with lamin A/C, thus confirming that SUN1 is a nuclear rim protein (Fig. 1.22B). Interestingly, mSUN1 distribution was not affected in lamin A null MEFs and also in cells with RNA interference (RNAi) knock-down of lamin A/C, which suggests that there are other proteins involved in anchoring SUN1 to the NE.

The NTD of mSUN1 was found to be responsible for interaction with lamin A and was also able to self-interact, as demonstrated by pull-down assays (Haque et al., 2006). In contrast, co-immunoprecipitation studies showed that the CTD of SUN1 interacts with nesprin-2. This suggests that, similar to their *C. elegans* homologues UNC-84 and ANC-1, SUN1 and nesprins can interact to position the nucleus within cells. To delineate the topology of SUN1, transfection studies were performed. The SUN1 N-terminus (residues 1-355) localized mainly in the NE, whereas the C-terminus (residues 450-913) was distributed evenly in the cytoplasm (Fig. 1.22B). Digitonin permeabilization studies (section 3.2) and immunogold-electron microscopy (in
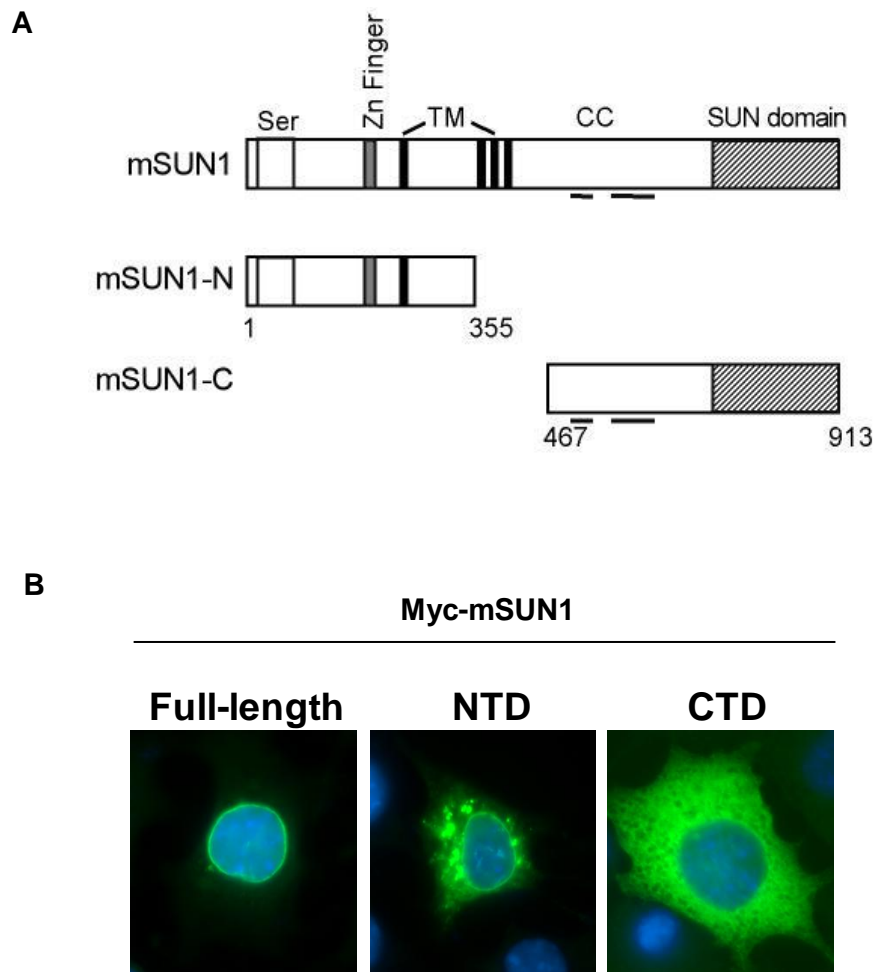
Fig. 1.22. Mouse SUN1 structure and subcellular localization. A) Schematic representation of full-length mSUN1, along with the NTD and CTD constructs used in preliminary studies. mSUN1 contain four putative transmembrane domains (TM) predicted by TMpred; a serine rich domain (Ser) and zinc (Zn) finger motif at the N-terminus and coiled-coil (CC) region and SUN domain (shaded box) at the C-terminus. A consensus nuclear localization signal was not identified in the sequence. **B)** Immunofluorescence microscopy showing localization of myc-tagged full-length mSUN1, NTD and CTD constructs transiently expressed in NIH 3T3 cells, as indicated, and stained with anti-myc 9E10 (green). DNA is stained with DAPI (blue). (Work performed by Dr. S. Shackleton).

A

B

C
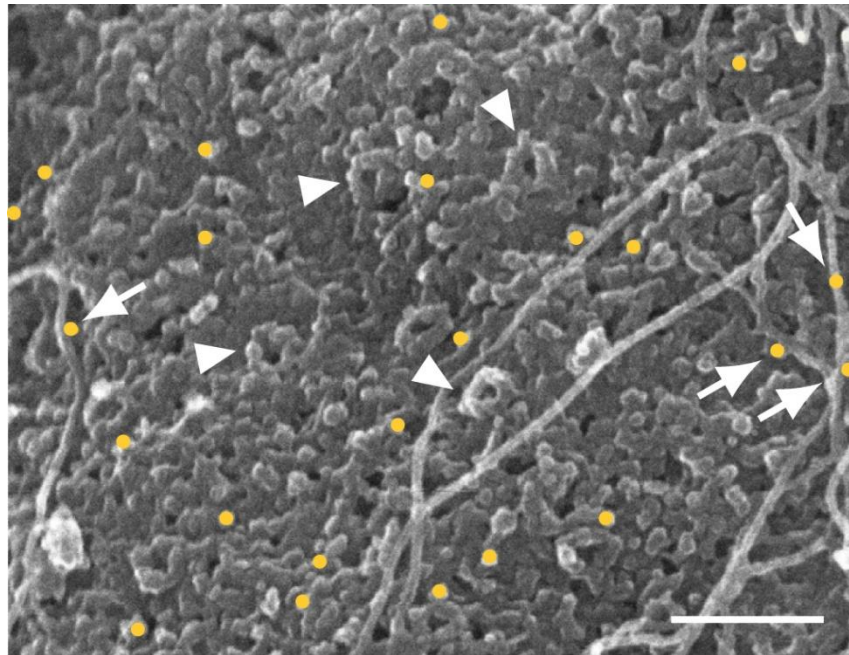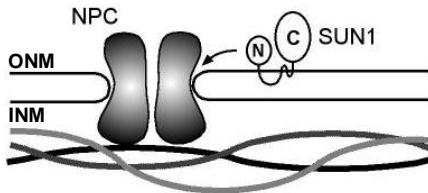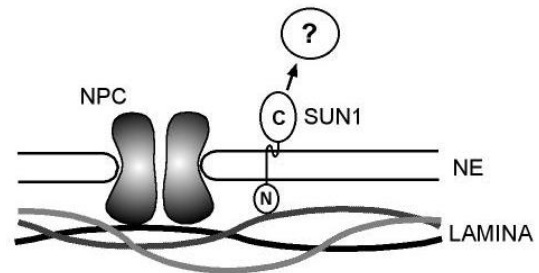
Fig. 1.23. Proposed topology of mSUN1 at the NE. A) NIH 3T3 cells were labelled with SSHR1 antibodies, followed by 10-nm gold-conjugated anti-rabbit secondary antibodies and subjected to immunogold-electron microscopy. A representative image of the cytoplasmic surface of the nucleus is shown. Gold particles are artificially coloured yellow. Arrows indicate gold particles co-localizing with microtubules. Arrowheads indicate nuclear pores. Scale bar, 250nm. **B** and **C)** Initial proposed model of mSUN1 topology at the nuclear envelope. (B) mSUN1 contains four membrane spanning sequences and is inserted into the ER/ONM such that the NTD and CTD both project into the cytoplasm. (C) On reaching the pore membrane domain, the NTD of mSUN1 passes through to the INM and is anchored on the nucleoplasmic face of the NE by interaction with the nuclear lamina. The extended sequence between the first and second transmembrane domains spans the NE lumen. The CTD remains on the outer face of the NE where it may interact with cytoskeletal proteins or nesprins (?) and control nuclear position. (Work performed by Dr. Shackleton in collaboration with Prof Terry Allen, Manchester).

collaboration with Prof. Terry Allen, Paterson Institute, Manchester) also suggested the SUN1 CTD to be located at the cytoplasmic face of the NE (Fig. 1.23). Therefore, the proposed topology was that the NTD resides at the INM, where it interacts with lamin A, whereas the CTD is located on the outer face of the NE. This suggests a highly novel topology where a single polypeptide spans both membranes of NE. The proposed topology was supported by fact that residues 1-355 localise to the NE by itself (Fig. 1.22B). Isolated NTDs of other NE proteins localize mainly to the nucleoplasm (Burke and Stewart, 2002), not the NE, suggesting that 1-355 contains a TMD, which is the first hydrophobic region on mSUN1 (Fig. 1.22A). Following the first TMD, mSUN1 could then traverse the NE lumen and span the ONM with the three clustered TMDs, locating the C-terminal domain to the cytoplasm (Fig. 1.23C).

1.7 AIMS OF THE PROJECT

The aim of this project was to carry out detailed characterization of the novel NE protein, SUN1, by investigating its topology and membrane dynamics, identifying binding partners of both SUN1 and SUN2 and determining whether they play any role in laminopathy disease mechanisms.

1.7.1. Characterization of the sequences required for targeting SUN1 to the NE and delineating its topology

Most INM proteins are targeted to the NE by sequences within their N-terminus and a few also have targeting signals in their membrane-embedded domain (section 1.3). Since SUN1 was a novel uncharacterized NE protein, the project firstly aimed to identify and narrow down the sequences required for targeting SUN1 to the NE. Various deletion constructs of mSUN1 were generated and their localization in NIH 3T3 cells were analyzed by immunofluorescence microscopy. SUN1 topology in the NE was not fully understood and potentially involved a novel conformation. Digitonin experiments were therefore performed to confirm mSUN1 topology in the NE and were compared with that of mSUN2.

1.7.2 Identification of mSUN1 and mSUN2 interacting proteins

SUN1 homologue, UNC-84, is hypothesized to bind to ANC-1 to link the nuclear lamina with the actin cytoskeleton. In addition to binding to lamin A, as found previously in the lab, SUN1 might have other binding partners, in particular nesprins. SUN1 was also found to be stably anchored at the NE in lamin A deficient cells (Haque et al., 2006), therefore SUN1 might also interact with other lamin isoforms or other NE proteins which accounts for its stable anchorage. Current knowledge about the cellular interactions and function of SUN1 are limited. The project therefore aimed to identify mSUN1 and mSUN2 interacting proteins, such as nesprins and other lamins and also map their sites of interaction, by immunoprecipitation and GST/MBP pull down assays.

1.7.3 Potential roles of SUN proteins in laminopathy disease mechanisms

To define the role of SUN proteins in laminopathies, mSUN1 and mSUN2 interaction with a range of lamin A mutants was performed by pull-down assay. Antibodies against human SUN, N- and C-terminus were also generated and used to observe SUN1/SUN2 localization in various laminopathy patient skin fibroblast cell lines. Since lamin A and nesprins have been shown to be mutated in human disease, it is possible that SUN proteins may be associated with these disorders.

CHAPTER 2

MATERIALS AND METHODS

2.1 MATERIALS

2.1.1 General reagents

All chemicals and reagents were purchased from Sigma-Aldrich (Poole, UK), VWR/BDH (Poole, UK) or Fisher Scientific (Loughborough, UK) apart from those listed below.

100 bp DNA ladder	New England Biolabs UK Ltd. (Hitchin, UK)
Agarose	Bio Gene (Kimbolton, UK)
Ampicillin	Melford Laboratories (Suffolk, UK)
dNTPs	GE Health care (St Giles, UK)
IPTG	Melford Laboratories (Suffolk, UK)
L-[^{35}S] methionine	GE Health care (St Giles, UK)
Long ranger acrylamide	FMC Bioproducts (Chicago, USA)
Nonidet P-40	ICN Biomedicals (High Wycombe, UK)
Nitrocellulose membrane	Schleicher and Schuell (Germany)
Protease inhibitor cocktail	Roche (UK)
ProtoGel	National Diagnostics (Hull, UK)
Bovine serum albumin	GE Health care
LE agarose	BioWhittaker Molecular Applications
Glutathione-Sepharose beads	GE Health care
Protein A-Sepharose beads	GE Health care
Amylose resin	New England Biolabs
CNBr-activated sepharose	GE health care
Slide-A-Lyzer dialysis cassettes	Pierce (Rockford, USA)
(3,500 molecular-weight cutoff (MWCO)	
Poly-prep column	BioRad (Hemel Hempstead, UK)

2.1.2 Enzymes

All enzymes and enzyme buffers were purchased from Life Technologies Ltd. (Paisely, UK) or New England Biolabs (Hitchin, UK) apart from those listed below.

AmpliTaq DNA polymerase	ABGene (Epsom, UK)

Pfu DNA polymerase   Stratagene (La Jolla, USA)

BigDye^{TM} terminator cycle sequencer (version 1.0)   Applied Bio System (UK)

2.1.3 Oligonucleotides and Plasmids

All oligonucleotides were purchased from Interactiva (Germany), Invitrogen or Fisher Scientific. Plasmid pMAL-c2G was purchased from New England Biolabs, pCIneo from Promega, pCMV-tag-3B from Stratagene, pGEX-4T3 from GE Health care, pET-28a from Novagen and pEGFP-C1 Clontech. See appendix (Table A.1-A.4 and Fig. A.1-A.5) for constructs used.

2.1.4 Molecular Biology Kits

BigDye terminator version 1.1   Applied Biosystems (Foster City, USA)

BigDye version3.1   Applied Biosystems (Foster City, USA)

Gel purification kit   Qiagen (Crawley, UK)

Midiprep kit   Qiagen (Crawley, UK)

Miniprep kit   Qiagen (Crawley, UK)

PCR purification kit   Qiagen (Crawley, UK)

TNT® Quick Coupled

transcription/translation System   Promega (Madison, USA)

Dye Ex Spin Kit   Qiagen (Crawley, UK)

ECL plus detection kit   GE Healthcare

Performa DTR Gel Filtration Cartridges   Edge BioSystems

2.1.5 Size Markers

1kb DNA ladder (Hyperladder 1)   Bioline

Dual colour protein marker   Biorad

2.1.6 Cell Culture Reagents

Most of the media, reagents and kits for cell culture and transfection were purchased from Invitrogen, UK.

Dulbecco's modified Eagle's medium   GIBCO

Optimem Medium   GIBCO

Foetal Bovine/Calf Serum   GIBCO

Penicillin-streptomycin   GIBCO

Lipofectamine 2000   Invitrogen

Glutamax   GIBCO

Sodium pyruvate   GIBCO

Plasmocin   Invivogen

Cells	Obtained from
NIH-3T3 mouse fibroblasts	ATCC (American Type Culture Collection)
U2OS (human osteosarcoma cells)	ATCC
NRK (normal rat kidney cells)	ATCC
hFF (human foreskin fibrobasts)	ATCC
HGPS, G608G fibroblasts (AG011498)	Coriell Repository
Progeria, T623 fibroblasts	Louise Wilson (Great Ormond Street Hospital, London)
EDMD patient fibroblasts	Manfred Wehnert (Greifswald, Germany)

Table 2.1 Tissue culture cells

2.1.7 Antibodies

Primary antibody	Host	Dilutions for WB	Dilutions for IF	Obtained from
mSUN1CTD (0545)	rabbit	1:500-1:1000	1:100-1:500	S. Shackleton
hSUN1CTD (2379)	rabbit	1:2000	1:500	generated
hSUN1CTD (2383)	rabbit	1:2000	1:500	generated
hSUN1NTD (2371)	rat			generated
hSUN1NTD (2373)	rat	1:400		generated
hSUN2 (2853)	rabbit	1:500	1:150-1:500	S. Shackleton
hSUN2	rabbit		1:2000	D. M. Hodzic (Washington University, USA)
LaminA/C (3262)	rabbit		1:200-1:500	E. Schirmer (Edinburgh University, UK)
Lamin A/C	mouse		1:100	Chemicon
LAP1	mouse		1:200-1:400	L. Gerace (Scripps

				Institute, California, USA)
emerin	rabbit	1:1000	1:500	Glenn Morris (Wolfson Centre for Inherited Neuromuscular Disease, Oswestry,UK)
emerin (AP8)	rabbit	1:3000	1:50	J. Ellis (King's College London, UK)
SREBP1 (H1-160)	rabbit	1:200-1:1000		Santa Cruz Biotechnology
myc (9E10)	mouse	1:500	1:250	Zymed
GFP	rabbit	1:6000-1:8000	1:1000	AbCam
HA (Hemagglutinin)	rabbit	1:500		Santa Cruz
β-actin	mouse	1:5000		Sigma-Aldrich
α-tubulin	mouse		1:10000-1:20000	Sigma-Aldrich
γ-tubulin	mouse		1:500	Sigma-Aldrich

Table 2.2 Primary antibodies (IF: Immunofluorescence microscopy, WB: Western blot)

Secondary antibody	Host	Dilutions	Obtained from
Anti-mouse HRP	rabbit	1:3000	Sigma-Aldrich
Anti-rabbit HRP	mouse	1:3000	Sigma-Aldrich
Anti-rat HRP	goat	1:2000	Sigma-Aldrich
Alexa Fluor® 594 anti-mouse	donkey	1:200	Molecular probes
Alexa Fluor® 488 anti-rabbit	goat	1:500	Molecular probes
Alexa Fluor® 594 anti rat	donkey	1:200	Molecular probes

Table 2.3 Secondary antibodies

2.1.8 Commonly used solutions

2.1.8.1 Common recipes

10× TBE

      890 mM Tris-base

      890 mM boric acid

      20 mM EDTA-NaOH pH 8.0

50× TAE

      2 M Tris-base

      50 mM EDTA

      5.71% (v/v) glacial acetic acid

6× sucrose loading dye

      6× TBE

      35% (w/v) sucrose

      0.25% (w/v) bromophenol blue

      0.25% (w/v) xylene cyanol

TE

      10 mM Tris-HCl pH7.4

      1 mM EDTA pH8

Transformation buffer (TB)

      15 mM $CaCl_2$

      250 mM KCl

      10 mM PIPES

      pH adjusted to 6.7

      55 mM $MnCl_2$

2.1.8.2 Immunofluorescence microscopy

Pre-extraction buffer

      10 mM HEPES pH 7.4

      80 mM KCl

      16 mM NaCl

      1.5 mM $MgCl_2$

      1 mM DTT

      30% Glycerol

      0.5% Triton X-100

      $10\times$ protein inhibitor cocktail

Mounting medium

      3% (v/v) n-propyl gallate

      80% (v/v) glycerol

2.1.8.3 Immunoprecipitation

Lysis buffer

      10 mM HEPES pH 7.4

      50 mM NaCl

      5 mM EDTA

      1% Triton X-100

      $1\times$ protease inhibitor cocktail

      1 mM PMSF

Wash buffer

      10 mM HEPES pH 7.4

      50 mM NaCl

      5 mM EDTA

      1% Triton X-100

2.1.8.4 Antibody purification

Coupling buffer

0.2 M $NaHCO_3$

0.5 M NaCl

Adjusted to pH 8.5 with NaOH

Acetate buffer

0.1M Sodium acetate/HCl,

0.5M NaCl

Adjusted to pH 4

2.1.8.5 Protein Analysis

$1\times$ PBS

137 mM NaCl

2.7 mM KCl

4.3 mM Na_2HPO_4

1.4 mM KH_2PO_4

Lower separating gel (7.5%)

1.5 ml of lower buffer

1.5 ml of Protogel

3 ml of dH_2O

75 µl of 10% APS

5 µl of TEMED

Upper stacking gel (4%)

325 µl of Protogel

625 µl upper buffer

1.5 ml dH_2O

75 µl of 10% APS

5 µl of TEMED

Laemmli buffer

    62.5 mM Tris-HCl pH6.8

    5% (v/v) β-mercaptoethanol

    20% (v/v) methanol

    2% (w/v) SDS

    0.2% (w/v) bromophenol blue

    10% (v/v) glycerol

$10\times$ SDS-PAGE running buffer

    250 mM Tris-base

    1.92 M Glycine

    1% (w/v) SDS

SDS-PAGE lower buffer

    1.5 M Tris-HCl pH 8.8

    0.4% (w/v) SDS

SDS-PAGE upper buffer

    0.5 M Tris-HCl pH 6.8

    0.4% (w/v) SDS

Coomassie stain

    40% (v/v) methanol

    10% (v/v) acetic acid

    0.05% (w/v) Coomassie blue

Destain

    40% (v/v) methanol

    10% (v/v) glacial acetic acid

NETN buffer

    0.5%-1.5% (v/v) Nonidet P-40

    1 mM EDTA

    20 mM Tris-HCl pH8

    100 mM NaCl

Transfer buffer

      25 mM Tris-base

      192 mM glycine

      20% (v/v) methanol

Ponceau S stain

      0.1% Ponceau S (w/v) in 5% acetic acid

Blocking buffer

      5% marvel (w/v) milk in PBS/0.1% Tween 20

PBS/Tween 20

      0.1% Tween (v/v) in $1\times$ PBS

$10\times$ Protease inhibitor cocktail (Roche)

      1 mini tablet

      1 ml H_2O

Stripping buffer

      100 mM β-mercaptoethanol

      2% (w/v) SDS

      62.5 mM Tris-HCL pH 6.7

2.1.8.6 Sequencing

Formamide loading dye (5:1 ratio)

      5 ml deionized formamide

      1 ml 25 mM EDTA (pH 8) containing 50 mg/ml blue dextran

5% acrlyamide sequencing gel

      10.8 g urea

      3 ml Long Ranger® acrylamide

      3 ml $10\times$ TBE

      15.6 ml dH_2O

      21 μl TEMED

      150 μl 10% APS

2.1.8.7 Bacterial Media

LB agar

      1 % (w/v) tryptone

      0.5% (w/v) yeast extract

      1 % (w/v) NaCl

      1.5% (w/v) agar

LB broth

      1% (w/v) tryptone

      0.5% (w/v) yeast extract

      1 % (w/v) NaCl

2.2 METHODS

2.2.1 Preparation of plasmid DNA

2.2.1.1 Miniprep

A 5 ml bacterial culture containing the desired plasmid and appropriate antibiotic, was grown overnight at 37°C in a shaking incubator (see section 2.2.8). The culture was then centrifuged at 3,500 rpm for 10 min at RT to form a pellet. The supernatant was discarded and the Qiagen miniprep kit was used to extract plasmid DNA from the bacterial pellet, following the manufacturer's protocol. Purified plasmid DNA was then eluted in 30μl of dH$_2$O and stored at –20°C.

2.2.1.2 Midiprep

A 50 ml bacterial culture was grown overnight and used for large-scale plasmid extraction. The culture was centrifuged at 3300×g for 15 min at RT. The supernatant was discarded and the bacterial pellet was used to obtain plasmid DNA, using a Qiagen midiprep kit according to the manufacturer's protocol. Purified plasmid DNA was resuspended in 200μl of dH$_2$O and then stored at –20°C. The DNA concentration was measured by OD at 260 nm, with a UV spectrophotometer.

2.2.2 Polymerase chain reaction (PCR)

2.2.2.1 Oligonucleotide design

Oligonucleotides for PCR-based cloning were designed to be 25-30 bp in length with an AT:CG ratio of 50-60%, thus ensuring an annealing temperature of around 55-60ºC. To incorporate appropriate restriction enzyme sites for cloning, additional bases were added to the 5' end of the oligonucelotide sequences. Further as necessary additional bases were added between restriction enzyme sites and coding sequence to ensure the maintenance of the correct reading frame upon insertion into the vector. Also four random nucleotides were added on the 5' end to ensure binding and cleavage by restriction enzymes.

2.2.2.2 PCR for cloning

Oligonucleotide primers (as shown in Table 2.4) were used to generate required constructs by PCR, using appropriate plasmid as template. PCR reactions were set up as follows:

10× PCR buffer	10 µl
2 mM dNTPs	10 µl
15 mM MgCl$_2$	10 µl
5 µM forward primer	5 µl
5 µM reverse primer	5 µl
Pfu DNA polymerase	0.1 µl
Taq DNA polymerase	0.9 µl
Template plasmid DNA	1-2 ng
Adjusted with dH$_2$O	100 µl

PCR reactions were placed in PCR tubes and performed on a DNA Engine Thermal Cycler (MJ Research Inc. Waltham, USA) or G-Storm Thermal Cycler (GRI). The PCR program used was as follows, the annealing temperature varied according to the primers used to increase the specificity of the PCR and the extension period also varied with the size of PCR product:

STEP	TEMP	TIME (min:sec)	PROCESS
1	94°C	1:00	Initial DNA denaturation
2	94°C	0:30	DNA denaturation
3	45-65°C ·	0:30	Oligonucleotide annealing
4	72°C	0:30	DNA polymerase extension (1min/kb of product length)
5	-	-	Go to STEP 2, 34 times
6	72°C	3:00	Final extension

The resulting PCR reactions were stored at -20°C until needed and 5-10 µl sample was separated on agarose gel to verify that correct sized product was produced (section 2.2.4). PCR products were purified using a Qiagen PCR column purification kit following the manufacturer's protocol.

Name	Primer sequence 5'-3'	Construct
LIPABamF	GTACGGATCCATGGACTTTTCTCGGCTGCACAC	SUN1(1-229)
LIPA229R2	ACTGGTCGACTACCTATCCAGGTAAAAGGACAC	
LIPA-229F	GTACGGATCCAGGACTCTGTGGCTGGCCAAG	SUN1(223-355)
LIPA355-SalR	GATCGTCGACTATCTAGTCCTTCGCAGTGCTTGAAC	
LIPABamF	GTACGGATCCATGGACTTTTCTCGGCTGCACAC	SUN1(1-432)
LIPA-432R	ACACGTCGACTAGGAGACACCAGCACCTAGTAA	
LIPA-355F	GTACGGATCCAGAGCTGCCGGGTGGTCTGT	SUN1(355-913)
LIPA-SalR	ACTGGTCGACCTACTGGATGGGCTCTCCGTGGACT	
LIPA-229F	GTACGGATCCAGGACTCTGTGGCTGGCCAAG	SUN1(229-913)
LIPA-SalR	ACTGGTCGACCTACTGGATGGGCTCTCCGTGGACT	
LIPA-EcoF	GATCGAATTCCATGGACTTTTCTCGGCTGCACAC	SUN1(1-138)
LIPA138R	CACAGTCGACCTCATCTAGCACAGGGTGCC	
mSUN2EcoF	CACGAATTCATCGAGACGAAGCCAGCGCCTC	SUN2(1-129)
mSUN2129R	CACAGTCGACCTAGGTGAGCCCATTGGCCTTGC	
mSUN2EcoF	CACGAATTCATCGAGACGAAGCCAGCGCCTC	SUN2(1-83)

mSUN283R	CACAGTCGACGCTGCCGATGTAGGACTCTCG	
hSUN1-EcoF	GAGAGAATTCATGGATTTTTCTCGGCTTCAG	SUN1(1-217)
hSUN1-Sal217R	GAGAGTCGACTAATTCCTGTCCCTAGAATAAAC	
hSUN1-Eco352F	GAGAGAATTCAGCATGCATAGAACACAGCGG	SUN1(352-812)
hSUN1-SalR	GAGAGTCGACTCACTTGACAGGTTCGCCATG	

Table 2.4 Primers used for PCR-based construct generation

2.2.3 Restriction enzyme digestion

Plasmids containing the required inserts and PCR products were digested with appropriate restriction enzymes in the appropriate 1× enzyme buffer. Most commonly, *EcoR*I and *Sal*I restriction enzyme sites were used for cloning PCR products into relevant vectors. For cloning purposes, reactions were performed in 50 μl volumes. In general, 5 μl of 10× restriction enzyme buffer (compatible for both enzymes, for example commonly used *EcoR*I buffer at 37ºC) and 0.5 μl of each enzyme were combined with 1-2 μg of plasmid DNA or 40 μl of purified PCR product and the final volume was adjusted to 50 μl with dH$_2$O. For verification of cloning products, 2-3 μl of minipreped plasmid DNA was digested in a 10 μl volume with 0.3 μl of restriction enzymes. Reactions were incubated at appropriate the temperature for 1-2 hours and electrophoresed on an agarose gel.

2.2.4 Agarose gel electrophoresis

DNA samples from plasmid digests or PCRs were analysed by adding 1/6th volume of 6x sucrose loading dye and were loaded on a 1% agarose gel (dissolved in 1× TBE or 1× TAE), containing 400 ng/ml of ethidium bromide. The gels were run at 120 V in 1× TBE or 1× TAE for approximately 60 minutes and viewed on a UV trans-illuminator. For cloning, digested insert or PCR and vector DNA were run on an agarose gel and viewed on the trans-illuminator to excise the gel bands with a scalpel.

2.2.5 DNA ligation

Restriction digested DNAs were firstly purified according to the manufacturer's protocol using a Qiagen PCR purification kit. For bands excised from an agarose gel,

the DNA was instead purified using a Qiagen gel purification kit. The purified DNA was then resuspended in dH_2O and stored at -20°C. DNA concentration was quantified by gel electrophoresis and comparing the band intensity to a quantified standard (usually the DNA ladder Hyperladder I).

Approximately 20 ng of vector was used in a ligation reaction. Insert was combined with vector to give 3:1 to 10:1 ratio. Ligation reactions were set up between insert and vector DNA using 1 µl of 10× T4 DNA ligase buffer and 1 µl of T4 ligase to a final volume of 10µl (adjusted with dH_2O) and incubated at 16°C overnight.

2.2.6 Generation of competent cells

Fresh *E. coli* strain (DH5α or BL21) was streaked on a LB agar plate and grown overnight at 37ºC. The following day, one colony of *E. coli* was picked and inoculated in 2 ml LB medium and grown overnight. The next day, 0.5 ml of the culture was inoculated in 500 ml of LB, containing 2.5 ml of 2 M $MgCl_2$ and incubated at 18-22ºC, 100 rpm until OD_{600}=0.3-0.6. The culture was then rapidly cooled on ice and centrifuge at 2,500× g, 0ºC for 10 min. The following steps were performed in the cold room. The supernatant was discarded and the pellet was resuspended in 150 ml of ice cold transformation buffer (TB) and centrifuged as before. The pellet was then gently resuspended in 40 ml of ice cold TB and 3 ml DMSO was added with gentle swirling. The cell suspension was then aliquoted in 100-500 µl into eppendrofs and immediately frozen by liquid nitrogen and stored at 80ºC.

2.2.7 Bacterial transformation

Purified circular plasmids (1ng) or 2 µl of ligation reactions were transformed into chemically competent *E. coli* strain DH5α or BL21 (for protein expression studies only). A 100 µl of competent bacteria (stored at −80°C) were thawed and incubated on ice with the plasmid for 30 min. The bacteria were then heat-shocked at 42°C for 90 sec and held on ice for 5 min for plasmids carrying ampicillin resistance gene the bacteria were plated onto LB agar media containing 100 µg/ml ampicillin. If the plasmid carried the kanamycin resistance gene, then the bacteria were incubated in 1.5 ml tube containing 500 µl LB media at 37°C for 30 min longer to allow expression of the kanamycin resistance gene and then 200 µl was plated on to an LB agar plate containing

30 µg/ml kanamycin. The plates were then incubated at 37°C overnight to allow colony formation and stored at 4°C until needed.

2.2.8 Growth and storage of bacteria

Bacterial colonies were picked from LB agar using a sterile tip and inoculated into 5 ml LB medium containing 50-100 µg/ml ampicillin or 30 µg/ml kanamycin, as appropriate, and incubated at 37°C, shaking at 220 rpm overnight and used as per requirement. For long-term storage, 750 µl of the bacterial overnight culture was mixed with 250 µl of 80% glycerol and stored at -80°C.

2.2.9 Fluorescent DNA sequencing of plasmids

2.2.9.1 *Sequencing with ABI 377 sequencer*

Initially, sequence reactions and acrylamide gels were run in the lab using an ABI377 sequencer. Later, completed sequence reactions were sent to the University of Leicester sequencing service (PNACL) and were run on an ABI 3730 sequencer (section 2.2.9.2). Plasmid DNAs were sequenced after miniprep and verified by restriction enzyme digestion, using primers flanking the vector multiple cloning site or primers internal to the cDNA.

Basic sequencing reaction:	Big Dye terminator mix	2 µl
	Primer (5 µM)	0.6 µl
	Plasmid DNA	200 ng
	Add dH$_2$O to	10 µl

Sequencing reactions were placed in 0.2 ml PCR tubes or in a 96 well micro-titre plate (ABGene, Epsom, UK), covered with an adhesive lid and placed in a DNA Engine Thermal Cycler (MJ Research Inc. Waltham, USA). Cycle sequencing was performed as follows:

Sequencing program

STEP	TEMP	TIME	PROCESS
1	96°C	10 sec	DNA template denaturation

2	50°C	5 sec	oligonucleotide annealing
3	60°C	4 min	DNA polymerase extension
4	-	-	Go to STEP 1, 28 times

The resulting sequencing reactions were stored at -20°C until needed. The sequencing reaction was purified from unincorporated dye terminator using a DyeEx spin kit following the manufacturer's protocol. The DNA samples were then dried in heated block at 70°C for 1 hr and resuspended in 3 μl of formamide loading buffer. This was denatured at 96°C for 2 min and held on ice.

Polyacrylamide gels were made using 36 cm well-to-read ABI glass plates. A 5% gel mix was made (section 2.1.8.6) and allowed to set for 2 hours. Samples were loaded on the gel and electrophoresed using 1× TBE on an ABI 377 DNA fragment analyser (Applied Bio systems. Foster City, USA). Raw data were saved for later analysis using the Sequencing Analysis v3.4.1 package (Applied Biosystems. Foster City, USA).

2.2.9.2 Sequencing using the PNACL service

Whilst using PNACL's service (University of Leicester) the sequencing reaction was performed as follows using PNACL protocol:

Big dye V3.1	0.5 μl
5 × Buffer (supplied)	1.75 μl
Plasmid DNA	1 μl of miniprep (200ng)
Primer (5 μM)	1 μl
Add dH$_2$O to	10μl

Sequencing reactions were placed in 0.2 ml PCR tubes or in a 96 well micro-titre plate (ABGene, Epsom, UK), covered with an adhesive lid and placed in a PCR machine. Cycle sequencing was performed as described in section 2.2.9.1. The finished sequencing reactions were purified using PNACL's protocol. 10 μl of dH$_2$O and 2 μl of 2.2% SDS was added to the reaction, mixed and then incubated at 98°C for 5 min, followed by 25°C for 10 min, in a PCR machine. Then Performa DTR Gel Filtration

Cartridges were used to remove dye terminators, using the supplier's protocol. The samples were then sent to PNACL for running on an Applied Biosyatem 3730 sequencer. The data were analyzed using computer software SeqEd.

2.2.10 Mammalian cell culture and transfection

2.2.10.1 Cell culture and propagation

Human osteosarcoma (U2OS) cells, mouse NIH 3T3 fibroblasts and normal rat kidney (NRK) cells were grown in DMEM medium containing 4500 mg/L glucose, supplemented with 10% fetal calf serum and 500 U/ml penicillin & 500 μg/ml streptomycin in a cell culture flask or petri dish. This was incubated at 37°C in 5% CO_2 and confluence of cell was checked daily under a microscope When cells reach approximately 90% confluence, they were washed in PBS and detached by incubation with $1\times$ trypsin (0.05%) in PBS for 5 min at 37°C. The cells were collected in a sterilin tube, centrifuged at 200g for 5 min using an Eppendorf 5840 benchtop centrifuge and resuspended in fresh new medium. For general propagation of the cell lines, cells were passaged at a 1:5-1:10 ratio into a new dish. To seed specific numbers of cells for experiments, trypsinised cells were counted using a haemocytometer (BS 748 Hawksley, UK). The haemocytometer is designed such that the number of cells in one set of 16 corner squares is equivalent to the number of cells x 10^4 / ml. The number of cells per ml was calculated using the following equation.

$$\text{Cells / ml} = \frac{\text{The total count from 4 sets of 16 corner squares}}{4} \times 10^4$$

A calculated amount of cells were seeded into appropriate sized dishes, as described in the following sections, with fresh medium.

2.2.10.2 Propagation of primary human dermal fibroblasts

Dermal fibroblast obtained from laminopathy patients were cultured in DMEM containing 4500 mg/L glucose, supplemented with 15% fetal calf serum, 500 U/ml penicillin & 500 μg/ml streptomycin, $1\times$ Glutamax, 1mM sodium pyruvate in small $25cm^2$ flask when recovered. Then the cells were transferred to $75cm^2$ flask for

expansion and propagated as described above and passaged at 1:3 ratio. When required, 2.5 µg/ml plasmocin was added to the medium to prevent mycoplasma infection and 25 µg/ml plasmocin was used if there was an infection. The slower growing cells were regularly passage at low confluence (40-50%) every 3-4 days, to keep them healthy. The cells were used between passage 9 and 12 for experiments.

2.2.10.3 Freezing and storage of cells

To freeze, cells were trypsinised and pelleted as described in section 2.2.10.1.Thereafter cells were resuspended in freezing medium (5% DMSO in DMEM) and 1 ml was transferred to labelled cryo-vials (Nunc). The cells were frozen at -80ºC for 48 hour using insulated boxes and then transferred to liquid nitrogen for long term storage.

2.2.10.4 Recovery of cells

Cells were removed from liquid nitrogen and thawed quickly by adding pre-warmed DMEM to the vial and pipetting up and down multiple times Then the cells were centrifuged at 1100 rpm in an Eppendorf 5840 benchtop centrifuge for 5 min and resuspended in appropriate fresh medium and transferred in a petri dish (10 cm) or small flask (25 cm^2) for propagation at 37ºC, 5% CO_2.

2.2.10.5 Preparation of acid-etched coverslips

Coverslips were incubated in a container with 1M HCl for 30 min at RT, on a rocking platform. Afterwards coverslips were turned over to ensure that the both surfaces of the coverslips are treated equally. The coverslips were then rinsed with ddH$_2$O and washed in 100% ethanol for another 30 min (15 min each side). Then the coverslips were dried on 3MM paper and sterilized by baking at 140ºC.

2.2.10.6 Transient transfection

For immunofluorescence (IF) microscopy, 2×10^5 U2OS or NIH 3T3 cells or 3×10^4 NRKs were seeded onto 22×22 mm coverslips in 6 well dishes and incubated overnight. The next day, the cells were transfected with mammalian expression vector containing appropriate constructs using Lipofectamine 2000, according to manufacturer's protocol.

Briefly, for U2OS and NIH 3T3 cells, 1 μg of plasmid DNA was mixed with 3 μl of Lipofectamine 2000, each previously diluted in 100 μl OPTI-MEM medium and incubated at RT for 20 min. The transfection mix was then added to wells of cells, mixed by gentle swirling and incubated at 37°C overnight in a 5% CO_2 incubator. NRK cells were particularly difficult to transfect and for optimal transfection, 4 μg of plasmid DNA and 6 μl of Lipofectamine 2000 were used following the protocol as above. For immunoprecitation (IP) or protein extraction studies 10 cm plates containing U2OS or mouse NIH 3T3 cells, were generally transfected with 4 μg of plasmid DNA and 12 μl of Lipofectamine 2000. Cells were the generally incubated for 24 hours, prior to fixation for IF microscopy (section 2.2.11) or for IP or protein extraction (section 2.2.12 and 2.2.16). In some instances, cells were incubated for 48, 72 or 120 hours post-transfection. In these cases, the cells were trypisinized and seeded at a 1:2 or 1:4 dilution, as appropriate to avoid over-confluence.

2.2.11 Immunofluorescence microscopy

Following the growth of a required cell line on acid-etched coverslips in 6 well dish, the medium was removed and cells washed twice in 1x PBS. Cells were then fixed and permeabilized in ice-cold methanol for 20 minutes at –20ºC or fixed with freshly prepared 4% paraformaldehyde solution in PBS, incubating for 30 minutes at room temperature. Thereafter cells were washed with 3× 5 minutes in PBS. If paraformaldehyde fixation was used, cells were the permeabilized by incubation at RT with 0.5% Triton-X 100 in PBS for 5 min. For digitonin permeabilization studies cells were instead permeabilized with freshly prepared digitonin 40 μg/ml on ice for a range of time, 5 minutes to 15 minutes. For Triton pre-extraction, cells were subjected to 0.5% Triton extraction before fixation. Cells were washed in cold PBS and then incubated on ice for 5 minutes with freshly prepared pre-extraction buffer, as described in materials section. The cells were fixed immediately with methanol without pre-washing with PBS.

The fixed and permeablized cells were washed 3× 5 minutes in PBS and then blocked with 1% bovine serum albumin (BSA) in PBS to block non-specific antibody binding and then incubated for 1 hour with primary antibodies diluted in 1% BSA in PBS. Thereafter, cells were washed with 1× PBS for 3-5 min four times. Following this, cells

were incubated for 1 hour with appropriate secondary antibody and 0.2 µg/ml Hoechst 33258 to stain the DNA. Antibodies used are listed in table 2.2 and 2.3. Cells were washed for $4\times$ 5 minutes in PBS after incubation with each antibody. Coverslips were mounted upside-down onto microscope slides with one drop of mounting medium, edges were sealed with clear nail varnish to prevent drying and slides were stored in the dark at 4ºC. Cells were viewed and photographed with a Nikon TE300 inverted microscope using an ORCA ER charge couple device camera (Hamamatsu) and Openlab 3.09 software (Impovision).

2.2.12 Immunoprecipitation

2×10^6 3T3 or 2.5×10^6 U2OS cells were seeded onto 10 cm petri dishes. The next day, when 70% confluent, the cells were transfected with appropriate plasmid constructs, as in section 2.2.10.6. The following morning, the medium was aspirated and cells were washed with 5 ml cold $1\times$PBS. Then 600 µl of lysis buffer (as described in materials) was added and the plate incubated on ice for 20-30 min. Afterwards, cells were scraped off from the plate and transferred to an eppendorf. This lysate was incubated on ice for 10 minutes. The lysate was then sonicated on ice $3\times$ 15 sec at 12 mA using Soniprep 150 (MSE), centrifuged at 13,000 rpm for 1 min at 4ºC to pellet the cell debris and the supernatant was removed to a new tube. At this point the sample could be snap-frozen in liquid nitrogen and stored at -80ºC for later use. Next, 20 µl protein A-Sepharose and 1 mM PMSF were added to the lysate and incubated for 1 hr at 4ºC, on a rotating wheel, for pre-clearance of non-specific binders of protein A-Sepharose. To prepare protein A-sepharose, 0.5 g was washed twice in 20 ml dH$_2$O, centrifuged for 2 min at 500 g at 4ºC. The beads were then resuspended in 5 ml PBS containing 0.1% sodium-azide and stored at 4ºC for future use.

The lysate was then centrifuged at 500 g for 5 min and the supernatant was transferred to a new tube. Thereafter, 1-2µg of appropriate antibody was added to the supernatant to bind its respective protein and was incubated for 2 hr at 4ºC on a rotating wheel. Next, 20 µl of protein A-Sepharose was added and incubated for 1 hr at 4ºC rotating, to pull down the antibody and co-precipitated proteins. The sample was centrifuged at 500 g for 5 min at 4ºC to pellet the protein A-Sepharose beads and the supernatant was discarded. The pellet was washed 3 times, with 1 ml wash buffer (lysis buffer without protease inhibitor and PMSF) and centrifuged at 500 g for 5 min at 4ºC. The supernatant

was discarded each time and after the last wash, 10 µl Laemmli buffer was added to the pellet, boiled for 5 min and then run on a SDS-PAGE gel for western blot (section 2.2.17 and 2.2.18).

2.2.13 MBP pull-down or GST pull-down

2.2.13.1 In vitro translation of proteins

The TNT® T7 Quick-Coupled transcription/translation system was used to perform in vitro translation of plasmids containing cDNA sequences downstream of a T7 promoter. Appropriate plasmid (1 µg) was combined with 40 µl of TNT® master mix, 2 µl of [^{35}S] methionine and the final volume was adjusted to 50 µl with nuclease-free dH$_2$O. This reaction was scaled up when necessary. Samples were incubated at 30°C for 90 min, and then stored at -80°C after snap freezing in liquid nitrogen, until needed.

2.2.13.2 Bacterial expression and purification of MBP- /GST-fusion protein

pMALc2G or pGEX-4T plasmids containing the appropriate cDNA sequences were transformed into *E. coli* strain BL21. A single colony was inoculated in 2 ml LB medium containing 50 µg/µl ampicillin and grown shaking at 220 rpm, 37°C overnight. The culture was diluted 20-fold in an appropriate volume of LB (to yield approximately 5 µg of fusion protein), supplemented with 50 µg/ml ampicillin and 0.2% glucose (in the case of MBP-fused constructs) and then grown for 2 hr at 30°C, shaking at 220 rpm. After that IPTG was added to a final concentration of 0.2 mM and the culture grown for another 2 or 3 hr. The culture was then centrifuged at 3,000 rpm for 10 min at 4°C using a bench-top centrifuge and the pellet resuspended in 1 ml of 0.5%-1.5% NETN supplemented (higher concentration of NETN was used to increase the stringency of the buffer to reduce non-specific binding of proteins) with 100 mM PMSF . Cells were sonicated 3 times for 15 sec at 12 mA using Soniprep 150 (MSE), and then centrifuged at 11,000× g for 10 min at 4°C using Sorvall® RC-5B refrigerated super-speed centrifuge. The supernatant was collected and 40 µl 50% amylose or 25 µl of 50% glutathione-Sepharose beads were added to the supernatant (section 2.2.13.4), as required and then incubated at 4°C in rotating wheel for 1 hr. The sample was

centrifuged at 1000×g for 2 min at 4°C, using a refrigerated microcentrifuge. The supernatant was discarded and the beads were washed 3 times in 1 ml NETN buffer and centrifuged at 1000×g for 2 min. The beads were then resuspended either in 15 μl of Laemmli buffer for direct loading on a protein gel or in 500 μl NETN buffer (4°C).

2.2.13.3 MBP pull–down

Purified MBP or GST proteins, bound to amylose or glutathione-Sepharose beads, respectively (section 2.2.13.2), were incubated with appropriate amounts of in vitro-translated protein (section 2.2.13.1) in a total volume of 500 μl of (0.5-1.5%) NETN (percentage varied according to the stringency of the required buffer), supplemented with 1 mM PMSF. These were incubated at 4°C on a rotating wheel for 2-3 hr. Samples were then centrifuged at 1000×g for 2 min, using a refrigerated microcentrifuge, and washed 3 times with 1 ml NETN buffer at 4°C. 15 μl of Laemmli buffer was added to the beads and heated to 96°C for 10 min. Samples were stored in –20°C until needed or directly loaded on an SDS-PAGE gel (section 2.2.17).

2.2.13.4 Preparation of amylose or glutathione beads

For preparation of 50% amylose resin or glutathione beads, 1.33 ml of respective beads were transferred to 15 ml tubes and centrifuged at 500 g for 5 min at 4ºC. The supernatant was removed and the pellet washed with 10 ml of cold 1×PBS, then re-centrifuged and the supernatant discarded. Finally the beads were resuspended in 1 ml cold 1× PBS and stored at 4 ºC for up to 2 months.

2.2.14 Large scale bacterial expression of MBP-fusion proteins as antigen for antibody production

For antigen production, appropriate plasmids containing MBP-fused hSUN1 NTD or CTD, pMAL-hSUN1(1-217) and pMALhSUN1(352-812), respectively or MBP alone were transformed into *E. coli* BL21. A culture of the appropriate colony was grown overnight in 75 ml LB media, supplemented with 50-100 μg/ml ampicillin and the following morning the culture was inoculated into 1.5 litre LB medium, supplemented with 50-100 μg/ml ampicillin and 0.2% glucose. As in section 2.2.13.2, the induction

was carried out. The culture was then centrifuged and the pellet was resuspended in 20 ml of 1.5% NETN supplemented with 1 mM PMSF. The sample was sonicated 6 times for 15 sec at 12 mA and then centrifuged at 11,000× g for 10 min at 4ºC. The supernatant was collected and 7.5 ml of 50% amylose beads added, then incubated at 4°C in rotating wheel for 3 hr. The sample was centrifuged at 500×g for 5 min at 4°C. The supernatant was discarded and the beads then resuspended in 10 ml of cold 1× PBS and poured into large polyprep chromatography columns and then washed 6× with 7.5 ml of cold 1× PBS. Proteins were ultimately eluted in 18× 1 ml fractions of cold 1× PBS containing 10 mM maltose and fractions were tested for protein expression by running on SDS-PAGE gel as described in section 2.2.17. Appropriate fractions were stored at -80°C after snap-freezing in liquid nitrogen.

2.2.15 Antibody purification

2.2.15.1 *Preparation of MBP-hSUN1CTD-CNBr affinity column*

MBP-hSUN1CTD protein generated was dialysed against coupling buffer. One slide-A-lyzer dialysis cassettes was used per 3 ml of protein sample. The cassette was briefly wet in the coupling buffer, then the protein sample was inserted to a cassette using a syringe. Any remaining air was removed and the cassettes were submerged in coupling buffer for dialysis, mixing gently overnight, at 4ºC.

1ml CNBr-activated Sepharose, which has binding capacity for 1-10 mg antigen, was swollen by adding 0.25 g of CNBr powder to 50 ml 1 mM HCl, rotating for 15 min at room temperature. The CNBr-Sepharose was then washed twice with 30-50 ml coupling buffer and centrifuged 2 min at 1000×g, at room temperature. The CNBr gel was then mixed with the dialysed protein, after carefully taking it out of the cassette with a syringe. The mixture was incubated in a 50 ml tube at room temperature for 2 hr and further incubated overnight at 4ºC on a rotating wheel. The next day, the mixture was centrifuged at 100×g for 2 min, the supernatant was removed and a 10 μl sample removed to test binding capacity of the beads. The pelleted beads were washed with 10 ml coupling buffer to remove unbound protein, then centrifuged again and 10 μl sample was removed to test for protein loss during washing. The remaining active groups on the CNBr gel were blocked with 0.2 M glycine pH 8.5, rotating for 2 hr at room

temperature. The gel was transferred to 10 ml polyprep chromatography column and excess blocking reagent and non-covalently adsorbed protein were washed away with 3 cycles of 50 ml coupling buffer, followed by acetate buffer (0.1 M sodium acetate/HCl/ 0.5M NaCl pH4). The column was stored at 4ºC with 9 ml PBS, containing 0.02% sodium-azide for later use. The percentage of protein bound to the CNBr beads was calculated by running the test samples on SDS-PAGE gel and deducting the amount of lost (unbound fraction after overnight binding to the beads and wash by coupling buffer) from initial dialysed protein.

2.2.15.2 *Affinity purification of SUN1 antibodies*

A 1ml aliquot of serum was diluted 1:4 with cold 1×PBS. Then the serum was centrifuged at 2000 rpm for 5 min at 4ºC to remove aggregates. A 20μl sample was removed for later analysis. The serum was then passed 5 times through an MBP affinity column (generated as in section 2.2.15.1), to remove anti-MBP antibodies and non-specifically bound antibodies. A 20μl sample was again removed for analysis.

Next, the MBP-hSUN1CTD affinity column prepared as in section 2.2.15.1 and then washed with 10 -15 ml cold 1× PBS. A stopper was inserted at the bottom of the column and the diluted serum that had been passed through the MBP column was added and sealed. Afterwards the column was incubated overnight at 4ºC, on a rotating wheel. The following day, the flow-through was collected on ice and a 30μl sample was removed for analysis. Then the column was washed with 20 ml of cold 10 mM Tris pH 7.5 and 20 ml of cold 20 mM Tris pH7.5/500 mM NaCl, to remove any loosely attached proteins. Thereafter, the antibody was eluted from the column with 100 mM glycine pH2.5 in 10× 500 μl fractions into eppendorfs containing 75μl of 1M Tris pH8. The fractions were stored at 4ºC with added 0.02% sodium-azide. Columns were washed with 10 ml of 10 mM Tris pH 7.5 and stored at 4ºC, with 10 ml cold 1× PBS/0.02% sodium-azide.

2.2.16 Preparation of total protein extracts from tissue culture cells

Confluent cells from a 75cm^2 flask were trypsinized and pelleted by centrifugation at 1,100 rpm for 5 min using eppendorf 5840 bench top centrifuge. Pellets were washed in PBS and recentrifuged. Then the pellet was resuspended in 250 μl of PBS. An equal volume of Laemmli buffer was added and samples were boiled for 10 minutes and stored at -20°C for later use.

2.2.17 Sodium dodecyl sulfate polyacrylamide gel electrophoresis (SDS-PAGE) analysis of proteins

Protein samples were mixed with an equal volume of 2× Laemmli buffer and heated at 96°C for 3 min prior to gel electrophoresis. SDS polyacrylamide gels were poured into 10× 7 cm glass plates with 0.75 mm thick spacers using the mini Protean III casting apparatus (Biorad. Hercules, USA). Firstly, a lower 7.5% separation gel was poured and this was covered with isopropanol to obtain a completely horizontal level and left to polymerise for 20-30 min. The isopropanol was washed off using dH2O and a 4% stacking gel was poured on top of the lower gel, a comb was inserted and the gel left to polymerise for 15-20 min. Protein samples (up to 25 μl) were loaded and electrophoresed at 150 V for 1 hr in 1× SDS-PAGE running buffer.

For visualization of bacterially expressed proteins and *in-vitro* translation products, gels were stained with Coomassie staining solution, with gentle agitation for 20 min and washed in destaining solution for 30-60 min or until background blue staining disappeared. Gels were dried on Whatman 3MM paper using a gel drying apparatus (Bio-Rad. Hercules, USA). For visualization of ^{35}[S]-labelled *in-vitro* translated proteins, autoradiography was performed, placing an X-ray film on the dried gel for 1-2 days or more and developing using a compact X4 X-ray film processor (Xograph imaging system).

2.2.18 Western Blotting

2.2.18.1 Blotting

After electrophoresis (section 2.2.17) protein gels were blotted on nitrocellulose membrane using a Hoefer semi-dry transfer apparatus. Nitrocellulose membrane was cut to 10 cm × 6 cm, soaked in transfer buffer for 10 min. After removing the gel from the gel running apparatus, the stacking gel was removed and the gel was soaked in transfer buffer for 5 min. Three pieces of 10.5 cm × 6.5 cm 3MM Whatman paper were soaked in transfer buffer, and stacked on the base of the transfer apparatus, taking care not to trap any air bubbles in between layers. The nitrocellulose membrane and gel were placed sequentially on top of the 3MM paper. Three more wet pieces of 3MM paper finally placed on top. A weight was placed on the lid and the blotter was set to run at 1 mA per cm^2 for 1 hr. The membrane was washed in water briefly and stained with ponceau S for 1 min to visualize transferred proteins.

2.2.18.2 Antibody staining

Transferred membranes were incubated in blocking buffer for 30 min at RT on a rocking platform. The membrane was then incubated with primary antibody, diluted to the appropriate concentration in 5 ml blocking buffer, for 1 hr with shaking and afterwards washed 4 times with PBS/0.1% Tween over 30 min. The filter was then incubated for 45 min with appropriate anti-mouse or anti-rabbit HRP-conjugated secondary antibody in 5 ml blocking buffer and washed 4 times with PBS/0.1% Tween over 30 min. An ECL plus detection kit was used according to manufacturer's protocol to visualise bound antibodies. Autoradiography was performed by placing an X-ray film on the membrane for 30 sec to 5 min or more and developed using a compact X4 X-ray film processor (Xograph imaging system).

CHAPTER 3

SUN1 TARGETING TO AND CONFIGURATION AT THE NUCLEAR ENVELOPE

3.1 INTRODUCTION

Integral membrane proteins of the nuclear envelope (NE) are produced on the rough endoplasmic reticulum (ER). The proteins traverse by lateral diffusion from the interconnected membranous ER to the outer nuclear membrane (ONM) and then, via the pore membrane (POM), they reach the inner nuclear membrane (INM). According to the 'diffusion-retention' model, membrane proteins are retained at the INM through their interaction with nuclear ligands such as the nuclear lamina, chromatin or other nuclear proteins (Holmer and Worman, 2001) (section 1.3). Moreover, some integral membrane proteins may contain a nuclear localization signal (NLS) within their nucleoplasmic domain and could be actively transported to the INM through the aqueous channel of nuclear pore complexes (NPCs) (Lusk et al., 2007). Although most INM proteins have a NE targeting sequence within their nucleoplasmic domain, some NE proteins have additional domains responsible for NE targeting. For example, in LBR, both the NTD and the first transmembrane domain (TMD) are capable of targeting the protein to the NE (Soullam and Worman, 1995). On the other hand, nurim can target itself to the NE despite lacking a proper NTD. Interaction of a different segment (either the TMDs, loops between the TMDs or the C-terminal domain) with other NE proteins is probably contributing to the NE targeting of nurim (Hofemeister and O'Hare, 2005). Most integral membrane proteins of the NE reside at the INM. These INM proteins generally have a nucleoplasmic N-terminal domain, one or several transmembrane domains and a lumenal C-terminal domain (Burke and Stewart, 2002, section 1.1.3). Giant nesprins and emerin are the only known ONM proteins, possessing a lumenal CTD and a cytoplasmic NTD (Wilhelmsen et al., 2006; Salpingiduo et al., 2007).

Work in this project involved investigating mammalian SUN proteins and studies were mainly carried out using murine SUN1. Murine SUN1 (referred to hereafter as SUN1) is comprised of 913 amino acids and contains four hydrophobic regions predicted to be TMDs, a coiled-coil region and a conserved SUN domain (Fig. 3.1A). The four predicted TMDs of SUN1 (referred to as H1, H2, H3 and H4, where 'H' represents hydrophobic sequence) are at positions 231-254, 358-383, 386-407, and 413-431 (Fig. 3.1A and B). Initial immunofluorescence studies in the lab had confirmed that SUN1 is
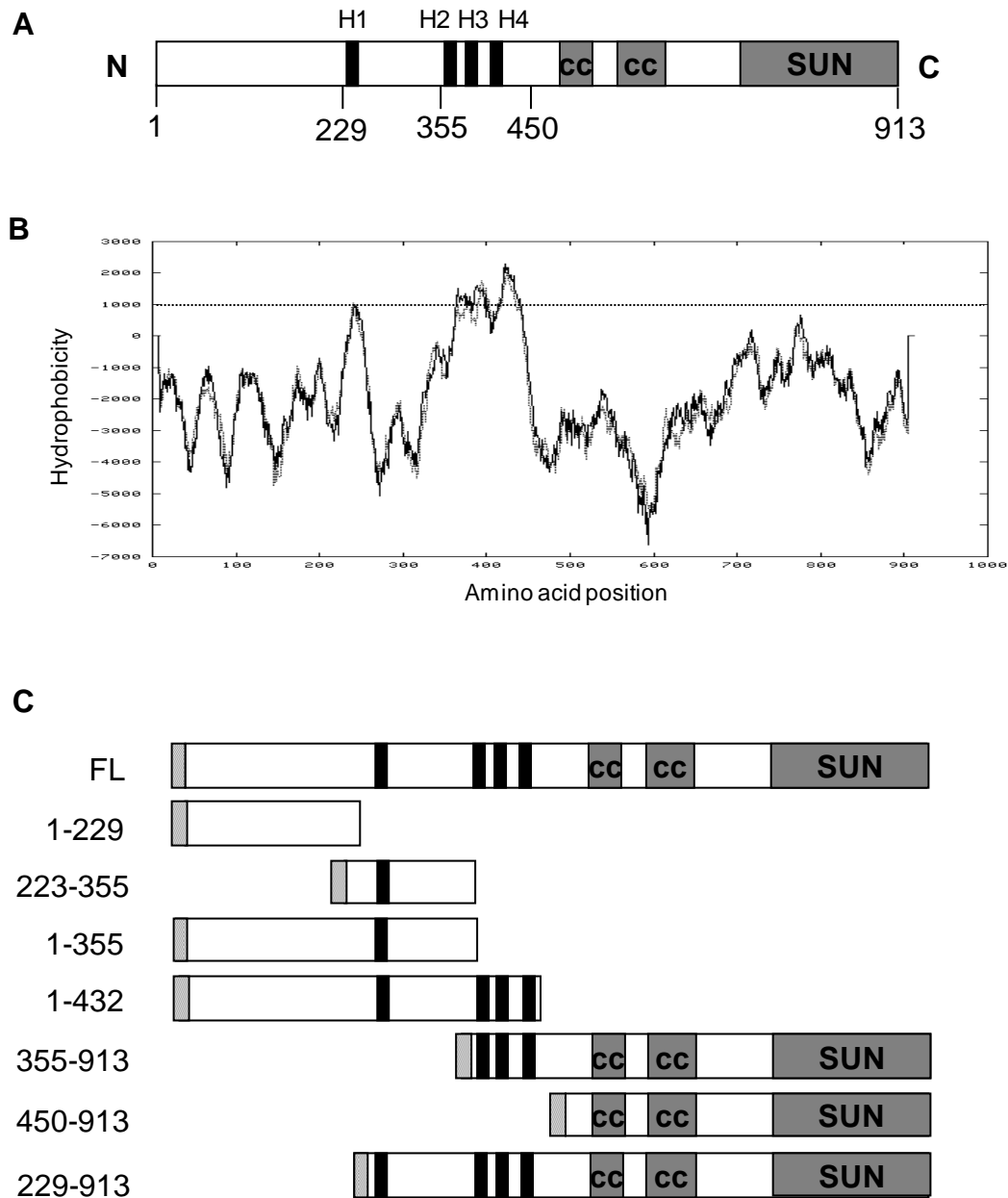
Fig. 3.1. Schematic representation of SUN1 structure and myc-tagged SUN1 deletion constructs used in this study. A) SUN1 domain structure, indicating the positions of the N-terminus (N), C-terminus (C), four potential transmembrane domains (H1, H2, H3 and H4; black bars), coiled-coil regions (cc) and conserved SUN domain (grey box). **B)** Hydropathy plot generated with TMpred software predicting four transmembrane domains at amino acids 231-254, 358-383, 386-407, and 413-431. Values above '0' indicate hydrophobic amino acids, and any peak comprising more than 20 amino acids and above value 1000 (dotted line) is considered to be a potential transmembrane domain. **C)** Schematic representation of myc-tagged SUN1 deletion constructs used in these studies. Hatched box denotes the position of myc tag. FL denotes full length SUN1.

a nuclear envelope protein, which co-localizes with lamin A in a rim like pattern at the periphery of the nucleus. Deletion fragments of SUN1, composing N-terminal sequences 1-355 and C-terminal sequences 450-913 were found to localize mainly at the NE and in the cytoplasm, respectively (section 1.6). This showed that the SUN1 NTD contains a NE targeting signal and, together with the fact that the NTD interacts with lamin A, suggested that SUN1 is an INM protein with a nucleoplasmic NTD like most other INM proteins.

However, no direct evidence confirming the topology of SUN1, or indeed any of the SUN proteins, had been obtained at this stage. Whilst *C. elegans* UNC-84 was shown to require Ce-lamin for its NE localization, no direct interaction between the two proteins had been detected (Lee et al., 2001). Existing models equally predicted UNC-84 to reside at the INM or at the ONM, where its role in nuclear migration could be more easily explained through a direct interaction with centrosomes (Malone et al., 1999; Raff, 1999).

Intriguingly, initial immuno-electron microscopy using gold-conjugated secondary antibody to detect SUN1 CTD, also suggested that the SUN1 CTD could be at the cytoplasmic face of the NE (section 1.6). Further studies were therefore required to understand the topology of SUN proteins at the NE.

Software prediction of the hydropathy plot of SUN1 sequence shows four transmembrane domains. It was not clear how many of the four predicted hydrophobic regions were bona fide TMDs. Hydropathy plots do not always accurately predict the presence of transmembrane domains. H1, in particular, has a relatively weak peak compared to H2-H4 in hydrophobicity the plot (Fig. 3.1 B) and therefore may not be a true membrane-spanning sequence. Together, these data led us to propose three different topologies of SUN1 at the NE, all of which assume that the N-terminus is located in the nucleoplasm due to its ability to interact with lamin A (Fig. 3.2, section 1.6). In the first model, H1 traverses the INM and then H2, H3 and H4 span the ONM three times, resulting in a cytoplasmic CTD (Fig. 3.2A). However, this topology is highly unusual, as there is no known INM protein that passes both the INM and the ONM, and thus spans the space between the two membranes. Secondly, the H1-H4 could traverse the INM four times resulting in a nucleoplasmic CTD (Fig. 3.2B). This is
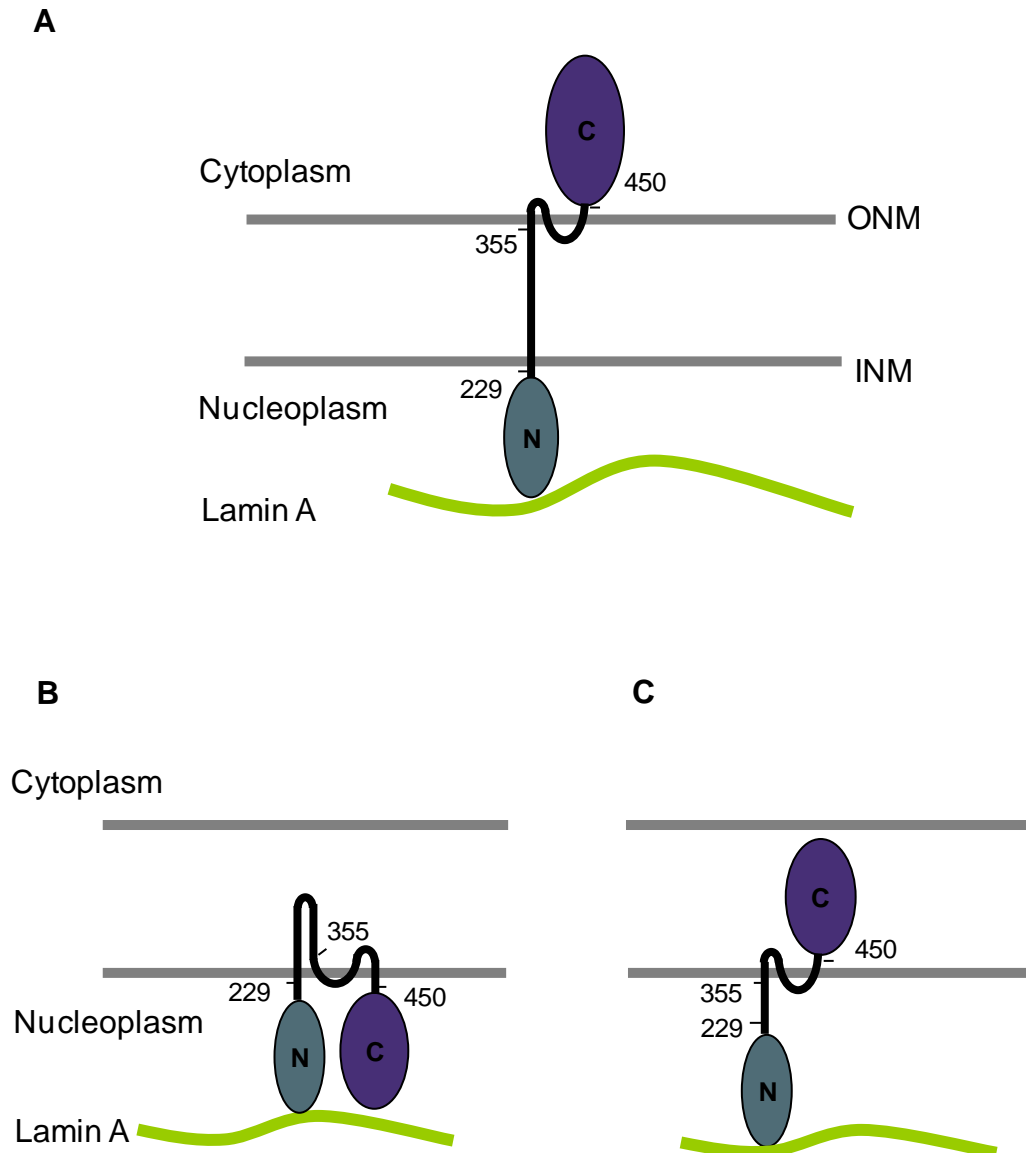
Fig. 3.2. Schematic representation of three different possible SUN1 topologies. In all cases the NTD is predicted to be nucleoplasmic, based on previous data. **A)** H1 traverses the INM, H2, H3 and H4, span the ONM and the CTD is cytoplasmic. **B)** H1-H4 all traverse the INM with the result that the CTD is nucleoplasmic. **C)** H1 is not membrane-spanning. H2, H3 and H4 each span the INM resulting in a lumenal CTD. Predicted locations of residues 229, 355 and 450 are indicated in each case.

also unlikely, since the UNC-84/SUN1 CTD is hypothesized to interact with the KASH domain of ANC-1/nesprins (Starr and Han, 2003) and this is most likely to occur in the NE lumen. The third possibility is that, H1 is not a membrane-spanning region, H2, H3 and H4 traverse the INM three times, resulting in a lumenal CTD (Fig. 3.2C).

The aim of the studies presented in this chapter was therefore to address the topology of SUN1 at the NE, and to delineate the exact sequences of SUN1 that are responsible for the NE targeting of the protein and the mechanism of its nuclear anchoring. To achieve this, further myc-tagged N- and C-terminal deletion constructs of SUN1 were generated, as shown in Figure 3.1C. These constructs were transiently transfected into different cell lines to observe their subcellular localization. The transfected cells were further subjected to biochemical extraction to analyse the association of the SUN1 deletion fragments with the nuclear matrix. To investigate the topology of SUN1, several experiments were performed by subjecting cells to digitonin permeabilization (section 2.2.11), using other INM or cytoplasmic proteins as controls. Furthermore, a range of full length SUN1 constructs, with myc tags inserted at different locations, were generated and the location of the myc tag in digitonin-treated cells was studied by immunofluorescence microscopy.

3.2 RESULTS

3.2.1 Generation of myc-tagged SUN1 deletion constructs

Previous SUN1 localization studies involved three SUN1 constructs: pCI-SUN1 full-length, pCI-SUN1(1-355) and pCI-SUN1(450-913) (Fig. 3.1). These SUN1 deletion fragments were engineered by PCR amplification of the relevant region of the SUN1 cDNA and included an N-terminal myc-tag. In addition to these three SUN1 constructs, further deletion constructs were generated to investigate the sequence requirements for SUN1 targeting to the NE (Fig. 3.1C and Fig. A.1). The previous deletion constructs, SUN1(1-355) and SUN1(450-913), do not include H2-H4. The new SUN1 constructs, SUN1(1-432) and SUN1(355-913) were therefore engineered to contain H2-H4, as the membrane spanning regions could also contribute to the NE targeting of SUN1. Two additional SUN1 constructs, encompassing residues 1-229 and 223-355, were generated to aid refinement of the SUN1 NTD NE targeting sequence. SUN1(1-229) sequence

does not contain any TMD, whereas SUN1(223-355) sequence has only H1. All new SUN1 deletion constructs were generated by PCR amplification of the relevant region of the SUN1 cDNA with specific primers (Table 2.4). The deletion fragments were then cloned into the *Bam*HI and *Sal*I sites of mammalian expression vector pCMV-Tag3B, which has the myc tag sequence upstream of the multiple cloning sites (Fig. A.1).

3.2.2 SUN1 contains two independent NE targeting sequences

3.2.2.1 Localization of SUN1 deletion fragments 16 hours post-transfection

The myc-tagged SUN1 deletion constructs, along with full-length (FL) SUN1, were transiently transfected into cultured NIH 3T3 cells to assess their subcellular localization. Sixteen hours of post-transfection, the cells were fixed with methanol and co-stained with anti-myc 9E10 and 3262 anti-lamin A/C antibodies and visualized by immunofluorescence microscopy after secondary staining with fluorescently labelled antibodies. Images of representative transfected NIH 3T3 cells are shown in Figure 3.3.

FL SUN1 was mainly concentrated at the NE where it co-localized with lamin A/C. In some cells the protein was present in cytoplasmic aggregates or had a reticular cytoplasmic distribution, presumably representing ER accumulation due to over-expression of the transfected protein (Fig. 3.3a). SUN1(1-432) and SUN1(1-355) also localized predominantly to the nuclear rim, with some cytoplasmic accumulation (Fig. 3.3b,c). This suggests that there is a NE targeting sequence present at the NTD of SUN1 within residues 1-355. In an attempt to further map the NE targeting sequence, NTD divisional constructs SUN1(1-229) and SUN1(223-355) were generated. Both SUN1(1-229) and SUN1(223-355) were poorly expressed, with a transfection efficiency around 2%. In the limited number of transfected cells observed, SUN1(1-229) was present in both the cytoplasm and the nucleoplasm, but not at the NE (Fig. 3.3d,e) whereas SUN1(223-355) was found as cytoplasmic aggregates in cells, with no clear distribution pattern (Fig. 3.3f,g).

Surprisingly, SUN1(355-913), which comprises H2-H4 and the CTD, was found to localize at the NE (Fig. 3.3h). This suggests that the SUN1 CTD, in conjunction with

Fig. 3.3. Localization of myc-tagged SUN1 full length (FL) and deletion proteins 16 hours post-transfection. NIH 3T3 cells were transiently transfected with SUN1 FL (a) and deletion constructs SUN1 1-432, 1-355, 1-229, 223-355, 355-913, 450-913 (b to i) and fixed in methanol 16 hours later. Cells were then co-stained with anti-myc 9E10 (in red) and anti-lamin A/C 3262 antibodies (in green). In (i), the merged image shows apparent co-localization of SUN1(450-913) with lamin A/C at the NE, as indicated by yellow staining at the nuclear periphery. Scale bar, 10 µm.

the middle TMDs can independently localize to the NE. Conversely, SUN1(450-913), that consisted of the CTD alone, did not associate with the NE and was evenly distributed in the cytoplasm (Fig. 3.3i). This suggests that the SUN1 CTD without H2-H4 is not capable of targeting itself to the NE. Co-staining with lamin A/C showed some overlapping staining at the NE for SUN1(450-913) (Fig. 3.3i). However, at the resolution of the light microscope it was not possible to determine whether SUN1(450-913) overlapping staining represented localization in the cytoplasm, at the ONM or in the NE lumen. Considering all of the above results, it seems likely that there are two independent sequences present in SUN1 for targeting to the NE or nuclear rim, the first in the NTD located within residues 1-355 and the second could be located in H2-H4 or possibly in the CTD itself.

3.2.2.2 NE localization of SUN1 deletion proteins is improved after expression for 72 hours

Transient transfection generally leads to over-expression of proteins, as multiple copies of plasmids are taken up by each transfected cell. This can result in aberrant localization of the exogenous protein due to overloading of the cells and could explain why some SUN1 constructs localized not only to the NE but also as cytoplasmic aggregates or within the ER, 16 hours post-transfection. Moreover, it may require more than 24 hours or one cycle of cell division, including NE breakdown and reassembly, to fully incorporate these proteins into the NE. In addition, it is possible that the binding sites for SUN1 at the NE are easily saturated, leading to diffusion of excess proteins back to the ER. To overcome these potential problems, a time course experiment was performed, where the cells were incubated for 24, 72 or 120 hours post-transfection prior to fixation.

NIH 3T3 cells were transfected with five SUN1 constructs, SUN1 FL, SUN1(1-432), SUN1(1-355), SUN1(355-913) and SUN1(450-913). The NTD divisional constructs SUN1(1-229) and SUN1(223-355) were not used as they previously showed poor transfection and did not show any obvious localization pattern. To carry out the time course experiment, 3 coverslips were prepared and were fixed at 24, 72 or 120 hours post-transfection and thereafter co-stained with anti-myc and 3262 anti-lamin A/C antibodies and visualized by immunofluorescence microscopy.

The subcellular localization of all the SUN1 fragments after 24 hours was similar to that of 16 hours post-transfection, as shown in section 3.2.2.1.   At 24 hours post-transfection, SUN1 FL and SUN1(1-432) were mainly localized to the nuclear rim with a little cytoplasmic distribution in some cells (Fig. 3.4b,g). After 72 hours, most of the cytoplasmic staining was lost, and SUN1 FL and SUN1(1-432) were found exclusively at the NE. This indicates that the SUN1 NTD plus the TMDs have all the necessary NE targeting sequences (Fig. 3.4c,h). Compared to SUN1(1-432), there was more cytoplasmic staining observed at 24 hours post-transfection for SUN1(1-355) (Fig. 3.4d,e,g). After 72 hours, the cytoplasmic distribution of SUN1(1-355) was much reduced, with localization of SUN1(1-355) mainly to the nuclear rim, suggesting that this protein may require more time than SUN1(1-432) to fully incorporate into the NE or nuclear periphery (Fig. 3.4f).

For SUN1(355-913), whilst, the majority of the protein localized to the NE, some cytoplasmic staining was visible 24 hours post-transfection (Fig. 3.4i), but was reduced following 72 hours of transfection (Fig. 3.4j). Not surprisingly, SUN1(450-913) was still in the cytoplasm after 72 hours. This further supports the notion that the CTD alone is not sufficient to target itself to the NE (Fig 3.4l).

At the 72 and 120 hours time points, similar distribution of the myc-tagged SUN1 FL and deletion proteins was observed, with the exception that there were fewer transfected cells at 120 hours. Therefore, only the results from the 72-hour timepoint are shown. Overall, these results confirm the localization pattern of the SUN1 deletion proteins described earlier and the presence of two individual NE targeting signals in SUN1.

One noticeable phenomenon during this experiment was that the expression of SUN1 FL, 1-355, 1-432 and 355-913 appeared to be more transient than that of SUN1(450-913). Compared to cells transfected with SUN1(450-913), there were very few cells maintaining expression of the other four proteins at 72 or 120 hours post-transfection. In addition, many of the cells that did still express these proteins had abnormal nuclei, generally observed as micronuclei, blebbing or very large nuclei (Fig. 3.5a-d). Occasionally nuclear abnormalities were also observed in untransfected cells on the same coverslips following prolonged expression, but were more prominent in the transfected cells. Since there were very few transfected cells remaining 72 or 120 hours
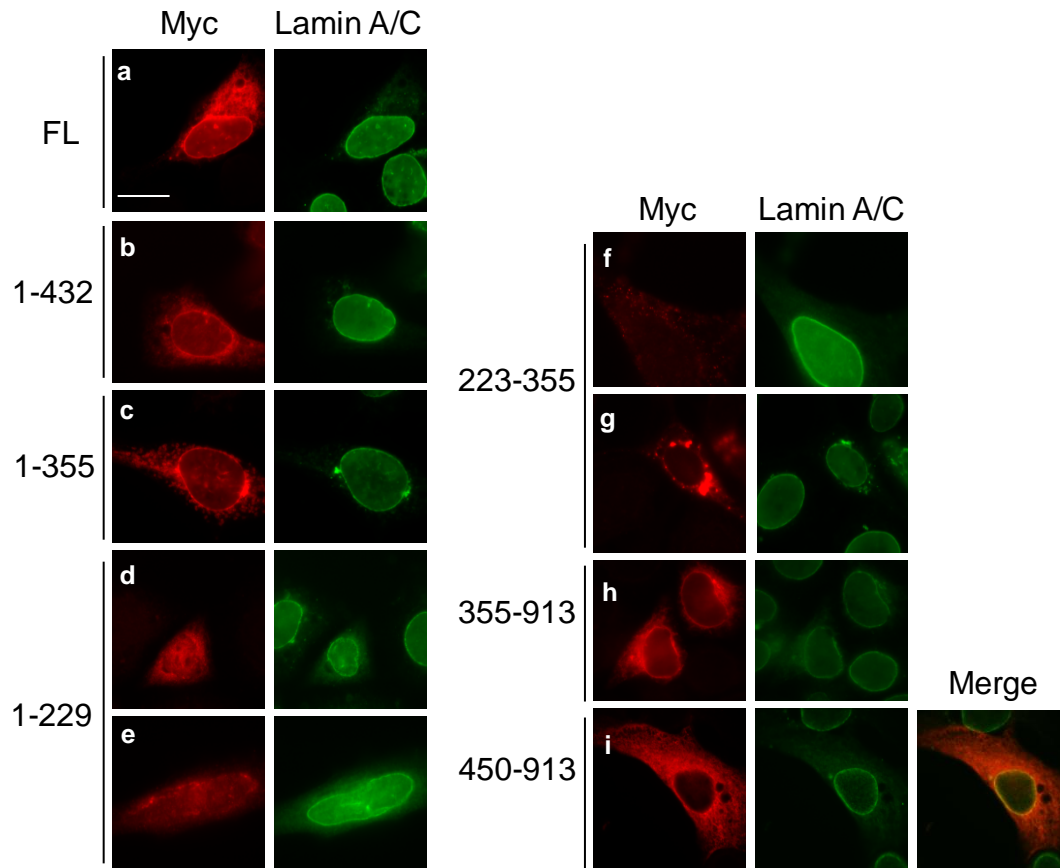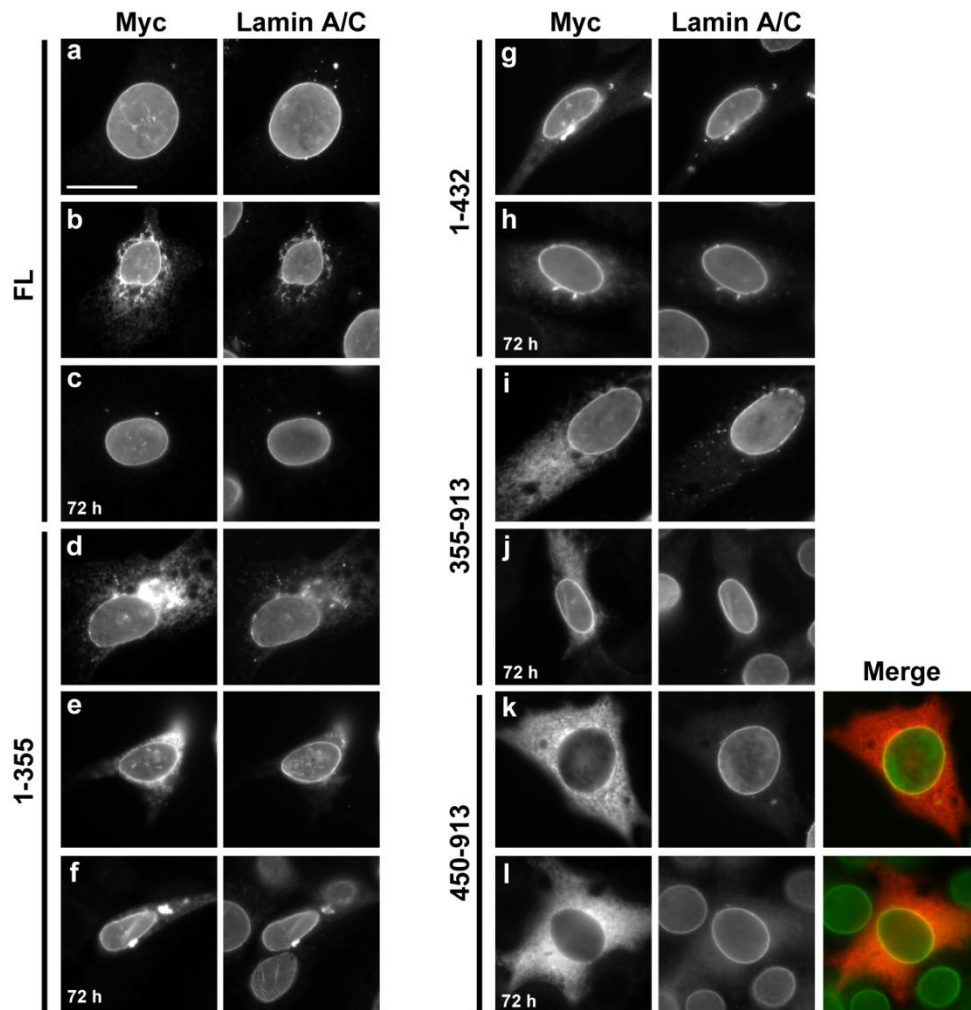
Fig. 3.4. Localization of myc-tagged SUN1 full length (FL) and deletion proteins 24 and 72 hours post-transfection. NIH 3T3 cells were transfected with myc-SUN1 FL and deletion constructs SUN1 1-355, 1-432, 355-913, 450-913 and fixed in methanol 24 hours (a, b, d, e, g, i, k) or 72 hours (c, f, h, j and l) post-transfection. Cells were then co-stained with anti-myc 9E10 (left panel) and anti-lamin A/C 3262 antibodies (right panel). Merged colour images in (k) and (l) show apparent co-localization of SUN1(450-913) (red) with lamin A/C (green) at the NE, as indicated by yellow staining. Scale bar, 10 μm.
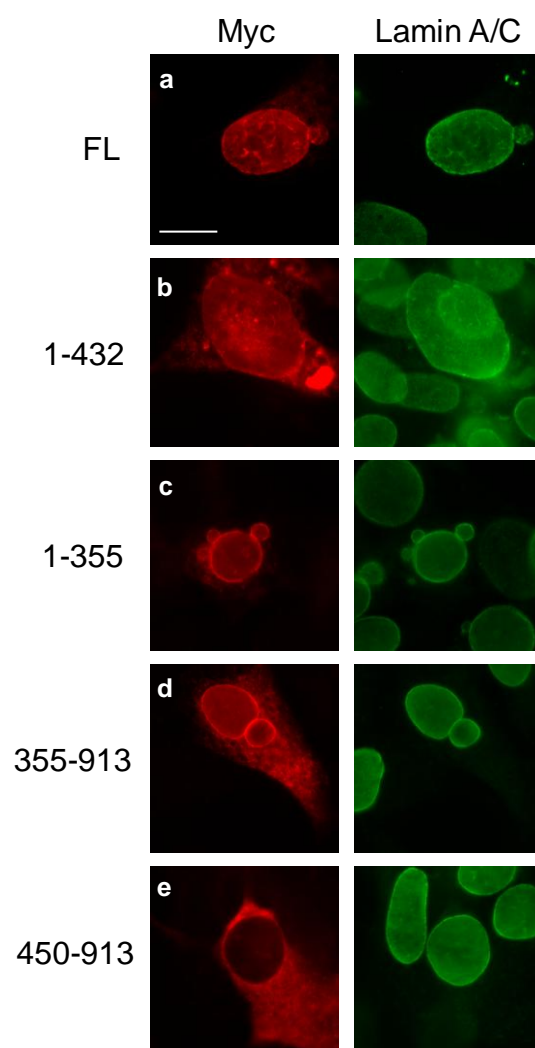
Fig. 3.5. Nuclear abnormalities detected in cells transfected with SUN1 constructs 72 hours post-transfection. NIH 3T3 cells were transfected with SUN1 constructs (FL, 1-432, 1-355, 355-913 and 450-913) and fixed in methanol 72 hours later. Cells were then co-stained with anti-myc 9E10 (in red) and anti-lamin A/C 3262 antibodies (in green). Scale bar, 10 μm.

post-transfection, cells were not counted for their abnormalities on this occasion. In another experiment using only FL SUN1 after prolonged expression, the nuclear abnormalities were counted. Around 34% (n=100) and 50% (n=48) of transfected cells showed nuclear abnormality after 72 and 120 hours respectively. On the other hand, in untransfected cells only 12% and 13% showed nuclear abnormality, respectively, after 72 and 120 hours. Altogether, these findings suggest that prolonged expression of SUN1 FL, 1-355, 1-432 and 355-913 could be toxic to the cells, leading to abnormal nuclear shape, nuclear blebbing and cell death.

3.2.3 The N-terminal domain of SUN1 is associated with the nuclear matrix

INM proteins that are associated with the nuclear matrix and the nuclear lamina have been found to be resistant to detergent extraction (Hofemiester and O'Hare, 2005). In order to determine which domain of SUN1 is associated with the nuclear lamina, cells transfected with the NE-localized SUN1 constructs were pre-extracted with Triton X-100 prior to fixation. After Triton treatment any protein that is not associated or only loosely associated with the nuclear matrix is solubilised and largely lost from the cells. The only nuclear proteins remaining are those that are associated with the insoluble nuclear lamina and the nuclear matrix. NIH 3T3 cells were transfected with the five SUN1 constructs (FL, 1-432, 1-355, 355-913, 450-913). After 72 hours the cells were subjected to pre-extraction with 0.5% Triton X-100 for 5 minutes on ice, then fixed with methanol and co-stained with anti-myc and 3262 lamin A/C antibodies to visualize by immunofluorescence microscopy.

Full length SUN1, as well as the NTD-containing fragments SUN1(1-355) and SUN1(1-432), were retained exclusively at the NE and any cytoplasmic staining that was present before was lost after Triton pre-extraction (Fig. 3.6a-c). This suggests that the NTD of SUN1 is bound to the nuclear lamina and that this association with the nuclear lamina might be responsible for the NE anchoring of SUN1 NTD. In contrast, SUN1 CTD-containing fragments SUN1(355-913) and SUN1(450-913) were completely lost from the NE and the cytoplasm (Fig. 3.6d,e). This shows that, although SUN1(355-913) is localized at the NE, it is not bound to the nuclear lamina and a
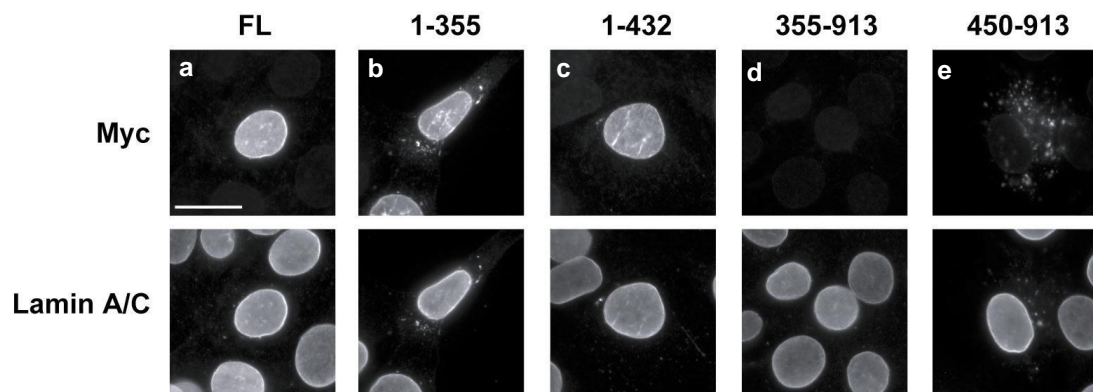
Fig. 3.6. Localization of full-length SUN1 and deletion mutants after Triton pre-extraction. NIH 3T3 cells were transfected with SUN1 FL and deletion constructs SUN1 1-355, 1-432, 355-913, 450-913, and 72 hours post-transfection were subjected to pre-extraction with 0.5% Triton X-100 for 5 minutes on ice and immediately fixed in methanol. Cells were then co-stained with anti-myc 9E10 (top) and anti-lamin A/C 3262 antibodies (bottom). Scale bar, 10 μm.

different mechanism is responsible for targeting of this fragment to the NE. It is possible that either H2-H4 have the NE targeting capacity or interaction of the CTD with other NE proteins such as nesprins, or its oligomerization with endogenous SUN1 is contributing to the NE localization of SUN1(355-913).

3.2.4 SUN1 residues 229-913 are not dependent on the nuclear lamina for the NE localization

A new construct, SUN1(229-913), was generated to further probe the sequence requirements for nuclear matrix association of SUN1. SUN1(229-913) contains all four putative TMDs (H1-H4) and the CTD (Fig. 3.7A). pCMV-SUN1(229-913) construct was generated by PCR of relevant region of SUN1 cDNA with appropriate primers and was cloned into *Bam*HI and *Sal*I sites of plasmid pCMV-Tag3B (Table 2.4 and Fig. A.1). NIH 3T3 cells were transfected with SUN1(229-913) as well as full length SUN1 and SUN1(355-913), as controls. One set of transfected cells was methanol fixed after 24 hours and then co-stained with anti-myc and 3262 anti-lamin A/C antibodies to visualize the localization of the SUN1 fragments by immunofluorescence microscopy. Another set of cells was pre-extracted with 0.5% Triton X-100 for 5 minutes on ice, before methanol fixation and then stained with the anti-myc and lamin A/C antibodies for immunofluorescence microscopy.

SUN1(229-913) was found to localize mainly at the NE similar to SUN1 FL and SUN1(355-913) (Fig. 3.7B a,b,c). Interestingly, similar to SUN1(355-913), SUN1(229-913) was not retained at the NE after Triton pre-extraction indicting non-association with the nuclear lamina (Fig. 3.7B e,f). This suggests that, although SUN1(229-913) fragment has a NE targeting capacity, it is not dependent on the nuclear lamina. Furthermore, as SUN1(1-355) was found to interact with lamin A previously in the lab by yeast two-hybrid screen and SUN1(229-913) is not associated with the nuclear lamina, this implies that the lamin A-binding region in SUN1 resides within residues 1-228.
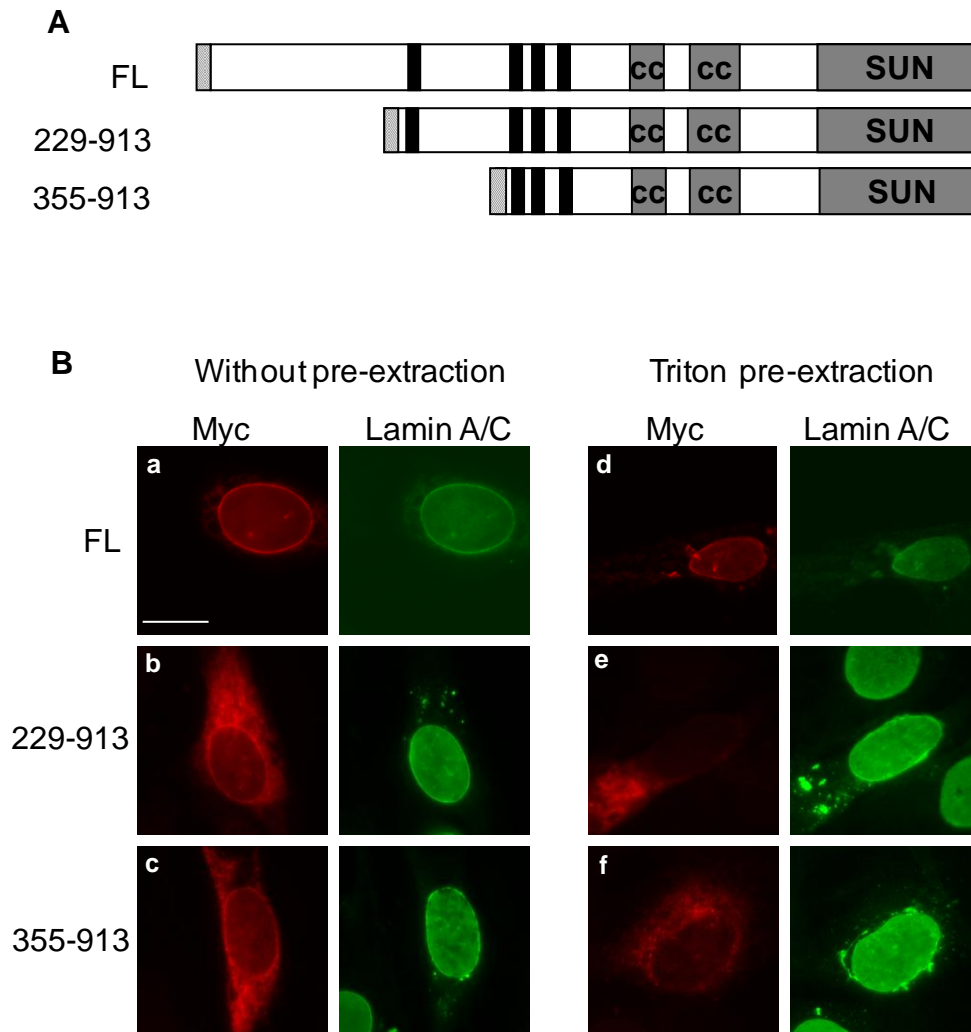
Fig. 3.7. SUN1(229-913) is not anchored at the nuclear envelope after Triton pre-extraction. A) Schematic representation of myc-tagged SUN1 FL, SUN1(229-913) and SUN1(355-913). Hatched box denotes myc tag. **B)** NIH 3T3 cells were transfected with SUN1(229-913) along with SUN1 FL and SUN1(355-913) and 24 hours post transfection were either fixed directly in methanol (left panels) or subjected to pre-extraction with 0.5% Triton X-100 for 5 minutes on ice and immediately fixed in methanol (right panels). Cells were then co-stained with anti-myc 9E10 (in red) and anti-lamin A/C 3262 antibodies (in green). Scale bar, 10 µm.

3.2.5 Determining the location of the SUN1 CTD following digitonin permeabilization of cells

To address the topology of SUN1 at the nuclear envelope, several experiments were performed by subjecting the cells to digitonin permeabilization. After paraformaldehyde fixation, cells were treated transiently with 40 µg/ml digitonin instead of Triton X-100. Triton permeabilizes all the membranes of a cell. On the other hand, brief incubation of cells at 4°C with digitonin selectively permeabilizes only the plasma membrane, leaving the NE and other internal membranes intact (Adam et al., 1990) (Fig. 3.8A). Digitonin can readily disrupt a higher cholesterol content membrane, such as the plasma membrane and it will progressively permeabilize all membranes if incubated for a longer period of time or at a higher temperature. Since treating cells with digitonin for a brief period leaves the NE intact, the nucleoplasm remains inaccessible to antibodies. Therefore, detection of the SUN1 CTD by immunofluorescence microscopy in digitonin-treated cells, compared to control Triton-treated cells, could give more insight into its topology by indicating whether the CTD resides in the nucleoplasm, the NE lumen or the cytoplasm.

3.2.5.1 Localization of the SUN1 CTD to the cytoplasmic face of the NE, using LAP1 as control

Digitonin permeabilization experiments were performed, using antibodies against the CTD of the INM protein LAP1 (kind gift from L. Gerace; Martin et al., 1995) as a control marker for integrity of the ONM. LAP1 has a lumenal CTD which should be inaccessible to the antibodies in digitonin-treated cells when the ONM is intact. Similarly, if the SUN1 CTD is lumenal, it will not be accessible to SUN1 antibody (0545, was raised previously in the lab, against residues 450-913 of mouse SUN1). Conversely, if the SUN1 CTD is cytoplasmic, it will be visible in digitonin-treated cells. LAP1 was used as control because this was the only protein with an available antibody generated against its lumenal domain. NRK cells were used as LAP1 and SUN1 antibody staining was better in these cells compared to NIH 3T3 cells.

A

Triton permeabilization

Digitonin permeabilization

B
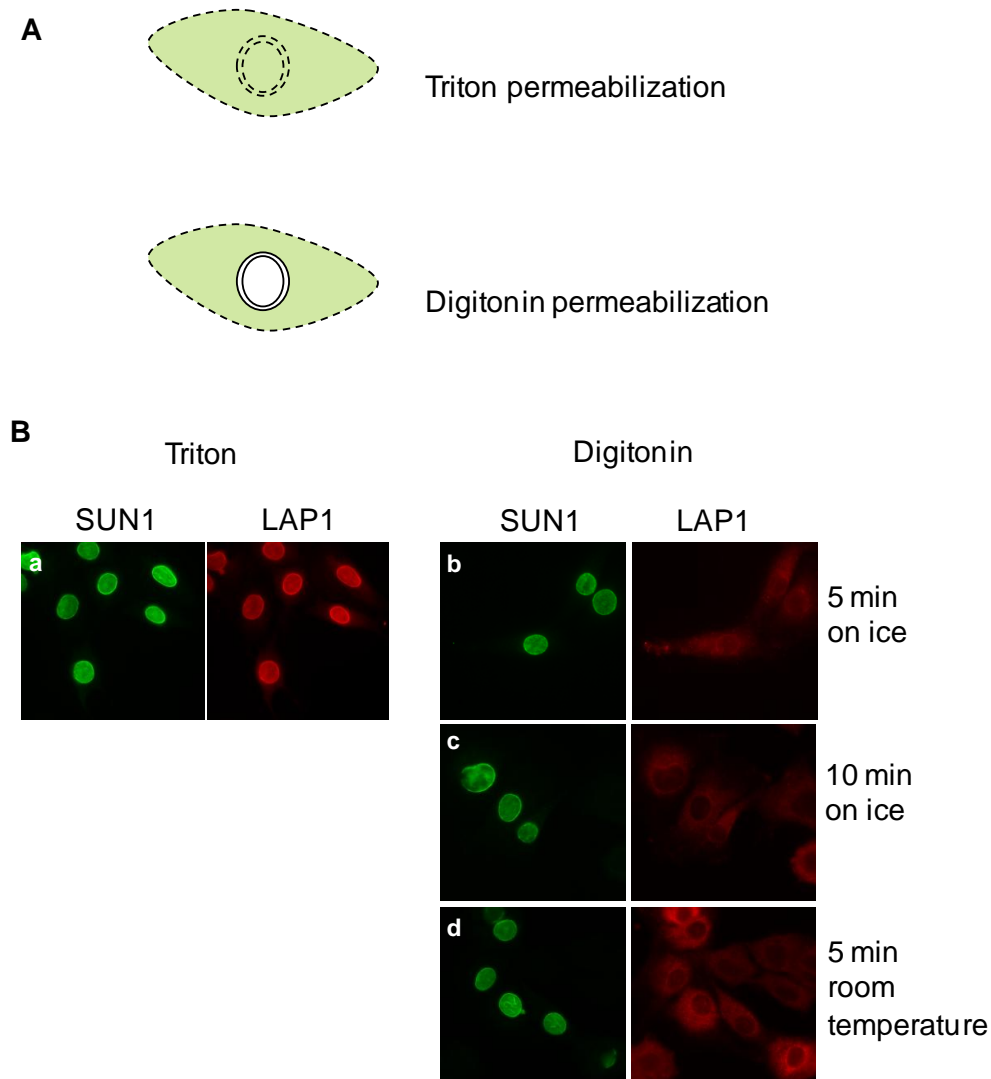
Fig. 3.8. Cytoplasmic localization of the SUN1 CTD detected using LAP1 antibodies as control. A) Schematic representation of a Triton-permeabilized cell, with both plasma membrane and nuclear envelope permeabilized, and a digitonin-treated cell with an intact NE. **B)** NRK cells were fixed with 4% paraformaldehyde and permeabilized with either Triton X-100 (a) or with digitonin on ice for 5 min (b), 10 min (c) or at room temperature for 5 min (d). Immunofluorescence staining was performed using antibodies against the SUN1 CTD (green) and the LAP1 CTD (red).

To determine whether the SUN1 CTD was lumenal or cytoplasmic, NRK cells were permeabilized with TritonX-100 or 40 µg/ml digitonin for varying times at 4°C or at room temperature, after fixation with paraformaldehyde. After Triton and digitonin treatment, the NRK cells were co-stained with antibodies against the SUN1 CTD and the lumenal domain of LAP1. Immunofluorescence staining of the control Triton-treated cells showed that both 0545 SUN1 and LAP1 antibodies were capable of detecting the respective proteins (Fig 3.8B a). In contrast, permeablizing cells with digitonin for 5 or 10 minutes on ice revealed that the SUN1 CTD was accessible to the antibodies whereas LAP1 was not (Fig. 3.8B b,c). With digitonin treatment at room temperature for 5 minutes, LAP1 staining was just becoming appearent (Fig 3.8B d). Since the lumenal LAP1 CTD was inaccessible to the antibody after 5 or 10 minutes of digitonin treatment on ice, this suggests that the ONM was intact. On the other hand, the SUN1 CTD was visible in many cells under these conditions, suggesting that the SUN1 CTD resides on the cytoplasmic face of the NE.

3.2.5.2 The ONM is permeabilized by digitonin earlier than the INM

Although in the literature, studies report using digitonin for 5 minutes at 4 °C to obtain an intact NE, the conditions required titration. In the previous experiment, LAP1 staining started to become visible after digitonin treatment of cells for 5 minutes at room temperature. Further experiments were therefore performed to determine whether the ONM and the INM are permeablized at different time points. NRK cells were treated with digitonin for 5, 8, 11 or 15 minutes at room temperature following paraformaldehyde fixation. The cells were then co-stained with LAP1 and 3262 lamin A/C antibodies and subjected to immunofluorescence microscopy. LAP1 antibody should detect the lumenal domain of LAP1 and lamin A is located inside the nucleus. Therefore sequential detection of these proteins by these antibodies would reveal the efficiency of digitonin in permeabilizing the nuclear membranes. In this experiment, LAP1 staining started to become visible in many cells at 5 minutes and gradually became more visible with increasing time, becoming maximum at 11 minutes (Fig. 3.9A). On the other hand, lamin A/C staining became apparent only after 8 minutes and reached maximal staining after 15 minutes. This indicates that, with digitonin treatment, the INM and ONM are not permeablized as a whole at the same time. Instead, there is

A

B
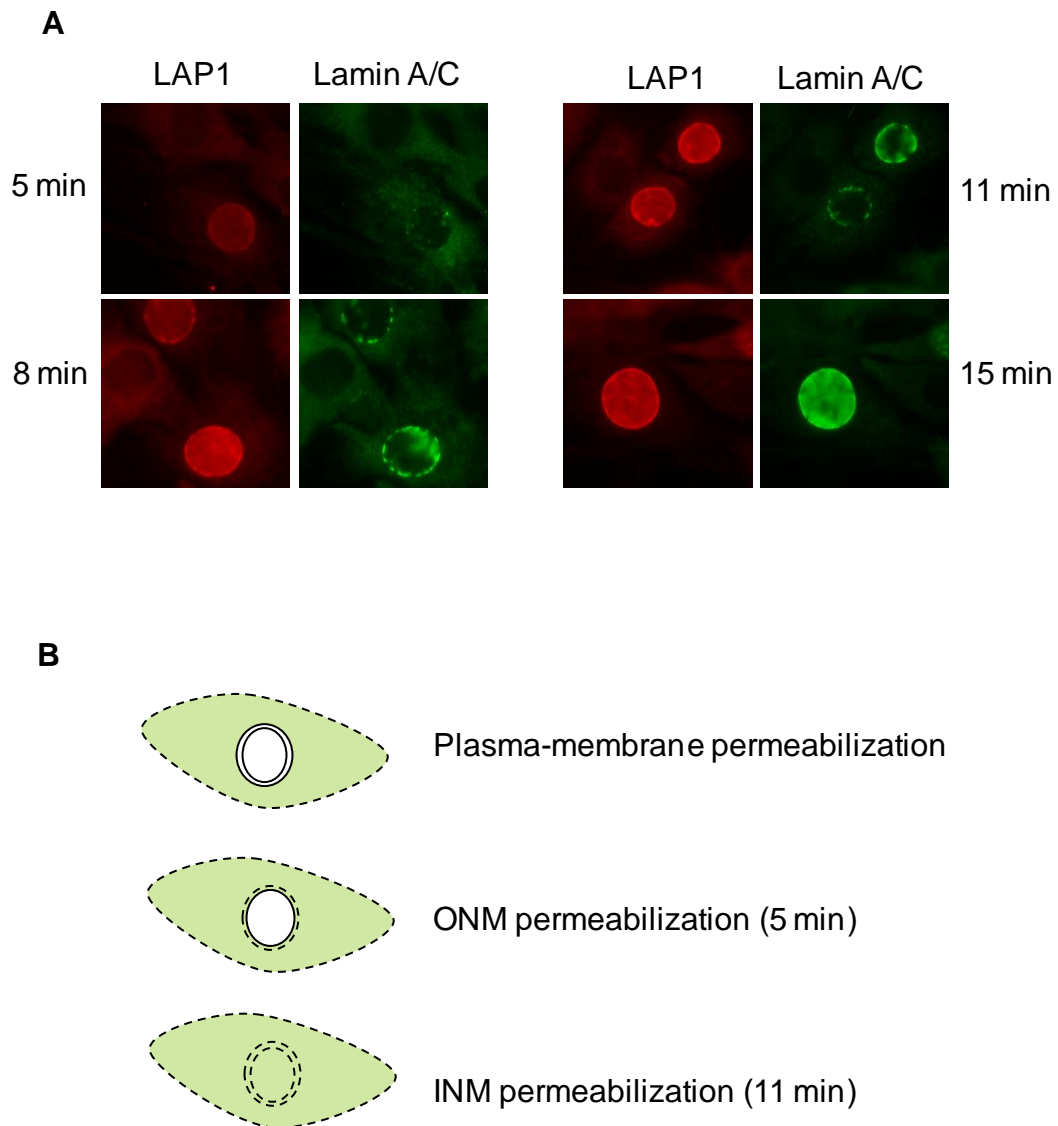
Fig. 3.9. The ONM is permeabilized earlier than the INM with digitonin treatment. A) NRK cells were fixed with paraformaldehyde and permeabilized with digitonin at room temperature for 5, 8, 11 or 15 min. Immunofluorescence staining was performed using antibodies against LAP1 (red) and lamin A/C (green). **B)** Schematic representation of digitonin-treated cells with sequential permeabilization of the plasma membrane, the ONM and the INM in a time-dependent manner.

gradual permeablization of the NE, with the ONM being permeabilized first and with longer digitonin treatment, the INM is then permeabilized (Fig. 3.9B).

3.2.5.3 The CTD of SUN1 and SUN2 have similar topology at the NE

During the course of this study, Hodzic et al. published work demonstrating that the SUN2 CTD is located in the NE lumen (Hodzic et al., 2004). In their studies, SUN2 CTD was not detectable in the cytoplasm in digitonin permeabilization assays while the control cytoplasmic tubulin was detected. Moreover, proteinase K protection assays revealed a protected C-terminal region of SUN2 in microsomes. Together these data demonstrated that the SUN2 CTD is not cytoplasmic but resides in the NE lumen.

As we expect SUN1 and SUN2 to have same topology, the previous result (section 3.2.5.1), where the SUN1 CTD was found at the cytoplasmic face of the NE using LAP1 as a control, conflicts with this data (Fig. 3.8B). To address this, we directly compared the topology of SUN1 with that of SUN2 in a digitonin permeabilization experiment. A rabbit polyclonal antibody raised against the CTD of human SUN2 was kindly donated by Didier Hodzic. This required the use of human cells and U2OS cells were chosen for these experiments. Furthermore, since the human SUN2 and 0545 SUN1 antibodies were both raised in rabbit, they could not be used together to co-stain the cells. Also, 0545 SUN1 antibody does not recognise human SUN1. Therefore, a C-terminally myc-tagged mouse SUN1 construct (SUN1-myc) was used to transiently transfect U2OS cells. The cells were then treated with digitonin for 5 and 10 minutes on ice after paraformaldehyde fixation and co-stained with anti-myc and human SUN2 antibodies. Both the SUN1 C-terminal myc tag and SUN2 CTD were visible after 5 and 10 minutes digitonin-treatment on ice (Fig. 3.10A c,e). This suggests that the SUN1 and SUN2 CTDs might have similar location in the NE lumen. However, it does not rule out that the CTD of SUN1 could be on the outer face of the NE.

One interesting observation made during this experiment was that, in SUN1-myc transfected cells, endogenous SUN2 was mislocalized from the NE. This was evident in most Triton-treated cells and also in many digitonin-treated cells (Fig. 3.10A b,d arrowheads). This observation is consistent with a study later published by Crisp et al. (Crisp et al., 2006).
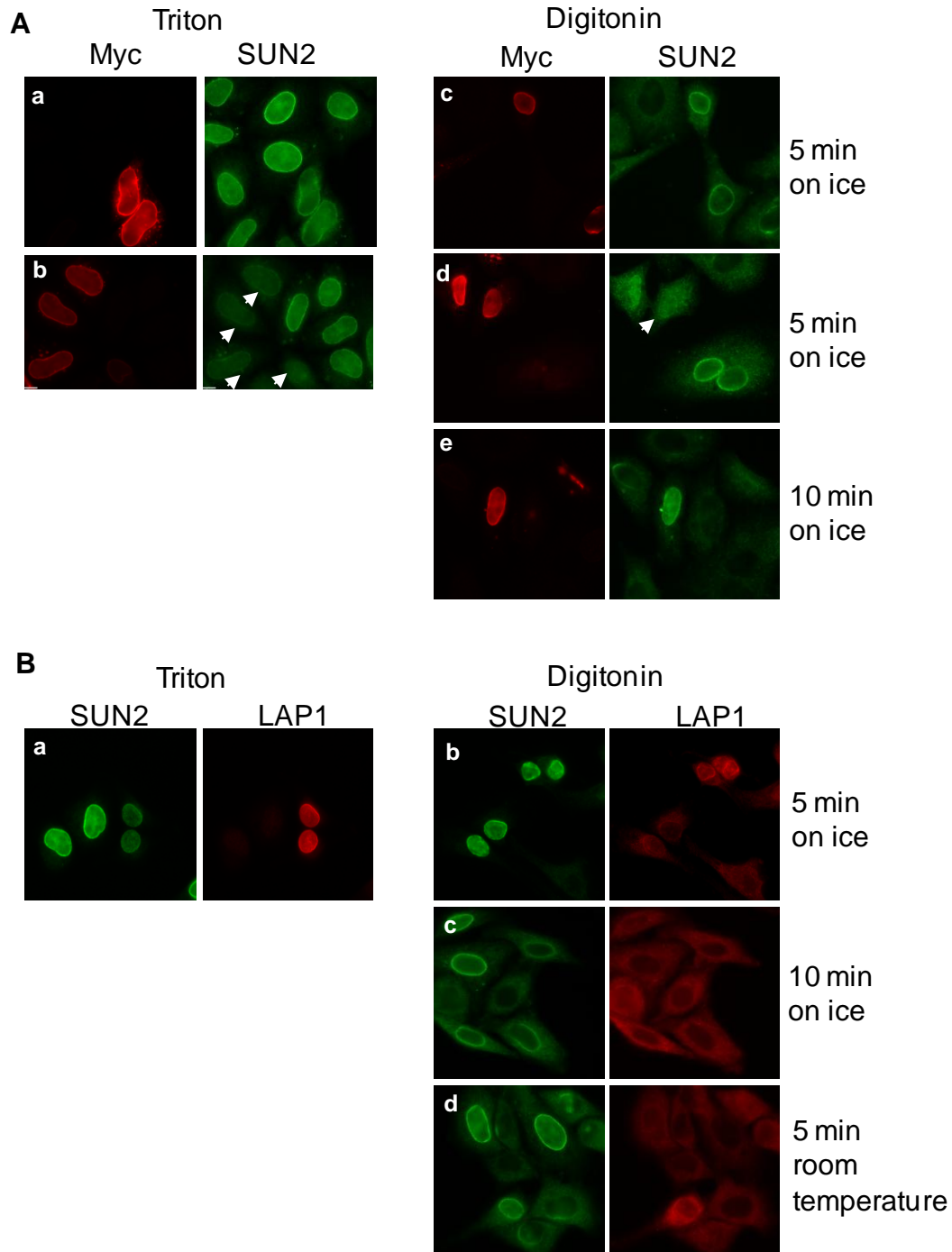
Fig. 3.10. The CTDs of SUN1 and SUN2 are in the same location. A) U2OS cells were transiently transfected with SUN1-myc, fixed with paraformaldehyde and permeabilized with Triton X-100 (a,b) or digitonin for 5 min (c,d) and 10 min (e) on ice. Immunofluorescence staining was performed with anti-myc (9E10) (red) and anti-SUN2 (green) antibodies. Arrowheads show mislocalization or reduction of SUN2 staining in the SUN1-myc transfected cells. **B)** NRK cells were fixed with paraformaldehyde and permeabilized with either Triton X-100 (a) or with digitonin on ice for 5 min (b) or 10 min (c) or at room temperature for 5 min (d). Immunofluorescence staining was performed using antibodies against the SUN2 CTD (green) and the LAP1 CTD (red).

Since we had now obtained conflicting results regarding the location of the SUN1 CTD, a further experiment was performed to confirm that the SUN2 CTD exhibit similar behaviour to the SUN1 CTD, using LAP1 antibodies as a control for ONM integrity. NRK cells were permeabilized with digitonin for 5 or 10 minutes on ice, or 5 minutes at room temperature, after fixation with paraformaldehyde and then co-stained with antibodies against the human SUN2 CTD (after verifying that they cross-react with rat SUN2) and the lumenal domain of LAP1. Immunofluorescence microscopy in control Triton-treated cells showed both SUN2 CTD and LAP1 staining in many cells (Fig. 3.10B a). In some Triton-treated cells, LAP1 staining was not as good as the SUN2 staining, which may have been due to poor permeabilization by Triton on this occasion. On the other hand, permeablizing cells with digitonin for 5 or 10 minutes on ice showed that SUN2 CTD was stained whereas there were very few LAP1 stained cells (Fig. 3.10B b,c). The result is similar to the previous result with the SUN1 CTD (Fig. 3.8B) and therefore suggests that the SUN2 CTD is also in the cytoplasm. As the published work of Hodzic et al. (Hodzic et al., 2004) contradicts this result, further experiments were required to definitively confirm the location of the SUN1 CTD. It is possible that the LAP1 antibody was not accessing the LAP1 CTD properly under the biochemical conditions used, giving different results to those of SUN1 and SUN2 antibodies.

3.2.5.4 Co-staining with antibodies against the cytoplasmic protein, α-tubulin, shows that the SUN1 CTD is not at the cytoplasmic face of the NE

As a follow-up to the previous studies, a further digitonin permeabilization experiment was performed where cytoplasmic α-tubulin was used as a control marker for plasma membrane integrity. Treating cells briefly with digitonin should only permeabilize the plasma membrane and not the NE. Therefore, both the SUN1 CTD and α-tubulin should be visible with brief digitonin treatment if the SUN1 CTD is located on the cytoplasmic face of the NE. NIH 3T3 cells were fixed with paraformaldehyde and then treated with digitonin on ice for 1, 2 and 5 minutes. The cells were then co-stained with anti-α-tubulin and 0545 SUN1 antibodies. NIH 3T3 cells were used as both anti-α-tubulin and 0545 SUN1 antibodies were raised against respective mouse proteins. Results showed that, with 1-2 minutes digitonin permeabilization, α-tubulin is visible, thus

demonstrating that the plasma membrane is permeabilized (Fig. 3.11d). Conversely, the SUN1 CTD was not visible at this time point. Only after 5 minutes digitonin treatment did the SUN1 CTD staining begin to appear, as found in previous experiments (Fig. 3.8B). This suggests that the SUN1 CTD is not located in the cytoplasm like α-tubulin, but more likely resides in the NE lumen like that of SUN2 and most other INM proteins.

3.2.5.5 The SUN1 CTD resides in the NE lumen

We suspected that the anti-LAP1 antibodies used in the initial experiments (section 3.2.5.1) were unable to detect their epitope under the biochemical conditions used (5 minutes, 4°C). To resolve this issue, another experiment was performed in the lab by Dr S. Shackleton using the INM protein, emerin, as a control marker for the ONM permeabilization. Since no other antibodies against lumenal domains of NE proteins were available, a C-terminally myc-tagged emerin construct was engineered. NIH 3T3 cells were transfected with the emerin-myc construct. Following digitonin treatment for 5 minutes on ice, both the lumenal myc tag and the SUN1 CTD were visible, whereas lamin A/C, used as a control marker for INM permeabilization, was not visible (Fig. 3.11b,f). This result is consistent with the α-tubulin control study and indicates that the SUN1 CTD is located in the NE lumen and not in the cytoplasm. In addition, the result also confirms the previous observation that digitonin-treatment for 5 minutes on ice permeabilizes only the ONM and not the INM.

3.2.6 Determining the location of four myc-tagged SUN1 proteins by digitonin permeabilization

Four full-length SUN1 constructs with a myc-tag at located different sites were generated in the lab (by Dr S. Shackleton and Dr C. Dent) to further probe the topology of SUN1. In addition to the N- and C-terminally myc-tagged constructs described previously, constructs containing a myc tag positioned internally after amino acid 355 (SUN1-355myc) and after amino-acid 456 (SUN1-456myc) were generated (Fig. 3.12A). The myc tag of the latter two constructs is located respectively, just upstream and downstream of H2-H4. These four myc-tagged SUN1 constructs were used for additional digitonin permeabilization studies. U2OS cells were transiently transfected
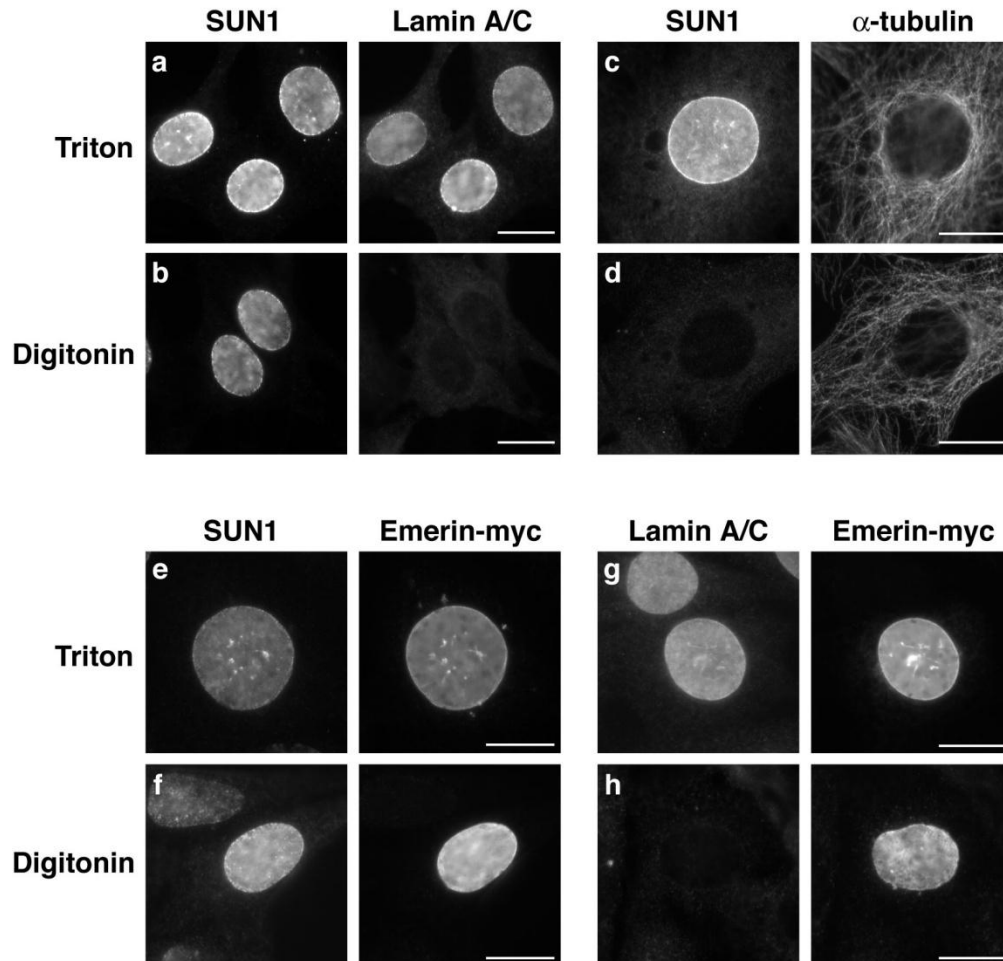
Fig. 3.11. The SUN1 CTD is located in the NE lumen. Untransfected (a to d) and emerin-myc transfected (e to h) NIH 3T3 cells were fixed with paraformaldehyde and permeabilized with either Triton X-100 (a,c,e,g) or with digitonin on ice for 5 min (b,f,h) or 2 min (d). Immunofluorescence staining was performed using antibodies against the SUN1 CTD, α-tubulin, lamin A/C and the myc epitope, as indicated. Scale bar, 10μm.
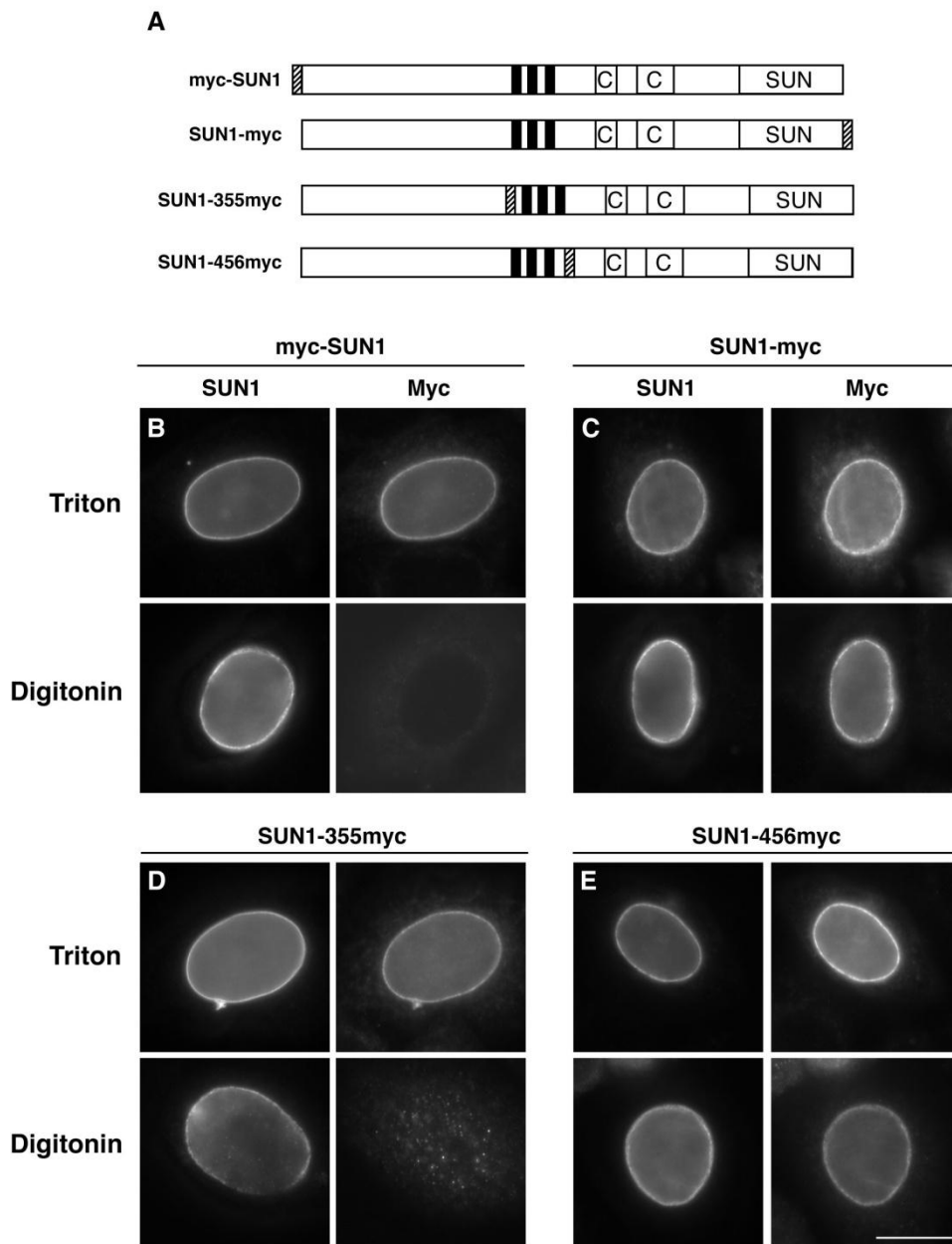
Fig. 3.12. Determination of SUN1 topology using myc-tagged SUN1 constructs.
A) Schematic representation of the myc-tagged SUN1 constructs, showing positions of myc tag as hatched boxes. **B-E)** U2OS cells were transiently transfected with the myc-tagged SUN1 constructs having myc-tag at the N-terminus (B) or the C-terminus (C) or internally after amino acid 355 (D) or after amino acid 456 (E). The cells were fixed with paraformaldehyde and permeabilized with either Triton X-100 (top) or digitonin for 5 min on ice (bottom). Immuonofluroscence co-staining was performed using antibodies against SUN1 (left side) and myc epitope (right side). Scale bar, 10μm.

with the myc-tagged constructs and then the cells were permeabilized with Triton X-100 or digitonin for 5 minutes on ice after paraformaldehyde fixation. They were co-stained with both anti-myc 9E10 and 0545 SUN1 antibodies. Anti-myc antibody staining was visible only in cells transfected with SUN1-myc and SUN1-456myc, both of which contain the myc tag within the CTD (Fig. 3.12C, E). On the other hand, the myc tag was not detectable in cells expressing myc-SUN1 and SUN1-355myc under the same biochemical conditions and these constructs contain the myc tag within the NTD (Fig. 3.12B, D). Since the ONM is disrupted but the INM is intact in cells treated with digitonin for 5 minutes on ice, this result therefore indicates residues 1-355 of SUN1 are located in the nucleoplasm. In addition, visualization of the myc epitope in SUN1-myc and SUN1-456myc transfected cells indicates that residues 450-913 are located in the NE lumen.

This result confirms the topology of SUN1 with the NTD in the nucleoplasm and the CTD in the NE lumen. As SUN1-355myc staining demonstrates the position of the myc-tag as being nucleoplasmic, this strongly suggests that the predicted transmembrane domain, H1 (residues 231-254), does not in fact span the INM. Therefore, of the three topologies proposed in Figure 3.2, topology C is the only one consistent with the data.

3.3 DISCUSSION

Almost all of the NE proteins characterized so far reside at the INM, except for the KASH domain proteins that reside at the ONM (Burke and Stewart, 2002; Zhen et al., 2002). Most INM proteins have a nucleoplasmic NTD, followed by one or more TMDs and a lumenal CTD. In general, NE proteins are targeted to the INM via their nucleoplasmic domain, assisted by a TMD and are retained there by interacting with the nuclear lamina (Holmer and Worman, 2001). SUN1 was previously found in the lab as a lamin A-binding protein in yeast two-hybrid screen that localized to the NE. SUN1 has an NTD, four predicted hydrophobic regions and a CTD with a coil-coiled region and a conserved SUN domain. On the commencement of this project, the characteristics of SUN1 protein were not known. Although the SUN1 NTD was expected to have a NE targeting sequence, further investigations were needed to delineate the sequence requirements for NE targeting of SUN1 and the mechanism of SUN1 nuclear anchoring. Moreover, although the SUN1 NTD was predicted to be located in the nucleoplasm, the location of the CTD was not known. Previous immuno-EM studies suggested that the SUN1 CTD is in the cytoplasm but this needed to be verified, as a topology with the CTD in the cytoplasm would be highly unusual for an INM protein. In addition, it was not clear whether H1 was a real TMD or not. The studies presented in this chapter give insights into the NE targeting behaviour and the topology of SUN1. During the period of this work, other groups have published data on SUN1 characteristics, which will be discussed along with the results of this study.

3.3.1 Delineation of the sequences required for the NE targeting of SUN1

Subcellular localization of various myc-tagged SUN1 deletion proteins was studied in order to define which sequence of SUN1 is responsible for the NE targeting. Surprisingly, both SUN1(1-355) and SUN1(355-913) were found to localize to the NE. This shows that both the SUN1 NTD and the CTD in conjunction with H2-H4, contain a NE retention sequence and can independently localize to the NE. In contrast, SUN1(450-913) was not concentrated at the NE but was found mostly in the cytoplasm. This indicates that in the absence of H2-H4, the SUN1 CTD cannot target itself to the NE. Experiments to determine the localization of the SUN1 deletion proteins after Triton pre-extraction produced interesting results. Following Triton pre-extraction only

the proteins that are tightly associated with the nuclear matrix are retained at the NE. Under these conditions, SUN1(1-432) and SUN1(1-355) remained at the NE, whereas SUN1(355-913) was no longer present. This indicates that the NE targeting of the SUN1 NTD is aided by its association with the nuclear lamina whereas SUN1(355-913) is targeted through a different mechanism. This therefore suggests that either the TMDs have intrinsic NE targeting capacity as observed for LBR (Smith and Blobel, 1993) or the CTD itself has a NE targeting signal. However, SUN1(450-913), which lacks H2-H4, was found exclusively in the cytoplasm, indicating that only in presence of H2-H4, is the SUN1 CTD anchored properly at the NE. Interestingly, Liu et al. showed that the SUN1 CTD fused to a heterologous TMD did not localize to the NE (Liu et al., 2007). Of note, Liu et al., also found that only H4 traverse the INM (section 3.3.2). However, although H2 and H3 do not span the membrane, they are important for localization of the SUN1 CTD at the NE, as H4 by itself was not sufficient enough to target the SUN1 CTD to the NE (Liu et al., 2007). This suggests that H2-H4 are all important for targeting SUN1(355-913) to the NE. In addition, Padmakumar et al. reported that SUN1(358-632), which includes H2-H4 and the coil-coiled region but lacks the SUN domain, can localize to the NE. Furthermore, SUN1(358-913Δcc), containing the CTD and H2-H4 but lacking the coil-coiled region, can localize to the NE (Padmakumar et al., 2005). Together these data indicate that H2-H4, rather than other regions in the SUN1 CTD, are essential for the NE localization of SUN1(355-913). However, H2-H4 sequences alone could not localize to the NE (Liu et al., 2007), suggesting that the SUN1 CTD domain has some function in facilitating the NE localization of SUN1(355-913). Nonetheless, the mechanism of retention of SUN1(355-913) at the NE is still not clear and oligomerization or association with other INM proteins or a nesprin/KASH domain protein might be responsible for targeting this fragment to the NE (Fig. 3.13B, C).

When expressed in the absence of a TMD, the NTD of most INM proteins, for example, LBR and emerin, accumulates only in the nucleoplasm and not at the NE (Holmer and Worman, 2001). From the above results, it is evident that SUN1(1-355) does not require H2-H4 to localize to the NE. The question therefore remains how SUN1(1-355) is able to localize to the NE. SUN1(1-355) contains H1 and it is possible that this is facilitating membrane attachment of this fragment. However, there was increasing doubt as to whether H1 is a real TMD, since SUN1(1-355) was found to be soluble in 7 M urea,

indicating that it does not contain a *bona fide* TMD (Haque et al., 2006). Moreover, Crisp et al. subsequently showed that H1 does not span the membrane using a proteinase K protection assay: an identical protease-resistant microsomal fragment was found for both full-length SUN1 and a mutant lacking the H1 (deletion of residues 222-343; Crisp et al., 2006). This indicates that, even though SUN1(1-355) does not have a membrane-spanning region, it can still target to the NE, a feature which is so far unique among those INM proteins that have been characterized. The likely explanation for this is that interaction with lamin A and/or other nuclear envelope proteins is contributing to the nuclear peripheral retention of this fragment (Fig. 3.13C). Crisp et al. also suggest that H1 can associate with the membrane, even though it does not span the lipid bilayer (Crisp et al., 2006) and thus it may still facilitate the NE targeting of the SUN1 NTD.

Further attempts to delineate the sequences within the NTD of SUN1 that are responsible for NE targeting were not successful. SUN1(1-229) and SUN1(223-355) did not localize to the NE. SUN1(223-355) was found as aggregates in the cytoplasm, while SUN1(1-229) was found in both the nucleoplasm and cytoplasm, although it may have been slightly concentrated in the nucleoplasm. Crisp et al. subsequently reported that SUN1(1-220) localises preferentially to the nucleoplasm but is recruited to the nuclear periphery upon co-transfection with prelamin A, the unprocessed form of lamin A (Crisp et al., 2006). In addition, Hasan et al. demonstrated that SUN1(1-300) is primarily found in the nucleoplasm but when fused with a heterologous TMD was re-located to the NE (Hasan et al., 2006). From the previous discussion it is evident that H1 is not a real TMD, therefore, neither SUN1(1-229) nor SUN1(223-355) contains a membrane-spanning region. To further investigate if these fragments can be located to the NE, the next logical step would be to attach these to a heterologous TMD and then analyse their localization in cells (discussed in section 7.1.1).

During the course of this investigation, it was observed that all SUN1 constructs that are capable of NE localization give rise to toxic effects in cells when expressed for 72 hours or longer. There were very few transfected cells remaining after 72 hours and many of these transfected cells showed nuclear deformity, seen mostly as micronuclei. The reason why nuclear abnormalities are caused is not clear, especially in the case of wild-type SUN1. One possibility is that the proteins may displace endogenous SUN1 and/or SUN2 and thus alter nuclear morphology by interfering with the normal binding

properties and functions of the endogenous proteins. In relation to this, Crisp et al. showed that over-expressed full-length SUN1 can displace endogenous SUN2 (Crisp et al., 2006). Moreover, in one of the digitonin permeabilization experiments presented in this chapter (Fig. 3.10A), it was found that exogenously expressed SUN1-myc can displace endogenous SUN2; this is discussed in more detail below (section 3.3.2). Furthermore, Liu et al. demonstrated that SUN1 CTD, H234SUN1L, equivalent to SUN1(355-913), can displace endogenous SUN1 from the NE (Liu et al., 2007). More recent work in our lab has also shown that SUN1(1-432) can displace both endogenous SUN1 and SUN2 (D. Mazzeo, unpublished data). Therefore, both SUN1 and SUN2 may need to be present to maintain NE structure. Significantly, Chi et al. reported that SUN1 may be involved in NE assembly after mitosis and that NE integrity is affected in SUN1 RNAi cells (Chi et al., 2007). Thus displacement of SUN1 and SUN2 may cause a NE assembly defect.

3.3.2 Determining the topology of SUN1 at the NE

At the beginning of this study, the topology of SUN1 was not known and indeed this was the case for all identified SUN proteins. From the Triton pre-extraction experiments it was evident that the N-terminus of SUN1 is anchored at the nuclear envelope by associating with the nuclear matrix. Furthermore, residues 1-355 of SUN1 were previously found to bind to lamin A (Haque et al., 2006). Together, this suggested that the NTD of SUN1 resides in the nucleoplasm, as for the majority of NE proteins. In support of this, a digitonin permeabilization experiment using N-terminally myc-tagged full-length SUN1 did not show any myc staining in cells where the INM was intact, therefore confirming that the SUN1 NTD is situated at the nucleoplasmic face of the NE.

Whilst the SUN1 NTD was found in the nucleoplasm, it was not known whether the SUN1 CTD is in the NE lumen, in the cytoplasm or in the nucleoplasm. A series of digitonin permeabilization experiments was therefore carried out to investigate the location of the SUN1 CTD. Initial experiments, using antibodies against the SUN1 CTD and the lumenal domain of LAP1, suggested that the SUN1 CTD is cytoplasmic. This was based on the fact that the SUN1 CTD was reliably detected in cells where LAP1 staining was absent. The lack of LAP1 staining strongly suggested that the ONM was

intact, leading to the conclusion that the SUN1 CTD was on the outer face of the NE, supporting the immuno-EM data (section 1.6). However, subsequent experiments using antibodies against the CTD of both SUN2 and SUN1 did not support this conclusion. Hodzic et al. already had shown that SUN2 has a lumenal CTD (Hodzic et al., 2004). In my digitonin experiments, SUN1 and SUN2 showed the same CTD location by antibody staining in cells where the ONM was permeabilized, suggesting that the SUN1 CTD is in the NE lumen. In support of this observation, a further experiment using antibodies against α-tubulin and the SUN1 CTD excluded the possibility that the SUN1 CTD resides in the cytoplasm. Here, α-tubulin staining was detected in the cytoplasm, whereas the SUN1 CTD was not detected, in cells where the ONM was intact. To unequivocally determine the location of the SUN1 CTD, a C-terminally myc-tagged emerin construct was engineered. As expected, both the SUN1 CTD and emerin CTD were found to be located in NE lumen. Based on all these results, the topology of SUN1, therefore, is that of a typical INM protein, with a nucleoplasmic NTD and a lumenal CTD.

It would have been highly unusual for the SUN1 CTD to reside anywhere other than the NE lumen. Since the SUN1 CTD was predicted to interact with the KASH domain of nesprins, this interaction would most likely occur in the NE lumen. Moreover, SUN1 is an INM protein and if the CTD were on the cytoplasmic face of the NE, the protein would have to traverse both the INM and the ONM, which has not been observed for any other INM protein so far. Therefore, the finding that the SUN1 CTD is in the NE lumen is more convincing. In support of this topology, Crisp et al. report the same configuration of SUN1 in proteinase K-protection assay (Crisp et al., 2006). However, why the LAP1 CTD was not detected under similar conditions was a mystery. The most likely explanation is that, as the LAP1 CTD antibody used was a monoclonal antibody, it had smaller binding surface and its epitope might have been masked or was not readily accessible after brief digitonin treatment. On the other hand, the SUN1 CTD antibody used was a polyclonal antibody and had a larger binding surface, which readily become accessible to antibodies upon ONM permeabilization. Moreover, the SUN1 CTD is quite large, comprising around 500 amino acids; in contrast the LAP1 CTD is half the size of the SUN1 CTD (around 200 amino acids, Martin et al., 1995). Thus the LAP1 CTD may be buried near the INM and be less accessible to the antibody

following partial digitonin permeabilization, while the SUN1 CTD being large was nearer to the ONM and was readily accessible.

Four myc-tagged full length SUN1 constructs were used to further delineate the configuration of SUN1 in digitonin permeabilization experiments. In accordance with the above results, it was found that the myc tag of myc-SUN1 (myc-tag at the N-terminus) and SUN1-myc (myc-tag at the C-terminus) reside at the nucleoplasm and at the NE lumen respectively. However, the myc tag of SUN1-355myc, which contains a myc tag after residue 355, was found to reside in the nucleoplasm. This suggests that SUN1(1-355) does not span the INM, and as discussed previously, this further supports the finding that H1 is not a real TMD. In addition, the myc tag of SUN1-456myc, containing a myc-tag after residue 456, was found in the NE lumen. This, therefore, indicates that there is a membrane-spanning region upstream of amino acid 456. Whilst it was not clear from these experiments, Liu et al. later reported that only H4 (residues 413 to 431) is capable of spanning the INM. In this study, C-terminally GFP or myc-tagged SUN1 chimeras containing only H4 did not show any staining with the respective antibodies, in digitonin permeabilized HeLa cells. In these cells the plasma membrane was permeabilized but the ER and the NE membranes remained intact. Therefore, the presence of membrane-spanning region H4 caused the GFP or myc tag to be within the PNS or the NE lumen, where it was not visible by immunofluorescence microscopy. However, this phenomenon was not observed with H2 or H3 containing GFP or myc-tagged SUN1chimeras, suggesting that only H4 traverse the INM (Liu et al., 2007). Similarly, SUN2 was also predicted to have two TMDs, but only the second was a true TMD (Hodzic et al, 2004). Therefore, both proteins have a hydrophobic region preceding the TMD, which presumably has some structural or functional importance.

As mentioned in the previous section, it was observed that SUN2 staining was reduced in SUN1-myc transfected cells. This indicates that over-expressed SUN1 can displace endogenous SUN2 and suggests that SUN1 and SUN2 have similar binding partners responsible for their anchoring at the INM. Crisp et al. observed the same effect but further found that transfected SUN2 could not displace endogenous SUN1 (Crisp et al., 2006). Interestingly, SUN2 was mislocalized from the NE in lamin A null cells in most cases whereas SUN1 was not (Haque et al., 2006; Crisp et al., 2006). This suggests that,

although SUN1 and SUN2 might share a subset of binding partners, SUN1 has additional binding partners that are contributing to its stable retention at the NE.

In summary, the results presented in this chapter show that SUN1 is an INM protein with a topology like most other INM proteins (Fig. 3.13B). SUN1 has an NTD that resides in the nucleoplasm and interacts with lamin A and also is responsible for anchoring the protein by associating with nuclear lamina. The CTD of SUN1 resides in the NE lumen. Results presented here and the observations of other groups show that H1 is not a true TMD and, like a typical type II membrane protein, SUN1 has only one TMD which is represented by H4 (Crisp et al., 2006; Liu et al., 2007). Investigation to determine the NE targeting sequences of SUN1 showed that both the SUN1 NTD and the CTD, in association with H2-H4, have independent NE targeting signals. The association of SUN1(1-355) with the nuclear lamina might be contributing to its NE retention, on the other hand, oligomerization or more extensive interactions in the NE lumen probably contribute to the NE retention of SUN1(355-913). However, the exact mechanism and signal behind the stable anchorage and the targeting of SUN1 at the NE is yet to be resolved.
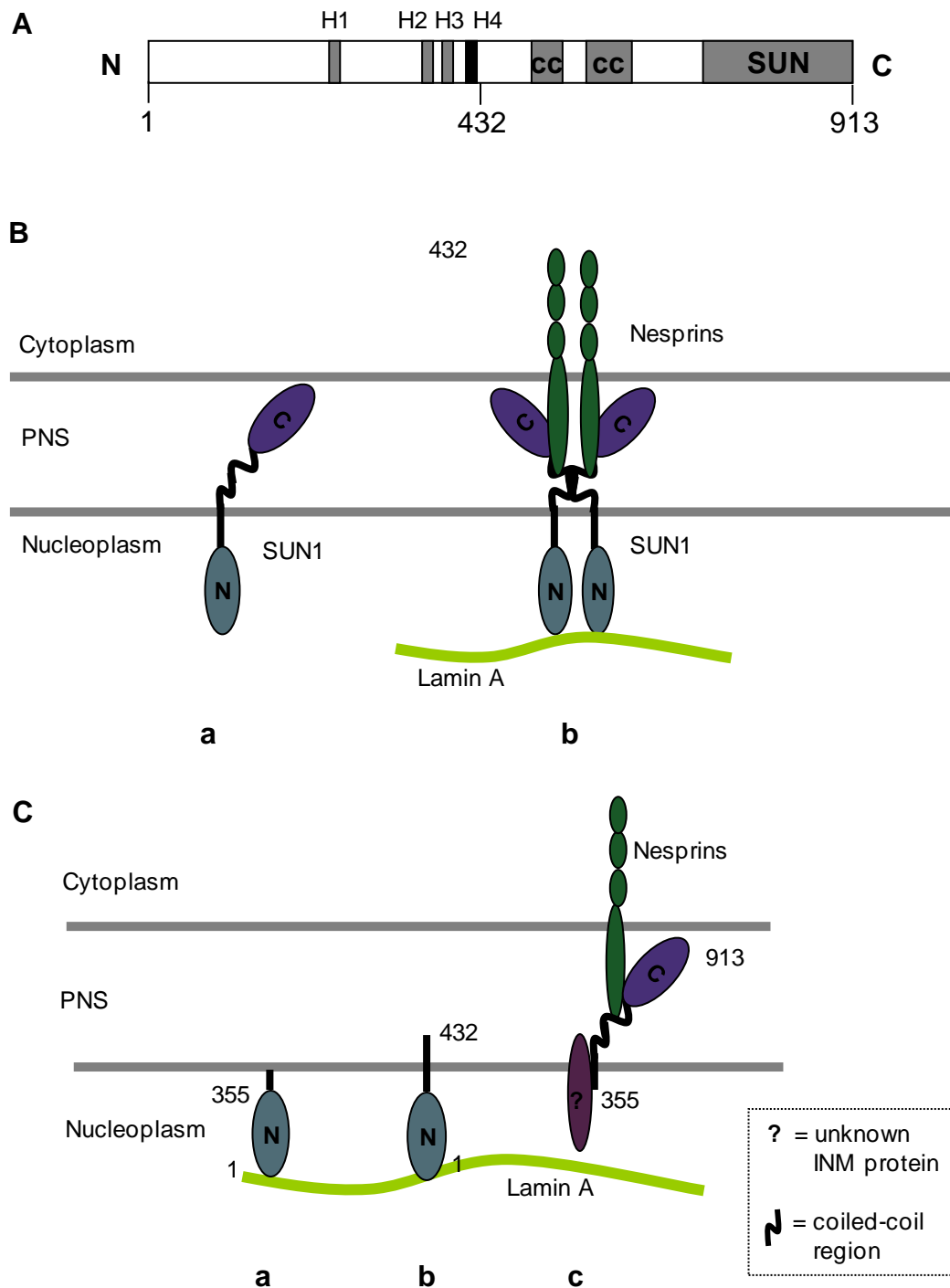
Fig. 3.13. Schematic representation of nuclear envelope   targeting and configuration of SUN1. A) SUN1 structure with only a single transmembrane domain (H4). **B)** SUN1 topology at the INM with the NTD in the nucleoplasm, a single TMD and the CTD in the lumen (a). Hypothesized SUN1 oligomerization and interactions at the NE (Padmakumar et al., 2005) (b). **C)** SUN1 residues 1-355 and 1-432 can target to the NE (a, b) by associating with lamin A. SUN1 residues 355 -913 can target to the NE possibly by interacting with nesprins or other INM proteins or oligomerization (c).

CHAPTER 4

CHARACTERIZING SUN PROTEIN INTERACTIONS WITH NUCLEAR LAMINS

4.1 INTRODUCTION

Nuclear lamins interact with a large number of proteins, which include both nucleoplasmic and INM-associated proteins. This allows them to have a wide range of roles in nuclear function. Interaction of INM proteins with the lamina is required for their localization to the INM, for example emerin does not localize to the INM in *LMNA* -/- cells (Sullivan et al., 1999). Conversely, interactions with INM proteins help attach the lamina to the INM. Regarding other functions, lamins interact with different transcription factors such as germ-cell-less (GCL) and retinoblastoma protein (Rb) to provide scaffolds for these complexes (Goldman et al., 2002; Gruenbaum et al., 2005). Lamins also interact with actin and nesprins that offer structural support to the nucleus (Zastrow et al., 2004). These interactions are required to establish extensive protein networks at the INM and to maintain nuclear integrity.

Mutations in proteins of the nuclear lamina, mainly lamin A/C and lamin-associated proteins are found in a number of inherited diseases in human, known as laminopathies. On the other hand, B-type lamins are essential for survival (Vergne et al., 2004). Laminopathies affect predominantly mesenchymal-derived tissues: skeletal and cardiac muscle, fat, skin and bone. Disease mutations of lamin A/C are distributed throughout the head, rod and tail domains, but in lipodystrophy, Hutchinson-Gilford progeria syndrome and mandibuloacral dysplasia, mutations are clustered within the C-terminus (Fig. 1.12; Mattout et al., 2006). Extensive research is being conducted to understand the mechanisms behind these laminopathies. Different lamin A-binding partners and their interactions are therefore being studied thoroughly.

The aim of this chapter was to investigate the interaction between the lamins and SUN domain proteins (SUN1 and SUN2). SUN proteins are homologues of Sad1 in yeast and UNC-84 in *C. elegans*. Of interest, yeast does not express lamins and *C. elegans* has only one lamin (Ce-lamin), which is a B-type lamin. NE localization of UNC-84 depends on its interaction with Ce-lamin (Lee et al., 2002). From the results of the last chapter, it is evident that the SUN1-NTD is associated with the nuclear lamina. Moreover, SUN1 was identified initially in our lab as a lamin A-binding protein in a yeast two-hybrid screen using the C-terminal domain (CTD) of lamin A as bait. *In vitro* interaction assays subsequently confirmed that SUN1(1-355) interacts with lamin A.

Interestingly, SUN1 was found stably anchored at the NE in the absence of lamin A/C (Haque et al., 2006, Crisp et al., 2006) whereas many INM proteins, for example, emerin and nesprins are mislocalized from the NE in the absence of lamin A/C (Sullivan et al., 1999, Libotte et al., 2005). This indicates that SUN1 has other binding partners that contribute to its NE anchoring in the absence of lamin A/C, and it is possible that SUN1 interacts with B-type lamin isoforms to contribute to this stable anchorage.

Here, further investigations were carried out to characterize SUN1 interactions with all of the major lamin isoforms. The binding sites of SUN1 and SUN2 for lamin A were mapped to understand their functional relevance and potential disease association. Several SUN1, SUN2 and lamin A sub-fragments were generated and their associations were tested by *in vitro* pull-down assays. Pull-down assays are a common and confirmatory approach to study protein-protein interactions *in vitro*. Here, the bait protein was expressed in bacteria as a glutathione-S-transferase (GST) or maltose binding protein (MBP) fusion protein and then purified and immobilized onto glutathione-Sepharose or amylose beads, respectively. Then the bait protein was incubated with an *in vitro*-translated [^{35}S]-labelled prey protein, so that if there was an interaction between the two, the prey protein would be pulled down along with the bait protein (Fig. 4.1). This interaction is then detected using sodium dodecyl sulphate-polyacrylamide gel electrophoresis (SDS-PAGE) and autoradiography. The results of these interaction assays between SUN1 or SUN2 and lamin A are described in this chapter.

Bacterial lysate expressing bait protein

In vitro translated [^{35}S]-labelled prey protein

Bait protein Incubated with glutathione – Sepharose beads

Glutathione-Sepharose beads

Glutathione-Sepharose beads

Immobilization of fusion proteins on beads

Incubation of bait and prey proteins

Glutathione-Sepharose beads

Detection of bound prey protein by SDS-PAGE and autoradiography

Fig. 4.1. Schematic representation of an *in vitro* pull-down assay. Bait proteins fused to glutathione-S-transferase (GST) or maltose binding protein (MBP) are expressed in bacteria. Bait proteins are then incubated with and immobilized on glutathione-Sepharose or amylose beads. Prey proteins are produced *in vitro* and labelled with [^{35}S]. Bait and prey proteins are incubated for potential interaction. Eluted proteins are subjected to SDS-PAGE and autoradiography to detect the bound proteins.

4.2 RESULTS

4.2.1 SUN1 NTD interacts with lamin A but not other lamin isoforms

SUN1 is retained at the NE in the absence of lamin A/C, whereas most other INM proteins diffuse to the ER in this situation (Haque et al., 2006). In order to identify whether SUN1 interaction with other lamin isoforms is contributing to its NE anchorage, direct interactions between SUN1 and lamin A, C, B1 and B2 were tested by MBP pull-down.

Construct pMAL-SUN1(1-355) was used to generate the MBP-SUN1(1-355) bait. pCI-LMNA and pCI-LMNB1 constructs were used to produce lamin A and lamin B1 prey proteins, respectively. These had been generated previously in the lab. pBS-LMNB2 was obtained from E. Schirmer (Edinburgh University, UK), as a kind gift. For production of lamin C, a new prey construct, pCI-LMNC, was generated by excising the *Apa*I and *Not*I insert fragment from the plasmid pCI-mycLMNC, which was used to replace the equivalent restriction fragment in pCI-LMNA by sequential digestion with the same enzymes. All prey constructs had an upstream T7 promoter to facilitate *in vitro*-transcription (Fig. A.2).

The bait plasmids, empty pMALc2g (containing only the MBP protein for use as a negative control) and pMAL-SUN1(1-355), were transformed into the BL21 strain of *E. coli* and cultures of these were grown accordingly and induced with IPTG. Soluble lysates were then incubated with amylose resin to immobilize the MBP-fusion proteins. MBP and MBP-SUN1(1-355) were incubated with equal amounts of *in vitro*-translated, [^{35}S] methionine-labelled lamin A, C, B1 or B2. The bound proteins from the amylose beads were eluted and SDS-PAGE was performed. The gel was subjected to autoradiography to detect the bound lamin A, C, B1, and B2.

From the result, it is apparent that only lamin A was efficiently pulled down by SUN1(1-355) (Fig. 4.2), confirming the interaction between the SUN1 NTD and lamin A. A weak interaction between lamin C and the SUN1 NTD was seen, but a band of similar intensity was produced in the presence of MBP alone, the control. This indicates that it was a residual interaction and the SUN1 NTD does not interact with

142
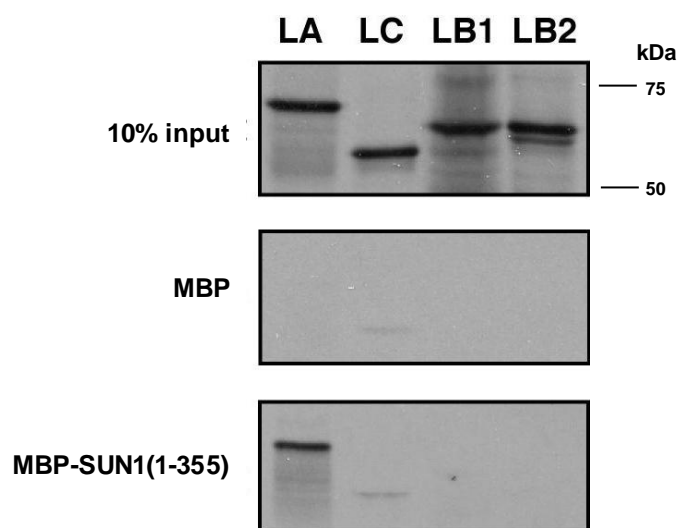
Fig. 4.2. SUN1 interaction with lamin A. [35S]-labelled lamin A (LA), lamin C (LC), lamin B1 (LB1) and lamin B2 (LB2) were produced by *in vitro* translation (top). The proteins were each incubated with MBP alone (middle) and MBP-SUN1(1-355) (bottom), previously bound to amylose beads. Bound proteins were detected by autoradiography, following SDS-PAGE.

lamin C. Furthermore neither isoforms of B-type lamins showed any interaction with the SUN1 NTD. This was unexpected and indicates that there might be binding factors other than the lamins present at the NE, that are contributing to the stable anchorage of SUN1 at the NE.

4.2.2 Mapping the SUN1 binding site for lamin A

4.2.2.1 Lamin A binds to SUN1 residues 1-229

In order to map the lamin A binding site on the SUN1 NTD, two GST-fused constructs comprising SUN1 N-terminus residues 1-229 and 223-355 were generated (Fig. 4.3A and Fig. A.4). The pGEX-SUN1(1-229) and pGEX-SUN1(223-355) plasmids were transformed into the BL21 strain of *E. coli.* Empty vector pGEX-4T3, encoding GST protein only, was used as a negative control and pGEX-SUN1(1-355) was used as a positive control. The GST-fused SUN1 proteins were bound to glutathione-Sepharose beads and were incubated with equal amount of lamin A, *in vitro*-translated from plasmid pCI-LMNA. SDS-PAGE of the eluted proteins was performed followed by autoradiography to detect bound [^{35}S]-labelled lamin A.

The results show that SUN1(1-229) interacts as strongly with lamin A as SUN1(1-355) (Fig. 4.3B), whereas SUN1(223-355) showed significantly weaker binding with lamin A. This indicates that the major binding site for lamin A on SUN1 lies within residues 1-229. However, the weak binding of lamin A to SUN1(223-355) suggests that there might be an additional binding site for lamin A on SUN1. Alternatively, this could also represent a non-specific interaction between these two proteins, for example due to misfolding of the SUN1 223-355 fragment.

4.2.2.2 Comparison of SUN1 and SUN2 sequences

The amino acid sequences of the N-terminal domains of mouse SUN1 and SUN2 were compared using ClustalW multiple sequence alignment software (Fig. 4.4), which revealed some regions of significant dissimilarity between the two sequences. Firstly, the SUN2 NTD, comprising 175 amino acids, is smaller than the 355 residues SUN1 NTD. This is because a major portion of the SUN1 N-terminal sequence is absent in the

A

B
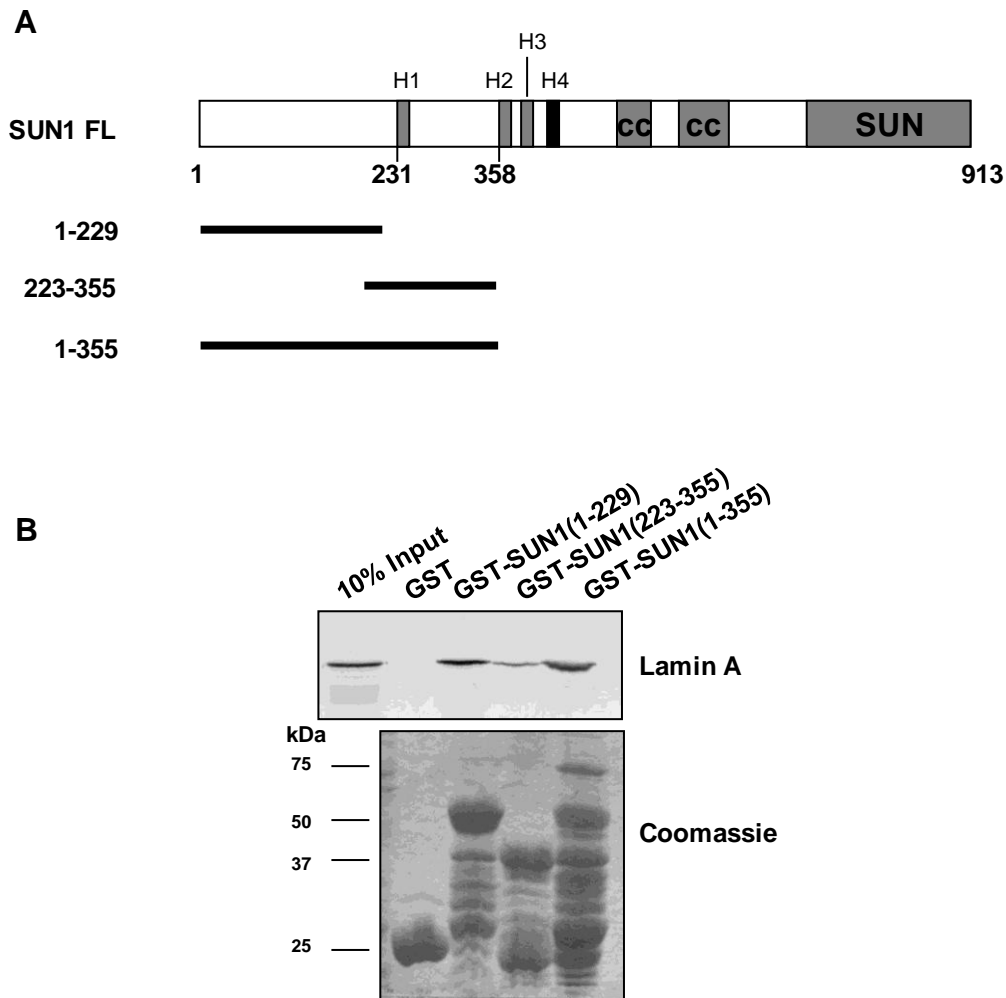
Fig. 4.3. Lamin A binds to residues 1-229 of SUN1. A) Schematic representation of SUN1 structure and SUN1 constructs used. H1, H2, H3 and H4 represent the four hydrophobic sequences present in SUN1. **B)** [35S]-labelled lamin A was produced by *in vitro* translation. Lamin A was incubated with GST and GST-SUN1 fusions, as indicated, previously immobilized on glutathione-Sepharose beads. Bound lamin A was detected by autoradiography. Coomassie-stained gel shows expression of the GST fusion proteins.
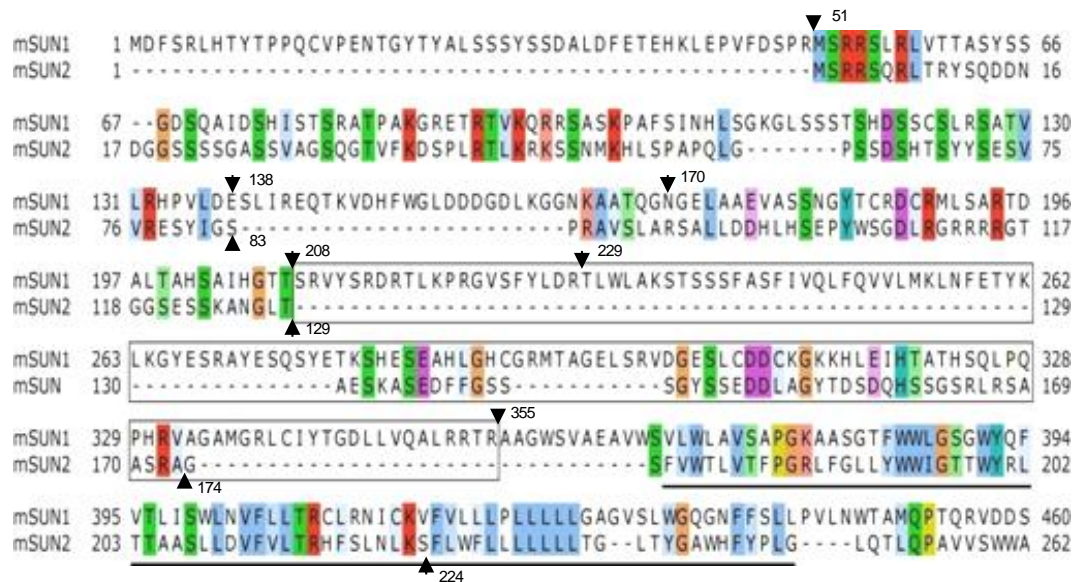
Fig. 4.4. Comparison of SUN1 and SUN2 NTDs. Alignment of murine SUN1 and SUN2 N-termini using ClustalW software. Coloured residues indicate related or identical amino acids between the two sequences. Boxed area indicates SUN1 residues 209 to 355. The hydrophobic region is underlined. Arrow-heads show amino acid positions used to make new constructs for interaction assay.

SUN2 N-terminus. The comparison shows that SUN1 and SUN2 have some homology up to residue 208 of SUN1 but then residues homologous to 209-355 of SUN1, which are immediately upstream of the hydrophobic regions of SUN1, are absent from SUN2. In the previous study, residues 1-229 and 223-355 were used as two sub-domains of the SUN1 NTD to test for interaction with lamins. The sequence comparison suggested that a better location for the breakpoint between the two halves of the NTD of SUN1 was after residue 208, rather than 229. Based on this, two additional GST-fused constructs, pGEX-SUN1(1-208) and pGEX-SUN1(209-355), were generated (Fig. 4.5A). These constructs were engineered by PCR amplification of the relevant region of the SUN1 cDNA, using appropriate primers and then cloning of the products into the *EcoR*I and *Sal*I site of plasmid pGEX-4T3.

Another GST-fused SUN1 construct comprising amino acids 1-170 was designed to map the binding site of lamin A on SUN1 NTD. Interestingly, the sequence comparison also showed that the first 50 amino acids of SUN1 are absent from SUN2 (Fig. 4.4). Therefore, to test whether these residues had any significance in lamin A binding of SUN1, constructs pGEX-SUN1(50-208) and pGEX-SUN1(50-170) were generated and used for the following interaction assay.

4.2.2.3 The lamin A binding site lies within the first 138 residues of SUN1 and the first 50 amino acids of SUN1 are essential for the interaction of SUN1 with lamin A

The GST-fused SUN1 constructs mentioned in the previous section were used in GST pull-down assays to test their interactions with lamin A. As shown in Figure 4.5B, SUN1(1-208) and SUN1(209-355) bind lamin A in an identical manner to SUN1(1-229) and SUN1(223-355) respectively, that is 1-208 interacts strongly, whereas 209-355 has a significantly weaker interaction with lamin A. The lamin A binding site was further narrowed to 1-170 by the observation that this fragment also interacts strongly with lamin A. Surprisingly, SUN1(50-208) and (50-170), lacking the first 50 amino acids, did not pull down lamin A, suggesting that this region of SUN1 is important with regard to binding lamin A or for correct folding of this domain.

A

B

C
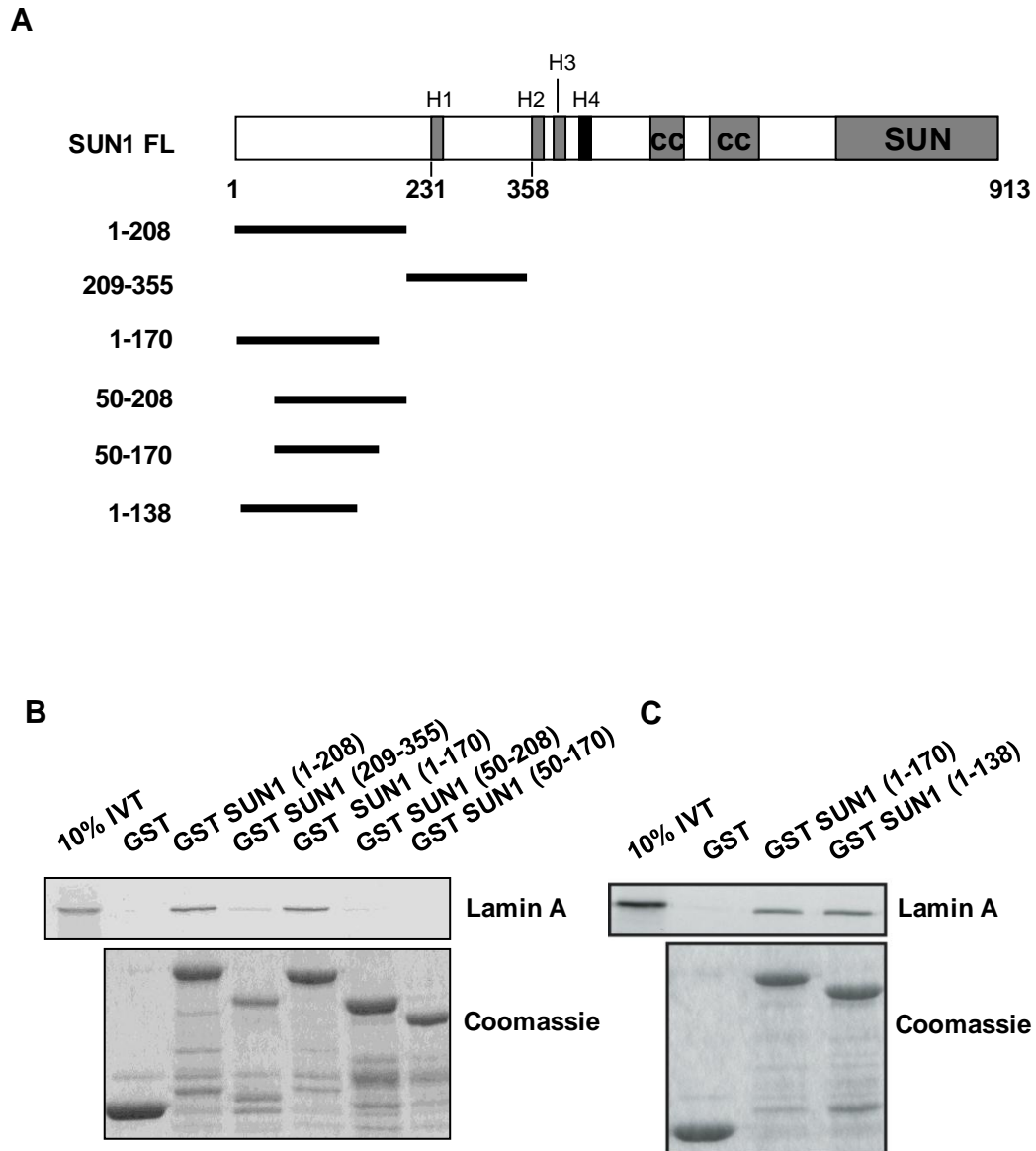
Fig. 4.5. Further narrowing down of the lamin A interaction site on the SUN1 NTD. A) Schematic representation of SUN1 structure and SUN1 constructs generated. **B,C)** [^{35}S]-labelled lamin A was produced by *in vitro* translation. Lamin A was incubated with GST or GST-SUN1 fusions as indicated, previously bound to glutathione-Sepharose beads. Bound lamin A was detected by autoradiography. Coomassie-stained gels show expression of the GST fusion proteins.

To further narrow down the binding site for lamin A on SUN1, additional N-terminal construct SUN1(1-138) was generated, following sequence comparison with SUN2. SUN1 and SUN2 sequences diverge after residue 138 of SUN1, as 24 amino acids are absent following this sequence in SUN2 (Fig. 4.4). pGEX-SUN1(1-138) was generated by PCR amplification of the relevant region of the SUN1 cDNA and then cloned into *Eco*RI and *Sal*I sites of the plasmid pGEX-4T3. pCI-LMNA was used to *in vitro* translate lamin A protein. GST pull-down assays were then performed to investigate the interaction between SUN1(1-138) and lamin A (Fig. 4.5C). GST and GST-SUN1(1-170) proteins were used as negative and positive controls, respectively. Equal amounts of lamin A were incubated with each of the SUN1 protein fragments. The results revealed that SUN1(1-138) binds as strongly with lamin A as SUN1(1-170). Thus, the shortest SUN1 fragment found to bind with lamin A is SUN1(1-138).

4.2.3 Mapping the binding site of lamin A on SUN2: the lamin A binding site lies within the first 129 residues of SUN2

A similar pull-down approach was used to map the SUN2 binding site for lamin A. Initially, based on the published topology of SUN2 (Hodzic et al., 2004), a GST-SUN2(1-224) construct was generated in the lab by Dr S. Shackleton, comprising the N-terminus and first hydrophobic region of SUN2 (Fig. 4.6A). Crisp et al. subsequently demonstrated that the first 165 residues of SUN2 are sufficient to bind lamin A in a GST pull-down assay (Crisp et al., 2006). After sequence comparison between SUN1 and SUN2, additional GST-fused SUN2 constructs were therefore generated. pGEX-SUN2(1-129) and pGEX-SUN2(1-83) were engineered (Fig. A.4) to be equivalent to pGEX-SUN1(1-208) and pGEX-SUN1(1-138) constructs (Fig. 4.4 and 4.6A). These constructs were generated by PCR amplification of the relevant regions of the SUN2 cDNA and then were cloned into the *Eco*RI and *Sal*I sites of plasmid pGEX-4T3.

The GST fusions encoded by these constructs were used in GST pull-down assays to assess their interaction with lamin A. The assays were carried out in the same manner as described previously. SUN2(1-129) interacted as strongly with lamin A as SUN2(1-224), whereas SUN2(1-83) showed a significantly weaker interaction (Fig. 4.6B). Although from sequence comparison, SUN2 residues 1-83 were equivalent to SUN1 residues 1-138 (the shortest SUN1 fragment to bind lamin A), SUN1 contains extra 50

A
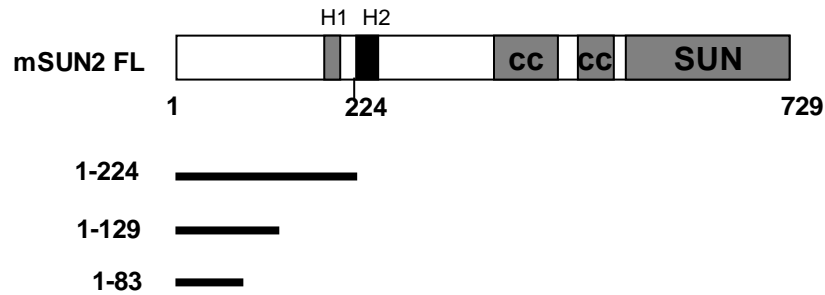
B
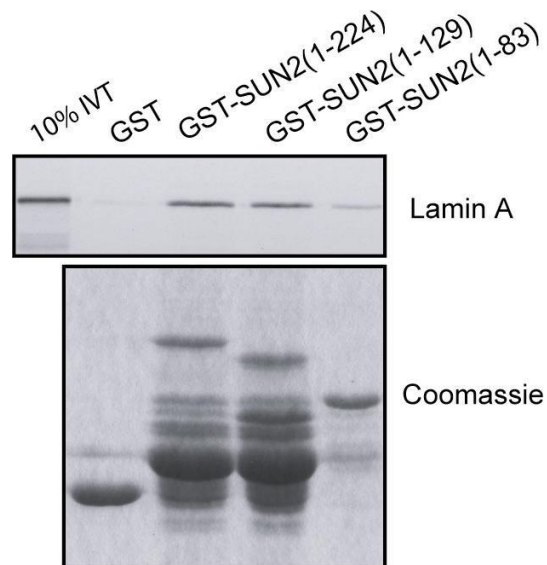
Fig. 4.6. Mapping SUN2 interaction with lamin A. A) Schematic representation of SUN2 constructs used, vertical bars denoting hydrophobic sequences. **B)** [^{35}S]-labelled lamin A was produced by *in vitro* translation. Lamin A was incubated with GST or GST-SUN2 fusions as indicated, previously immobilized on glutathion-Sepharose beads. Bound lamin A was detected by autoradiography. Coomassie-stained gel shows equal expression of the GST fusion proteins.

amino acids at the N-terminus that are absent in SUN2. These suggest SUN2(1-83) might not be correctly folded and residues between 84-129 are important for lamin A binding. Thus, the shortest SUN2 sequences found to bind lamin A are residues 1-129.

4.2.4 The SUN1 NTD interacts with the CTD of lamin A

4.2.4.1 SUN1 interacts with the C-terminal residues 389-664 of lamin A

Many INM proteins such as emerin, nesprin-2 and LAP2α interact with the globular C-terminus of lamin A (Goldman et al., 2002; Libotte et al., 2005). Previously in our lab, SUN1 was identified as a novel lamin A interacting protein in a yeast two-hybrid screen, using the lamin A CTD as a bait. Here, MBP pull-down assays were performed to confirm whether SUN1 interacts with the N-terminal head and rod domain or the C-terminal globular domain of lamin A. MBP-SUN1(1-355) was used to test its interaction with *in vitro*-translated lamin A sub-fragments comprising amino acids 1-389 and 389-664 residues of lamin A (Fig. 4.7A). Constructs pMAL-SUN1(1-355) and pET-laminA(1-664), pET-laminA(1-389) and pET-laminA(389-664) were utilized for this experiment and were generated previously in the lab.

As shown in Figure 4.7B, the SUN1 NTD interacted with laminA(389-664), comprising the CTD, but did not pull down laminA(1-389), comprising the head and rod domain. The interaction between SUN1 and laminA(389-664) was as strong as SUN1 interaction with the full length (FL) lamin A. This result confirmed that the SUN1 binding site lies within the C-terminal region lamin A. Of note, the FL lamin A construct encodes 664 amino acids, which represents the prelamin A sequence. It was not known whether *in vitro* translation using the rabbit reticulocyte system would facilitate proteolytic processing to produce mature lamin A or whether unprocessed prelamin A would remain. In contrast to mature lamin A, the prelamin A contains an extra 18 amino acids and can also be farnesylated at the C-terminus (section 1.1.2.3). Further tests were, therefore, performed to see whether SUN1 interacts preferentially with the CTD of mature lamin A or prelamin A.

A

B
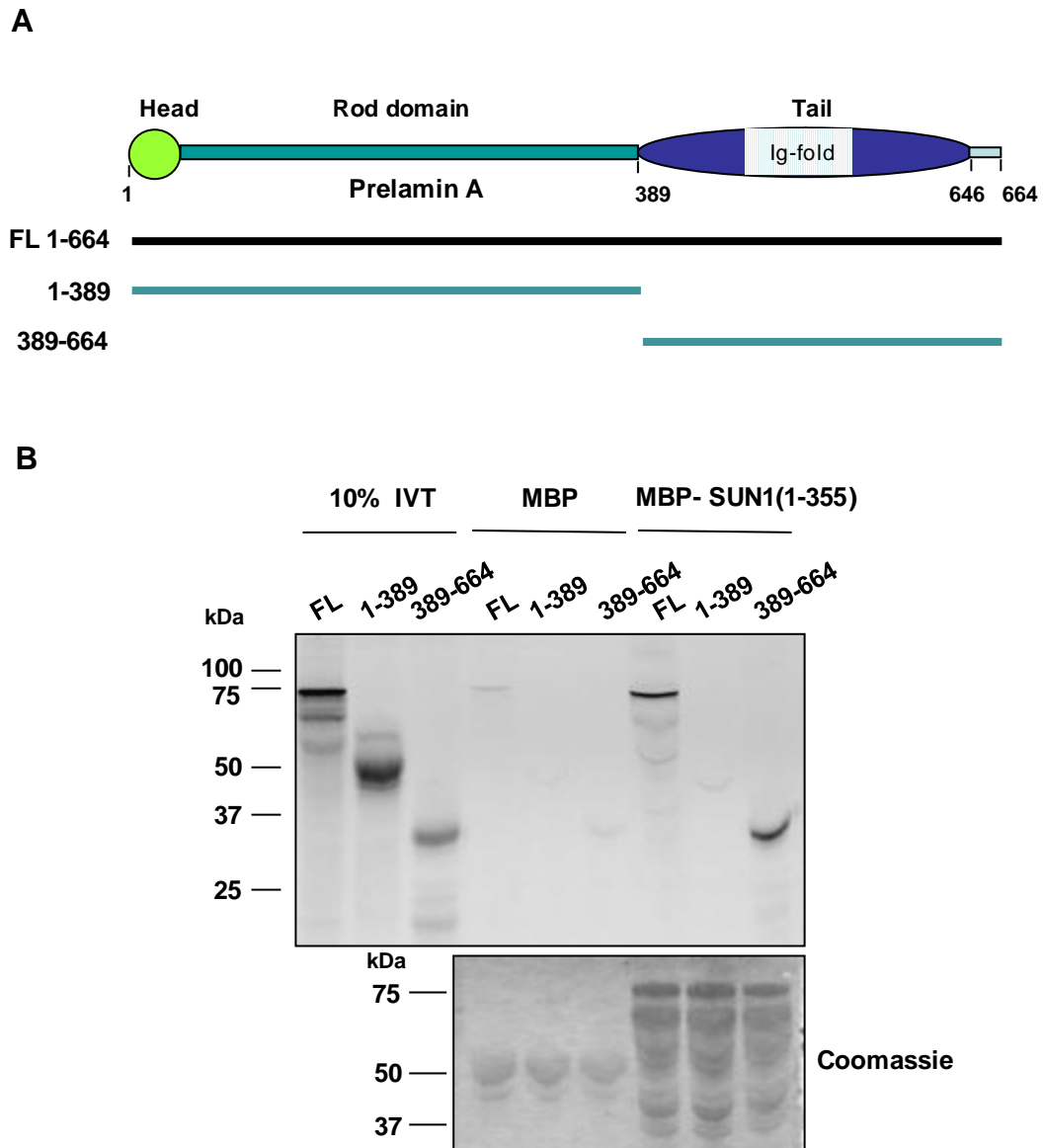
Fig. 4.7. SUN1 NTD interacts with the CTD of lamin A. A) Schematic representation of prelamin A and lamin A constructs used. Here, FL denotes pre-lamin A, comprising 664 amino-acids. Hatched area shows Ig-fold in the lamin A tail. **B)** [^{35}S]-labelled FL lamin A, lamin A (1-389) and lamin A (389-664) were produced by *in vitro* translation. The lamin A fragments were each incubated with MBP and MBP-SUN1(1-355) as indicated, previously immobilized on amylose beads. Bound lamin A fragments were detected by autoradiography. Coomassie-stained gel shows equal expression of the MBP fusion proteins.

4.2.4.2 SUN1 interacts with the C-terminus of both mature lamin A and prelamin A

Research carried out by Crisp et al. demonstrated that SUN1 interacts preferentially with prelamin A. In a GST pull-down assay, they found that SUN1(1-220) binds significantly more strongly to prelamin A than to mature lamin A (Crisp et al., 2006). To confirm this finding in our hands, an MBP pull-down assay was performed. A pET-laminA(389-L647X) construct was generated (by Dr S. Shackleton) which has a stop (X) codon incorporated at residue 647 in place of leucine (L), thus mimicking the processing that produces mature lamin A. Interaction between laminA(389-L647X) encoding residues 389-646 and MBP-SUN1(1-355) was tested along with control laminA(1-389) and laminA(389-664) (Fig. 4.8B). SUN1(1-355) appeared to interact with the C-terminus of both mature laminA(389-646) and prelaminA(389-664) with equal affinity. This result contradicts the findings of Crisp et al, as mentioned above. Further investigations are, therefore, required to verify this result.

4.2.4.3 Additional mapping of SUN1 binding on the lamin A CTD

Further narrowing down of the SUN1 binding site on the CTD of lamin A was attempted. Two additional constructs pET-laminA(389-510) and pET-laminA(450-664) were therefore generated (Fig. 4.8A and Fig. A.5). These constructs were used to test their interactions with SUN1(1-355) by MBP pull-down assay. MBP protein and *in vitro*-translated lamin A(1-389) were used as negative controls. The result shows that SUN1 interacted with both the C-terminal sub-fragments, laminA(389-510) and laminA(450-664) (Fig. 4.8B). The presumption was that SUN1 would bind to the extreme C-terminus of lamin A. The extreme C-terminus of lamin A is absent in lamin C, and previous finding shows that SUN1 does not interact with lamin C. However, the SUN1 binding region within the C-terminus of lamin A could not be determined from this result, as both C-terminal sub-fragments of lamin A interacted by equal intensity with SUN1.

An alternative approach was therefore taken to narrow SUN1 binding region on lamin A by performing the pull-downs in the opposite orientation. Existing GST-fused C-terminal fragments of lamin A (residues 389-664, 389-510, 450-664, 450-510 and 510-664) were utilized to pull down *in vitro*-translated SUN1 NTD (Fig. 4.9A). Plasmid
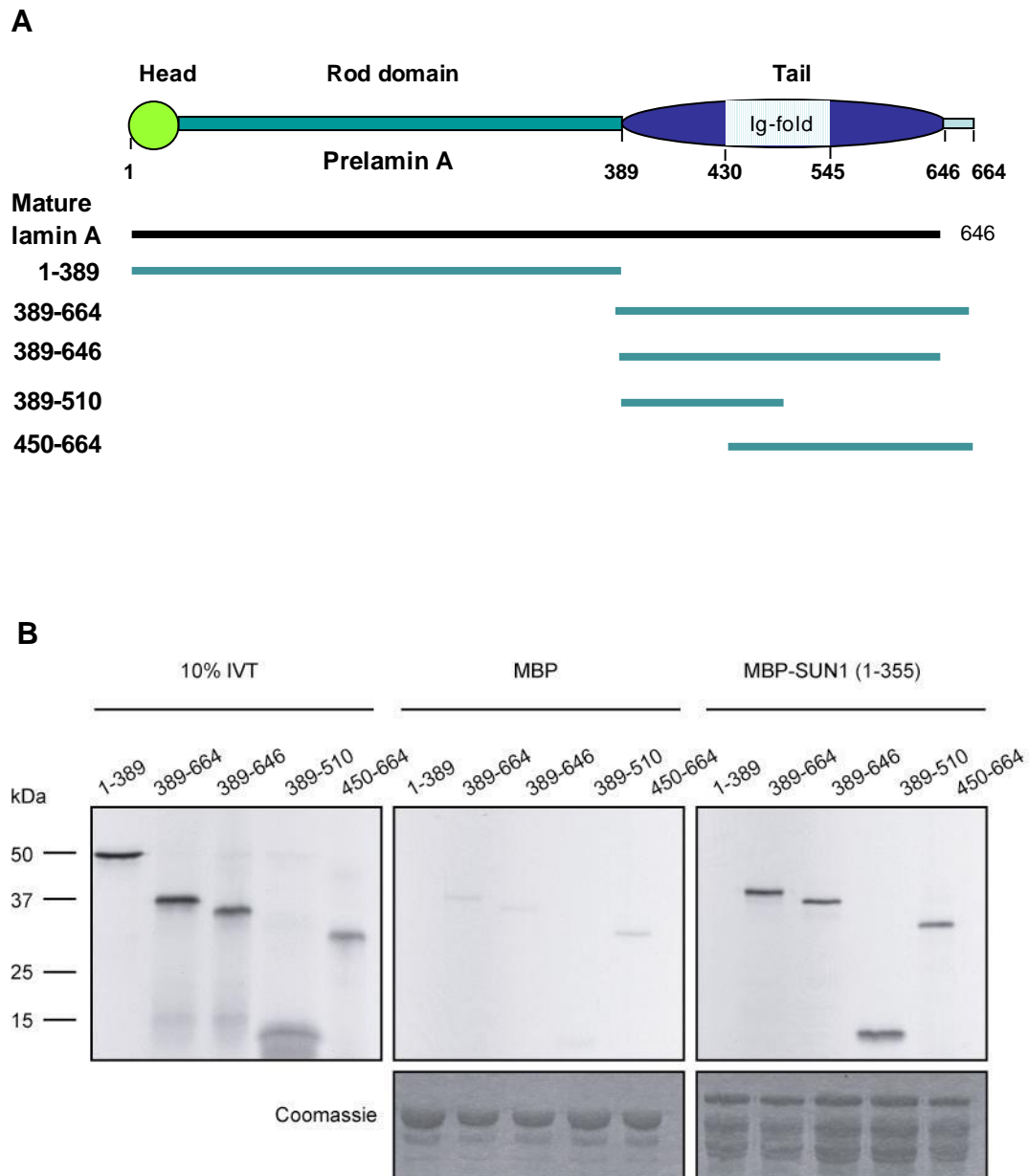
Fig. 4.8. Interaction of the SUN1 NTD with the CTD of pre-lamin A and lamin A.
A) Schematic representation of prelamin A and lamin A constructs used. **B)** [^{35}S]-labelled lamin A (1-389), lamin A (389-664), lamin A (389-646), lamin A (389-510) and lamin A (450-664) were produced by *in vitro* translation (left panel). The proteins were each incubated with MBP (middle panel) and MBP-SUN1(1-355) (right panel), previously immobilized on amylose beads. Bound lamin A protein was detected by autoradiography. Coomassie-stained gel shows equal expression of the MBP fusion proteins.
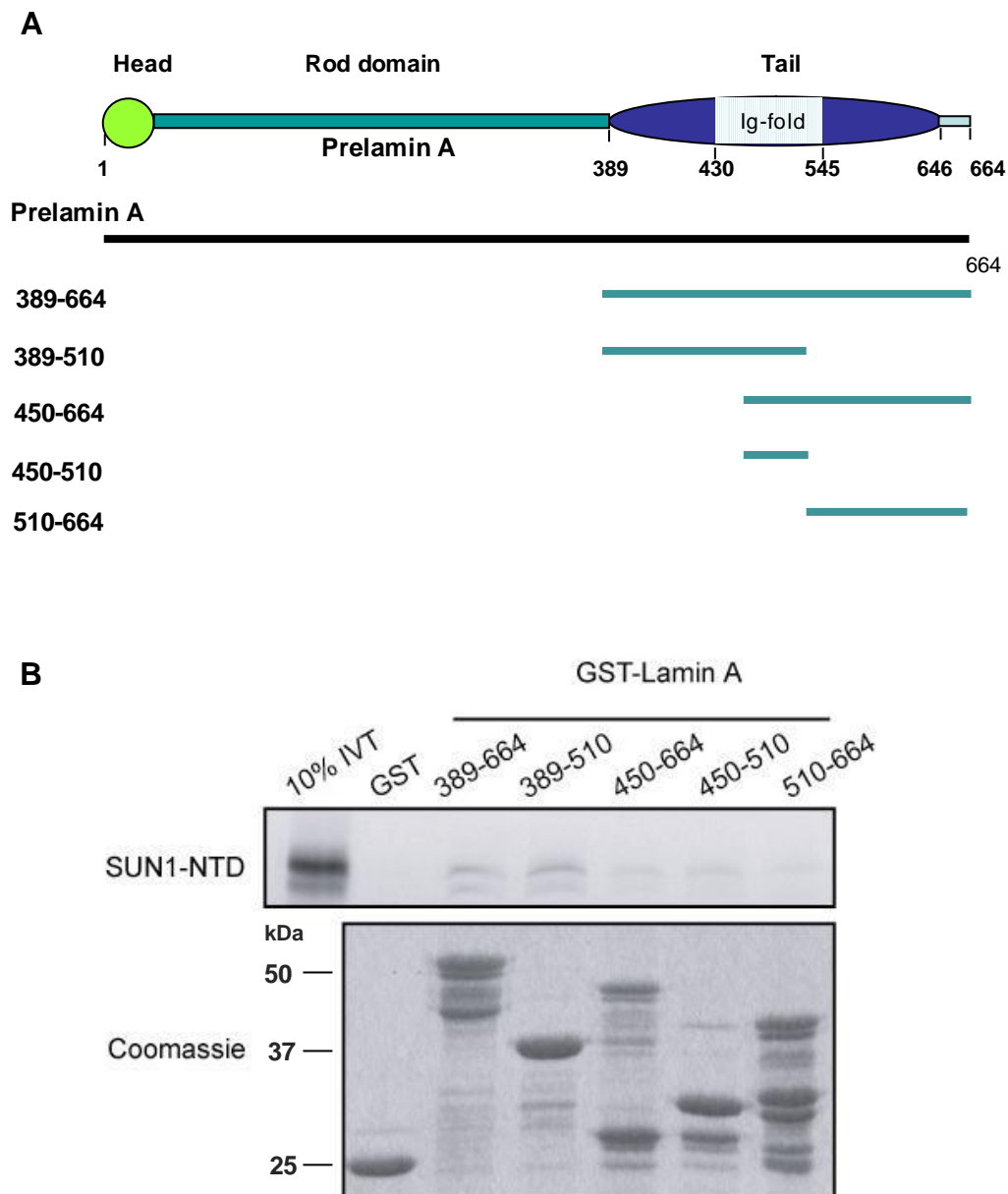
Fig. 4.9. Narrowing down of the SUN1 NTD binding region on the CTD of lamin A. A) Schematic representation of prelamin A and GST-fused lamin A constructs used. **B)** [35S]-labelled SUN1-NTD was produced by *in vitro* translation. The protein was incubated with GST and GST-lamin A fusion proteins, previously bound to glutathione-Sepharose beads. Bound SUN1 NTD was detected by autoradiography. Coomassie-stained gel shows expression of the GST fusion proteins.

pCI-SUN1(1-355) was used for *in vitro* translation of the SUN1 NTD. The GST-lamin A sub-fragments were transformed into the BL21 strain of *E. coli* and their expression determined following small-scale IPTG induction. It was difficult to optimize the expression of these sub-fragments of lamin A, as many underwent significant degradation. Regardless of this limitation, the proteins were expressed and incubated with equal amounts of *in vitro*-translated SUN1 NTD. The pull down assay was performed as described before. According to the results, SUN1 interacted with all the sub-fragments of lamin A very weakly (Fig. 4.9B). SUN1 interacted most strongly with residues 389-664 and 389-510 of lamin A and less strongly with residues 450-664, whilst the remainder were very weak but above background. The result suggests that the lamin A binding site is located within residues 389-510, but this again contradicts the previous findings that lamin C does not interact with SUN1 and that prelamin A interacts more strongly with SUN1 than mature lamin A. However, the very weak binding observed for all of these fragments makes any conclusion difficult to be made from these experiments.

4.3 DISCUSSION

Lamins bind to a large number of proteins at the nuclear envelope. Lamins and lamin binding partners have multiple functions in the cell. These binding proteins can be grouped into the following categories: architectural partners, chromatin partners, gene regulatory partners and signalling partners (Zastrow et al., 2004). It is important to study all the binding partners of lamins to understand their functions and also their potential roles in laminopathies. At the beginning of this study SUN1 was found as a novel binding partner of lamin A. In this chapter, the interactions between SUN1 and SUN2 with lamin A were investigated in detail in order to map their respective binding sites on lamin A. Although interaction of the deletion fragments may not fully represent the binding affinity of the full length protein, these methods (as discussed in this chapter) within their limitations give valuable insights for mapping the binding sites, which could be important for disease association of the protein.

Interactions between the SUN1 N-terminus and the major lamin isoforms (A, C, B1 and B2) were tested by *in vitro* pull-down assay. SUN1 NTD (1-355) was found to interact specifically with lamin A. Interestingly, although lamin A and lamin C are alternate splice variants of the *LMNA* gene, SUN1 did not interact with lamin C. Lamin A and lamin C are identical for the first 566 amino acids and differ at the extreme C-terminus. Lamin C then has 6 unique residues whereas lamin A has 98 additional residues (section 1.1.2.2; Mounkes et al., 2003). This finding, therefore, suggests that the SUN1 binding site on lamin A includes residues in this extreme C-terminus. SUN1 also did not bind to lamin B1 or B2, suggesting that SUN1 exhibits specificity in binding to different lamin isoforms. Crisp et al., also demonstrated similar findings that SUN1(1-220) interacted more strongly with lamin A than lamin C and B1, by GST pull-down assay (Crisp et al., 2006). Lamin isoform binding preferences have also been observed for other INM proteins, such as LBR, which preferentially binds lamin B; and emerin, which shows higher affinity for lamin C than lamin A (Ye and Worman, 1994; Vaughan et al., 2001). Importantly, lamin A is expressed only in differentiated tissues and, as SUN1 binds only to lamin A, it is possible that SUN1 might have specific role in differentiated tissues. Intriguingly, SUN1 was found to be stably anchored at the NE in the absence of lamin A, whereas emerin and nesprins mislocalize from the NE under these conditions (Haque et al., 2006, Sullivan et al., 1999, Libotte et al., 2005). As SUN1 does not bind other

lamin isoforms, these findings therefore suggest that there are additional binding factors contributing to the NE anchorage of SUN1.

Several *in vitro* interaction assays were performed to map the lamin A binding site on SUN1. Crisp et al., showed that SUN1(1-220) binds lamin A (Crisp et al., 2006). Our initial studies also revealed that SUN1(1-229) preferentially binds to lamin A compared to SUN1(223-355). Comparison of SUN1 and SUN2 sequence homology indicated that SUN1 residues 223-355 are mostly absent in SUN2. As both SUN1 and SUN2 interact with lamin A, this suggests that the extreme N-termini of the SUN proteins are responsible for this interaction. However, SUN1(223-355) also binds weakly to lamin A, which suggests that the SUN1 N-terminus might have two binding sites for lamin A, although the major binding site lies within residues 1-208 of SUN1. Further mapping narrowed the lamin A binding site to residues 1-138 of SUN1. Significantly, the first 50 amino acids of SUN1 were found to be essential in mediating this interaction, as SUN1 N-terminus fragments lacking the first 50 amino acids did not interact with lamin A. Crisp et al. showed that residues 1-165 of SUN2 bind lamin A by GST pull-down (Crisp et al., 2006). We performed further mapping of the lamin A binding region on SUN2 and narrowed the lamin binding site to residues 1-129 of SUN2. However, SUN2(1-83) was found to bind weakly to lamin A compared to the equivalent SUN1(1-138). These two NTD fragments are highly homologous, except that the SUN2 fragment lacks the first 50 residues of SUN1. This indicates that SUN1 and SUN2 might differ in their mechanism of binding with lamin A.

Experiments were next performed to map the SUN1 binding site on lamin A. SUN1 was found to bind the C-terminal globular tail domain of lamin A (389-664), similar to many other INM proteins such as emerin, actin, LAP2α and SREBP1 (Zastrow et. al, 2004). Crisp et al., reported preferential interaction of SUN1(1-220) with prelamin A, rather than mature lamin A, suggesting that the binding site for SUN1 lies at the extreme C-terminus of prelamin A. (Crisp et al., 2006). When I attempted to replicate this result, I instead found that the CTDs of both mature lamin A and prelamin A interacted with equal intensity with SUN1. One possible explanation for this apparently different result is that here, only the C-terminal globular domains of the lamin A proteins were used in the pull down assay, whereas Crisp et al., used the full length proteins. It is possible that dimerization of lamin A, via the coiled-coil region, is required for optimal binding to

SUN1. In support to this, and in agreement with Crisp et al., a later experiment where the SUN1 NTD interaction was compared with the FL mature lamin A and prelamin A isoforms (discussed in chapter 6, section 6.3.2), where prelamin A showed preferential binding to the SUN1 NTD. This finding, therefore, emphasizes that either the farnesylation of prelamin A or the last 18 residues of prelamin A are important for mediating the SUN1-lamin A interaction. Importantly, lamin C is not farnesylated and does not have the extreme C-terminus residues of lamin A, and lamin C does not interact with SUN1. This further stresses that the farnesylation and the final residues of lamin A may be critical for SUN1 and lamin A binding.

Although we found that the SUN1 NTD binds the CTD of lamin A, further attempts to map the binding site of SUN1 on the lamin A CTD proved to be difficult. SUN1 bound to the CTD sub-fragments of lamin A, 389-510 and 450-664 with equal intensity. This suggests there could be two SUN1 binding sites on lamin A, as there are for actin, which binds two different C-terminal regions of lamin A, located in residues 461-536 and residues 563-646 (Zastrow et. al., 2004). Conversely, SUN1 might bind to a region that is common in both the fragments that is amino acids 450-510, which contribute to the lamin A Ig-fold (amino acids 430-545) (Dhe-Paganon et al., 2002). However, narrowing the binding site to detect whether the extreme C-terminus of lamin A is responsible for SUN1 and lamin A interaction, using GST-fused lamin A fragments and *in vitro*-translated SUN1, was not successful. SUN1 showed preferential binding with laminA(389-510), but this was not conclusive as the binding was weak. Moreover, the GST-fused lamin A sub-fragments did not express very well. It seems likely that these fragments were not folded correctly or dimerization via the coil-coiled region might require for optimal binding.

In summary, from the observations presented here, it is evident that SUN1 binds specifically to lamin A rather than other lamin isoforms and the binding region is comprised of the CTD residues 389-664 of lamin A. Also, the lamin A binding site was mapped to residues 1-138 on SUN1 and residues 1-129 on SUN2. Mapping the binding sites is important for studying protein-protein interactions and understanding their structural and functional relevance to disease. In laminopathies, mutations are found in different domains of lamin A and in lamin-interacting proteins. Studying these mutation

sites, as well as their relevant proteins binding sites, such as SUN1 and SUN2, may give valuable insights in our understanding of laminopathy disease mechanisms.

CHAPTER 5

IDENTIFICATION OF FURTHER SUN PROTEIN BINDING PARTNER

5.1 INTRODUCTION

The NTD of SUN1 has been found to interact with the nuclear lamina where it interacts with lamin A only and not other lamin isoforms (section 4.2.1). Interestingly, SUN1 is stably anchored at the NE in the absence of lamin A, whereas, many INM proteins, such as emerin and nesprins, mislocalize to the ER in this condition (Haque et al., 2006; Crisp et al., 2006; Sullivan et al., 1999; Libbotte et al., 2005). Therefore, SUN1 is likely to have additional binding partners at the NE, which might be contributing to this stable anchorage. Candidate SUN1-interacting proteins are nesprins, emerin, actin and chromatin.

UNC-84 in *C. elegans*, had been the most extensively studied SUN protein at this stage. On the commencement of this work, little was known about the binding partners of UNC-84. UNC-84 was proposed to interact with the giant outer nuclear membrane protein, ANC-1, a nesprin homologue (Starr and Han, 2005). There are now known to be at least four nesprin proteins, nesprin-1, nesprin-2, nesprin-3 and nesprin-4 (section 1.5.5.3). The giant nesprin isoforms are located at the ONM. The smaller isoforms of nesprin-1 and nesprin-2 are found at the INM and some isoforms that lack transmembrane domains are predicted to reside within the nucleoplasm (Mislow et al., 2002a; Mislow et al., 2002b; Zhang et al., 2005). Previously, giant isoforms of nesprin-1 and nesprin-2 were found to interact with the SUN1 CTD through their KASH domains in the NE lumen to form the LINC complex (linker of nucleoskeleton and cytoskeleton) (Haque et al., 2006, Padmakumar et al., 2005; Crisp et al, 2006). However, it was not known whether SUN1 interacts with different nesprin isoforms residing within different cellular compartments. In this chapter, SUN1 interaction with other nesprin isoforms was investigated.

The next candidate protein that might interact with SUN1 is emerin. Nesprin-1 and nesprin-2 interact with both lamin A and emerin at the INM (Mislow et al., 2002b; Zhang et al., 2005). Emerin is a small INM protein. Emerin and lamin A mutations are involved in the disease causation of the first known laminopathy, Emery-Dreifuss muscular dystrophy (EDMD). Approximately 60% of EDMD patients do not have mutations in emerin or lamin A (Ellis, 2006, Bengtsson and Wilson, 2004). Recently, mutations in nesprin-1 and nesprin-2 were also found in some EDMD patients (Zhang et

al., 2007b). Importantly, nesprins, lamin A and emerin all interact with each other and any defect in these interactions might contribute to the pathogenesis of EDMD (Zhang et al., 2007b). SUN1 interacts with both lamin A and nesprins and potentially, any protein that interacts with lamin A could be involved in a laminopathy disease mechanism. The question arose whether SUN1 also interacts with emerin and is involved in the EDMD pathology.

As SUN1 is stably anchored at the NE in the absence of lamin A, while both emerin and nesprins are mislocalized form the NE to the cytoplasm under these conditions, this poses the question of, if not lamin A, nesprin or emerin, what is anchoring SUN1 at the NE in these cells (Haque et al., 2006, Crisp et al., 2006, Sullivan et al., 1999, Libotte et al., 2005). Nuclear actin is also a possible candidate in this regard. Nuclear actin is composed of β-actin that is thought to form short polymers within the nucleus. Nuclear actin has structural and regulatory functions in the nucleus, such as chromatin remodelling, RNA transcription, processing and export. Nuclear actin interacts with lamin A and emerin and was proposed to form a cortical actin network at the inner face of the NE, which might help anchorage of other NE proteins (Bettinger et al., 2004, Holaska et al., 2004). Giant nesprin-2 interacts with F-actin via its N-terminal actin binding domain (ABD) and was also hypothesized to interact with nuclear actin while residing at the INM (Zhen et al., 2002). Therefore, it is not unlikely that SUN1 might interact with nuclear actin as well, and this could be a factor for the stable anchorage of SUN1 at the NE.

In order to delineate SUN1 characteristics and role in the cell, SUN1 interaction with these candidate proteins was tested. Furthermore, potential heterodimerization between SUN1 and SUN2 was assessed. Where appropriate, the binding sites were mapped by *in vitro* pull-down assays and immunoprecipitation (IP) studies. Results of these interaction assays are discussed in this chapter.

5.2 RESULTS

5.2.1 Identification of a second SUN1-nesprin-2 interaction site

5.2.1.1 Nesprin-2 interacts with both the NTD and CTD of SUN1

Immunoprecipitation (IP) studies with FL SUN1 showed that SUN1 interacts with the KASH domains of both nesprin-1α and nesprin-2α (Haque et al., 2006). This indicates that the interactions between these two proteins are occurring at the NE lumen, presumably by interaction of the SUN1 CTD with the KASH domain of nesprins (Fig. 3.13). In order to define the binding region of nesprin-2 on SUN1, MBP pull-down assays were performed. Interaction of the SUN1 NTD and CTD with nesprin-2α and nesprin-2β was investigated. Nesprin-2α and nesprin-2β are short isoforms of nesprin-2 that lack the N-terminal actin binding domain and have fewer spectrin repeats than the giant nesprin isoform (Fig. 5.1A and Fig. 1.21). pMAL-SUN1(1-355) and pMAL-SUN1(450-913) constructs were employed to produce the bait proteins. Nesprin-2α and nesprin-2β were produced by *in vitro* translation from plasmids pCDNA3-nesprin2α and pCDNA3-nesprin2β, respectively (kind gifts from C. Shanahan, King's College, London). MBP pull-down assays were then performed as described in the section 2.2.13.

As expected, both nesprin-2α and nesprin-2β interacted with the CTD of SUN1, although interaction was very weak with nesprin-2β compared to nesprin-2α (Fig. 5.1B and C). However, this result confirms that the SUN1 CTD is interacting with nesprin-2α and nesprin-2β at the NE lumen, where the SUN1 CTD resides. Surprisingly, the NTD of SUN1 also interacted weakly with nesprin-2α and nesprin-2β (Fig. 5.1B and C). In a repeat experiment, the SUN1 NTD rather interacted more strongly with nesprin-2β than the SUN1 CTD (data not shown). The SUN1 NTD resides within the nucleoplasm. This result therefore suggested that the SUN1 NTD may interact with the nucleoplasmic isoforms of nesprin.

Co-immunoprecipitation experiments were performed to investigate the possibility that SUN1 interacts with the nucleoplasmic nesprin isoforms. GFP-nesprin-2α fusions were employed for this purpose, kindly provided by C. Shanahan (King's College, London).

164
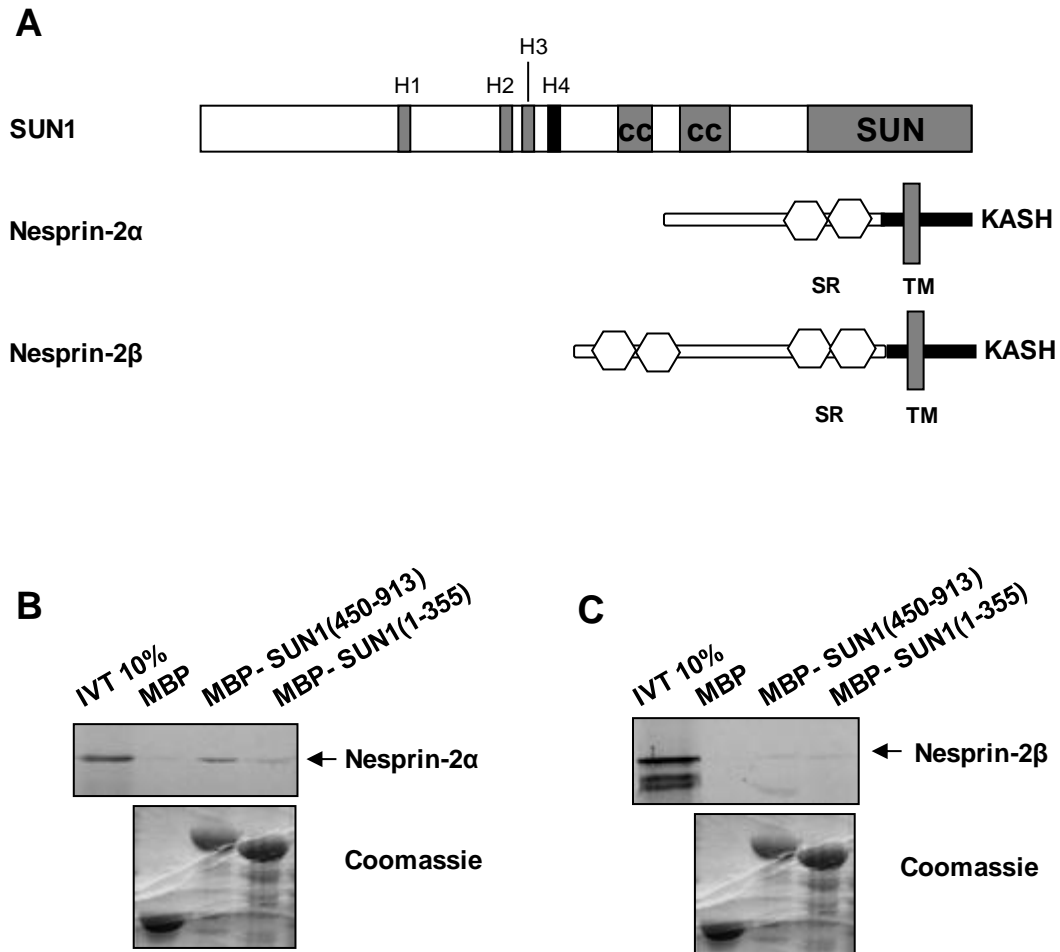
Fig. 5.1. Both termini of SUN1 interacts with nesprin-2. A) Schematic representation of SUN1, nesprin-2α and nesprin-2β. In SUN1 the vertical grey bars hydrophobic regions and the black bar represents the transmemebrane domain. 'CC' denotes the coiled-coil region. The hatched area is the SUN domain. In nesprins, the horizontal grey box is the KASH domain and the vertical grey bar represents the transmembrane domain. The hexagons are the spectrin repeats regions (SR). **B and C)** [35S]-labelled nesprin-2α and nesprin-2β were produced by *in vitro* translation. The proteins were incubated with MBP, MBP-SUN1(450-913) and MBP-SUN1(1-355), previously bound to amylose beads. Bound proteins were detected by autoradiography. Coomassie-stained gels show expression of MBP fusion proteins.

In addition to full-length pEGFP-nesprin2α, two deletion constructs were used: pEGFP-nesprin2αKASH and pEGFP-nesprin2αΔTM, which comprise the KASH domain and nucleoplasmic domains, respectively (Fig. 5.2A). U2OS cells were co-transfected with pCI-mycSUN1 and each of the GFP-tagged nesprin-2α constructs. Anti-GFP antibodies (AbCam) were used to immunoprecipitate the GFP-nesprin-2α proteins and the precipitates were probed with 9E10 anti-myc antibodies in order to detect bound myc-SUN1.

Myc-SUN1 was immunoprecipitated by all the GFP-nesprin-2α fragments, but not by the GFP control (Fig. 5.2B). In accordance with the previous findings, this result also indicates that SUN1 has two binding sites on nesprin-2α: one located in the KASH domain and the other in the nucleoplasmic domain. Therefore, this result also suggests that SUN1 might be interacting with nucleoplasmic isoforms of nesprins.

5.2.1.2 Mapping the SUN1 binding site for nucleoplasmic nesprins

The nucleoplasmic binding site for nesprin-2 was mapped by *in vitro* pull-down. To avoid potential confusion with the lumenal SUN1-KASH domain interaction, the plasmid pTNT-nesprin2βΔTM (kind gift from C. Shanahan, King's College, London) was used to generate *in vitro* translated nesprin-2βΔTM. MBP-fused SUN1 fragments encoding residues 1-355, 450-913, 1-229 and 223-355 were initially used in these pull-down assays. Unlike full-length nesprin-2β, nesprin-2βΔTM showed a specific interaction with only the NTD of SUN1 and did not interact with the SUN1 CTD (Fig. 5.3A). This indicates that the interaction with nesprin-2 is occurring at the inner face of the NE, with a nesprin-2 isoform that is located either at the INM or in the nucleoplasm.

Whilst nesprin-2βΔTM bound weakly to both SUN1(1-229) and SUN1(223-355), there was a consistently higher level of binding to residues 223-355 (Fig. 5.3A). As mentioned in chapter 4 (section 4.2.2.2), new GST-fused SUN1 constructs (1-209 and 209-355) were generated after sequence comparison of SUN1 and SUN2. These constructs were also employed to examine the binding site for nesprin-2βΔTM. As shown in Figure 5.3B, SUN1(209-355) showed a stronger interaction with nesprin-2βΔTM than either SUN1(1-208) and SUN1(223-355). This indicates that the binding site of nesprin-2βΔTM lies within residues 209-355 of SUN1. Interestingly, this binding
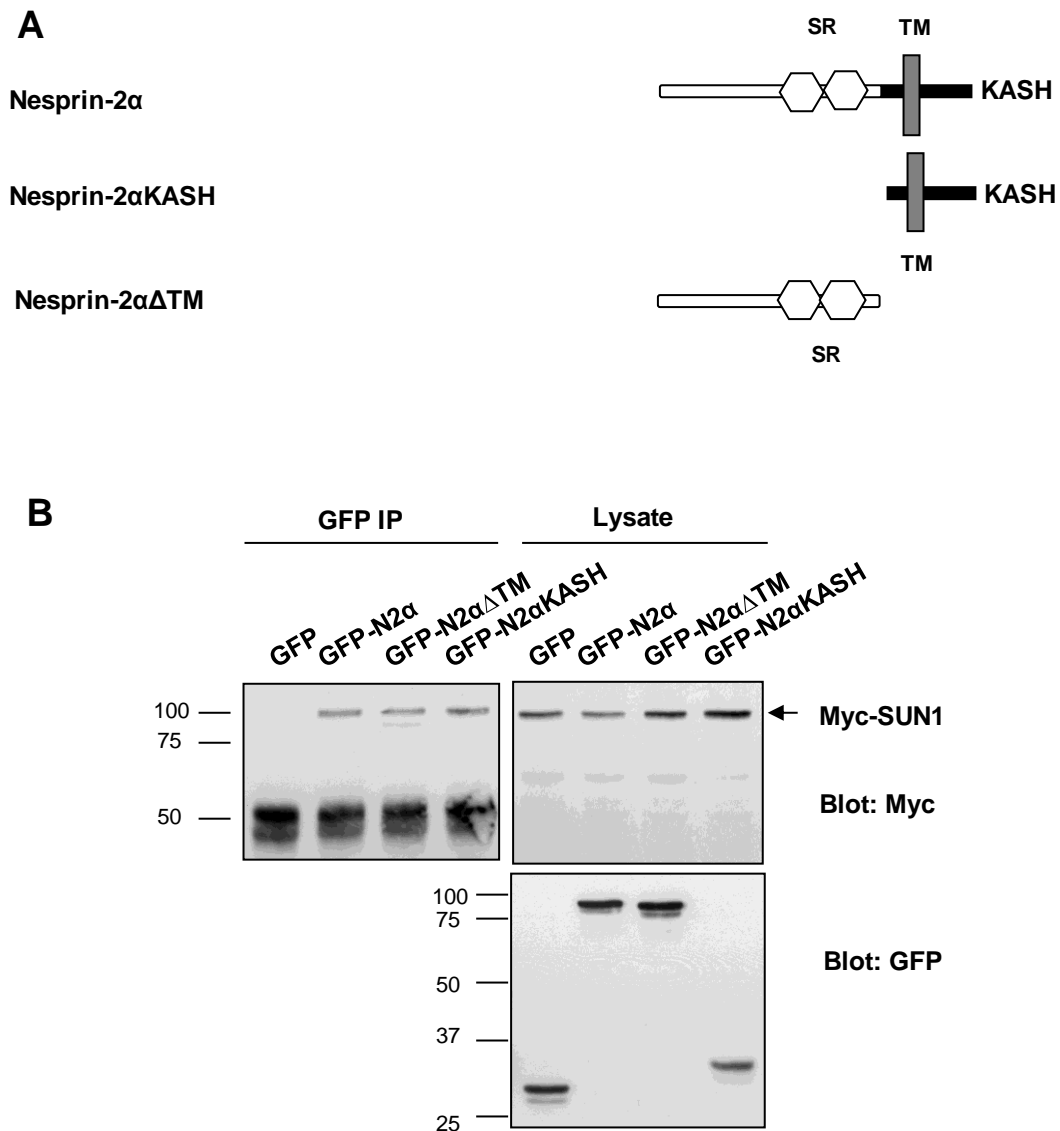
Fig. 5.2. Nesprin-2α contains two SUN1 binding sites. A) Schematic representation of FL nesprin-2α, nesprin-2αKASH and nesprin-2αΔTM. Here, hexagons are the spectrin repeat regions (SR), vertical grey bar is the transmembrane region and the horizontal grey box is the KASH domain. **B)** U2OS cells were co-transfected with myc-SUN1 and GFP or GFP-nesprin-2 fragments, as shown. Expression of myc- and GFP-tagged proteins were confirmed by immunoblotting (upper and lower right panels, respectively). Anti-GFP immunoprecipitates (IP) were probed with myc-antibody to detect co-precipitating myc-SUN1 (left panel).
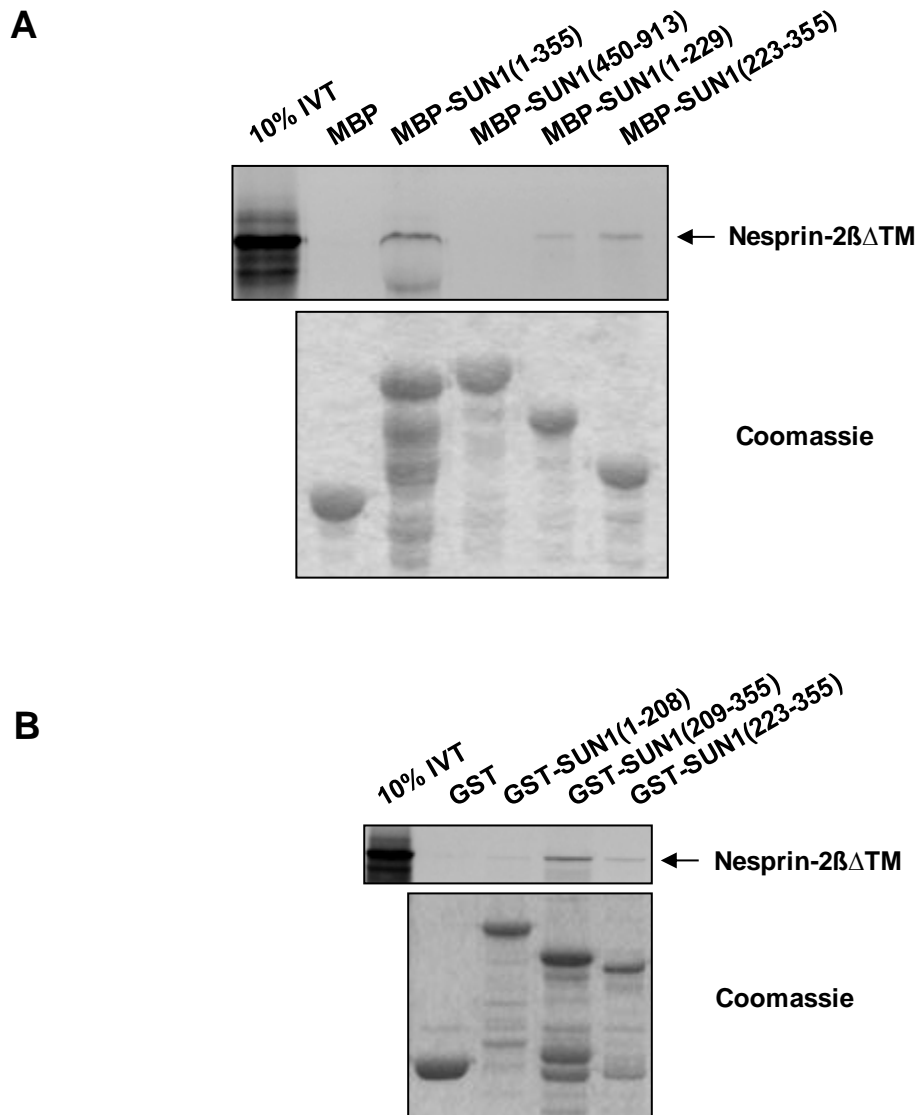
Fig. 5.3. Mapping the binding site of nesprin-2βΔTM on SUN1. A) [35S]-labelled nesprin-2βΔTM was produced by *in vitro* translation. Nesprin-2βΔTM was incubated with MBP and MBP-SUN1 fusions as indicated, previously bound to amylose beads. Bound proteins were detected by autoradiography. Coomassie-stained gel shows expression of the MBP fusion proteins. **B)** [35S]-labelled neprin-2βΔTM was produced by *in vitro* translation. Nesprin-2βΔTM was incubated with GST and GST-SUN1 fusions as indicated, previously bound to glutathione-Sepharose beads. Bound proteins were detected by autoradiography. Coomassie-stained gel shows expression of the GST fusion proteins.

preference is opposite to that observed for lamin A, which bound more strongly to 1-208 residues of SUN1 in a similar experiment (Fig. 4.5).

5.2.1.3 SUN1 binds weakly to nesprin-1αΔTM

The KASH domains of both nesprin-1 and nesprin-2 had previously been shown to interact with SUN1 (Haque et. al., 2006, Crisp et al., 2006, Padmakumar et al., 2005). Having identified a second interaction site between the nucleoplasmic domains of SUN1 and nesprin-2, I next carried out experiments to determine whether the nucleoplasmic domain of nesprin-1 also binds to the SUN1 NTD. Initial immuonoprecipiation experiments to examine the interaction between GFP-nesprin-1αΔTM and myc-SUN1 were not successful (results not shown). Therefore, MBP pull-down assays were carried out to compare the interaction of the SUN1 NTD with nesprin-1αΔTM and nesprin-2βΔTM. Nesprin-1αΔTM and nesprin-2βΔTM were *in vitro* translated from pTNT-nesprin1αΔTM and pTNT-nesprin2βΔTM, respectively (kind gifts from C. Shanahan, King's College London). The result shown in Figure 5.4B indicates that the SUN1 NTD interacted weakly with nesprin-1αΔTM compared to nesprin-2βΔTM. Together with the inability to immunoprecipitate nesprin-1αΔTM and SUN1, this suggested that nesprin-1α may not interact with the nucleoplasmic domain of SUN1. However, interaction with the nesprin-1β isoform, which has additional spectrin repeats that could mediate a stronger interaction, was not tested (Fig. 1.20).

Although the SUN1 NTD shows a weak interaction with nesprin-1αΔTM, further mapping of the binding region of nesprin-1αΔTM on SUN1 was attempted by MBP pull-down. MBP-SUN1 fusion proteins were used as baits and MBP alone was used as a negative control. *In vitro*-translated nesprin-1αΔTM was incubated with SUN1(1-355, 450-913, 1-229, and 223-355). According to the results shown in Figure 5.4C, nesprin-1αΔTM interacts relatively more strongly with the SUN1 NTD than the CTD, but is not much above background binding to MBP. Attempts to further map this potential binding site with SUN1 NTD sub-fragments (1-229, 223-355) were inconclusive, although SUN1(223-355) showed slightly higher binding than SUN1(1-229). In repeated experiments, the binding of nesprin-1αΔTM to the SUN1 NTD was found not to be as obvious as the nesprin-2βΔTM binding, and therefore clear evidence of interaction could not be established.

A

Nesprin-1αΔTM

Nesprin-2βΔTM

B

Nesprin-1αΔTM   Nesprin-2βΔTM

IVT 10%   MBP   SUN1(1-355)   IVT 10%   MBP   SUN1(1-355)

Coomassie

C

10% IVT   MBP   MBP-SUN1(1-355)   MBP-SUN1(450-913)   MBP-SUN1(1-229)   MBP-SUN1(223-355)

← **Nesprin-1αΔTM**

Coomassie
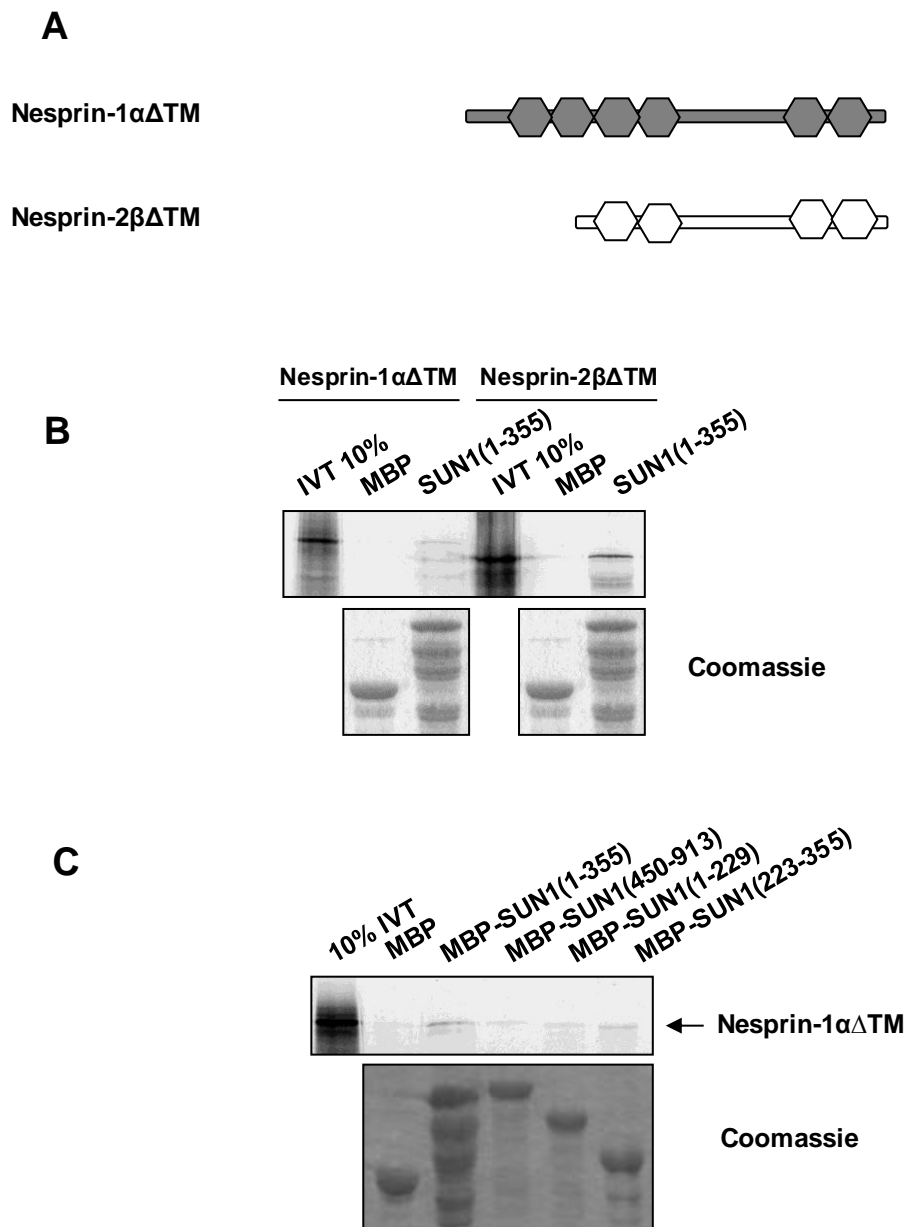
Fig. 5.4. Nesprin-1αΔTM interacts weakly with the NTD of SUN1. A) Schematic representation of nesprin-1αΔTM and nesprin-2βΔTM, lacking the KASH domain. **B)** [^{35}S]-labelled nesprin-1αΔTM and nesprin-2βΔTM were produced by *in vitro* translation and were incubated with MBP and MBP-SUN1(1-355), previously bound to amylose beads. Bound proteins were detected by autoradiography. **C)** [^{35}S]-labelled nesprin-1αΔTM was produced by *in vitro* translation and incubated with MBP and MBP-SUN1 fusions as indicated, previously bound to amylose beads. Bound proteins were detected by autoradiography. Coomassie-stained gel shows expression of the MBP fusion proteins.

5.2.1.4 SUN2 binds weakly to nesprin-2βΔTM

An investigation was carried out to determine whether the SUN2 NTD is capable of interaction with nesprin-2βΔTM. Full length SUN2 interaction with the nesprin-2βΔTM was not examined, because of the limited SUN2 constructs available to carry out investigations at that time. GST-fused SUN2(1-224) and positive control SUN1(1-355) were used as baits and *in vitro* translated nesprin-2βΔTM was used as prey in a pull-down experiment. The SUN1 NTD bound strongly with nesprin-2βΔTM, while the SUN2 NTD showed a weak interaction (Fig. 5.5). Previous results show that SUN1 residues 209-355 bind nesprin-2βΔTM and, interestingly, this sequence is mostly absent from SUN2 (section 4.2.2.2). This therefore could explain the weaker binding of SUN2 with the nesprin-2βΔTM. However, the interaction of FL SUN2 with the nesprin-2βΔTM should be investigated to draw a proper conclusion.

.
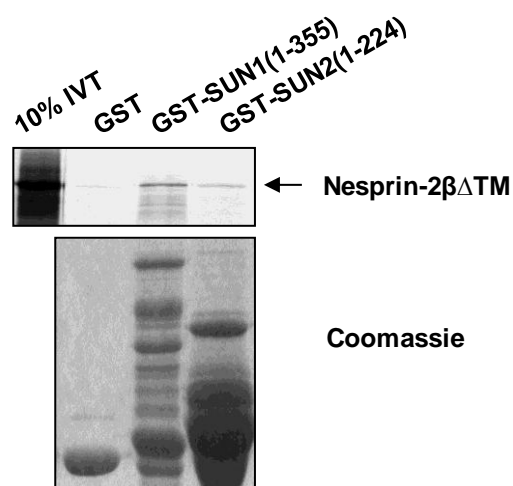
Fig. 5.5. Comparison of SUN1 and SUN2 NTD interactions with nesprin-2βΔTM.
[^{35}S]-labelled nesprin-2βΔTM was produced by *in vitro* translation. Nesprin-2βΔTM was incubated with GST, GST-SUN1(1-355) and GST-SUN2(1-224) as indicated, previously bound to glutathione-Sepharose beads. Bound proteins were detected by autoradiography. Coomassie-stained gel shows expression of the GST fusion proteins.

5.2.2 Identification of a novel interaction between SUN proteins and emerin

5.2.2.1 SUN1 interacts with emerin

Given that lamin A and nesprins interact with emerin and that SUN1 interacts with both nesprins and lamin A, potentially SUN1 could also interact with emerin. This possibility was, therefore, investigated by immunoprecipitation. U2OS cells were transfected with pCI-mycSUN1 and anti-emerin antibodies (AP8; a kind gift from J. Ellis, King's College, London) were used to immunoprecipitate endogenous emerin. Whilst anti-HA antibodies were used as a negative control. The precipitates were probed with anti-myc antibody to detect any bound co-precipitated myc-SUN1. FL myc-SUN1 was successfully precipitated by endogenous emerin but not by the control HA antibodies (Fig. 5.6). A novel interacting partner of SUN1, emerin, was therefore identified, which opened a new avenue in our research. The binding was further investigated as described below.

5.2.2.2 The nucleoplasmic NTD SUN1 binds emerin

Investigations were performed to determine which domain of SUN1 binds emerin. MBP pull-down assays were performed in order to examine whether the NTD or the CTD of SUN1 binds emerin and further narrowing down of the binding region was then carried out. MBP-fused SUN1(1-355), SUN1(450-913), SUN1(1-229) and SUN1(223-355) were used as baits. Emerin as a prey, was *in vitro* translated from plasmid pCDNA3.1-emerin (a kind gift from J. Ellis, King's College, London).

Emerin was found to interact with the SUN1 NTD and did not show any interaction with the SUN1 CTD (Fig. 5.7A). This suggests that the interaction is occurring at the nucleoplasmic face of the NE. Further narrowing down of the binding region on the SUN1 NTD shows that SUN1(223-355) binds more strongly than the SUN1(1-229). Interestingly, this binding preference is similar to that of nesprin-2β (section 5.2.1.2) and opposite to that of lamin A (section 4.2.2.1). However, a weaker interaction was observed with residues 1-229, indicating that there may be two binding sites for emerin on SUN1.
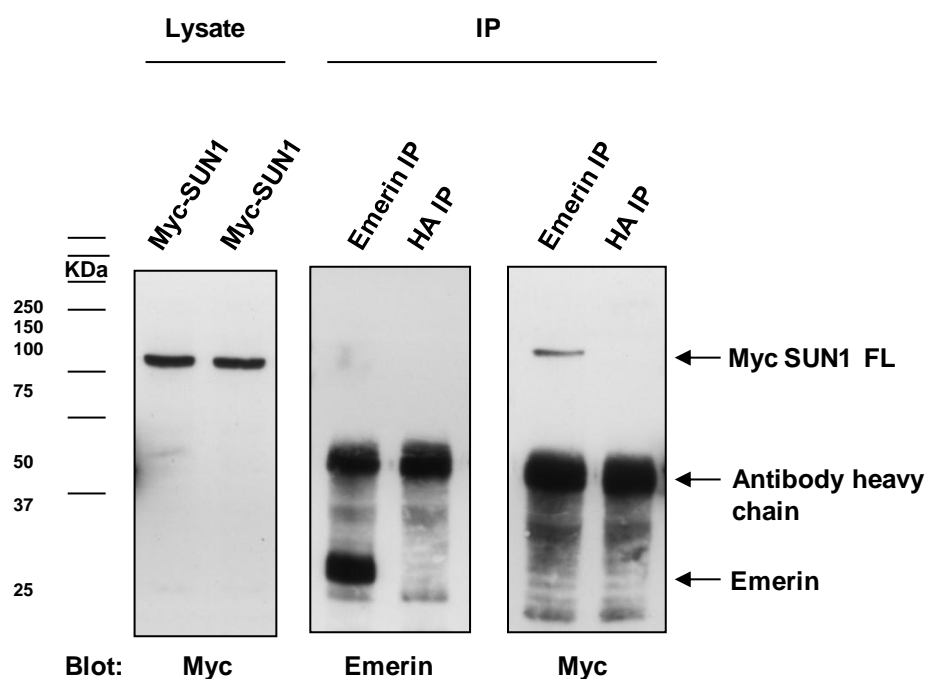
Fig. 5.6. SUN1 interacts with emerin. U2OS cells were transfected with myc-tagged SUN1. Expression of myc-SUN1 was confirmed by immunoblotting (left panel). Anti-emerin and control anti-HA immunoprecipitates (IP) were probed with emerin antibody to detect precipitated emerin (middle panel) and with myc antibody to detect co-precipitating myc-SUN1 (right panel).
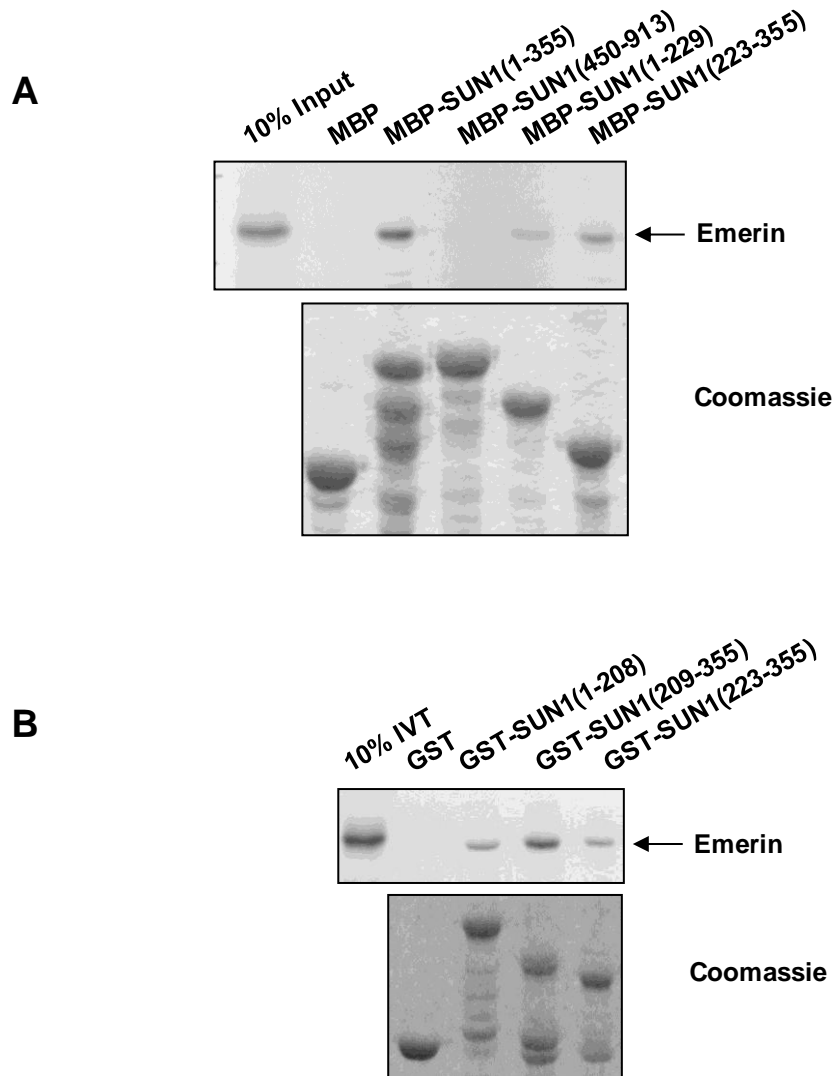
Fig. 5.7. Mapping binding site of emerin on SUN1. A) [^{35}S]-labelled emerin was produced by *in vitro* translation and incubated with MBP and MBP-SUN1 fusions as indicated, previously bound to amylose beads. Bound proteins were detected by autoradiography. Coomassie-stained gel shows expression of the MBP fusion proteins. **B)** [^{35}S]-labelled emerin was produced by *in vitro* translation and then incubated with GST and GST-SUN1 fusions as indicated, previously bound to glutathione-Sepharose beads. Bound proteins were detected by autoradiography. Coomassie-stained gel shows expression of the GST fusion proteins.

Further mapping of the binding site for emerin on SUN1 was carried out using the constructs that were generated after sequence comparison of SUN1 and SUN2 (section 4.2.2.2). GST-fused SUN1(1-208), SUN1(209-355) and SUN1(223-355) were used as baits with GST alone as a negative control. *In vitro* translated emerin, from pCDNA3.1-emerin construct, was used as a prey. The results, shown in Figure 5.7B, indicate that SUN1(209-355) binds emerin more strongly than either SUN1(223-355) or SUN1(1-208). This suggests that the major binding site for emerin lies within residues 209-355 of SUN1, although it is possible that the binding site might include residues within SUN1(1-208).

5.2.2.3 SUN2 interacts with emerin

Investigations were carried out to determine whether SUN2 interacts with emerin. Interaction of full-length SUN2 with emerin was tested in immunoprecipitation experiments and was compared with that of SUN1. U2OS cells were transfected with either pCI-HAmSUN1 or pCDNA3.1TOPO-V5/HIS-hSUN2 (a kind gift from D. Hodzic, Washington University, USA), expressing HA-tagged mouse SUN1 or His-tagged human SUN2, respectively (Table 2.2). AP8 anti-emerin antibodies were used to immunoprecipitate endogenous emerin and anti-SREBP1 antibodies were used as a negative control. The precipitates were probed with anti-mSUN1 0545 antibody or anti-hSUN2 2853 antibody (both raised in the lab; Haque et al., 2006; Haque et al., 2010), to detect precipitated mSUN1 and hSUN2 respectively. Both SUN1 and SUN2 were successfully co-precipitated by endogenous emerin (Fig. 5.8A), which indicates that emerin is also a novel binding partner of SUN2. In fact, SUN2 appeared to be more efficiently pulled down than SUN1, suggesting a stronger interaction.

The binding of SUN2 to emerin was confirmed by GST pull-down assays and was compared with that of SUN1. GST-fused emerin(1-221), encoding the nucleoplasmic domain of emerin, was used as a bait, produced from pGEX-emerin(1-221) (a kind gift from J. Ellis, King's College, London). FL mSUN1 and FL hSUN2 proteins were *in vitro* translated from pCI-mycSUN1 and pCDNA3.1TOPO-V5/HIS-hSUN2, respectively, and were used as preys. The result of the GST pull-down shows that both SUN1 and SUN2 interact with emerin (Fig. 5.8B). Although SUN1 shows relatively weaker binding than the corresponding SUN2, the input of SUN1 was also lower than that of SUN2. The result, therefore, confirms SUN2 binding with the nucleoplasmic
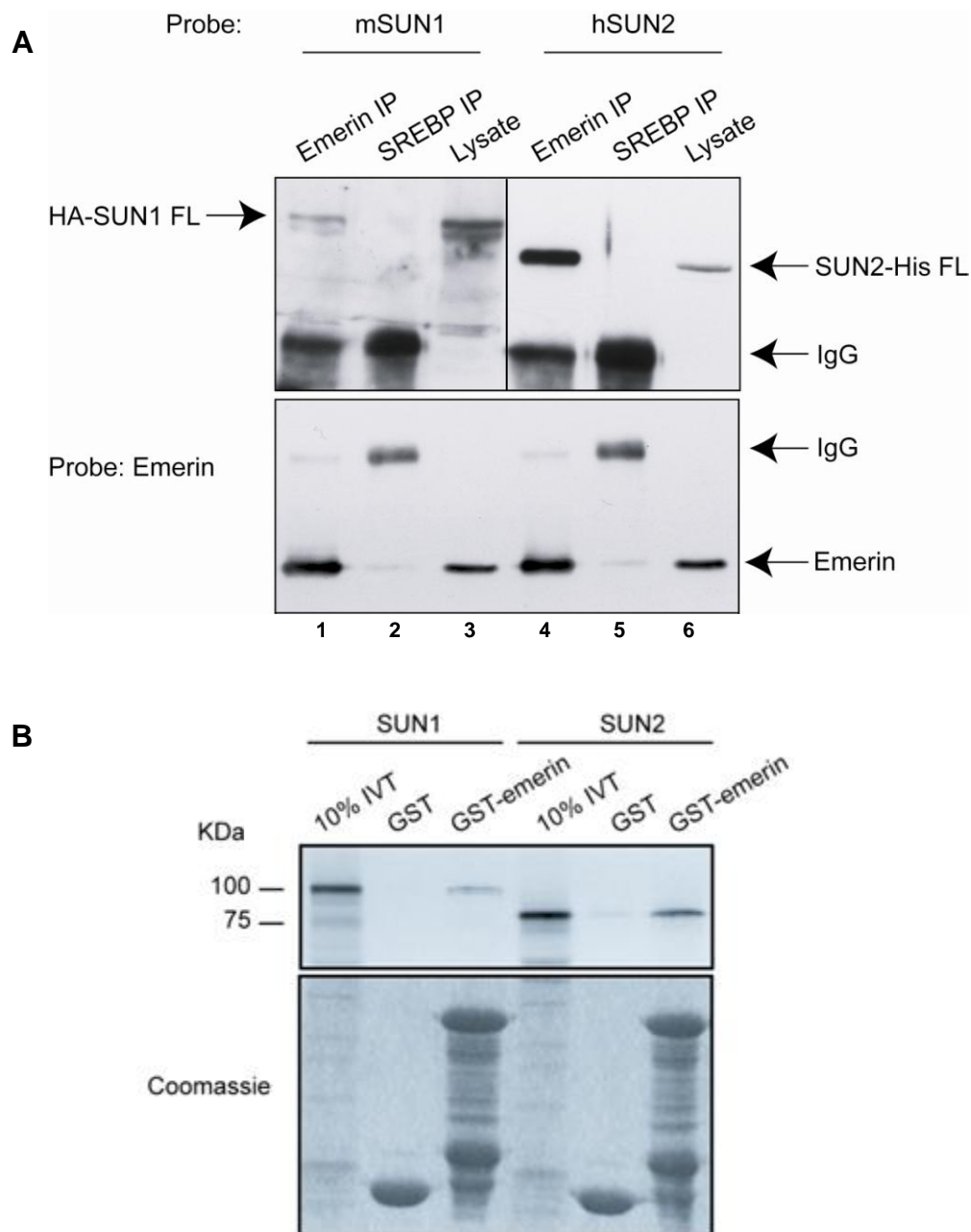
Fig. 5.8. SUN2 interacts with emerin. A) U2OS cells were transfected with FL HA-tagged mSUN1 and His-tagged hSUN2. Expression of HA-SUN1 and His-SUN2 was confirmed by immunoblotting (upper panels, lanes 3 and 6). Anti-emerin and control anti-SREBP1 immunoprecipitates (IP) and lysates were probed with emerin antibody to detect precipitated emerin (lower panel). Lysate and precipitates were probed mSUN1 or hSUN2 antibodies to detect expressed proteins and co-precipitating HA-SUN1 (upper panel, lane 1 and 2) or His-SUN2 (lanes 4 and 5). **B)** [^{35}S]-labelled SUN1 and SUN2 were produced by *in vitro* translation. SUN1 and SUN2 were incubated with GST and GST-emerin, previously bound glutathione Sepharose beads. Bound proteins were detected by autoradiography. Coomassie-stained gel shows expression of the GST fusion proteins.

domain of emerin and suggests that the interaction is occurring at the nucleoplasmic face of the NE.

5.2.2.4 Mapping the binding site of emerin on SUN2

In order to map the emerin binding site on SUN2, GST pull-down assays were performed. Having shown that the nucleoplasmic NTDs of SUN1 and emerin mediate this interaction, the assumption was made that SUN2 would also interact with emerin via its NTD. To verify this, a pull-down assay was performed using GST-SUN1(1-355) and GST-SUN2(1-224) as baits to pull down *in vitro* translated emerin. As shown in Figure 5.9, SUN2(1-224) did not show any interaction with emerin. The result contradicts the immunoprecipitation results described in section 5.2.2.3. This was surprising, given that SUN1 and SUN2 are predicted to have the same membrane topology. It is possible that a different region in SUN2 is responsible for mediating this interaction or it might need additional residues to augment the binding with emerin. However, GST-SUN2(1-224) is not expressed well as a GST-fused protein and generates a lot of degradation products. Also, SUN2(1-224) contains the first hydrophobic region (H1) that might interfere with the proper folding of the protein. Notably, GST-SUN2(1-224) does bind with lamin A (section 4.2.3) and also weakly interacts with nesprin-2β (section 5.2.1.4). There could be two possible explanations for this non-interaction: one is that the folding of GST-SUN2(1-224) is incomplete and therefore the binding site is not in correct conformation, hindering the interaction or, alternatively the binding site may lie elsewhere in the protein. Further investigation is required to map the binding site of emerin on SUN2.

5.2.2.5 Mapping the binding site of SUN1 and SUN2 on emerin

Experiments were performed to identify the binding region of SUN1 on emerin using GST pull-down assays. Studies have shown that nesprin-1α and nesprin-2β bind to residues 140-176 of emerin and that the lamin A binding region lies within residues 70-164 of emerin (Wheeler et al., 2007). A range of GST-fused emerin fragments was used to pinpoint the SUN1 binding site on emerin. pGEX-emerin 1-221, 140-176 and 170-220 were kind gifts from J. Ellis, King's College London and pGEX-emerin 1-120, 120-221 and 140-221 were generated in the lab, by R. Mckenzie (Table A.3). Prey protein, SUN1 NTD was *in vitro* translated from pCI-mycSUN1(1-355).
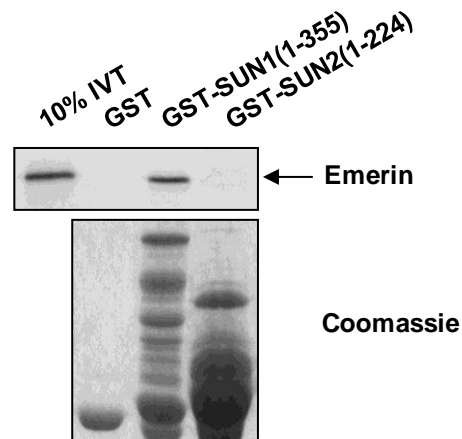
Fig. 5.9. Mapping the emerin binding site on SUN2. [^{35}S]-labelled emerin was produced by *in vitro* translation. Emerin was incubated with GST, GST-SUN1(1-355) and GST-SUN2(1-224), previously bound to glutathione-Sepharose beads. Bound proteins were detected by autoradiography. Coomassie-stained gel shows expression of the GST fusion proteins.

The result shows that the SUN1 NTD bound strongly to emerin(1-221) as expected (Fig. 5.10B), although the interactions in this assay were, in general, weak. It is possible that the fusion proteins do not fold correctly when produced in this way. However, within the limitation of the procedure, emerin(120-221) appeared to be interacting with the SUN1 NTD more strongly than emerin(1-120). Further narrowing revealed that emerin(140-221) also interacts with the SUN1 NTD. In order to define the binding region further, two additional sub-fragments of emerin, 140-176 and 170-221 were tested, but these small fragments failed to show any obvious interaction. Therefore, according to this result, the binding region of SUN1 on emerin most likely lies within residues 140-221 of emerin, which is similar to that of nesprin-1α and nesprin-2β (Wheeler et al. 2007). A similar experiment was carried out in order to identify the SUN2 binding site on emerin but was not successful, as no obvious binding preference was detected for any of the emerin fragments, except emerin(1-221) (Fig. 5.10C).

5.2.3 SUN1 also interacts with SUN2 via its NTD

SUN1 has a coiled-coil region at the proximal end of the CTD and was predicted to oligomerize through self-interaction of this region (Padmakumar et al., 2005). However, MBP pull-down assays show that SUN1 also self-interacts through its NTD (Haque et al., 2006). While looking at different binding partners of SUN1, the binding of SUN1 with SUN2 was investigated using MBP pull-down assays. MBP-fused SUN1(1-355) and SUN1(450-913) were used as baits to determine their interaction with FL SUN2, *in vitro* translated from pCDNA3.1TOPO-V5/HIS-hSUN2. SUN2 was found to interact with the NTD of SUN1 and no interaction was detected with the SUN1 CTD (Fig. 5.11). This indicates that SUN1 does interact with SUN2 and the interaction is occurring at the nucleoplasmic face of the NE through the N-terminus of SUN1, as for most other binding partners of SUN1.

A

B

C
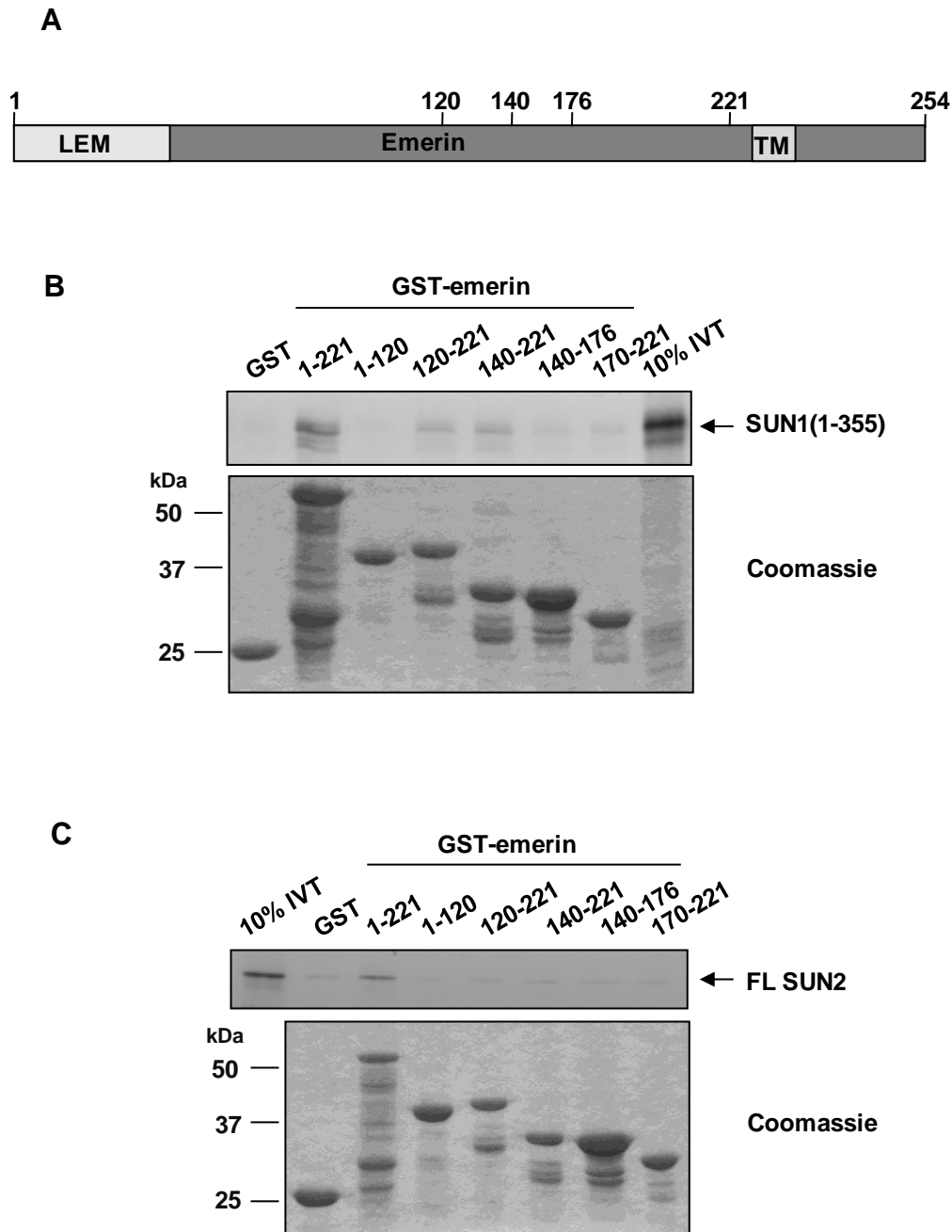
Fig. 5.10. Mapping SUN1 and SUN2 binding on emerin. A) Schematic representation of emerin showing LEM domain and transmembrane domain (TM). **B)** [^{35}S]-labelled SUN1-(1-355) was produced by *in vitro* translation and incubated with GST and GST-emerin fusions as indicated, previously bound to glutathione-Sepharose beads. Bound proteins were detected by autoradiography. Coomassie-stained gel shows expression of the GST fusion proteins. **C)** [^{35}S]-labelled FL SUN2 was produced by *in vitro* translation. SUN2 was incubated with GST and GST-emerin fusions as indicated, previously bound to glutathione-Sepharose beads. Bound proteins were detected by autoradiography. Coomassie-stained gel shows expression of the GST fusion proteins.
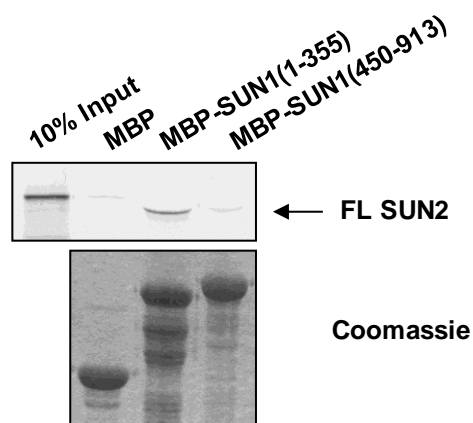
Fig. 5.11. SUN1 interacts with SUN2. A) [^{35}S]-labelled FL SUN2 was produced by *in vitro* translation. The protein was incubated with MBP, MBP-SUN1 NTD and MBP-SUN1 CTD, previously bound to amylose beads. Bound proteins were detected by autoradiography, following SDS-PAGE.

5.2.4 Potential SUN1/SUN2 interaction with actin

SUN1 is localized at the NE in the absence of lamin A (Haque et al., 2006, Crisp et al., 2006). Therefore, other factors are involved in SUN1 anchorage and it is possible that SUN1 interaction with nuclear actin is contributing to this. SUN1 interaction with nuclear actin was investigated in immunoprecipitation experiments. NIH 3T3 cells were transfected with pCI-HAmSUN1. An anti-HA antibody was used to immunoprecipitate HA-SUN1 and anti-SREBP1 antibody H-160 was used as a negative control. The precipitates were probed with an anti-βactin antibody. The result depicts that although actin was co-precipitated with the control anti-SREBP1 antibody, more actin was co-precipitated with HA-SUN1, suggesting an interaction between SUN1 and nuclear actin may occur (Fig. 5.12). However, it is not clear whether this interaction represents binding specifically to nuclear actin, as cytoplasmic actin was also present and actin is known to be 'sticky', so can easily contaminate the pelleted sample. Although the experiment was repeated using various cell lines and antibody controls, the result could not be reproduced to support this initial observation. Similar experiments were conducted to determine whether SUN2 interacts with nuclear actin but the results were not conclusive in repeated experiments (data not shown). Further investigations are therefore required, preferably using isolated nuclei to focus on interactions between the SUN proteins and nuclear actin.
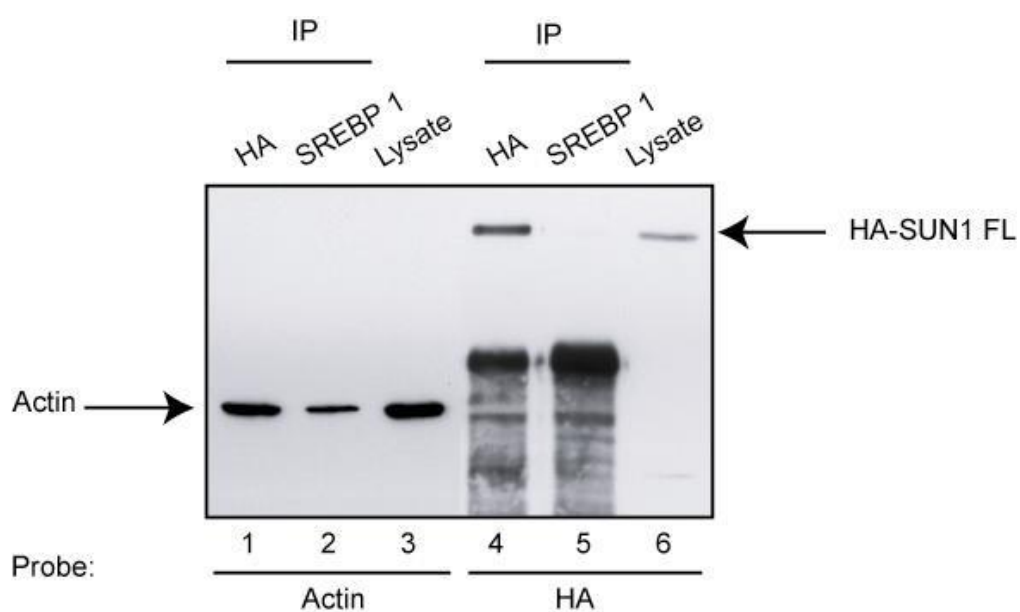
Fig. 5.12. SUN1 interaction with actin. NIH 3T3 cells were transfected with HA-SUN1. Expressions of actin and HA-SUN1 were conformed by immunoblotting (lane 3,6). Anti-HA and control anti-SREBP1 immunoprecipitates (IP) were probed with actin and HA antibodies to detect co-precipitating actin (lane 1,2) and precipitated HA-SUN1 (lane 4,5), respectively.

5.3 DISCUSSION

SUN1 was originally identified as a lamin A binding protein and its interaction with the KASH domain of nesprin has also been well established (Padmakumar et al., 2005; Haque et al., 2006; Crisp et al., 2006). In order to elucidate SUN1 function in cells, interaction of SUN1 with other candidate NE and nuclear proteins was investigated. SUN1 interaction with nucleoplasmic isoforms of nesprins, emerin, SUN2 and nuclear actin were studied in this chapter.

5.3.1 SUN proteins interaction with nucleoplasmic nesprin isoforms

Nesprin-1 and nesprin-2 have many isoforms, including the giant nesprins with an actin binding domain (ABD) and the KASH domain, plus smaller isoforms that lack the ABD and are located at the INM or within the nucleoplasm (section 1.5.5.3). While investigating the SUN1-nesprin-2 binding sites, SUN1 was found to interact with nesprin-2, not only through its lumenal CTD, as predicted, but also via the nucleoplasmic NTD. This strongly suggested that the N-terminus of SUN1 binds nesprin-2 isoforms located at the INM or within the nucleoplasm. Although the interactions detected were weak in the initial pull-down experiments, for both nesprin-2α and nesprin-2β, subsequent immunoprecipitation experiments with nesprin-2αΔTM (lacking the KASH domain) show strong binding with FL SUN1. This further supported an interaction between the nucleoplasmic domain of nesprin and that of SUN1. In addition, nesprin-2βΔTM, that is predicted to locate within the nucleoplasm, showed a strong binding with SUN1. Together, these data confirmed that SUN1 interacts with nesprins at two sites: firstly via the lumenal KASH domain and secondly via the nucleoplasmic domain of nesprin-2. Lamin A and emerin interact with the nucleoplasmic spectrin repeats regions (SR) of nesprin-2, more specifically with SR 19-22 and SR 21-22, respectively (Libotte et al., 2005). It is therefore possible that the SUN1 NTD also binds the SR regions of nesprin-2 at the inner face of the NE. As both nesprin-2α and nesprin-2β nucleoplasmic domains, interact with SUN1, it is likely that SUN1 interacts with the SR region that is common to both, namely SR 21-22. This interesting finding shows that SUN1-nesprin-2 connections are present not only in the NE lumen but also at the INM, thus SUN1 may bridge both the nuclear and cytoplasmic nesprins. Whether this provides only a mechanical support or has other functional relevance within the nucleus should be the subject of further investigation.

Mapping of the nesprin-2βΔTM binding site showed that the binding region lies within the SUN1 N-terminal residues 209-355, which is distinct from that of lamin A (residues 1-208) but identical to that of emerin (as discussed in the next section). Initial pull-down experiments also showed that the SUN1 CTD binds nesprin-2 as expected, so presumably it is the KASH domain of nesprin which is responsible for this binding, as both domains reside within the NE lumen. Investigations to further map the binding of nesprin-2 on the SUN1 CTD, using sub-fragments of the SUN1 CTD, were not successful. However, Padmakumar et al., showed that nesprin-1 binds to the SUN1 CTD, at a segment between the SUN domain and the coiled-coil region (Padmakumar et. al., 2005). It is therefore likely that, nesprin-2 also binds to a similar region on the SUN1 CTD, but this requires further investigation.

SUN1 binding to the nucleoplasmic domain of nesprin-1 isoforms was not convincingly established. Weak binding of nesprin-1αΔTM to the SUN1 NTD was observed in *in vitro* pull-down assays. However, I failed to detect an interaction between FL SUN1 and nesprin-1α by immunoprecipitation. It is therefore possible that the nucleoplasmic SUN1-nesprin interaction is specific to nesprin-2 isoforms. Alternatively SUN1 may interact with longer nucleoplasmic nesprin-1 isoforms, such as nesprin-1β, which was not tested.

Of note, recent bioinformatic analyses show less support for biological relevance nesprin-1β1, nesprin-1α1, nesprin-2β1, nesprin-2γ and isoforms lacking the KASH domain for nesprin-2 (Simpson and Roberts, 2008). However, this was not known at the start of this project and evidence of existence of different isoforms in mRNA level was shown by different groups, although it is possible that some of these isoforms may not be detected at protein level (Zhang et al., 2001; Zhang et al., 2005; Padmakumar et al., 2004). Nonetheless, experiments presented in this chapter show binding of SUN1 with different deletion fragments of nesprin-2α as well, which supports nesprin-2 interaction with SUN1 in the nucleoplasm.

SUN2 binding to nesprin-2βΔTM also was investigated by GST pull-down and a weak interaction was detected, although this was not confirmed by immunoprecipitation due to lack of a suitable FL SUN2 construct at that time. However, GST-SUN2(1-224), the NTD fusion protein of SUN2 employed to test the interaction is poorly expressed, and

although capable of interaction with lamin A, it may be partially misfolded and this could be the reason for a weak interaction seen. More investigations are required to conclude whether SUN2 interact with the nucleoplasmic nesprin-2 isoforms.

5.3.2 SUN proteins interaction with emerin

A novel interaction between SUN domain proteins, SUN1 and SUN2, and emerin was convincingly established by both immunoprecipitation and *in vitro* pull-down. This added another protein to the long list of emerin binding proteins.

The binding site of emerin was mapped to the nucleoplasmic N-terminus of SUN1. Further mapping revealed a major binding region within residues 209-355. However, weaker yet significant binding was also observed for SUN1 residues 1-208 and it is possible that the binding region might include residues from this fragment. Interestingly, the major emerin binding site, residues 209-355, is identical to that of nesprin-2. Thus emerin and nesprin-2 might compete with one another for binding or may bind in a co-operative fashion. These binding data suggest that a multi-protein complex is present at the inner face of the NE involving the lamin A, emerin, nesprins and SUN1.

Mapping of the emerin binding site on SUN2 was not successful as experiments with GST-SUN2(1-224), the N-terminus of SUN2, did not show any interaction. It is noteworthy that the SUN1 binding region, residues 209-355, are mostly absent from SUN2, which could explain why no interaction was detected with SUN2(1-224). However, interaction of the SUN2 CTD and emerin was not investigated, which could shed more light on the strong interaction observed for full length SUN2 and emerin.

In reciprocal mapping studies, SUN1 and SUN2 were both found to bind to the nucleoplasminc domain of emerin, residues 1-221. This result confirms that it is the nucleoplasmic domains of these proteins that associate. Therefore, it is difficult to explain why an interaction between GST-SUN2(1-224) and emerin was not seen. This GST fusion does not express very well, and may be misfolded and fail to interact *in vitro* with emerin.

Further narrowing of SUN proteins binding site on emerin was difficult. GST-fused emerin sub-fragments as a whole did not interact very strongly with the N-terminus of SUN1 or FL SUN2 in the pull-down experiments. Within the limitation of the procedure, residues 140-221 of emerin were found to interact preferentially with SUN1, whereas binding of SUN2 on emerin could not be mapped using this method. Interestingly, nesprin-1α and nesprin-2β bind to residues 140-176 of emerin, which are located within the same region (Wheeler et al., 2007). This again indicates that there could be competitive or co-operative binding at this site between SUN1 and nesprins and suggests the existence of a protein-complex between emerin, nesprins and SUN1 at the INM. Emerin also binds a number of other proteins, including actin, BAF, GCL, β-catenin. How all these come into play within the cells to maintain muscle tissue and cardiac conduction still remains a mystery.

5.3.3 SUN1 and other binding partners

SUN1 was also found to interact with SUN2. Although the current models predict that SUN proteins homodimerize via the coiled-coil domain (Crisp et. al. 2006), instead I found that it was the N-terminus of SUN1 that interacts with SUN2. Previously, pull-down assays in the lab had also shown that SUN1 self-interacts through its N-terminus (Haque et al., 2006). These suggest that the SUN proteins can form homodimers or heterodimers at the inner face of the NE through interaction of their nucleoplasmic domains. As most binding partners of SUN1 also interact with SUN2, this association suggest that SUN proteins may have an overlapping range of functions. Therefore defects in one may be able to compensate for absence of other. SUN1 is not dependent on lamin A for its NE localization, while SUN2 is partly mislocalized in lamin A/C null cells, but remains at the NE in cells where RNAi of lamin A was performed (Crisp et al., 2006). Hetero-oligomerization of SUN2 with SUN1 could help SUN2 to remain at the NE in the absence of lamin A.

Emerin, nesprins and SUN2 interact with SUN1, yet all of these proteins mislocalize from the NE in lamin A/C null cells (Sullivan et al., 1999; Libotte et al., 2005; Crisp et al., 2006; Haque et al. 2006). Therefore these proteins cannot be responsible for anchoring SUN1 at the NE in absence of lamin A. To understand SUN1 anchoring at the NE, SUN1 interaction with nuclear actin was investigated. The preliminary

experiment presented here suggests that SUN1 may interact with actin, however it was not reproducible and also SUN2 interaction with actin could not be established. Nevertheless, this was the first indication that SUN1 might interact with actin, which could be responsible for the stable anchorage of SUN1 at the NE. Actin is predicted to form a cortical supporting network at the nucleoplasmic side of the NE. Since nuclear actin interacts with lamin A, emerin and possibly nesprins (Bettinger et al., 2004; Zhen et al., 2002), it is possible that SUN proteins interact with actin as well. Further tests, such as actin co-sedimentation assays and immunoprecipitation assays, preferably using isolated nuclei, are required to confirm the interaction between these two proteins. However, it cannot be ruled out that other proteins are responsible for SUN1 anchoring at the NE, such as hALP, histone H2B and telomeres (discussed in section 7.3.4; Chi et al., 2007; Ding et al., 2007; Schmitt et al., 2007).

SUN protein interactions with several proteins were investigated in this chapter. Whilst only nesprins have so far been found to interact with the C-terminus of SUN1, I have demonstrated that emerin, nesprins, lamin A and SUN2 interact with the nucleoplasmic N-terminus of SUN1. Due to technical difficulties with the expression of deletion fragments, SUN2 interactions could not be mapped. Although the interaction of the nesprin KASH domain with SUN1 denotes a major function of SUN1, as a linking protein between the nucleoplasm and cytoplasm, interaction with multiple proteins at the nucleoplasmic face of the NE suggests that SUN1 may have other roles besides providing structural support. SUN1 may help in relaying signals in mechanotransduction from the cell surface to inside of the nucleus. SUN1 interaction with lamin A, emerin and nesprin also indicates that it might have a role in pathogenesis of EDMD and potentially other laminopathies. Further studies to understand SUN1 role in cells therefore would also shed light in our understanding of laminopathy disease pathologies.

CHAPTER 6

EXAMINING THE INVOLVEMENT OF SUN1 AND SUN2 IN LAMINOPATHIES

6.1 INTRODUCTION

Nuclear lamins are associated with a number of inherited diseases known as laminopathies. Over 180 mutations are found in the *LMNA* gene alone, which are distributed throughout its head, rod and tail domain (Fig. 1.12). There are at least 13 laminopathies known so far (Capell and Collins, 2006). Among these are Emery-Dreifuss muscular dystrophy and related myopathies, familial partial lipodystrophy, Charcot-Marie-Tooth disease and progeroid disorders (Worman and Bonne, 2007). How mutation in a single gene can cause such a wide range of disease phenotypes is a question still remaining to be answered. Lamin A and its interacting proteins have been studied intensively to understand the mechanisms lying behind laminopathies. A few INM proteins, namely emerin, LBR and nesprins are also involved in laminopathies, alternatively known as nuclear envelopathies. Emerin mutations are responsible for causing X-linked EDMD. Recently, mutations in nesprin-1 and -2 have also been found in a few, mainly sporadic, cases of EDMD (Zhang et al., 2007b).

From the previous chapters, we have come to know that SUN1 and SUN2 interact with lamin A, emerin and nesprins. All of these interacting partners of SUN1 and SUN2 are involved in laminopathies, particularly EDMD. It is thought that perturbation of interactions between lamin A and its binding partners might lead to EDMD (Ellis, 2006). Weakening of the NE, impaired mechanical stiffness or altered mechanotransduction, are the mechanisms hypothesized to cause EDMD (section 1.4.6). SUN proteins, being a part of this multi-protein complex involving lamin A-emerin-nesprins and SUN proteins at the NE, also have the potential to play some role in laminopathies. In order to shed light on SUN proteins involvement in laminopathies, several investigations were performed. Firstly, SUN1 and SUN2 interactions with several lamin A mutants occurring in laminopathies, were investigated. Initially, lamin A mutants that represent most of the laminopathy phenotypes were employed, to study interactions by *in vitro* pull-down. SUN1 interactions with a variety of emerin missense mutants were also tested in similar way, using P183H, P183T, del 95-99, Q133H, S54F, 1-169(208) and del 236-241 emerin mutants. To further extend our studies, antibodies against the N- and C-termini of human SUN1 were generated and purification of the antibodies was attempted. Afterwards, using these antibodies and a human SUN2

antibody generated in the lab, SUN1 and SUN2 localization in fibroblast cells obtained from patients with a range of laminopathy phenotypes, was studied and compared.

6.2 RESULTS

6.2.1 SUN protein interaction with a range of laminopathy-associated lamin A mutants

6.2.1.1 EDMD and HGPS lamin A mutants have reduced interaction with SUN1 and SUN2

We have previously shown that SUN1 interacts with lamin A (LA), by both co-immunoprecipitation and pull-down assays (section 4.2.1; Haque et al., 2006). In order to investigate potential SUN1 association with laminopathies, SUN1 interactions with a range of different lamin A mutants representing most of the laminopathy phenotypes were tested. These mutants were: R482W (familial partial lipodystrophy), E203G (dilated cardiomyopathy), L530P (EDMD), R60G (dilated cardiomyopathy), R453W (EDMD), R298C (Charcot-Marie-Tooth disease), R527H (mandibuloacral dysplasia) and G608G (HGPS). Lamin A mutant G608G causes an internal 50 aa deletion in the lamin A C-terminus (section 1.4.4) and is referred as LA-G608G or LAΔ50, which results in aberrant permanent fanesylation. These lamin A mutants were engineered previously in the lab by site-directed mutagenesis and were cloned into the pCIneo mammalian expression vector along with an N-terminal myc tag. The interaction of the *in vitro* translated lamin A mutants with MBP-SUN1(1-355) was tested by MBP pull-down assay in comparison with wild type (WT) lamin A. The experiment was repeated four times and a representative experiment is shown in Fig. 6.1. According to the results, SUN1 interacted strongly with all the mutants except LA-L530P, an EDMD mutant, and LA-G608G, the most common HGPS mutant. MBP alone did not bind significantly to WT or mutant lamin A. The lamin A constructs used in this experiment produced a doublet, which probably corresponds to myc-tagged and untagged products, since a western blot with anti-myc antibody detected only one band (S. Shackleton, unpublished data).

To validate this result, the intensity of the interactions was measured using Image J software and was plotted on a graph (Fig. 6.1C). Firstly, intensity of the interacting

Fig. 6.1. Interactions between SUN1 and lamin A mutants interaction. A) Schematic diagram of lamin A, indicating locations of mutations. **B)** [35S]-labelled myc-tagged lamin A mutants causing laminopathies (as indicated above) were produced by *in vitro* translation. These were separately incubated with MBP and MBP-SUN1(1-355), previously bound to amylose beads. Bound proteins were resolved by SDS-PAGE and were detected by autoradiography. Coomassie-stained gel shows expression of the MBP fusion proteins. **C)** The graph plotted shows interaction between SUN1 and different lamin A mutants, averaged from four experiments. Lamin A mutant interactions were quantified by densitometry using Image J and normalized against the corresponding input lane. Values were expressed as a percentage of the WT value. The error bars represent ±SEM and asterisk shows statistical significance of the binding (** = p<0.01).

bands of SUN1 and lamin A mutants and WT lamin A were quantified. Then the values measured were inversed and the background value was deducted from these values. Next, the values of interactions were normalized against the corresponding 10% input bands. Finally, the values were expressed as a percentage of the wild type value. Student's t-test analysis was performed, which demonstrated a significant reduction of SUN1 binding to LA-L530P ($p<0.0001$) and LA-G608G ($p<0.0001$). This finding was very exciting and was the first correlation found between SUN1 and laminopathies. This shows that SUN1 might play a role in EDMD and HGPS disease processes.

As a follow up to this finding, similar investigations were performed for SUN2, by GST pull-down assay. GST-SUN2(1-224) interactions with the same range of lamin A mutants were tested in three independent experiments. A representative result is shown in Figure 6.2B and demonstrates that SUN2 interactions with LA-L530P and LA-G608G were reduced in a similar manner to SUN1. However, the reduction in binding was not as obvious as observed for SUN1. To validate the finding, intensity of the interactions was measured using Image J software and was plotted on a graph. However, the interaction of SUN2 with WT lamin A was weaker than that of SUN1, so the background was relatively higher, which may limit the significance of quantification. Nevertheless, statistical tests confirmed that there is significant reduction in binding of SUN2 with LA-L530P ($p=0.002$) and LA-G608G ($p=0.002$). SUN2 interaction with LA-R482W ($p=0.05$) was also found to be slightly reduced.

6.2.1.2 Reduced SUN protein interaction with both L530P and R527P EDMD lamin A mutants

Having observed reduced interaction of SUN protein with the EDMD-associated lamin A mutant L530P, I sought to determine whether this was a common feature of EDMD-associated lamin A mutants. Previous experiments showed that SUN1 interacts with the CTD of lamin A (section 4.2.4). Therefore, SUN1 interaction with several AD-EDMD lamin A mutants occurring mainly at the C-terminus was tested. The lamin A mutants employed for this study were E358K, R453W, W520S, R527P, L530P, and R541C. These mutants were generated previously in the lab by site-directed mutagenesis and cloned into pCIneo vector with an N-terminal myc tag. MBP pull-down assays were performed using MBP-SUN1(1-355) and *in vitro* translated lamin A EDMD mutants. An average of three experiment is shown in Figure 6.3, which shows a significant

WT= Wild type lamin A
R482W = Familial partial lipodystrophy
E203G= Dilated cardiomyopathy
L530P= Emery-Dreifuss muscular dystrophy
R60G= Dilated cardiomyopathy
R453W= Emery-Dreifuss muscular dystrophy
R298C= Charcot-Marie -Tooth Disease 2
R527H= Mandibuloacral dysplasia
G608G= Hutchinson -Gilford progeria syndrome

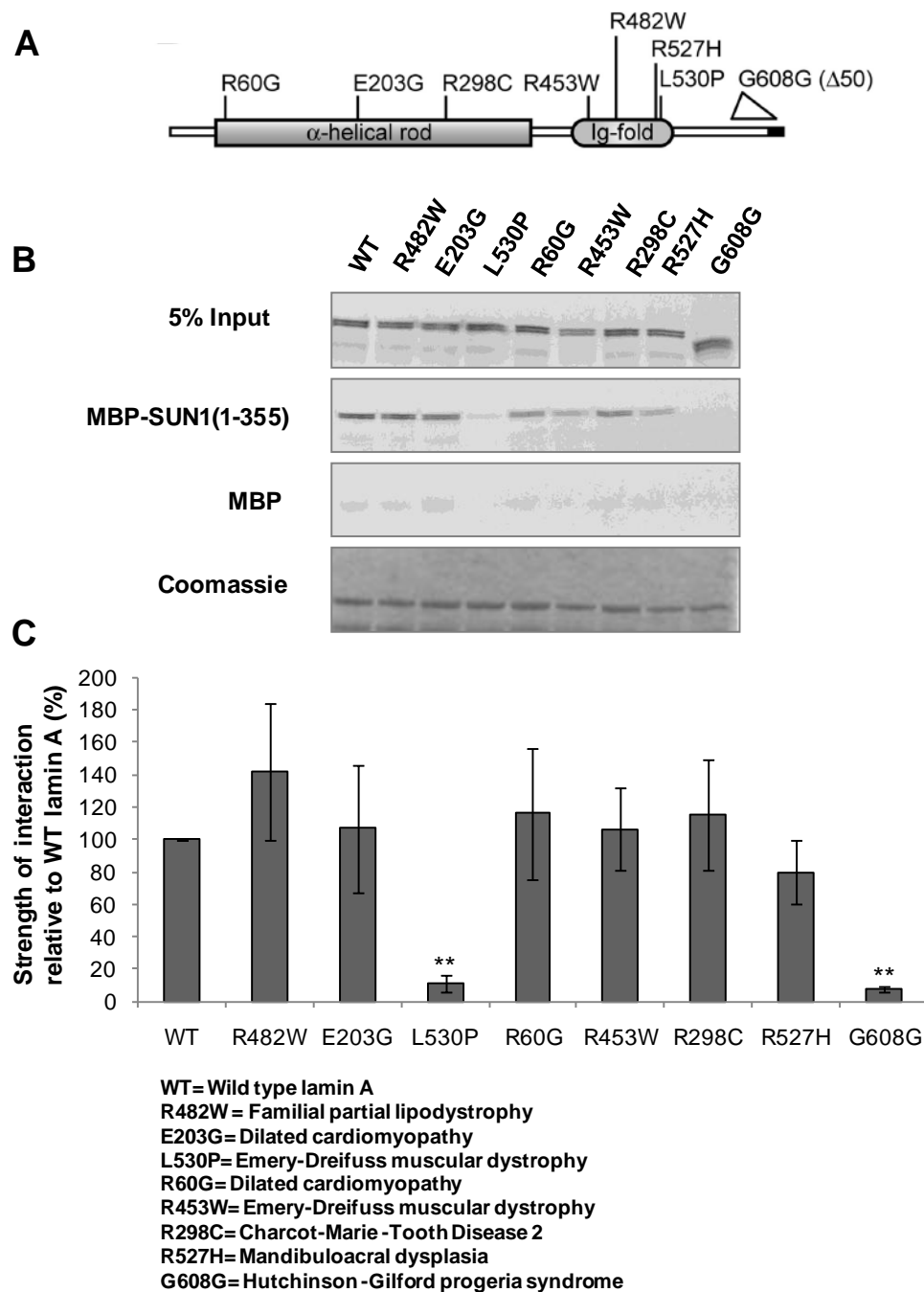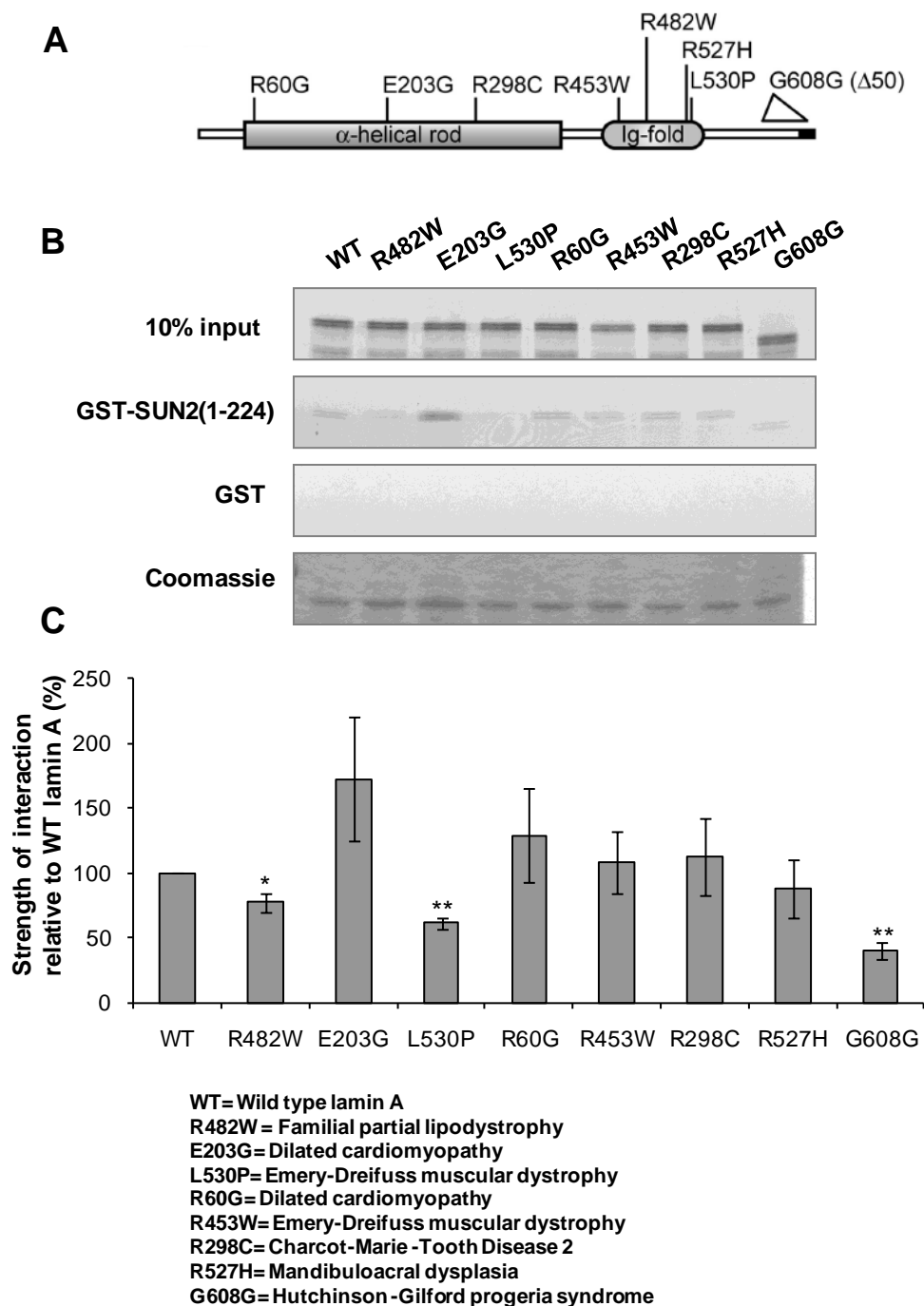**Fig. 6.2. Interactions between SUN2 and lamin A mutants. A)** Schematic diagram of lamin A, indicating locations of mutations. **B)** [^{35}S]-labelled myc-tagged lamin A mutants causing laminopathies (as indicated above) were produced by *in vitro* translation. These were separately incubated with GST and GST-SUN2(1-224) previously bound to glutathione-Sepharose beads. Bound proteins were resolved by SDS-PAGE and detected by autoradiography. Coomassie-stained gel shows expression of the GST fusion proteins. **C)** The graph plotted shows interaction between SUN2 and different lamin A mutants, averaged from three experiments. Lamin A mutant interactions were quantified by densitometry using Image J and normalized against the corresponding input lane. Values were expressed as a percentage of the WT value. The error bars represent ±SEM and asterisk shows statistical significance of the binding (* = $p<0.05$; ** = $p<0.01$).

Fig. 6.3. Interaction of SUN1 with EDMD-associated lamin A mutants. A) Schematic diagram of lamin A, indicating locations of mutations. **B)** [35S]-labelled myc-tagged lamin A mutants causing EDMD were produced by *in vitro* translation. These mutants were separately incubated with MBP and MBP-SUN1(1-355), previously bound to amylose beads. Bound proteins were resolved by SDS-PAGE and were detected by autoradiography. Coomassie-stained gel shows expression of the MBP fusion proteins. **C)** The graph plotted shows interaction between SUN1 and different EDMD lamin A mutants, averaged from three experiments. Lamin A mutant interactions were quantified by densitometry using Image J and normalized against the corresponding input lane. Values were expressed as a percentage of the WT value. The error bars represent ±SEM and asterisk shows statistical significance of the binding (* = $p<0.05$; ** = $p<0.01$).

reduction in binding of SUN1 with LA-L530P (p=0.0006), as found previously, and also with LA-R527P (p=0.007). In contrast, increased interaction with LA-W520S (p=0.01) was observed. This further stresses the possibility that SUN1 might have a role in EDMD pathology.

SUN2 interaction with the same range of lamin A EDMD mutants was also investigated, using GST-SUN2(1-224). Interestingly, as for SUN1, SUN2 showed reduction in interaction with both LA-L530P (p=0.0004) (as found previously) and LA-R527P (p=0.0006) EDMD mutants (Fig. 6.4). In addition, SUN2 interaction with LA-R541C (p=0.01) was found to be reduced, whereas the binding with LA-E358K (p=0.02) was increased. These findings suggest that both SUN1 and SUN2 might have a role in the EDMD disease process due to interference of SUN protein binding with mutant lamin A.

6.2.1.3 Reduced SUN protein interaction with two progeria lamin A mutants, G608G and T623S

In an analogous manner, SUN1 interaction with several progeria lamin A mutants was tested by MBP pull-down. The progeria lamin A mutants employed for this investigation were T528M, K542N, G608G, T623S and L647R. The T528M and K542N are recessive lamin A mutations and do not affect farnesylation (Verstraeten et al., 2006; Plasilova et al., 2004), while T623S mutation results in 35 aa deletion similar to G608G, that also results in permanent farnesylation (Fukuchi et al., 2004; Shalev et al., 2007; section 1.4.4). The L647R mutation produces an uncleavable prelamin A mutant, due to mutation of the second ZMPSTE24 cleavage site (Fig. 1.6) and, is expected to yield a permanently farnesylated and carboxymethylated protein. Therefore L647R mutation mimics the effect of ZMPSTE24 mutations that cause progeroid disorders such as MAD, RD and some rare cases of classical HGPS (section 1.4.4). These lamin A mutant constructs were generated previously in the lab by mutagenesis and were cloned into pCIneo vector with an N-terminal myc tag. It was not clear at this stage whether the wild type lamin A protein employed in these experiments was correctly processed (section 1.1.2.3), when translated *in vitro* using the rabbit reticulocyte system. Therefore, another lamin A construct, pCI-mycLMNAL647X, was used which directly produces a mature lamin A. LA-L647X has a stop codon at residue 647, therefore mimics mature lamin A, which is 18 residues shorter than prelamin A.

A

B

C

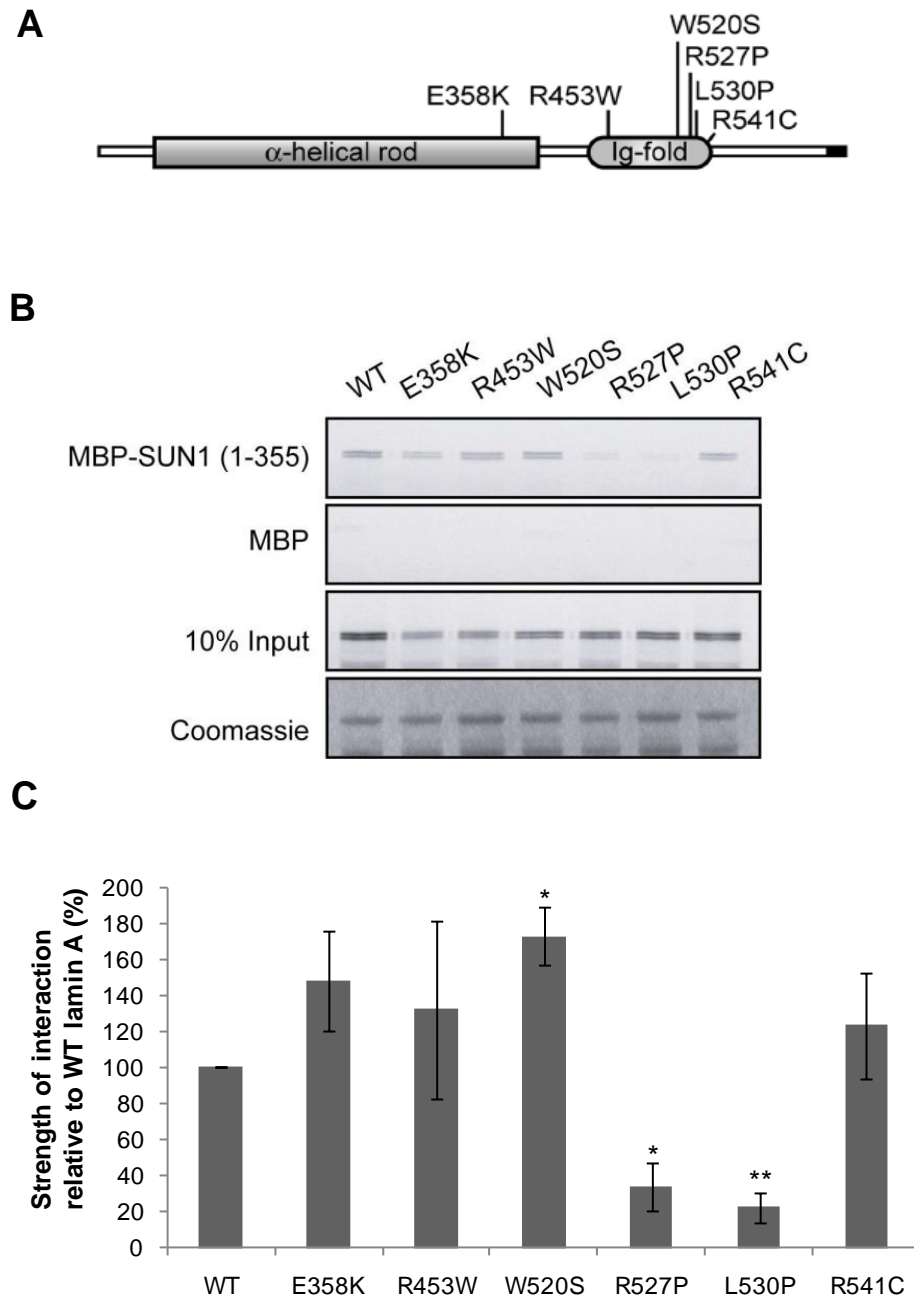**Fig. 6.4. Interaction of SUN2 with EDMD-associated lamin A mutants. A)** Schematic diagram of lamin A, indicating locations of mutations. **B)** [^{35}S]-labelled myc-tagged lamin A mutants causing EDMD were produced by *in vitro* translation. These were incubated separately with GST and GST-SUN2(1-224) previously bound to glutathione-Sepharose beads. Bound proteins were resolved by SDS-PAGE and detected by autoradiography. Coomassie-stained gel shows expression of the GST fusion proteins. **C)** The graph plotted shows interaction between SUN2 and different EDMD lamin A mutants averaged from three experiments. Lamin A mutant interactions were quantified by densitometry using Image J and normalized against the corresponding input lane. Values were expressed as a percentage of the WT value. The error bars represent ±SEM and asterisk shows statistical significance of the binding (* = $p<0.05$; ** = $p<0.01$).

As shown in Figure 6.5 (a representative of three repeat experiments), MBP-SUN1(1-355) interaction was again reduced with the LA-G608G (p<0.001) and, interestingly, was also significantly reduced for LA-T623S (p<0.001), which causes a similar 35 aa internal deletion near the C-terminus of lamin A, also referred as LA-Δ35 (Fukuchi et al., 2004). This suggests that the residues deleted are essential for interaction. From comparison of the sizes of wild-type lamin A, LA-L647R and LA-L647X, it was apparent the WT lamin A protein was in fact unprocessed prelamin A, as it migrated at the same position as the L647R mutant, whilst lamin A-L647X was noticeably smaller (Fig. 6.5B). In agreement with a study by Crisp et al. (Crisp et al., 2006), SUN1 interacted more strongly with prelamin A (WT and LA-L647R) than with mature lamin A (LA-L647X). Interestingly, SUN1 showed a significantly stronger interaction with L647R than WT lamin A, possibly due to the leucine to arginine substitution. There was also an apparent increase in interaction between SUN1 and LA-T528M and LA-K542N, but this did not reach statistical significance.

In an analogous manner, GST-SUN2(1-224) was used to test its interaction with progeria lamin A mutants, as described above. The experiment was repeated two times and a representative result is shown in Figure 6.6. Results were similar to those obtained with SUN1 in that SUN2 also interacted less efficiently with LA-G608G (p=0.004) and LA-T623S (p=0.001) lamin A mutant. However, SUN2 interaction was slightly increased with LA-T528M (p=0.04). SUN2 interaction was also very much reduced with LA-L647X (mature lamin A) and increased with LA-L647R, suggesting that both SUN1 and SUN2 interact better with unprocessed farnesylated lamin A.

6.2.2 SUN1 interaction is reduced with X-EDMD emerin mutant, 1-169(208)

Emerin mutation is associated with X-EDMD. Having detected reduced binding between SUN1 and two AD-EDMD lamin A mutants, I next examined whether SUN1 interaction with emerin mutants is altered. Therefore, MBP-SUN1(1-355) binding with several emerin mutants was tested by pull-down assay. The emerin mutants used for this test were P183H, P183T, del 95-99, Q133H, S54F, 1-169(208) and del 236-241. Most emerin mutants occurring in X-EDMD are effectively null (due to a truncation or

A

B

C

Fig. 6.5. Interaction of SUN1 with progeria-associated lamin A mutants. A) Schematic diagram of lamin A, indicating locations of mutations. **B)** [^{35}S]-labelled myc-tagged lamin A mutants causing progeria and mature lamin A (L647X) were produced by *in vitro* translation. These were incubated separately with MBP and MBP-SUN1(1-355) previously bound to amylose beads. Bound proteins were resolved by SDS-PAGE and detected by autoradiography. Coomassie-stained gel shows expression of the MBP fusion proteins. **C)** The graph plotted shows interaction between SUN1 and different progeria lamin A mutants averaged from three experiments for the first 5 samples, and from two experiments for the last two samples. Lamin A mutant interactions were quantified by densitometry using Image J and normalized against the corresponding input lane. Values were expressed as a percentage of the WT value. The error bars represent ±SEM and asterisk shows statistical significance of the binding (** = p<0.01).
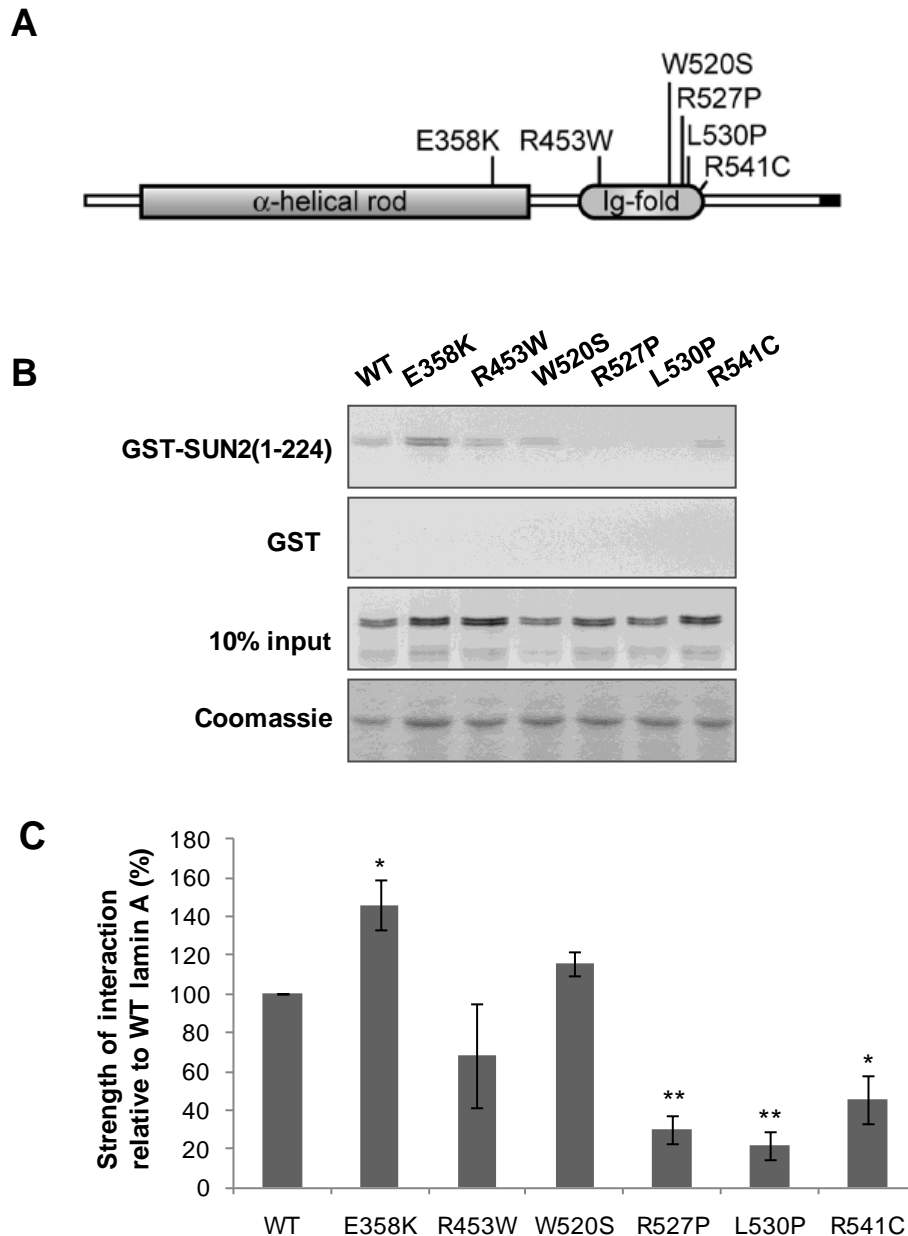
A

B

C
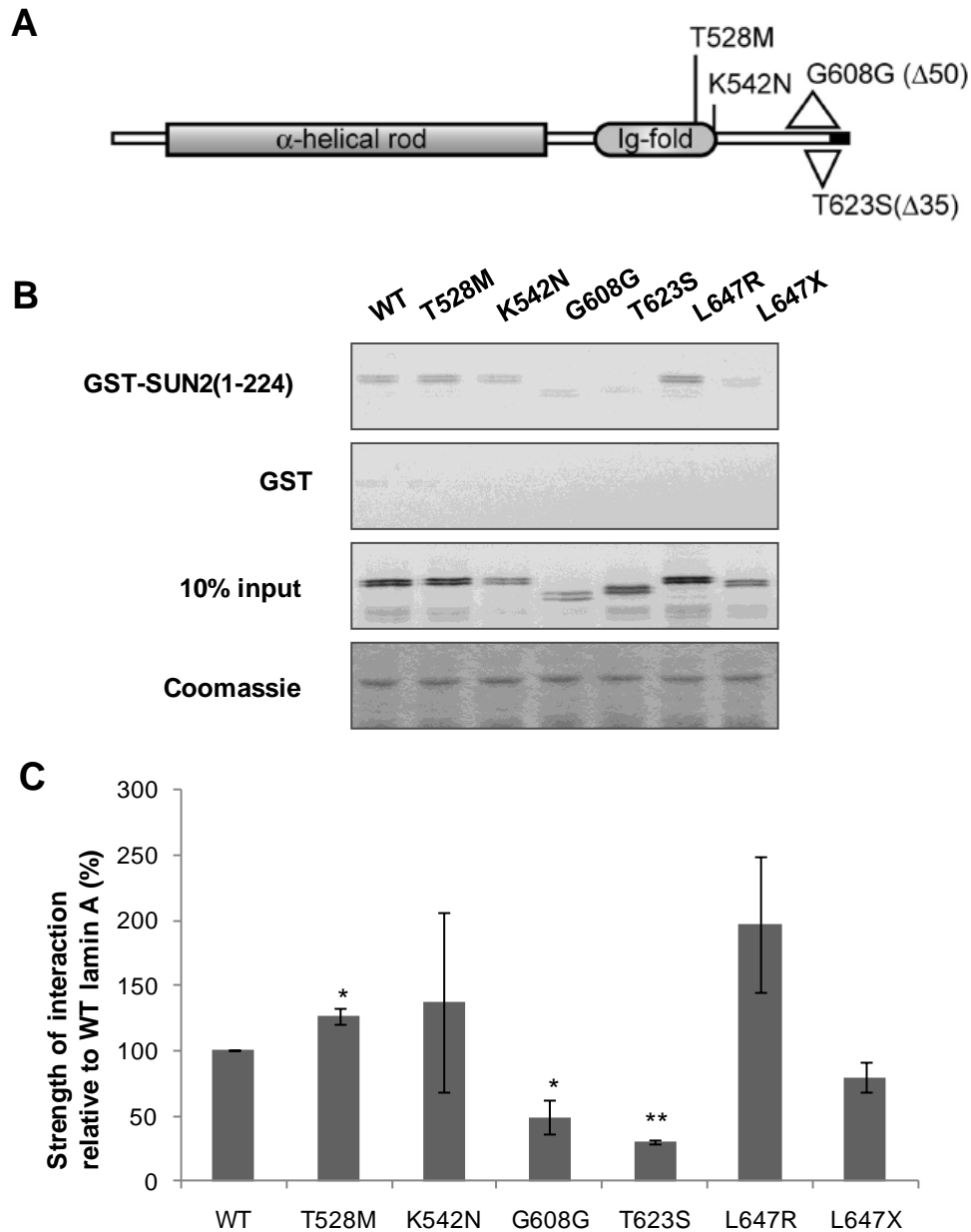
Fig. 6.6. Interaction of SUN2 with progeria-associated lamin A mutants. A) Schematic diagram of lamin A, indicating locations of mutations. **B)** [^{35}S]-labelled myc-tagged lamin A mutants causing progeria and mature lamin A (L647X) were produced by *in vitro* translation. These were incubated with GST and GST-SUN2(1-224) previously bound to glutathione Sepharose beads. Bound proteins were resolved by SDS-PAGE and detected by autoradiography. Coomassie-stained gel shows expression of the GST fusion proteins. **C)** The graph plotted shows interaction between SUN2 and different progeria lamin A mutants, averaged from two experiments. Lamin A mutant interactions were quantified by densitometry using Image J and normalized against the corresponding input lane. Values were expressed as a percentage of the WT value. The error bars represent ±SEM and asterisk shows statistical significance of the binding (* $= p<0.05$; ** $= p<0.01$).

frameshift), but the emerin mutants employed in this experiment do not alter the stability of emerin and also all of these emerin mutants, except del 236-241, are localized at the NE (Ellis et al., 1998; Fairley et al., 1999; Bengtsson and Wilson, 2004; Cartegni et al., 1997). The 1-169(208) emerin mutation involves a frame shift at residue 169, resulting in a novel hydrophobic stretch of 39 residues ending with a premature stop codon (Cartegni et al., 1997). These mutants were *in vitro* translated from plasmids pCDNA3emerinP183H, pCDNA3emerinP183T, pCDNA3emerindel(95-99), pCDNA3emerinQ133H, pCDNA3emerinS54F and pCDNA3.1emerin1-169(208) and pCDNA3.1emerindel(236-241) accordingly (kind gifts from J. Ellis, King's College London) (Ellis et al., 1998). The results in Figure 6.7, an average of three experiments performed, show significant reduction in binding between SUN1 and emerin mutant 1-169(208) (p=0.03). There was also apparent reduction in binding with P183T emerin mutant, but this did not reach statistical significance. SUN2 interaction with these emerin mutants was not tested and should be the subject of investigation in future studies.

6.2.3 Human SUN1 antibody generation

Having the aim to broaden our experiments to study localization of SUN proteins in laminopathy cell lines, antibodies against human SUN1 were generated. Antibodies against both the N-and C- terminal domains of human SUN1 were raised, in rat and rabbit, respectively, so that these antibodies could also be used in topology experiments to detect the respective termini of hSUN1. The hSUN1 cDNA available at the time was used to generate the antigens for the antibody production and it was a shorter splice version of the full length hSUN1 that lacks exon 7 and 8. This encodes a protein of 812 aa, in contrast to the full length protein of 916 aa (Fig. 6.8A). Therefore the N-terminus of hSUN1 used for antigenic stimulation in rat (residues 1-217) is approximately 100 residues shorter than the full length version (Fig. 6.8A). Amino acids 352-812, including the SUN domain at the C-terminus, were selected to use as antigen in rabbit.

6.2.3.1 Generation of MBP-hSUN1(1-217) and MBP-hSUN1(352-812) proteins

Two constructs, pMAL-hSUN1(1-217) and pMAL-hSUN1(352-812), were generated that encode MBP-fused hSUN1 NTD and CTD, respectively (Fig. A.3). These constructs were introduced into the BL21 strain of *E. coli* for expression of the proteins.
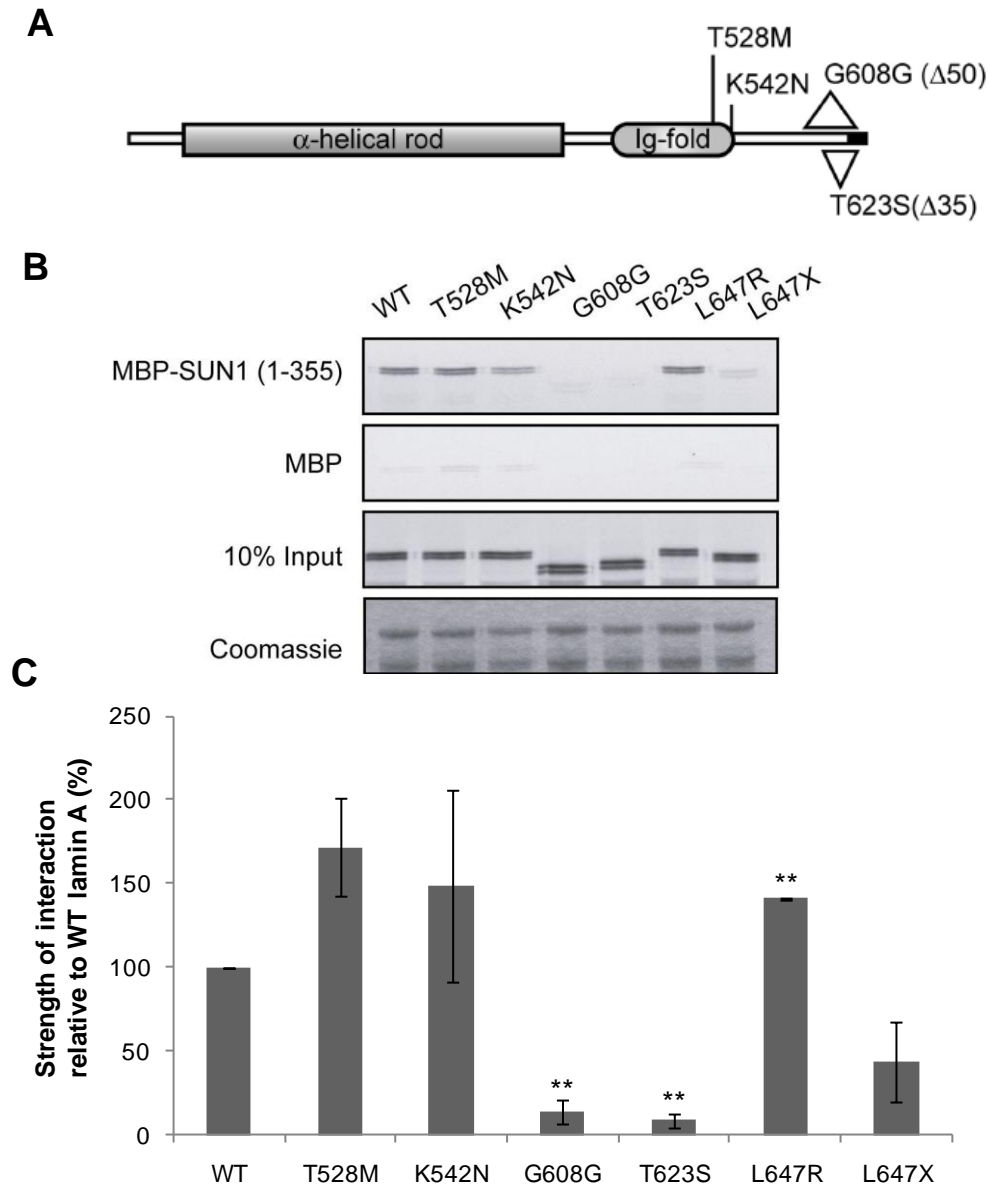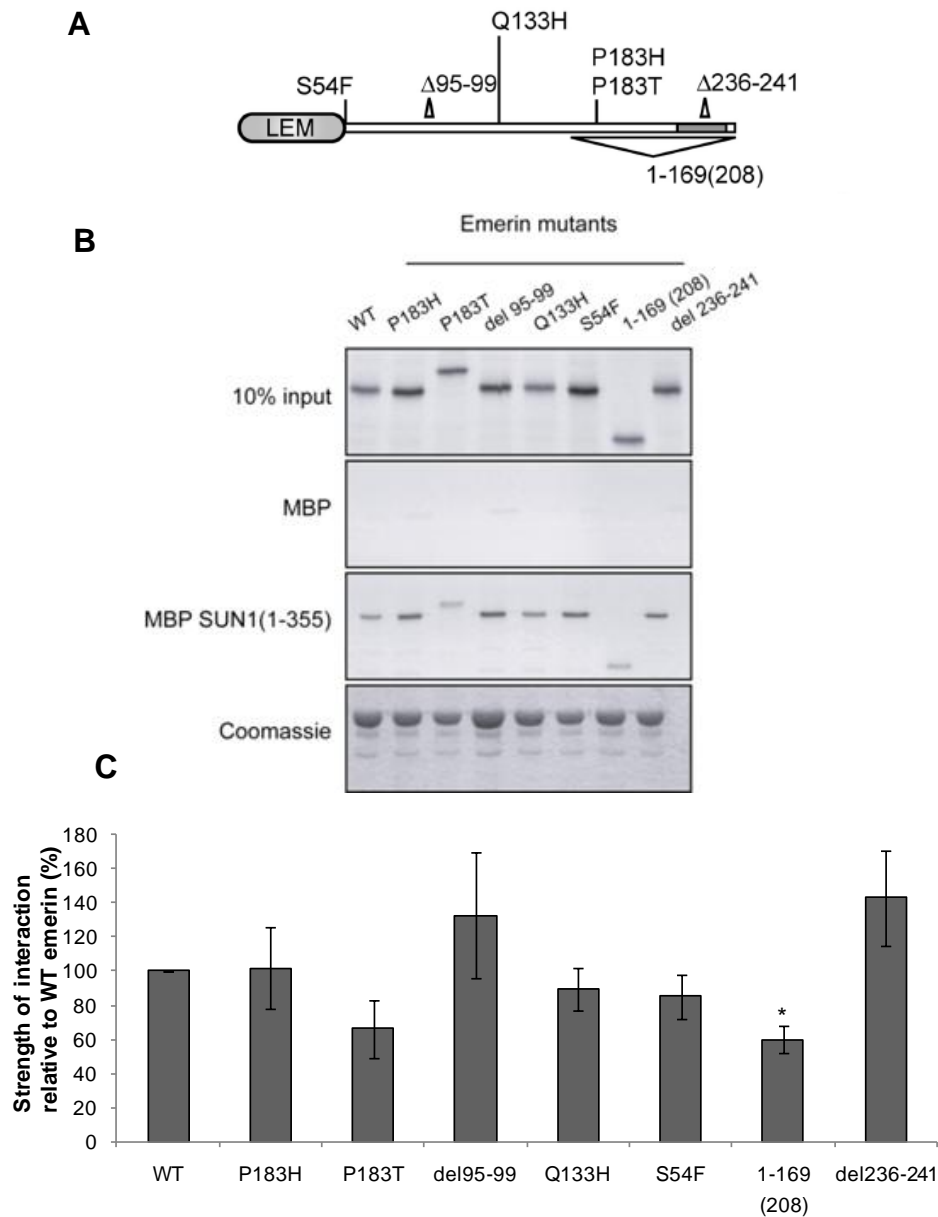
Fig. 6.7. Interaction of SUN1 with X-EDMD-associated emerin mutants. A) Schematic diagram of emerin, indicating locations of mutations. **B)** [35S]-labelled emerin mutants causing X-EDMD were produced by *in vitro* translation. These were incubated separately with MBP and MBP-SUN1(1-355) previously bound to amylose beads. Bound proteins were resolved by SDS-PAGE and detected by autoradiography. Coomassie-stained gel shows expression of the MBP fusion proteins. **C)** The graph plotted shows interaction between SUN1 and different emerin mutants, averaged from three experiments for the first six samples and two experiments for the last two samples. Values were expressed as a percentage of the WT value. The error bars represent ±SEM and asterisk shows statistical significance of the binding (* = p<0.05).
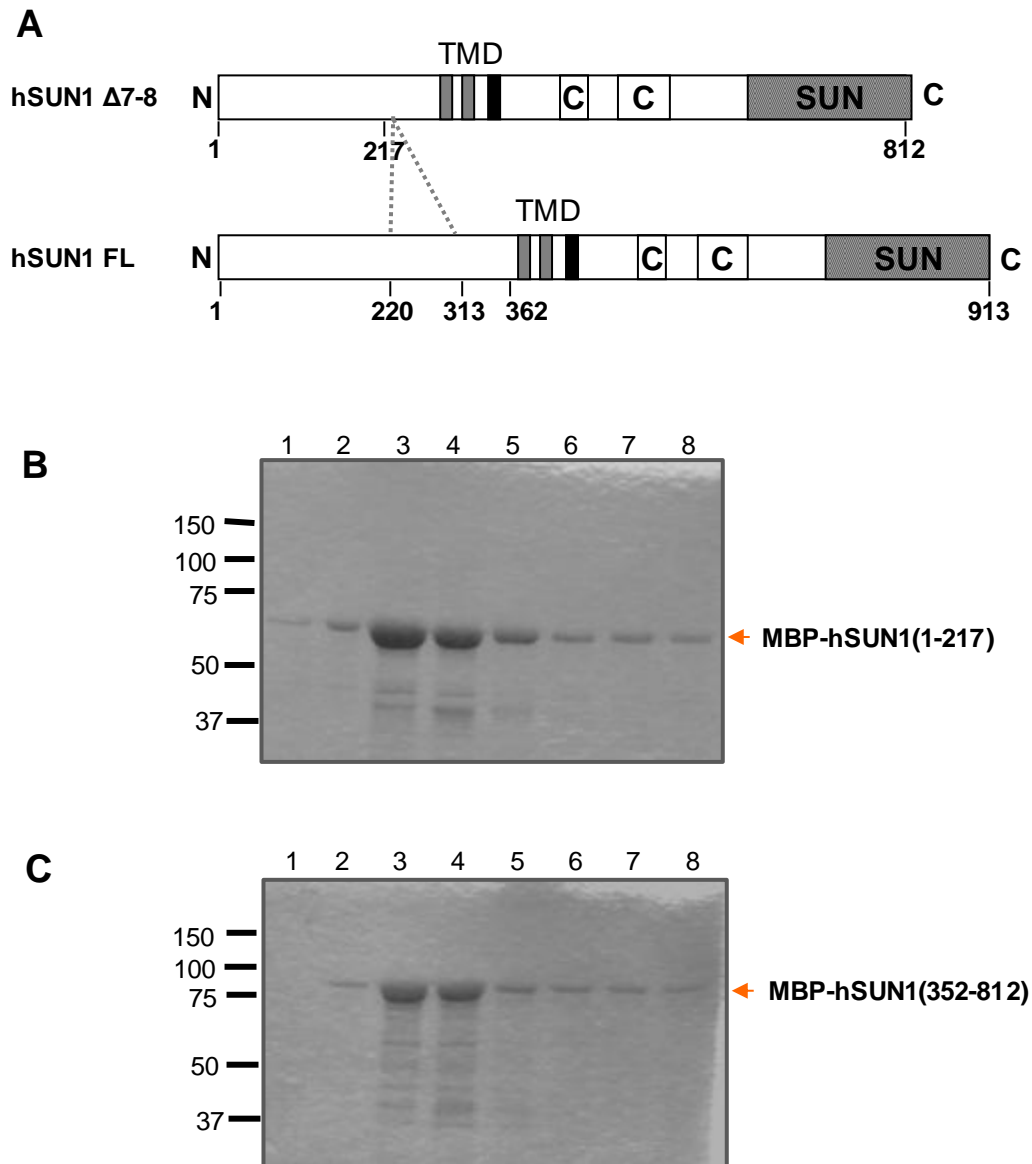
Fig. 6.8. MBP-fused human SUN1 NTD and CTD, antigen production. A) Schematic representation of hSUN1 full length and the splice variant (hSUN1Δ7-8) used for antigen production. (TMD=Transmembrane domain, CC=coiled coil region, SUN=SUN doamin, N=N-terminus, C=C-terminus) **B)** Coomassie stained protein gel showing MBP-hSUN1(1-217) antigen samples from different elutions as indicated (arrow). **C)** Coomassie stained protein gel showing MBP-hSUN1(352-812) antigen samples from various elutions as indicated (arrow). Numbers on left of each panel indicate sizes (kDa) of protein size markers .

In order to produce antibodies, approximately 2 mg and 3 mg of protein were required for proper antigenic stimulation in rat and in rabbit, respectively. After a test expression, 1.5 litre cultures of bacteria containing each plasmid were grown. As described in section 2.2.13, the bacteria were centrifuged, sonicated and the soluble lysate was incubated with amylose beads. This allowed the MBP-fused protein to bind with the beads. Later the protein was eluted from the beads using 10 mM maltose. The appropriate fractions of the eluted protein were selected after running the samples on protein gel (Fig 6.8B and C) and quantification of samples was performed by comparing with a known quantity of control sample (data not shown). Ultimately, 2 mg of MBP-hSUN1(1-217) and 3 mg of MBP-hSUN1(352-812) were sent to Cambridge Research Biochemicals for antibody production.

6.2.3.2 Selection of rats for hSUN1 NTD immunization

Sera from eight rats were tested by both western blot and immunofluorescence microscopy to ensure that they did not produce any bands of the same size as SUN1, or give any NE staining prior to immunization. HeLa cell extracts were run on a protein gel and then western blotted and probed with the eight rat sera. Three sera did not show any band of 90-100 kDa (the size of SUN1) on western and also had fewer non-specific bands (Fig 6.9A). To further test the sera, U2OS cells were cultured on coverslips, fixed in methanol and processed for immunofluorescence microscopy using the eight rat sera. All eight sera did not show any obvious localization or staining pattern in cells and had a general background in immunofluorescence microscopy (data not shown). Rats 2371 and 2373 met the required criteria and were selected for immunization with MBP-hSUN(1-217) protein.

6.2.3.3 Characterization of hSUN1 NTD antibodies

The pre-immune test bleed and production bleeds 1, 2, 3 and 4 were received from Cambridge Research Biochemicals after the respective antigen doses. The antisera were tested by both western blot and immunofluorescence microscopy. For western blot a range of dilutions (1/100, 1/200, 1/400) of each serum were tested. For animal 2371, only bleed 3 showed a cross-reacting band with a protein of the expected size for SUN1 (100kDa) (Fig 6.10A), although, if anything the band migrated at a position too high in comparison to that seen for mouse SUN1 (Haque et al., 2006). In contrast, serum from

A

Rats
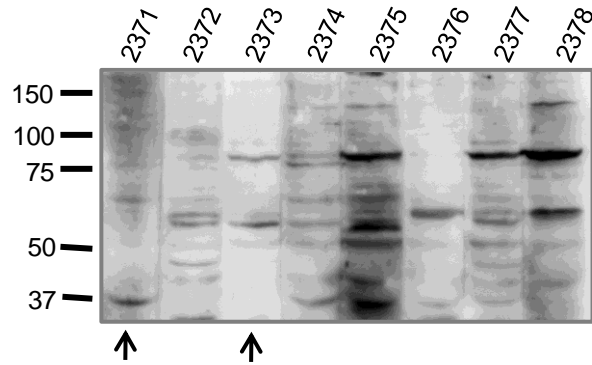
B

Rabbits
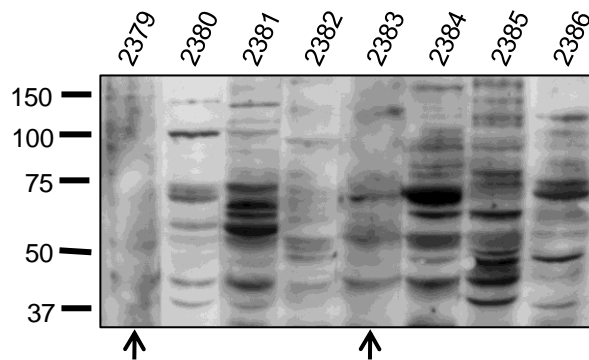
Fig. 6.9. Test of animal sera by western blot. A) Western blot of HeLa cell extract probed with pre-immune sera from 8 rats, before antigenic stimulation by MBP-hSUN1(1-217), as indicated. Arrows indicate the rats chosen for antibody production. **B)** Western blot of HeLa cell extract probed with pre-immune sera from 8 rabbits, before antigenic stimulation by MBP-hSUN1(352-812), as indicated. Arrows indicate the rabbits chosen for antibody production. Numbers on left of each panel indicate sizes (kDa) of protein size markers.
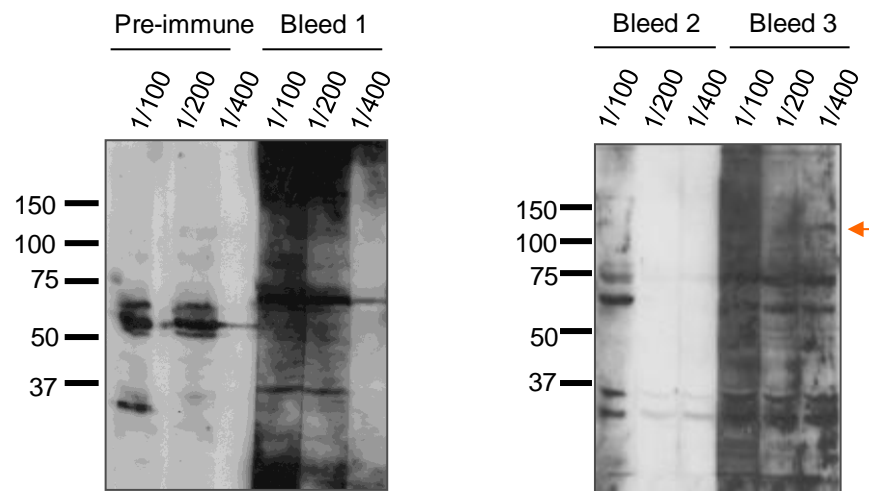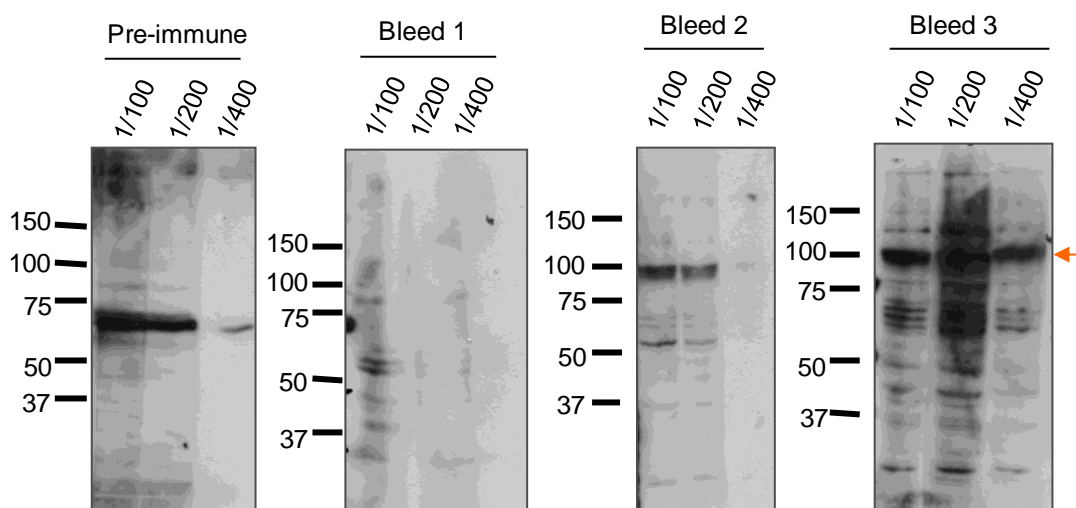
Fig. 6.10. Characterization of human SUN1 NTD antibody by western blot. Western blot of U2OS cell extract probed with pre-immune serum and production bleed 1, 2 and 3 after antigenic stimulation by hSUN1 NTD (1-217), at the indicated dilutions for rat 2371 (A) and 2373 (B). Arrows indicate 100kDa band in 2371 bleed 1 and 2373 bleed 2 and 3 (arrow). Numbers on left of each panel indicate sizes (kDa) of protein size markers. Dilutions used for each serum are indicated at the top of each panel.

bleeds 2 and 3 of animal 2373 showed strong cross-reacting bands with a protein migrating just below the 100 kDa size marker and appeared to be a doublet (Fig. 6.10B). This mirrors quite closely the bands produced by 0545 mouse SUN1 antibody (Haque et al., 2006), therefore is likely to represent detection of human SUN1 by the 2373 anti-serum.

However, immunofluorescence microscopy results were not very satisfactory. U2OS cell were cultured and then stained with the antisera. Unlike the nice western result, bleed 3 of animal 2373 showed faint NE staining in only a few cells (data not shown). This suggests that the antiserum was effective only for western blot and not for immunofluorescence microscopy. Thus the antibody generation against the hSUN1 NTD was only partially successful. It is possible that the fixation methods (methanol and paraformaldehyde) used for immunofluorescence staining are masking the epitope thus rendering the 2373 antibody inaccessible to the antigen. Also, since only part of NTD of FL hSUN1 (lacking exon 7 and 8) was used as an antigen, this region may be important for recognition of the full length protein. However, the original purpose for production of both N- and C-terminal antibodies was for simultaneous detection of the N- and C-terminal domains by immunofluorescence microscopy in topology experiments, therefore as it did not work for immunofluorescence staining, the antibody was not further used.

6.2.3.4 Selection of rabbits for hSUN1 CTD antibody production

Antigen MBP-hSUN1(352-812) was generated as described in section 6.2.3.1 and was sent to Cambridge Research Biochemicals for antibody production. Pre-immune sera from eight rabbits were tested before antibody production, with the aim of selecting two for antigenic stimulation. The sera were tested by western blotting and immunofluorescence microscopy. HeLa cell extract was run on a protein gel and then western blotted and probed with the eight different rabbit sera. All sera had non-specific bands and most had cross-reacting bands equivalent to 100kDa (SUN1 size) on western except two, which were rabbit 2379 and 2383 (Fig. 6.9B). For immunofluorescence microscopy, U2OS cells were cultured and stained with the 8 rabbit sera. The sera 2379 and 2383 did not show any obvious localization pattern (data not shown). As rabbits 2379 and 2383 did not cross-react significantly by either western blot or

immunofluorescence, these were selected for antigenic stimulation with MBP-hSUN1(352-812) protein.

6.2.3.5 Characterization of hSUN1 CTD antibodies

The pre-immune test bleed and production bleed 1, 2, 3 and 4 were received from Cambridge Research Biochemicals after the respective antigen doses. The antisera were tested by both western blot and immunofluorescence microscopy. Production bleeds 2 and 4 of both animals 2379 and 2383 detected a 100 kDa doublet, which was not present in pre-immune sera (Fig 6.11). Immunofluorescence microscopy with U2OS cells was then performed to detect endogenous SUN1. Both animals 2379 and 2383 showed nice NE staining, which was not very apparent with bleed 2 but was more detectable with bleed 4 (Fig 6.12). Therefore the antiserum is effective for detection of hSUN1 both by western and immunofluorescence microscopy and was used for subsequent experiments.

6.2.3.6 Affinity purification of hSUN1 CTD antibodies

As there was non-specific bands present in western and also some cytoplasmic staining present in cells by immunofluorescence microscopy, purification of the hSUN1-CTD antibodies was attempted. Purification was performed by affinity purification using a CNBr column, as described in the material and methods (section 2.2.14). Firstly, the MBP-fused hSUN1CTD(352-812) antigen was produced by induction of a two litre culture of *E. coli* BL21 containing pMAL-hSUN1(352-812). After binding to an amylose column, the MBP-hSUN1(352-812) protein was eluted with 10 mM maltose in PBS. After several attempts, approximately 4.6 mg of MBP-hSUN1CTD was generated (Fig 6.13A). The protein was dialysed against coupling buffer and then coupled to the CNBr gel and washed with coupling buffer to generate the hSUN1CTD-CNBr column. Approximately 3 mg of hSUN1 CTD was attached to the column.

Next, 1 ml of 2379 rabbit serum from the terminal bleed was diluted with PBS. As the antigen is fused to MBP, it may contain antibodies against MBP protein as well as the required antibody. Therefore the serum was passed through a previously generated MBP column to remove anti-MBP antibodies. The serum was then passed though the

A

2379 Rabbit
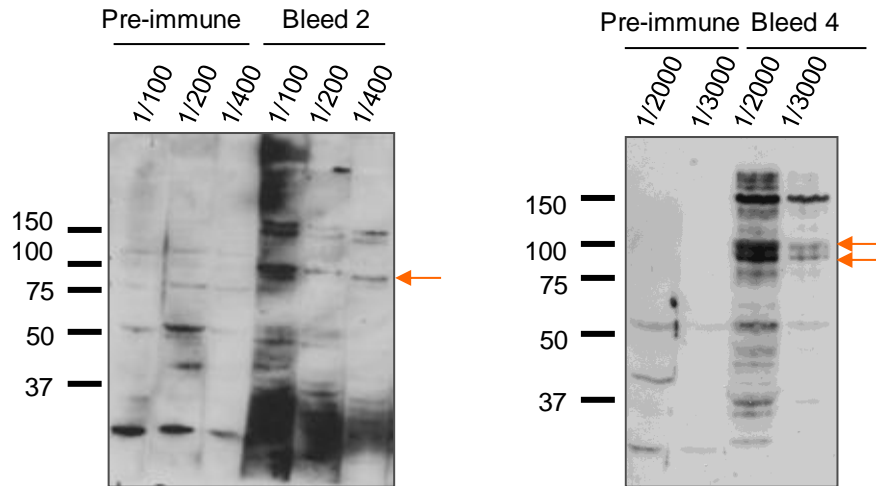
B

2383 Rabbit
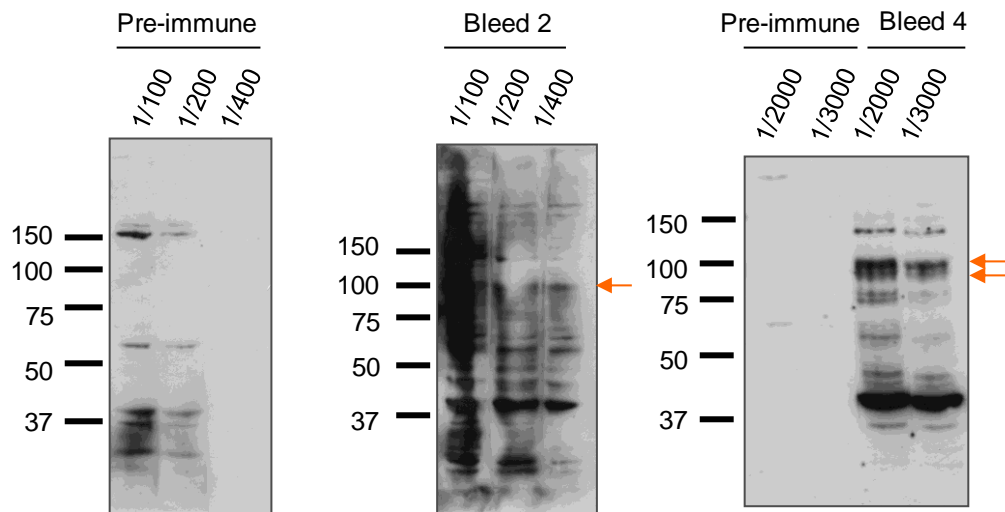
Fig. 6.11. Characterization of human SUN1 CTD antibody by western blot. A) Western blot of U2OS cell extract probed with pre-immune and production bleed 2 and 4 antisera of rabbit 2379 after antigenic stimulation by hSUN1 CTD (352-812). 100 kDa band is detected in bleed 2 and 4 (arrow). **B)** Western blot pre-immune and production bleed 2 and 4 of rabbit 2383, also showing 100kDa band (arrow). Numbers on left of each panel indicate sizes (kDa) of protein size markers. Dilutions used for each serum are indicated at the top of each panel.

A

B
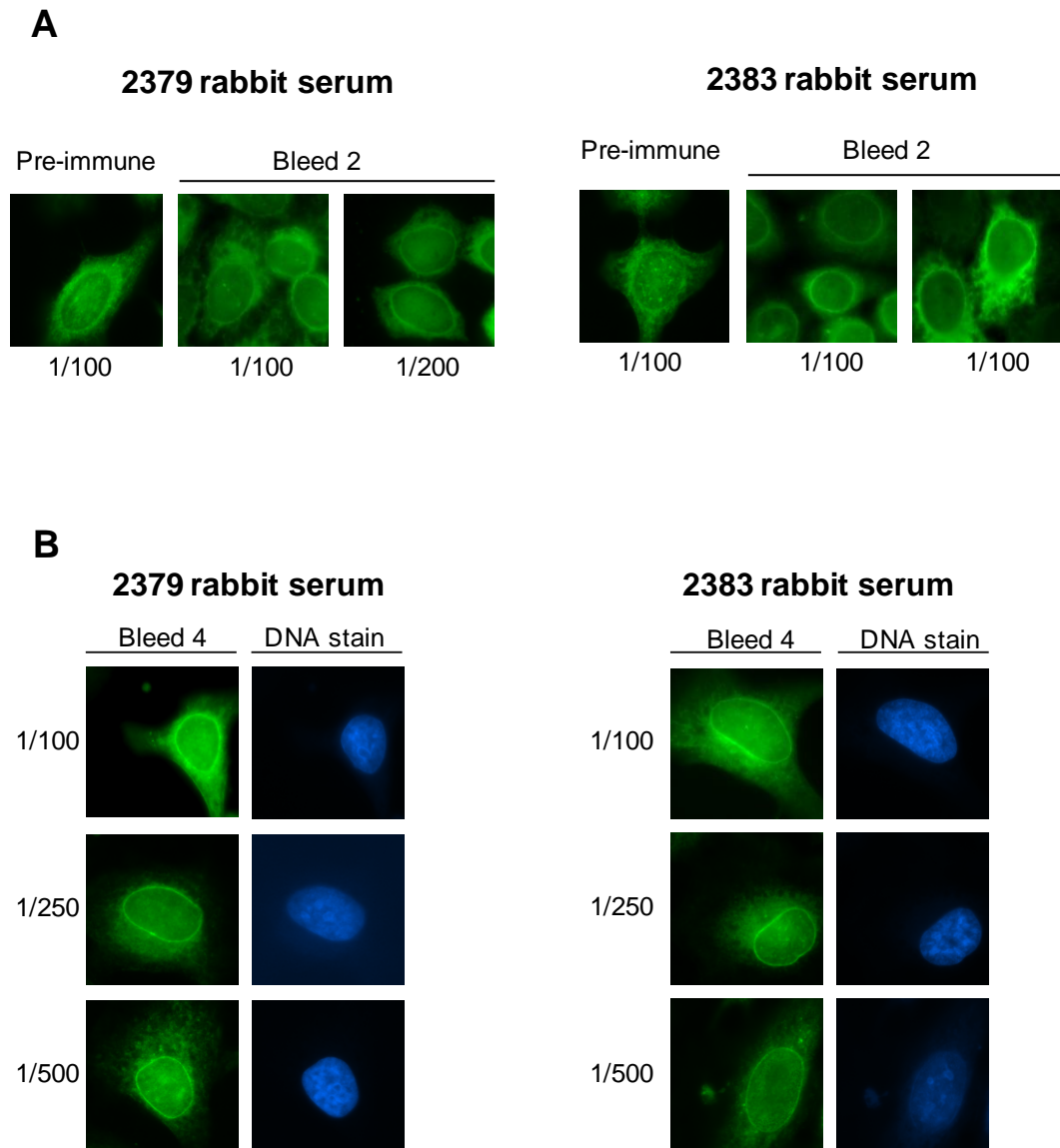
Fig. 6.12. Characterization of human SUN1 CTD antibody by immunofluorescence. Immunofluorescence microscopy of U2OS cells with 2379 and 2383 rabbit antisera. **A)** Cells were stained with 2379 and 2383 pre-immune serum and bleed 2. **B)** Cells were stained with 2379 and 2383 antiserum bleed 4 and showed a distinct nuclear rim pattern for both antisera.
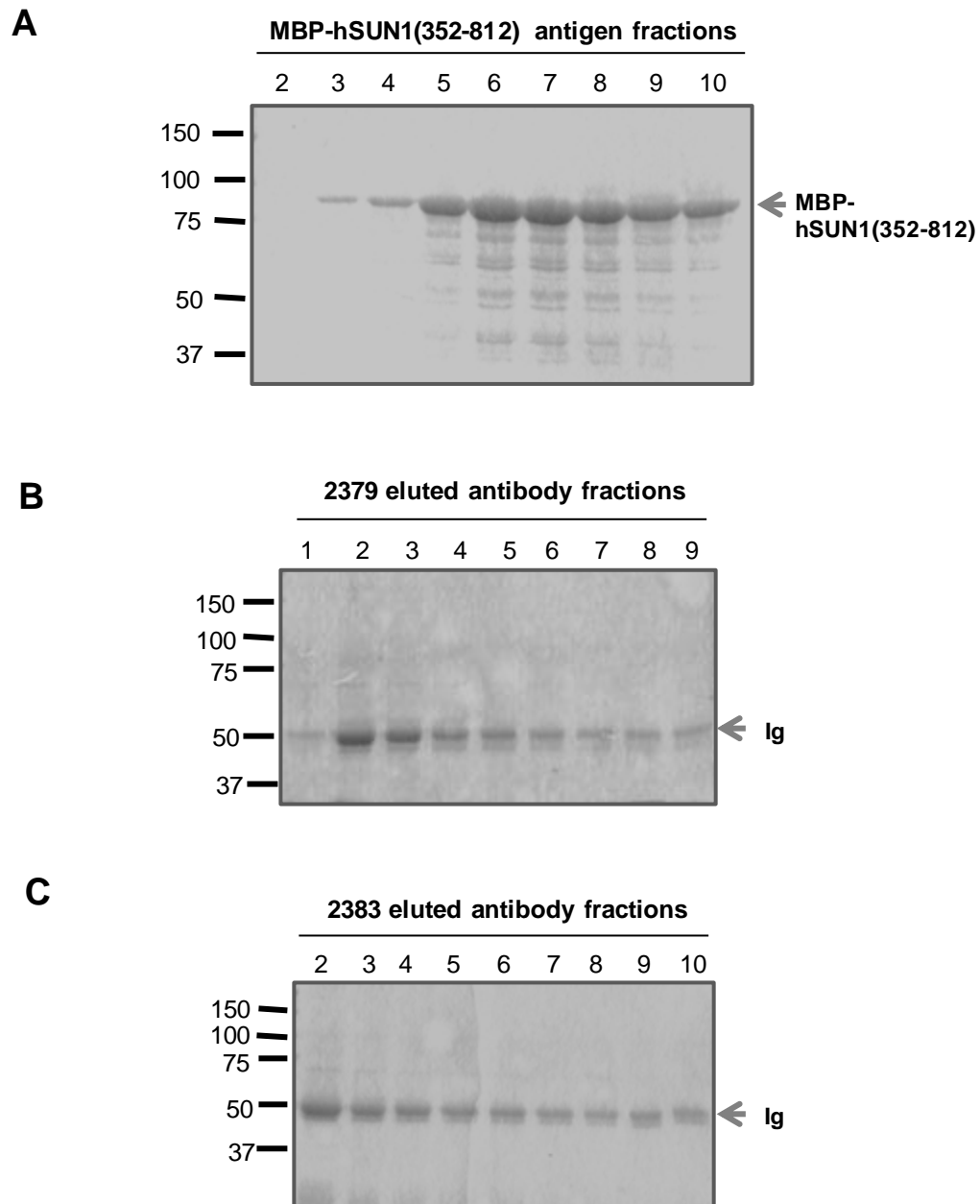
Fig. 6.13. Antigen production and eluted antibody fractions after purification.
A) Coomassie stained SDS-PAGE of MBP-hSUN1(352-812) antigen produced for capturing the antibody for purification. **B)** Coomassie stained SDS-PAGE gel showing 2379 hSUN1CTD antibody eluted fractions (as indicated) after purification. **C)** Coomassie stained SDS-PAGE gel showing 2383 hSUN1CTD antibody eluted fractions (as indicated) after purification. Numbers on left of each panel indicate sizes (kDa) of protein size markers.

CNBr column for binding of the anti-hSUN1 antibodies with their respective antigen. Subsequently, the column was washed with PBS and the antibodies eluted with glycine at pH 2. The eluted antibody fractions samples were examined by SDS-PAGE (Fig. 6.13B). As there was a significant amount of protein in fractions 2 and 3, these were pooled, as were fraction 4 and 5. The two sets of pooled fractions were tested by western blot, along with the pre-immune, initial serum before and after binding with the CNBr column, for their ability to detect hSUN1 from U2OS total cell extract. According to the results, in Figure 6.14, the affinity column appears to have been rather non-specific, as all the bands detected by the antibodies in the initial serum have been removed after binding to the CNBr colmn. Therefore, the purified antibody is not cleaner than the initial serum. However, there was a doublet at 100 kDa, in non-purified 2379 serum and the top band was lost after purification. The purified fractions showed two distinct bands, one at 100 kDa and another at 75 kDa. The 100 kDa band corresponds to the size of hSUN1 and the 75 kDa band could either be a splice variant of hSUN1 or a cross-reacting hSUN2 band or a non-specific band.

The 2383 antibody was purified in a similar manner (Fig. 6.13C) and was tested by western blot against U2OS total cell extract. After purification, the 2383 antibody fractions detected two bands at 100 and 75 kDa, similar to those observed with 2379, and also showed two more bands at approximately 45 and 50 kDa (Fig. 6.14). Since, even after purification, non-specific bands were present in western blot for 2383 antibody, it was not further characterized.

As 2379 antibody, pooled fraction 2+3, demonstrated relatively better detection of hSUN1 antibody by western blot, only this fraction was tested by immunofluorescence microscopy on U2OS cells and NIH 3T3 cells. However, the staining of the NE was weak in comparison with crude serum, even at 1/100 dilution, where there was some cytoplasmic staining still present. Although the 1/500 dilution looks very clean, it was very weak (Fig. 6.15A and 6.16). In addition, there was no cross reaction of 2379 antibodies with mouse SUN1 (Fig. 6.15A). Interestingly, the antibody also stained the centrosomes, which was initially an exciting finding since the LINC complex is now known to connect to the centrosome in some cases (Razafsky and Hodzic, 2009). However after careful comparison, the pre-immune serum also showed staining of the

A   **2379**
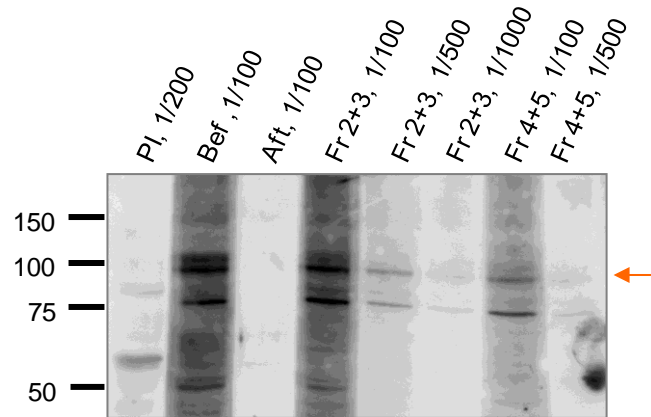
B   **2383**
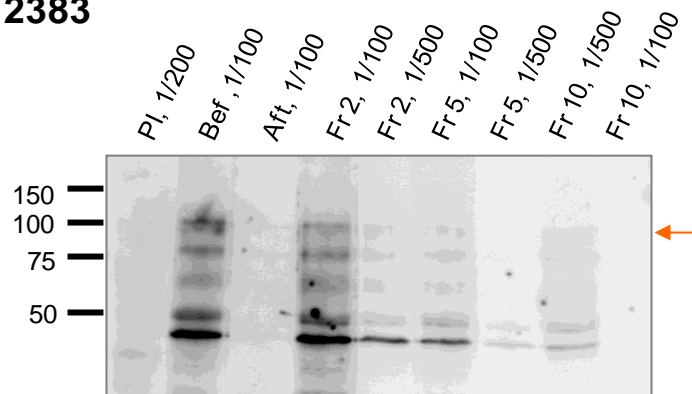
Fig. 6.14. Characterization affinity purified 2379 and 2383 human SUN1 CTD antibodies by western blot. A) Western blot showing U2OS cell extract probed with pre-immune (PI) and 2379 serum before (Bef) and after (Aft) binding with CNBr column or unbound fraction, as well as pooled fractions (Fr) 2+3 and 4+5, used at various dilutions, as indicated. Purified fractions show approxiamtely100 kDa band (arrow). **B)** Western blot showing U2OS cell extract probed with pre-immune (PI) and 2383 serum before (Bef) and after (Aft) binding with CnBr column or unbound fraction, as well as fractions (Fr) 2, 5 and 10. Purified fractions show faint 100 kDa band (arrow). Numbers on left of each panel indicate sizes (kDa) of protein size markers.

A
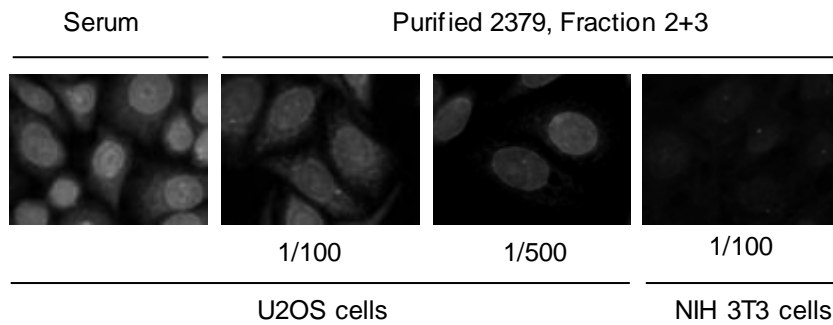
B
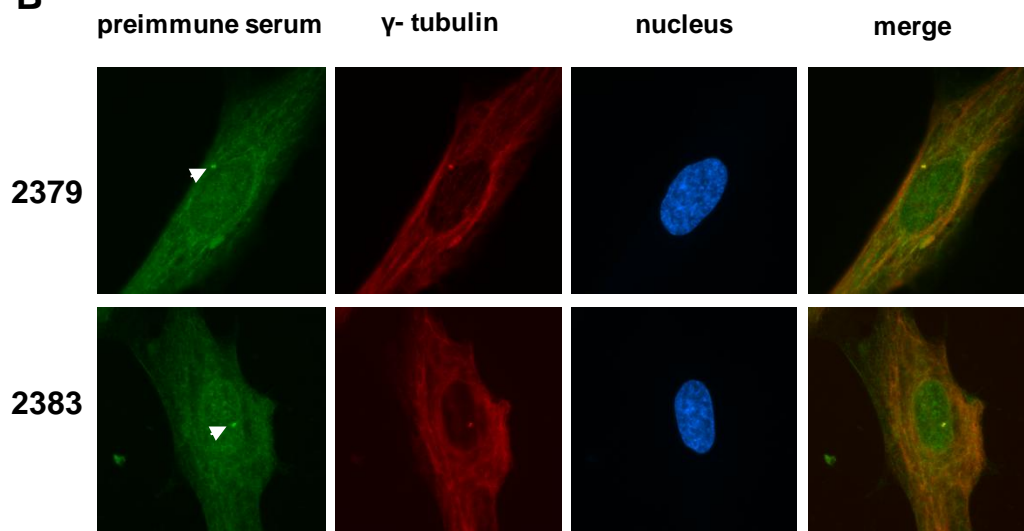
Fig. 6.15. Characterization of affinity purified 2379 human SUN1 CTD antibody and 2379 and 2383 rabbit pre-immune serum by immunofluorescence microscopy. A) Cells stained with 2379 antiserum before and after purification, showing endogenous SUN1 in a rim pattern. In NIH 3T3 cells, SUN1 is not detected by 2379 hSUN1 CTD antibody. **B)** U2OS cells co-stained with 2379 or 2383 pre-immune serum (green), together with centrosomes with γ-tubulin (red). Arrows indicate regions of co-localization.
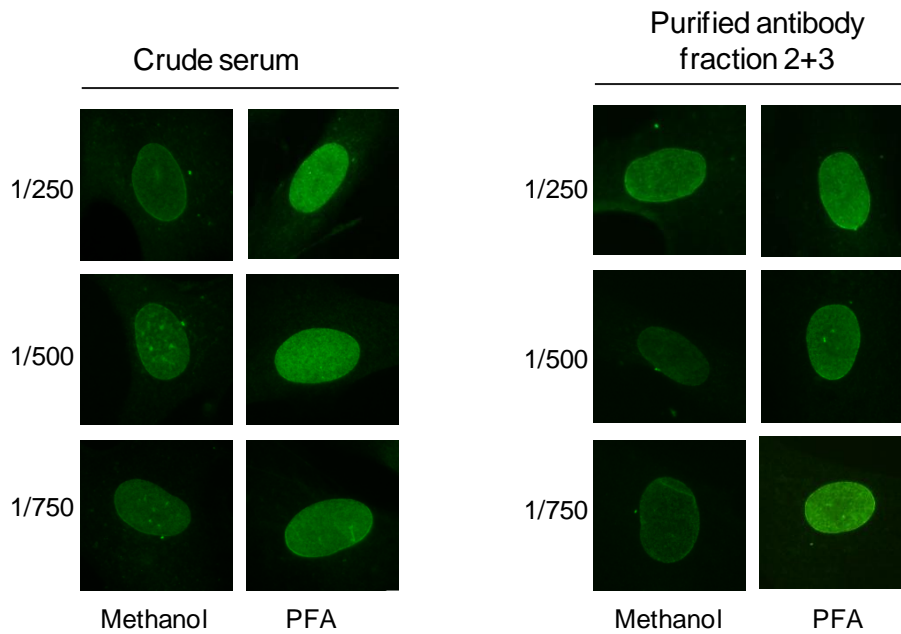
Fig. 6.16. Comparison of different fixation methods with 2379 human SUN1 CTD antibody. Immunofluorescence microscopy of hFF cells with 2379 rabbit antiserum, before and after affinity purification, tested by methanol and paraformadehyde (PFA) fixation of the cells. Dilutions are indicated on the left of each panel.

centrosomes, as judged by co-localization with centrosomal protein γ-tubulin. A similar phenomenon was observed for 2383 serum (Fig. 6.15B).

Up to this point, only methanol fixation had been used for testing the antibodies by immunofluorescence, whereas other methods of fixation could be more suitable. Therefore, fixation of U2OS and hFF (human for skin fibroblasts) cells, with both methanol and 4% paraformaldehyde was compared for immunofluorescence microscopic detection of hSUN1, with 2379 crude serum and purified pooled fractions 2+3. Representative images of hFF cells are shown in Figure 6.16. After methanol fixation, the NE staining was discrete but fainter than the corresponding paraformaldehyde fixation. In addition, the centrosome staining was very bright in methanol fixation, compared to paraformaldehyde fixation. Therefore, we decided to use the 2379 crude serum after paraformaldehyde fixation, for later studies on laminopathy patient cells.

6.2.4 SUN protein localization in laminopathy patient cell lines

SUN protein localization in different laminopathy patient cell lines was investigated, in order to determine whether disruption of lamin A-SUN protein interactions leads to mislocalization of SUN1 or SUN2 from the NE, in laminopathies. Initially, SUN1 and SUN2 localization was tested in skin fibroblasts obtained from individuals with mild progeria, HGPS and FPLD (Table 2.1), carrying T623S, G608G and R482W, respectively. Earlier in this chapter, I demonstrated that the G608G and T623S-associated deletion at the C-terminus of lamin A abolish interactions with SUN1 and SUN2, whereas R482W has no effect on interaction with SUN1, although R482W interaction with SUN2 is slightly reduced. The 2379 crude serum was used to detect SUN1, whilst SUN2 was detected using rabbit 2853 antibody, raised in the lab by Dr S. Shackleton against an N-terminal hSUN2 peptide (Haque et al., 2010). The cells were grown on coverslips, fixed in methanol and then stained with rabbit 2379 hSUN1 or 2853 hSUN2 antibodies and co-stained for lamin A/C. As shown in Figure 6.17, both SUN1 and SUN2 localized well to the NE and there was no obvious mislocalization visualized. Interestingly, SUN1 antibody staining of the NE was very variable from cell to cell in both the progeria patient cell lines, compared to control cells which had uniform SUN1 staining. In contrast, SUN2 antibody staining of the NE in progeria cells
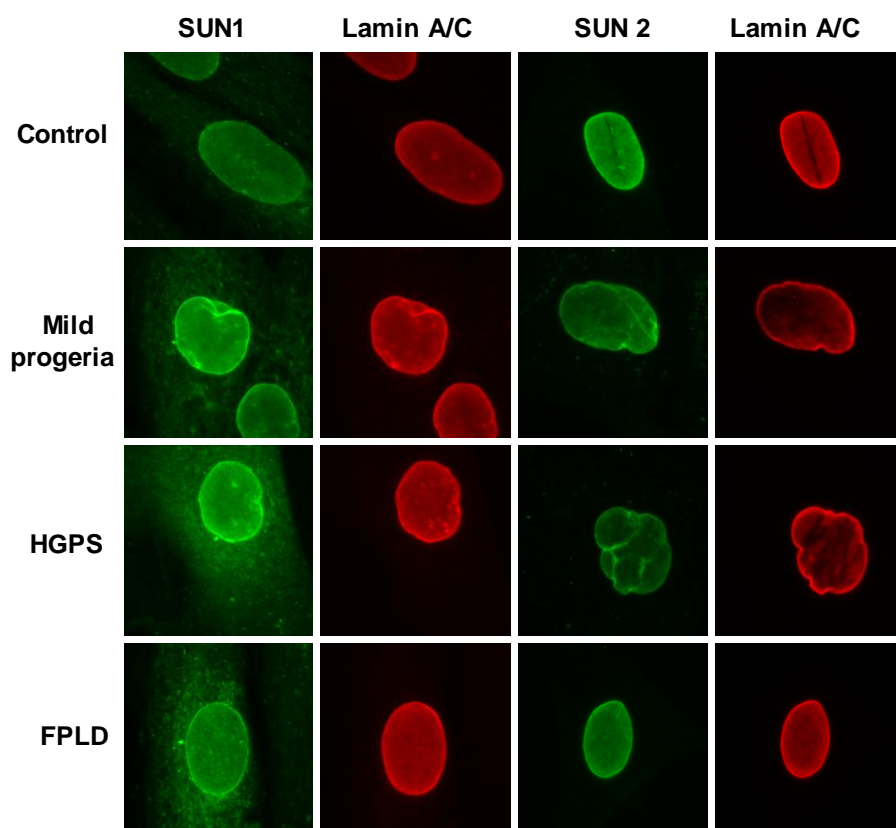
Fig. 6.17. Localization of SUN1 and SUN2 in laminopathy patient cells. Immunofluorescence staining of progeria and lipodystrophy patient skin fibroblasts with 2379 hSUN1 (green) and Chemicon lamin A/C antibodies (red), reveals no defect in SUN1 and SUN2 localization to the NE.

was uniform, similar to that of control cells. This suggests there might be increased interaction of SUN1 with lamin A in progeria. However, this conflicts my previous finding that interaction of LA-G608G and LA-T623S with SUN1 and SUN2 is reduced (section 6.2.1.3). We hypothesized that this might be due to the fact that many HGPS cells accumulate prelamin A and that, since SUN1 preferentially interacts with prelamin A (as shown in Figure 6.5; Crisp et al., 2006), this interaction was leading to enhanced recruitment of SUN1 to the NE in prelamin A-expressing HGPS cells. Indeed, further studies in the lab, carried out by D. Smallwood, where co-staining of HGPS cells with SUN1 and prelamin A antibodies were performed, the results showed that SUN1 staining was more intense in HGPS cells expressing more prelamin A, while SUN2 staining was unchanged (Fig. 6.18B). However, overall expression of SUN proteins in HGPS cells was found reduced by western blot (Fig. 6.18A). These suggest that although overall SUN1 expression in progeria is reduced, its recruitment at the NE is maintained in those cells that express significant levels of prelamin A.

SUN protein localization in a range of AD-EDMD and X-EDMD was also examined. Since SUN protein interaction was found reduced with LA-L530P and LA-R527P EDMD mutants (section 6.2.1.2), it would have been interesting to see whether there is any mislocalization of SUN proteins in these patients cell lines. However, we were unable to obtain cell lines from these patients. Therefore, fibroblasts from AD-EDMD patients with R249Q, R377H and R453W *LMNA* mutations and from X-EDMD patient with g329del59 and Δ236-241 emerin mutations were used for this experiment (Table 2.1). The R249Q and R377H mutations are located in the rod domain and C-terminal domain of lamin A and potentially affect polymerization or lamina assembly (Fig. 1.12; Holt et al., 2006; Reichart et al., 2004). On the other hand, the R453W mutation is located at the tail domain of lamin A and might affect emerin binding (Holt et al., 2003). In contrast, the two emerin mutations analysed disrupt expression of the protein, resulting in a null effect in affected males (Talkop et al., 2002; Yates et al., 1999; Fairley et al., 1999).

The cells were cultured on coverslips and fixed with paraformaldehyde for 2379 hSUN1 antibody staining or with methanol for 2853 hSUN2 antibody staining. Another set of cells was co-stained with lamin A/C (Chemicon) antibody and emerin (Glenn Morris) antibody, as controls. In all of the cell lines analysed, both SUN1 and SUN2 localized
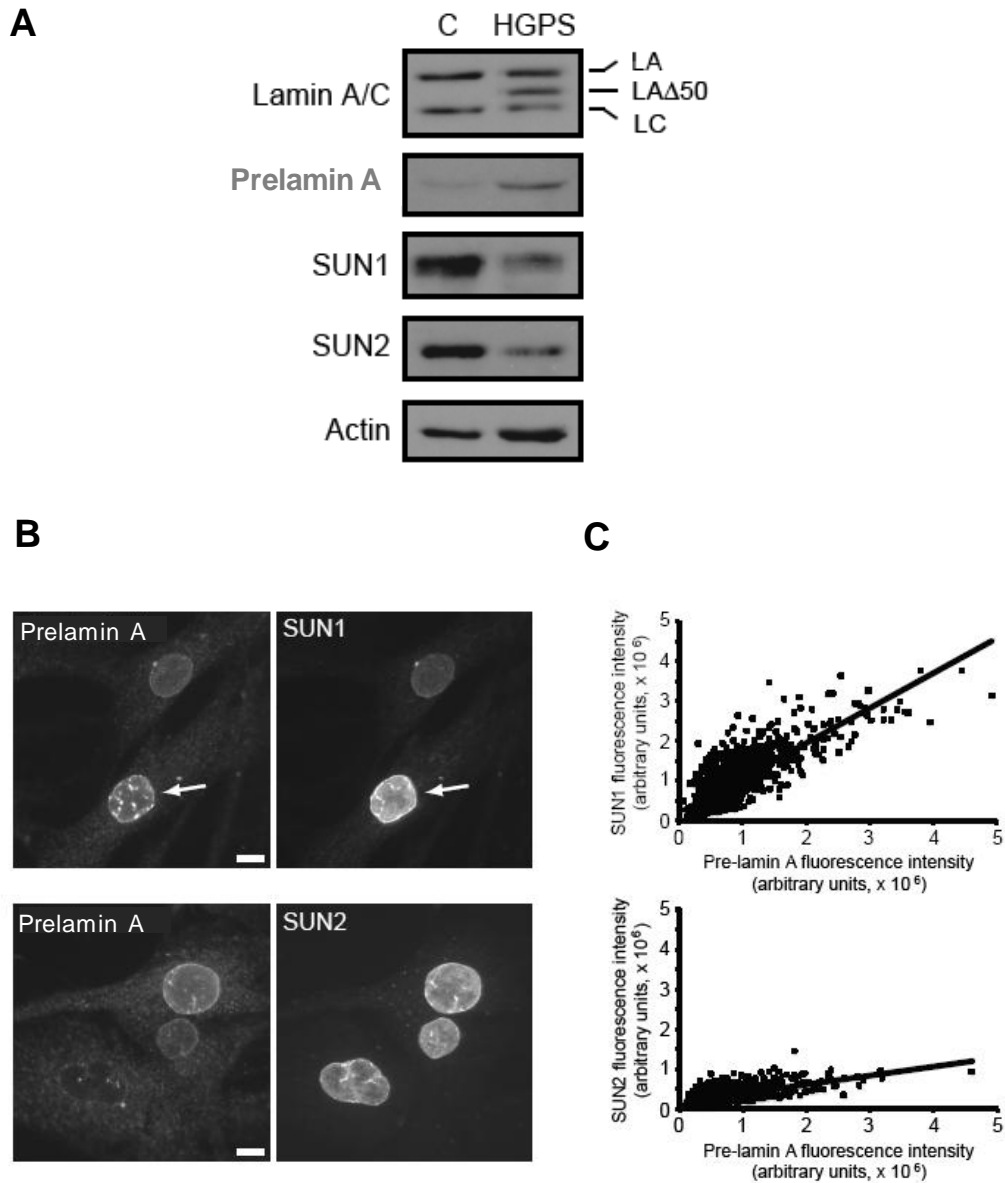
Fig. 6.18. Correlation of SUN protein and prelamin A in HGPS cells. A) Immunoblot analysis of total protein lysates from control (C) and G608G-carrying HGPS cells using lamin A/C, pre-lamin A, hSUN1 (2379), and hSUN2 (2853) antibodies. **B)** HGPS cells display variable intensity of SUN1 staining. Co-staining of HGPS cells carrying the G608G mutation with antibodies against prelamin A (left panels) and either SUN1 (upper, right panel) or SUN2 (lower, right panel). Arrows illustrate that, in cells with accumulation of pre-lamin A, SUN1 expression is correspondingly higher. In contrast, expression levels of SUN2 are not affected by accumulation of pre-lamin A. **C)** Scatter plot of pre-lamin A versus SUN1 or SUN2 fluorescence intensity in 1000 cells reveals a strong positive correlation between pre-lamin A and SUN1 intensities, whereas SUN2 intensity does not vary significantly and does not correlate with prelamin A intensity. This is highlighted by the gradient of the best-fit line. Scale bars, 10m. Reproduced from Haque et al. (2010).

well to the NE (Fig. 6.19). Therefore, none of the three lamin A mutations analysed disrupts SUN proteins localization. Moreover, SUN1 and SUN2 can localize at the NE in emerin null cells as well suggesting that SUN proteins are not dependent on emerin for their anchorage at the NE.
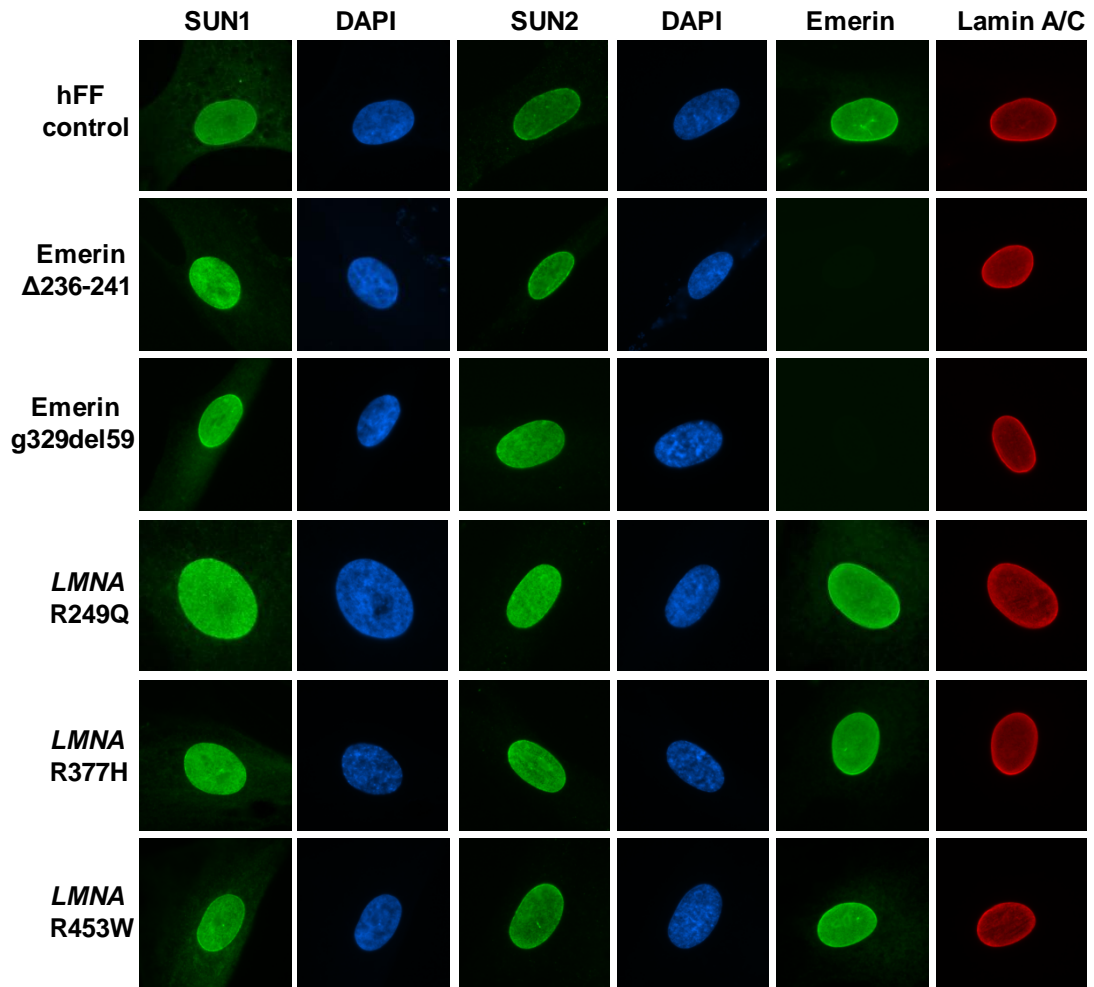
Fig. 6.19. Localization of SUN1 and SUN2 in EDMD patient cells. Immunofluorescence staining of control (hFF) and EDMD fibroblast from patients carrying emerin or lamin A mutations, as indicated, with 2379 hSUN1, 2853 hSUN2, emerin and lamin A/C antibodies. DNA was stained with DAPI. The result reveals no defect in localization of SUN1 and SUN2 to the NE.

6.3 DISCUSSION

Lamin A/C and associated NE proteins are mutated in a range of diseases, termed laminopathies (Holaska, 2008). In this chapter, the potential involvement of SUN proteins in laminopathy disease was investigated and defects were found to be specifically associated with EDMD and progeria.

6.3.1 SUN1 and SUN2 involvement in EDMD

EDMD is proposed to arise from disruption of interaction between emerin, lamin A and its associated proteins resulting in weakening of the nuclear lamina (Bengtsson and Wilson, 2004). The pull-down experiments performed in this chapter demonstrate that interaction of both SUN1 and SUN2 is significantly reduced with two EDMD-associated lamin A mutants, LA-L530P and LA-R527P, but increased with LA-W520S; although most of the mutations tested had no effect on interaction with SUN proteins. All of the LA-mutants that have shown to affect SUN proteins interaction are located within the immunoglobulin (Ig) fold of lamin A (Fig. 6.20). Residue L530 resides at the core of the domain and residue R527 resides at the surface of the Ig domain, but both have been predicted to disrupt the fold structure and decrease protein stability when mutated (Krimm et al., 2002; Dhe-Paganon et al., 2002), thereby potentially hindering the interaction of SUN proteins with lamin A. Residue W520S also has the potential to disrupt the Ig fold structure but interaction of SUN protein with this mutant was found to be increased instead, which could be a localized effect of this mutation. Interestingly, although SUN protein interactions were reduced with LA-R527P, they were normal for LA-R527H, which is associated with mandibuloacral dysplasia. This further demonstrates the effect of localized amino-acid substitutions on protein interactions and disease pathology. However, SUN protein interaction with LA-R527C (associated with progeria) was not examined and should be subject of future study.

Whilst most mutations had similar effects on interaction with SUN1 and SUN2, some mutations had specific effects on one protein only. SUN2 interaction with LA-R541C was found to be decreased, whilst interaction with LA-E358K was increased. Although we have not mapped SUN2 binding site on lamin A, decreased binding of SUN2 with these lamin A mutants suggests that the SUN2 binding region also might lie at the CTD of lamin A, as for SUN1 (section 4.2.4). Similar to our finding, interaction of
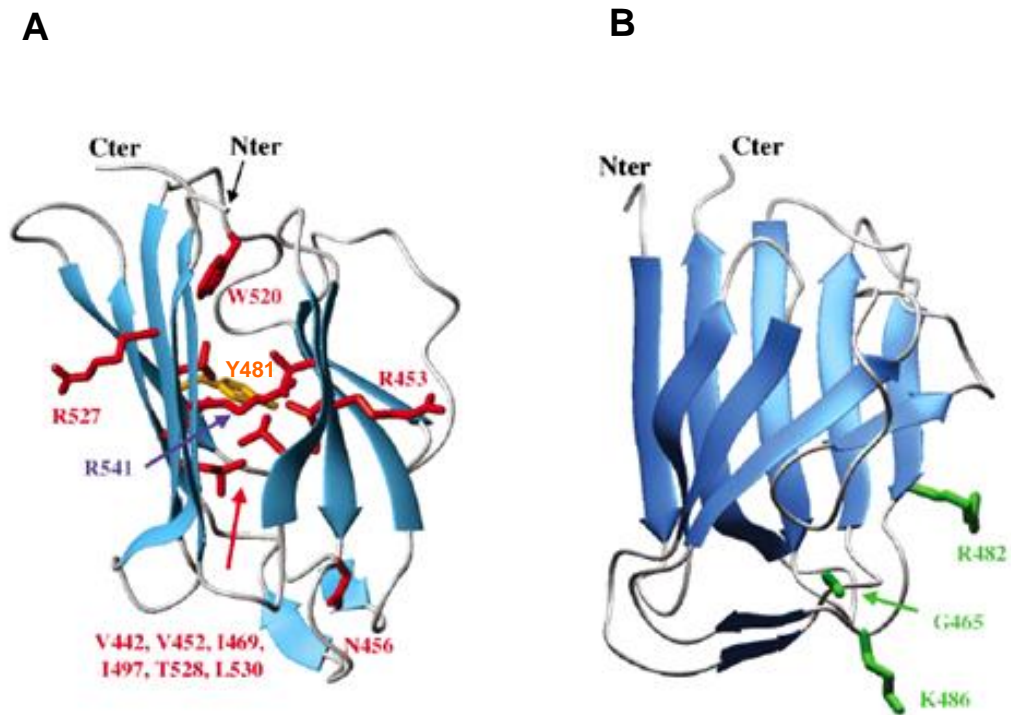
Fig. 6.20. Immunoglobulin-fold of lamin A CTD, with mutations associated in laminopathies. A) Localization of mutations associated with cardiac and skeletal muscle diseases. **B)** Localization of mutations causing FPLD. Residues mutated in EDMD are highlighted in red, LGMD in orange, and FPLD in green. Arg 541 is purple as it is mutated in both EDMD (R541H) and DCM (R541C). Reproduced from Krimm et al. (2002).

emerin was also found to be diminished with LA-L530P by co-immunoprecipitation (Raharjo et al. 2001). In addition, LA-L530P, LA-R527P and LA-W520S lamin mutants can also reduce localization of emerin to the NE (Raharjo et al. 2001, Holt et al., 2003). Lloyd et al. also demonstrated that SREBP1 (sterol regulatory element binding protein1) interaction with LA-L530P is reduced (Lloyd et al., 2002). Together, this shows that L530P mutation is likely to disrupt the whole structure of the Ig fold so that most, if not all, binding sites for other proteins are destroyed. Thus, disruption in interaction of lamin A, with its various binding partners including SUN proteins, could be a common mechanism in the EDMD disease process. Most EDMD lamin A mutants are autosomal dominant, possibly causing a dominant negative effect (Morris 2001). The rod domain mutants are thought to cause an assembly lamin A assembly defect, while the C-terminal mutants cause various interaction defects in the pathology of EDMD (Holt et al., 2003). Although I did not test all EDMD-associated lamin A mutant interactions with SUN proteins, it is possible that EDMD mutations present in the rod domain of lamin A (Fig. 1.12) could also disrupt SUN protein-lamin A interaction.

Most emerin mutations involved in X-EDMD are either truncating or frameshift mutations, resulting in a producing null effect for emerin in affected males. Only a subset of point mutations result in stably expressed protein, including P183H, P183T, Q133H, S54F, 1-169(208), del 95-99 and del 236-241, although the later two mutations cause reduced emerin expression. However, all except del 236-241, can still localize to the NE (Ellis et al, 1998; Fairley et al., 1999, Bengtsson and Wilson, 2004, Cartegni et al., 1997). Pull-down experiments performed here reveal that SUN1 interaction is significantly reduced only with the 1-169(208) emerin mutant. 1-169(208) involves a frame shift at residue 169, resulting in a novel hydrophobic stretch of 39 residues ending with a premature stop codon (Cartegni et al., 1997). I previously found that the SUN1 binding site on emerin lies within residues 140-221 (section 5.2.2.5). As the SUN1 binding site is mostly missing in the 1-169(208) emerin mutant, this could explain the reduction in interaction observed. Although not statistically significant, SUN1 interaction was also apparently reduced with P183T. However, SUN1 interacted well with other emerin mutants including P183H. As only 1-169(208) mutant has reduced interaction with SUN1, disruption of the SUN1-emerin interaction may not be a common feature of EDMD, associated with emerin missense mutations. Interestingly, contrary to SUN1, nesprin-1α and -2β binding affinity for 1-169(208) emerin is

increased (Wheeler et al., 2007). The binding site for nesprins (residues 140-176) is still mostly present in this mutant; on the other hand SUN1 binding site is mostly lost. Therefore, the mechanism of EDMD in these patients may lie in perturbing the SUN1-emerin interaction. Some emerin mutants have been shown to disrupt other interactions between components of the LINC complex. It is thought that specific emerin mutations may target specific binding partners. For example, the interaction of lamin A is reduced with the del95-99 emerin mutant (Lee et al., 2001). Nesprin-1α binding is reduced with the P183T emerin mutant. However, nesprin-1α and -2β binding is increased with the P183H mutant (Wheeler et al., 2007). Together, these findings suggest that alteration of emerin binding with one or more of its binding partners might lead to X-EDMD. Therefore, EDMD could result from disruption of interaction between any of the components of the LINC complex. Thus, weakening of SUN protein interactions with either the lamin A mutants or emerin mutants may in turn weaken the LINC complex, rendering muscle nuclei vulnerable to mechanical strain in EDMD. Alternatively, increased interaction with the lamin A EDMD mutants might increase the stiffness of the nuclear envelope and contribute to EDMD pathology via a different pathway, such as restricting deformability of the nucleus.

To determine whether defects in SUN protein interactions in EDMD affect their ability to be anchored at the INM, SUN protein localization in AD-EDMD and X-EDMD patient cells was investigated. Although SUN protein interactions were reduced with some EDMD lamin A mutants, I did not find any mislocalization of SUN1 and SUN2 in skin fibroblasts from patients carrying R249Q, R377H and R453W *LMNA* mutations. However, although SUN protein interactions were reduced with LA-L530P and LA-R527P, their localization in fibroblasts from patients carrying these mutations was not investigated, as these cell lines were not available to us. So it was not possible to determine whether the SUN proteins were mislocalized. Interestingly, SUN proteins were not mislocalized in emerin null cells obtained from X-EDMD patients, suggesting that SUN proteins are not dependent on emerin for their localization. Of interest, SUN1 can localize at the NE in absence of lamin A (Haque et al., 2006, Crisp et al., 2006). Therefore SUN protein mislocalization might not be a common feature of EDMD. Although there is no localization defect detected for SUN proteins in these patient cells, still weakening of SUN protein interaction with either lamin A or emerin could potentially weaken the nuclear lamina and/or connection of the nucleus with the

cytoskeleton, therefore increasing nuclear vulnerability to mechanical strain. Since lamin A/C-deficient and emerin-deficient cells exhibit impaired expression of mechano-sensitive genes (Lammerding et al., 2004; Lammerding et al., 2005), impaired SUN/lamin A/emerin interaction could also alter responsiveness of mechano-sensitive genes, due to defective mechanotransduction by disruption in LINC complexes (reviewed in Dahl et al., 2008).

6.3.2 SUN protein involvement in progeria

Experiments on SUN protein interaction with a range of progeric lamin A mutants located in the CTD revealed that both SUN1 and SUN2 has reduced interaction with LA-G608G and LA-T623S. This suggests that SUN proteins might play a role in progeria disease process. The G608G and T623S lamin A mutations cause internal deletion of 50 amino acids and 35 amino acids, respectively, close to the C-terminus of lamin A. This remove the ZMPTE24 cleavage site with the result that prelamin A cannot be fully processed and remains permanently farnesylated (Fig. 1.6). Since interaction of SUN1 with these two lamin A mutants was diminished, this also suggests that the SUN1 and SUN2 binding site might lie in the deleted region. However, I had previously been unable to map the SUN1 binding site to this region, as in the pull-down assay performed (section 4.2.4) all the small deletion constructs of lamin A CTD bound equally to SUN1 and, in a reciprocal study the binding of SUN1 with lamin A deletion constructs were very weak.

Interestingly, SUN1 and SUN2 binding to LA-L647X that mimics mature lamin A, was also found to be reduced compared to wild-type unprocessed lamin A, but was apparently increased with LA-L647R, which mimics the farnesylated prelamin A intermediate. LA-L647R mutation disrupts the second cleavage of ZMPSTE24 on lamin A (Fig. 1.6). Therefore, LA-L647R protein remains farnesylated which might account for the stronger interaction observed. Alternatively, the enhanced interaction observed could be a localized effect of the amino acid substitution. In the rabbit reticulocyte system used for *in vitro* translating lamin A, the protein may become farnesylated without going through further processing (Vorburger et al., 1989). This is supported by the fact that the wild type lamin A construct was several kilodaltons larger than the L647X mature lamin A mimic, but identical in size to the L647R mutant. Therefore,

similar to the findings of Crisp et al., this suggests that SUN1 and SUN2 interact more strongly with prelamin A than with mature lamin A; however, Crisp et al., have also found that SUN1 interacts more strongly with prelamin A than SUN2 (Crisp et al., 2006). Since the G608G and T623S mutants also remain permanently farnesylated, their lack of interaction with SUN1 and SUN2 suggests that the missing amino acids in G608G and T623S are of importance in binding of SUN1 and SUN2 to lamin A.

SUN protein localization in progeria patient skin fibroblast cells showed interesting results. Fibroblasts from HGPS patients carrying G608G and T623S mutations exhibit variable staining of SUN1 at the NE, but this was not observed for SUN2. This suggests a different mechanism for SUN1 and SUN2 in the pathophysiology of progeria. In HGPS, there is accumulation of prelamin A via an unknown mechanism (Goldman et al., 2004). As SUN1 interacts more strongly with prelamin A than mature lamin A, this could explain the variable staining observed in the HGPS patient cell lines. Further experiments in the lab also support this conclusion as the intensity of SUN1 staining correlated closely with that of prelamin A in HGPS cells. In contrast, SUN2 expression was independent of prelamin A level. However, although there was increase recruitment to the NE, overall SUN1 expression was reduced in these cells (Haque et al., 2010). Since quantification of the intensity of staining in HGPS versus control cells were not performed in the experiment described in this chapter, it is possible that the actual expression level of SUN1 is lower in most HGPS cells, except those expressing prelamin A. However, it is difficult to explain why the same was not seen for SUN2 Crisp et al. found that SUN2 interact less strongly with prelamin A than SUN1 (Crisp et al., 2006), which might explain why variable expression with SUN1 was observed but not with SUN2. Increased nuclear stiffness is a feature of HGPS cells (Verstraeten et al., 2008), which could result from the increased level of SUN1 and prelamin A found at the NE in the HGPS that is strengthening the connection of nucleus and cytoskeleton, via the LINC complex. As there is increased recruitment of SUN1 in HGPS cells, it is possible that its binding partner nesprins will also be accumulated at the NE. However, in contrast, nesprin-2 level was found to be reduced at the NE in HGPS cells (Kandert et al., 2007). Further study is therefore required to understand the relationship of SUN proteins and its binding partners in progeria.

Interestingly, slight but significant reduction of SUN2 interaction with R482W lipodystrophy lamin A mutant was also observed, but it was not observed for SUN1 and no defect in localization was visualized in R482W patient skin fibroblasts. Therefore, more study is required in this regard to understand its significance.

In conclusion, in our search for role of SUN1 and SUN2 in laminopathies, we have found defects in their behaviour in EDMD and progeria, but not in other laminopathies. SUN1 and SUN2 have reduced interaction with specific mutants associated with EDMD (L530P, R527P) and progeria (G608G, T623S). Further research on SUN protein involvement in EDMD and progeria could advance our understanding of the mechanism behind these diseases.

CHAPTER 7

FINAL DISCUSSION

7.1 SUN1 IS A TYPICAL INM PROTEIN WITH A LUMENAL CTD

Previous studies in the lab have confirmed SUN1 as a NE protein, which co-localizes with lamin A in a rim-like fashion around the nucleus. Proteomic and NE fractionation studies to identify NE proteins have also detected SUN1 in the NE fractions (Dreger et al, 2001, Schirmer et al., 2003). However, whether SUN1 is localized at the INM or ONM was still unknown at the beginning of this project. SUN1 homologue UNC-84, in *C. elegans*, was predicted to be at the ONM and was thought to anchor KASH domain proteins at the ONM (Starr and Han, 2003; Gruenbaum et al., 2005). However, UNC-84 is mislocalized in the absence of Ce-lamins in *C. elegans*, which suggests that UNC-84 interacts with Ce-lamin (Lee et al., 2002). Indeed, SUN1 was initially found as a lamin A binding protein in a yeast two-hybrid screen in our lab (Haque et al., 2006).

Most of the work presented in this project is based on mouse SUN1. SUN1 N-terminal residues 1-355 were found to interact with lamin A in an in-vitro pull-down assay, which indicates that the SUN1 N-terminus is located at the nucleoplasm. In support of this conclusion, SUN1 residues 1-355 also exhibited tight association with the nuclear matrix in Triton X-100 pre-extraction assays. Digitonin permeabilization experiments using N-terminally myc-tagged SUN1 full length construct have also confirmed that the SUN1 N-terminus is located at the nucleoplasm (Section 3.2.6).

At the beginning of this study, it was predicted that SUN1 traverses the NE four times with its four hydrophobic regions (H1-H4), identified using TMpred software. In this model, it was thought that the C-terminus of SUN1 might be located in the cytoplasm (Fig. 3.2). This topology of the SUN1 C-terminus was deduced from initial immuno-EM and digitonin permeabilization experiments (section 1.6 and 3.2). However, from later digitonin experiment results presented in this thesis, it is now clear that the SUN1 CTD is in fact located in the periplasmic lumen between the ONM and the INM. Therefore, SUN1 adopts a topology of a typical INM protein, where the N-terminus is located at the nucleoplasm and the C-terminus is located at the periplasmic lumen. Other groups have also reported similar findings for SUN1 topology and Hodzic et al. described a similar topology for SUN2 (Hodzic et al., 2004; Crisp et al, 2006).

Unexpectedly, recent studies by Liu et al. have demonstrated that SUN1 actually traverses the INM only once, with a single TMD, which is the hydrophobic region H4 (Liu et al., 2007). However, although H1, H2 and H3 of SUN1 do not traverse the nuclear membrane, these residues still confer membrane association of SUN1 (Crisp et al., 2006; Liu et al., 2007). SUN2 also has a hydrophobic region upstream of the TMD, but function of these residues is not known (Hodzic et al., 2004). Therefore, as most INM proteins, SUN1 also has one TMD rather than multiple as initially predicted.

7.1.1 Both the N- and C-termini of SUN1 are capable of NE localization

In order to define the NE targeting sequences of SUN1, several localization studies with SUN1 deletion constructs were performed. Surprisingly, unlike other INM proteins, both N- and C-termini of SUN1 can localize to the NE independently. SUN1(1-355) could associate with the NE even though it lacks a proper TMD. As already mentioned, SUN1(1-355) is associated with the nuclear matrix, even after Triton X-100 pre-extraction. Therefore, interaction with either lamins or other INM proteins is likely to be conferring the NE localization of this domain. Although SUN1(1-355) does not have a TMD, it contains hydrophobic region H1 which might associate this domain to the INM (Liu et al, 2007).

SUN1(355-913), containing hydrophobic regions H2-H4 and the lumenal domain, can localize to the NE. However, it is lost from the NE after Triton X-100 pre-extraction. This indicates that a different mechanism is responsible for SUN1(355-913) retention at the INM. Interaction of the SUN1 CTD at the lumen with KASH domain proteins might recruit SUN1(355-913) to the NE. However, SUN1(450-913), which lacks H2-H4 sequences, does not localize to the NE even though it interacts with KASH domain proteins. Therefore, mere interaction of the SUN1 CTD with KASH domain proteins is not enough for its NE localization and membrane association of this domain likely to be necessary. However, heterologous fusion of the SUN1 CTD with a different TMD does not localize this domain to the NE (Liu et al., 2007).

Padmakumar et al. have demonstrated that SUN1(358-717), containing H2-H4, along with the coiled-coil region, is important for the NE targeting of SUN1, and is retained at the NE even without a nesprin-1 binding region (residues 632-737) (Padmakumar et

al., 2005). Therefore, binding to nesprins/KASH domain proteins does not confer NE retention of SUN1(355-913) or SUN1(358-717), suggesting that SUN1 H2-H4 may have some intrinsic NE targeting signals as do the TMDs of LBR (Smith and Blobel, 1993). However, Hasan et al. show that SUN1 (200-499), containing only H1-H4 does not localize to the NE (Hasan et al., 2006).Therefore, presence of both TMDs and the lumenal domain of SUN1 are necessary for its NE targeting. Liu et al. have explained further that, although H4 is the only membrane spanning region in SUN1, H2 and H3 also are required for proper NE localization of the lumenal domain of SUN1 (Liu et al., 2007).

SUN1 can self-interact through the N-terminus, as demonstrated by pull-down assays previously in the lab (Haque et al, 2006). In the present project, pull-down assays also revealed that SUN1 interacts with SUN2 via the N-terminus and similar findings were also observed by Wang et al. (Wang et al., 2006). In contrast, other groups have found that it is the coiled-coil region in SUN1 that self-interacts and also interacts with SUN2 (Padmakumar et al., 2005; Lu et al., 2008). Therefore it is likely that SUN1 and SUN2 displays homo- or heterophilic association at both N and C-termini and forms homodimers or heterodimers at the NE (Fig. 7.1).

Since the coiled-coil regions of SUN1 can self interact (Padmakumar et al., 2005), the SUN1 proteins may oligomerize to retain SUN1(355-913) at the NE. However, this SUN1 deletion construct can displace endogenous SUN1 from the NE; therefore SUN1 oligomerization may not be the only cause for its NE retention (Padmakumar et al., 2005; Liu et al., 2007). Although various possibilities have been suggested, it is still unclear how this segment is retained at the NE and perhaps multiple mechanisms are involved to retain individual SUN1 segments at the NE.

Liu et al. have further demonstrated that SUN1(221-380), containing H1 and H2, can localize to the NE, thus suggesting a NE targeting motif is contained within this sequence (Liu et al., 2007). Investigations in the present study reveal that SUN1(229-355) interacts weakly with lamin A, however, it interacts strongly with emerin and also with nesprin-2β. Hence, it is possible that interaction with emerin and nesprin-2β is conferring NE retention for SUN1(221-380). Further studies in our lab have demonstrated that 209-228 residues SUN1 are important for NE anchorage of the SUN1
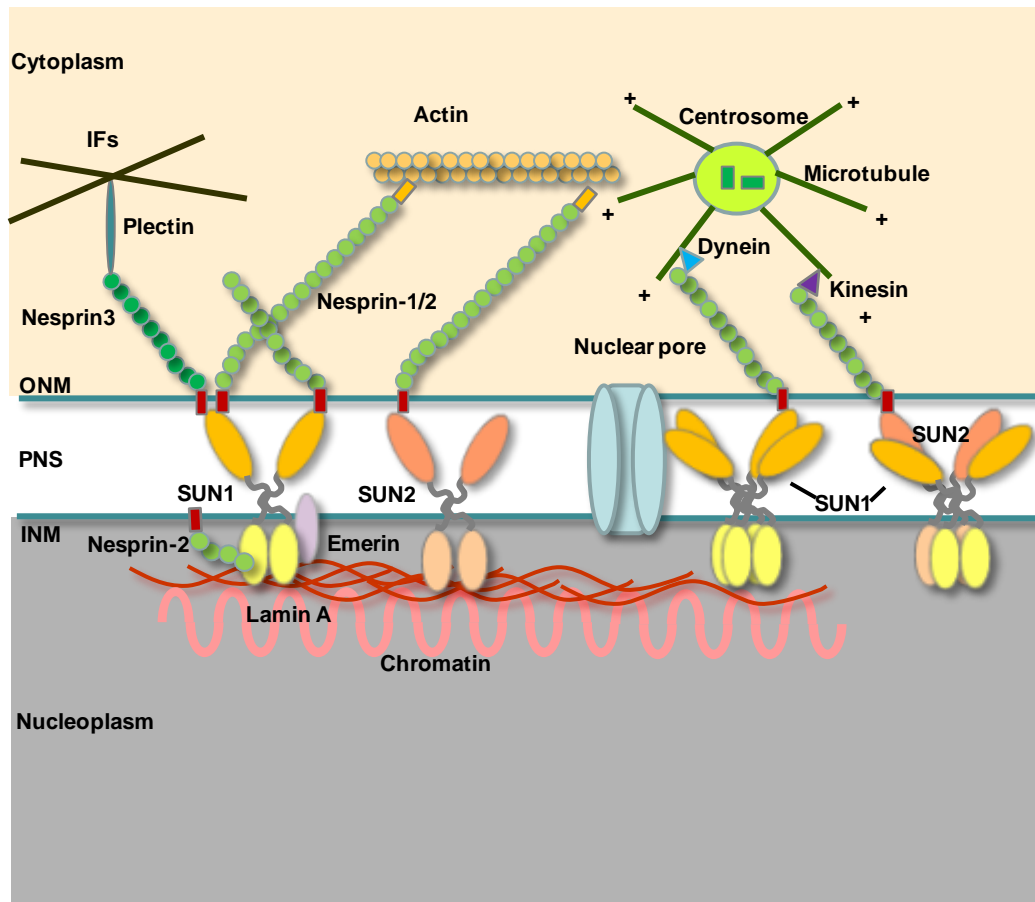
Fig. 7.1. Model illustrating SUN- and KASH-domain proteins forming LINC complexes at the NE. SUN1 and SUN2 can form dimers, interacting at coiled-coil region and the N-terminus. SUN1 and SUN2 also can form tetramers. SUN proteins promiscuously interact with all three nesprins, linking the nuclear surface to the cytoskeleton. ONM: outer nuclear membrane; PNS: perinuclear space; INM: inner nuclear membrane; NPCs: nuclear pore complexes; IFs: intermediate filaments. Adapted from Lu et al. (2008).

NTD (Haque et al., 2010). In these studies, deletion construct SUN1(209-913) was retained at the NE after Trion X-100 pre-extraction, whereas SUN1(229-913) was not. Also, integrin fused SUN1(1-208) was not retained at the NE after Triton pre-extraction, while integrin fused SUN1(1-229) was located at the NE under these conditions. Together, these experiments suggested that SUN1(209-228) is important for NE targeting of SUN1 (Haque et al., 2010). However, since none of the known SUN1 binding proteins interact significantly with this region, there are likely to be other binding factors present within the nucleus to anchor SUN1, potentially chromatin or DNA itself or nuclear actin, which may also account for the NE localization of SUN1 in *Lmna*$^{-/-}$ cells.

Of note, Hasan et al., demonstrated that SUN1 is highly immobile at the NE by FRAP analysis (Hasan et al., 2006). However, in comparison, SUN1 deletion mutants SUN1(1-412) and SUN1(358-913) that localize to the NE are more mobile as observed by FRAP. Therefore, although the described N- and C-termini of SUN1 can individually locate at the NE, all the NE targeting signals are necessary for the stable anchorage of FL SUN1 (Liu et al., 2007, Lu et al., 2008).

7.2 SUN1 AND SUN2 ARE COMPONENTS OF THE LINC COMPLEX

SUN1 and SUN2 have now been shown to interact with the KASH domains of nesprin-1 and -2 by several groups through immunoprecipitation studies, pull-down assays and yeast two-hybrid screens (Haque et al., 2006; Crisp et al., 2006; Padmakumar et al., 2005) (Fig. 7.1). Therefore, the hypothesis that UNC-84 anchors ANC-1 and forms bridges to connect the nucleoskeleton to cytoskeleton is now established from yeast to man, forming the LINC complex (Linker of nucleoskeleton and cytoskeleton) (Starr and Han, 2002; Crisp et al., 2006). In the present study, pull-down assays have demonstrated interaction between the lumenal domain of SUN1 (residues 450-913) and nesprin-2. However, further narrowing of the binding site was not successful. Although it is presumed that the SUN domain of SUN proteins interacts with the KASH domain of nesprins, Padmakumar et al. have shown that residues 632-737 of SUN1, that lie between the coiled-coil domain and the SUN domain, are responsible for mediating its interaction with nesprin-1 (Padmakumar et al, 2005). In contrast, Stewart-Hutchinson et al. have narrowed the SUN-KASH binding region to the last 20 amino acids of the SUN

domain in SUN2 and the last 23 amino acids of the KASH domain (Stewart-Hutchinson et al., 2008). This therefore confirms the importance of the SUN domain for SUN-KASH interaction as predicted.

Crisp et al. have further demonstrated that the anchoring of the KASH domain of nesprin-2 at the NE is dependent on SUN proteins, by RNAi experiments. Co-depletion of SUN1 and SUN2 from HeLa cells mislocalized nesprin-2 from the ONM, while individual depletion of the SUN proteins did not (Crisp et al., 2006). This demonstrates the redundant function of SUN1 and SUN2 in anchoring nesprins. SUN1 and SUN2 knock-out mice cell also show mislocalization of nesprin-1 and nesprin-2 from the NE (discussed in section 7.2.1; Lei et al., 2009; Zhang et al., 2009). Intriguingly, in SUN1 and SUN2 double RNAi-treated cells, the ONM and INM are separated in various places with expansion of the perinuclear space (Crisp et al., 2006). Therefore, SUN proteins maintain an even spacing of the INM and ONM, by interacting with nesprins. Nesprin-1 and -2 in turn interact with actin to maintain connection of nucleus with the actin cytoskeleton.

Recently, SUN1 and SUN2 have been found to interact with nesprin-3, which links the SUN proteins and therefore the nucleus, to plectins and IF proteins (Ketema et al., 2007). Roux et al. have also found that SUN1 and SUN2 are responsible for NE anchoring of nesprin-4, which is a kinesin binding protein, thus linking the nucleus to the MT network (Roux et al., 2009). Importantly, Stewart-Hutchinson et al. have demonstrated that the SUN1 and SUN2 lumenal domains bind promiscuously with KASH domains of nesprins-1, nesprin-2 and nesprins-3, further demonstrating the redundancy of SUN1 and SUN2 in anchoring nesprins at the NE (Stewart-Hutchinson et al., 2008). The LINC complexes are thus capable of connecting the nucleus to all three cytoskeletal networks and through these they are likely to maintain the position of the nucleus within the cell, as hypothesized initially.

Intriguingly, Stewart-Hutchinson et al. revealed that disruption of the LINC complex or SUN-KASH interaction can reduce the mechanical stiffness of cells, similar to lamin A/C null cells (Stewart-Hutchinson et al., 2008; Broers et al., 2004). Lamin A/C knock-out mice have been shown to develop an EDMD phenotype (Sullivan et al., 1999). Of note, mice with a deletion of the KASH domain of nesprin-1 also show an EDMD-like

phenotype (Puckelwartz et al., 2009). Together these findings indicate that disruption of LINC complex may have role in the pathogenesis of EDMD.

7.2.1 Defect in nuclear anchorage and migration in SUN1 and SUN2 knock-out mice

Recent discoveries have demonstrated that SUN1 and SUN2 do play a role in nuclear anchorage and nuclear migration, as hypothesized initially for its founding proteins (Lei et al., 2009; Zhang et al., 2009). *Sun1$^{-/-}$* mice have partial nuclear anchorage defects in synaptic nuclei of skeletal muscle. SUN1 and SUN2 double knock out (DKO) mice die soon after birth, and studies on the embryos demonstrate reduced number of synaptic nuclei at the neuro-muscular junction and clustering of non-synaptic nuclei in skeletal muscles. As nesprin-1 is mislocalized from the NE in SUN1/2 DKO mice muscle cells, this would lead to the defect in anchorage of nuclei (Lei et al., 2009), demonstrating the importance of the LINC complex in viability of animals.

Zhang et al. have further demonstrated that SUN1/2 DKO mice are very similar to nesprin-1/nesprin-2 DKO mice, both of which die having brain defects with impairment in neurogenesis and neuronal migration. Studies on SUN1/2 DKO mouse brains revealed that the NE localization of nesprin-2 is disrupted in cells and the nuclear-centrosomal distance is increased and nuclei fail to follow centrosomes during neuronal migration. Nesprin-2 interacts with dynein-dynactin complexes and kinesin, which connect SUN1/2 to MTs and thereby generate force to move the nucleus (Zhang et al., 2009). This therefore confirm that SUN-KASH protein though LINC complex play essential role in nuclear anchorage and migration in cells, which if disrupted may account for some laminopathies, such as muscular dystrophies and yet to be documented brain diseases.

7.3 SUN PROTEINS ARE COMPONENTS OF A MULTI-PROTEIN COMPLEX AT THE INM

Stable anchorage of SUN proteins at the NE of *Lmna* $^{-/-}$ cells suggests presence of other binding partners at the INM, other than lamins (Haque et al., 2006; Crisp et al., 2006). In this project, apart from interaction with lamin A, novel interactions of SUN1 with emerin, nucleoplasmic nesprin-2 isoforms, SUN2 and potentially also actin have been identified (Fig. 7.2). Furthermore emerin was also found to interact with SUN2. Together, these data indicate that SUN proteins not only form links between the nucleus and the cytoplasm, but also form a multi-protein complex inside the nucleus, along with lamin A, emerin, nesprins and possibly actin. Interestingly, all these protein interact with each other (Zastrow et al., 2004) (Fig. 7.3).

7.3.1 SUN1 interacts with only with the lamin A isoform, with an increased affinity for prelamin A

Intriguingly, although SUN1 interacts with lamin A, it was found that SUN1 can localize to the NE even in the absence of lamin A, in lamin A/C null cells. In contrast, other NE proteins such as, emerin and nesprins mislocalize to the ER in these cells (Haque et al., 2006; Crisp et al., 2006; Sullivan et al., 1999, Libotte et al., 2005). To shed light on this matter, SUN1 interaction with all major isoforms of lamins was tested. Surprisingly, it was found that SUN1 binds only to lamin A. Other groups have also demonstrated similar findings that SUN1 and SUN2 bind to lamin A more strongly than lamin C and B1 (Crisp et al., 2006). Also, combined RNAi of lamin A/C, lamin B1 and lamin B2 has no effect on SUN1 localization at the NE, therefore SUN1 is not dependent on lamins for its NE anchorage (Hasan et al., 2006). SUN1 and SUN2 are highly immobile at the NE, as demonstrated by FRAP studies (Hasan et al., 2006; Ostlund et al., 2009). However in lamin A/C null MEFs, although SUN1 and SUN2 still localize at the NE, their mobility at the NE increases significantly, again demonstrated by FRAP. Stability of SUN1 can be restored by introducing lamin A in these cells; however, stability of SUN2 is not restored. Therefore, although lamin A is not responsible for anchoring SUN proteins, it might be required for stabilizing SUN1 at the NE (Ostlund et al., 2009).
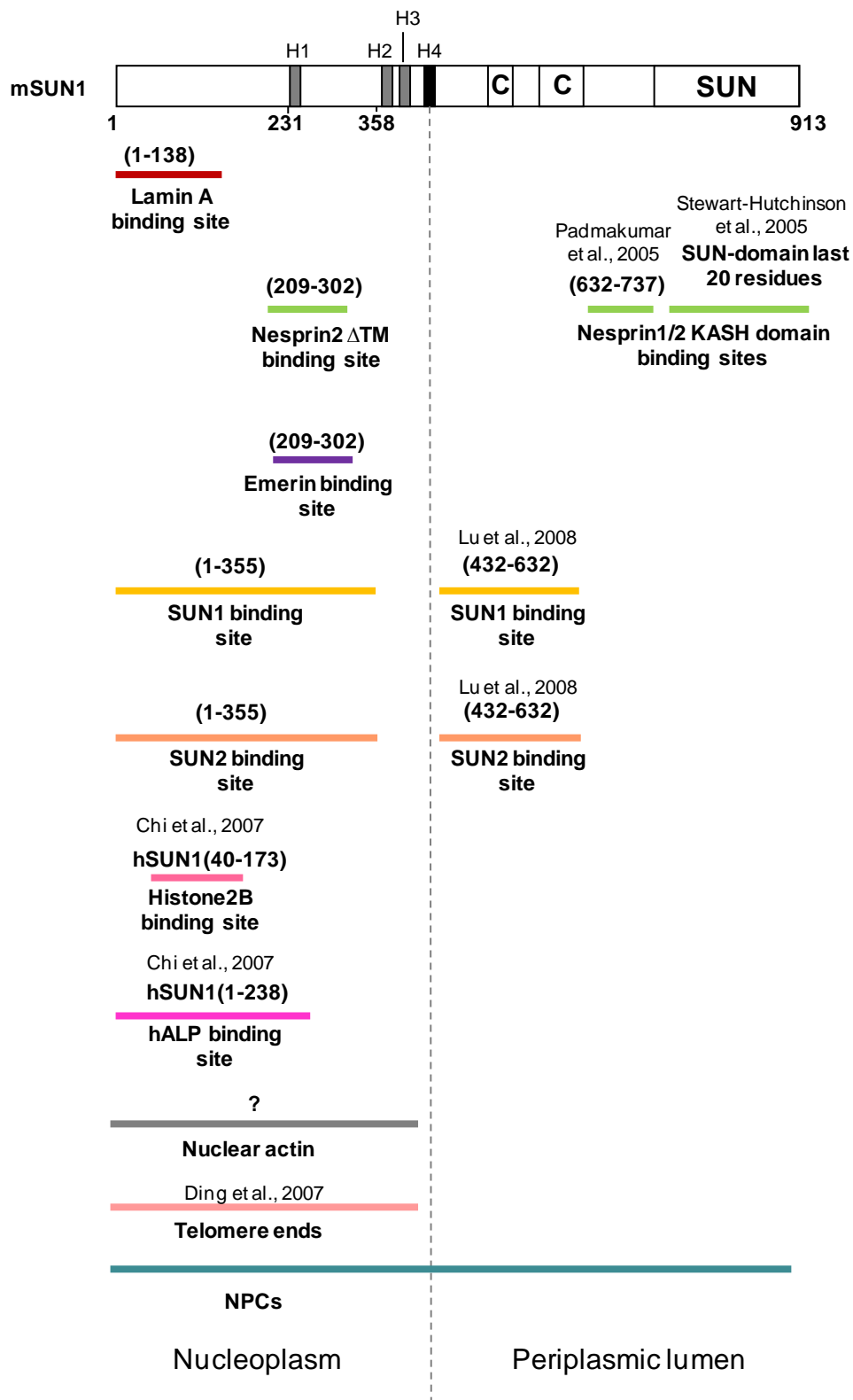
Fig. 7.2. Schematic representation of mSUN1 protein and its interacting proteins. mSUN1 is comprised of 913 amino-acids. H1, H2, H3 and H4 represent the four hydrophobic sequences present in mSUN1 and C is a coiled-coil region. SUN1 interacting partners are shown, along with their binding sites. '?' represents a possible interaction.
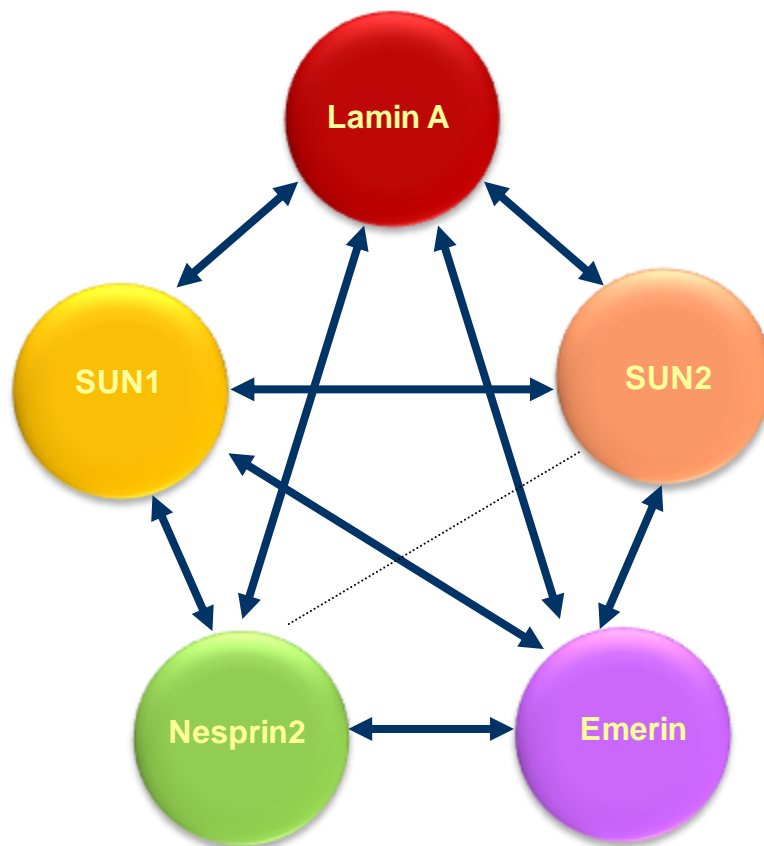
Fig. 7.3. Multi-protein complex at the inner-face of the NE that includes SUN proteins and their interacting partners. SUN1 interacts with various proteins at the inner nuclear membrane, potentially providing a stable platform. Almost all of its binding partners, lamin A, nesprins, emerin and SUN2 interact with each other as indicated by double arrowed lines. Most of these proteins can self associate. The dotted line represents an as not yet identified interaction.

Interestingly, Crisp et al., have found that SUN1 preferentially binds to prelamin A rather than mature lamin A (Crisp et al., 2006). In contrast, SUN2 bound relatively weakly to both prelamin A and mature lamin A, although it did show a slight preference for prelamin A (Crisp et al., 2006). In this project, experiments investigating SUN protein interaction with various lamin A mutants have demonstrated increased interaction of both SUN1 and SUN2, with prelamin A compared to mature lamin A. Although a direct comparison of SUN1 versus SUN2 binding to lamin A was not made, the relative binding of SUN2 did appear to be weaker than that of SUN1, thus agreeing with the data of Crisp et al. (2006). Together these studies suggest that the extreme C-terminus of prelamin A, which is absent in lamin C and mature lamin A, is responsible for its strong association with SUN1. As prelamin A is farnesylated, this might also increase the binding affinity between SUN1 and prelamin A. However, it should be noted that, in spite of being permanently farnesylated, lamin B1 and B2 do not interact with SUN1. Therefore, farnesylation may not be playing a role in the increased interaction observed between SUN1 and prelamin A. Nevertheless, it is not clear why SUN1 binds preferentially to prelamin A.

Pull-down experiments in the present project have confirmed that the lamin A CTD residues 389-664 interacts with the SUN1 NTD residues 1-355, similar to other INM proteins (Zastrow et al., 2004). However, several experiments to narrow the sequences on the CTD of lamin A that bind SUN1, were not successful. Nevertheless, the lamin A binding region on SUN1 and SUN2 was successfully delineated. The extreme N-terminus of SUN1 and SUN2 is responsible for binding lamin A, namely residues 1-138 and 1-129 of SUN1 and SUN2, respectively. Of interest, the first 50 amino acids of SUN1, which are absent from SUN2, were found to be important for lamin A interaction. Notably, other studies have revealed that SUN1 has higher affinity for lamin A compared to SUN2, as demonstrated by fluorescence resonance energy transfer (FRET) analysis (Ostlund et al., 2009). It is possible that the first 50 amino acids of SUN1 are mediating the stronger interaction observed between SUN1 and lamin A and possibly prelamin A.

7.3.2 Novel interaction of SUN proteins with emerin

In immunoprecipitation experiments, both SUN1 and SUN2 were found to interact with emerin. Emerin also interacts with numerous other proteins. Among them are structural proteins such as lamin A, nesprins, actin and also transcription factors, such as BAF, GCL and Btf (Section 1.1.3.2). Emerin mutation is the cause of X-EDMD (Bione et al., 1994). However, the exact pathophysiology for EDMD is still unknown. Only 40% of the EDMD mutations are found in emerin and lamin A (Burke and Stewart, 2006). As SUN1 and SUN2 are binding partners for both lamin A and emerin, this also makes SUN proteins candidates to be involved in EDMD. In the present study, pull-down assays demonstrated that SUN1(209-355) preferentially binds emerin. Further studies in the lab have since narrowed the binding region to residues 209-302 (Haque et al, 2010). In a reciprocal study, SUN1 showed preference in binding to residues 140-221 of emerin, which is also the binding site for nesprins (Wheeler et al., 2007). Study of SUN1 interaction with X-EDMD associated emerin mutants demonstrated reduced SUN1 binding with 1-160(208) emerin mutant. This mutant lacks most of the predicted SUN1 interacting region, which further supports that the binding region of SUN1 on emerin lies at residues 140-221, and also indicates that SUN1 might have role in EDMD.

7.3.3 Novel binding site of nesprin-2 for SUN1

It is now well known that the KASH domains of nesprin-1 and -2 interact with the SUN1 CTD. Intriguingly, in this project another binding region on nesprin-2 for SUN1 was identified. This interaction, which was consistent but relatively weak, occurs at the nucleoplasmic face of the NE, between SUN1 (1-355) and a nesprin-2β isoform that lacks the KASH domain. However, SUN2 binding to nesprin-2βΔTM was weak. Also, SUN1 binds weakly to a similar nesprin-1α isoform, lacking the KASH domain. Together, these findings suggest that only SUN1 is interacting with nucleoplasmic or INM specific isoforms of nesprin-2.

Nesprin-2βΔTM interacted most strongly with SUN1(209-355), which is also the binding region for emerin. Therefore, it is possible that emerin and nesprin-2 compete with each other for binding SUN1, or they may bind co-operatively. Another possibility

is that the interaction between SUN1 and nesprin-2 is indirect and is mediated through emerin. This could explain why the interaction detected by *in vitro* pull-down was rather weak. One way to test this possibility in the future would be to use purified proteins. Notably, SUN1(209-355) region is mostly absent from SUN2, as observed by sequence comparison. This might be the reason why only very weak interaction seen between SUN2 and nesprin-2βΔTM. Further studies in the lab narrowed nesprin-2βΔTM binding region on SUN1 to residues 209-302, similar to emerin binding site (Haque et al., 2010). These novel findings indicate that SUN1 is bridging nesprins not only on the outside, but also on the inside of the nuclear membranes, therefore playing a major structural role at the NE (Fig. 7.1).

7.3.4 SUN1 interaction with other proteins, NPCs and telomeres and anchorage at the NE

The mechanism of SUN1 anchoring at the NE in absence of lamin A is still not resolved. As discussed in section 7.1.1 SUN1 can self-interact (Haque et al, 2006) and also interacts with SUN2 suggesting SUN proteins might form homodimers and heterodimers at the NE (Fig. 7.1), which might account for its stable anchorage at the NE. In addition, a possible interaction between SUN1 and actin is observed in this study. Therefore, actin could also be the missing link that anchors SUN1 at the NE in absence of lamin A.

As mentioned, lamins are not responsible for anchoring SUN1 at the NE (section 7.3.1). Also, SUN1 and SUN2 localize normally at the NE in nesprin-1/-2 DKO mice muscle cells, and are therefore not dependent on nesprins for their localization (Lei et al., 2009). In addition, emerin is unlikely to anchor SUN1 (section 7.4.1). Therefore, other factors such as chromatin might be responsible for its anchorage. Recent studies by Chi et al. revealed that SUN1 interacts with chromatin. Chromatin immunoprecipitation studies showed that hSUN1(40-173) interacts with histone H2B (Chi et al., 2007). However, this sequence does not represent the NE targeting motif mSUN1(208-229) suggested by recent studies in our lab, so interaction with histones may not be responsible for anchoring these residues at the NE (Haque et al., 2010). Interestingly, Chi et al. also demonstrated that hSUN1(1-238) interacts with hALP, a histone deacetyl transferase protein, and contribute to chromatin decondensation after mitosis (Chi et al.,

2007). However, whether interaction with hALP promotes SUN1 NE anchoring is not known.

Liu et al. have found that SUN1, but not SUN2, has punctuate NE distribution, which is concentrated at the NPCs. SUN1 knock down cells also demonstrate clustering of NPCs (Liu et al., 2007; Chi et la., 2007). During mitosis, at anaphase stage, SUN1 is found with the lateral margins of the chromatids, where NPC assembly is initiated, while SUN2 is concentrated at the core region of the chromatids. SUN1 is therefore thought to be associated with NPCs and also to recruit NPCs during NE reformation (Liu et al., 2007). However, although SUN1 remains anchored at the NE, NPC distribution is altered in lamin A null cells (Sullivan et al., 1999). Therefore, NPCs are unlikely to be contributing to SUN1 anchorage.

Notably, SUN1 and SUN2 are widely expressed in cells, with increased expression in testis (Liu et al. 2007). Recent studies by other groups have shown that SUN1 knock-out mice are sterile with defects in gametogenesis, while SUN2 knock-out mice are fertile and do not demonstrate obvious defects in development (Ding et al., 2007; Lei et al., 2009). During meiotic prophase, SUN1 and SUN2 co-localize with the telomere attachment site at NE and remain associated with the telomere ends during dynamic movement of the telomeres for chromosomal for bouquet formation (Ding et al., 2007; Schmitt et al., 2007). $Sun1^{-/-}$ spermatocytes and oocytes fail to anchor telomere ends to the NE during meiosis. Therefore, SUN proteins are required for tethering telomeres to the NE during meiosis (Ding et al., 2007; Schmitt et al., 2007). The SUN protein homologues in yeast, Sad1 and Mps3, also function in tethering telomeres for bouquet formation (Chikashige et al., 2006, Bupp et al., 2007). Bqt1 and Bqt2 proteins in *S. pombe* mediate interaction between Sad1 and the telomere (Chikashige et al., 2006). However, homologue proteins of Bqt1 and Bqt2 in mammals have not been identified. These findings revealed new dimensions of SUN proteins roles in cells, which are conserved from yeast to mammals.

Together, these studies demonstrate that the SUN1 N-terminus is interacting with various proteins. Since SUN1 is highly immobile at the INM (Hasan et al., 2006; Lu et al., 2008) and SUN1 and SUN2, by homo- or heterophilic association, can form dimers

and tetramers, it is suggested that they are providing a stable platform for various macromolecular assemblies at the INM (Lu et al., 2008) (Fig. 7.1).

7.4 EMERGING ROLE OF SUN PROTEINS IN LAMINOPATHIES

Since SUN proteins show extensive interactions with lamin A, emerin and nesprins and, as all these proteins are involved in laminopathies, it was logical to investigate whether SUN proteins are involved in laminopathy or not. Indeed SUN proteins demonstrate reduced interaction with both EDMD and progeric lamin A mutants.

7.4.1 Disruption of SUN proteins interaction in EDMD

Over 200 missense mutations in lamin A/C are responsible for causing AD-EDMD. Emerin missense, null and truncating mutations are also found in X-EDMD. Furthermore, several nesprin-1 and -2 mutations were recently found in mainly sporadic EDMD patients (Zhang et al., 2007b). In this project, pull-down assays demonstrated that both SUN1 and SUN2 have dramatically reduced interaction with a subset of EDMD-associated lamin A and emerin mutants, most notably the L530P and R527P lamin A mutants. L530 and R527 are situated at the core of Ig-fold of lamin A and mutation of these residues disrupts the fold structure and may lead to the interference in binding of the two proteins. 1-169(208) emerin mutant interaction with SUN1 was also reduced. However, increased interactions were observed between lamin A W520S and SUN1 and, between lamin A E358K and R541C and SUN2, therefore different a mechanism might be contributing to EDMD in these patients. Nonetheless, decreased affinity of SUN1 and lamin A might weakens the NE integrity or increased affinity might increase the stiffness of the NE, consequently, both of these phenomena may lead to impaired NE mechanics, causing EDMD. Ostlund et al. have demonstrated that the stability of the LINC complex is decreased in lamin A/C null cells, by FRAP analysis (Ostlund et al., 2009). Intriguingly, Stewart-Hutchinson et al. also have found that disruption of the LINC complex (by introducing the isolated KASH domain of nesprins, which in turn displaces endogenous nesprins) lowers the mechanical stiffness of cytoskeleton in cells (Stewart-Hutchinson et al., 2008). This therefore indicates that any disruption of SUN-lamin A interaction may also lead to mechanical instability of cells.

In this project, studies with skin fibroblast from EDMD patients carrying *LMNA* mutations did not demonstrate mislocalization of SUN1 or SUN2 from the NE. SUN1 and SUN2 were also retained at the NE in emerin null patient fibroblasts. Therefore, SUN protein mislocalization is not a common feature for EDMD. These findings also indicate that SUN proteins are not dependent on emerin for their NE localization. Similar to this, Ostlund et al. also demonstrated that, in emerin null cells, SUN1, SUN2 and nesprin-2 still localize at the NE (Ostlund et al., 2009). However, Randle et al., demonstrates that in emerin null skin fibroblasts nesprin-2 is mislocalized to the cytoplasm, but nesprin-1 remains at the NE (Randles et al., 2010). Therefore, emerin may not be necessary for anchoring most of the LINC complex proteins. Notably, emerin is not dependent on SUN proteins for its NE localization, as emerin is retained at the NE in cells co-depleted for SUN1 and SUN2 by RNAi (Haque et al., 2010). Therefore, although SUN proteins and emerin interact with each other, they are not the major determinant for each other to localize at the NE. In general, INM proteins are not responsible for anchoring each other at the NE, except lamin A/C which anchors emerin and nesprins, and emerin may be responsible for anchoring giant nesprin-2 (Sullivan et al., 1999; Libotte et al., 2005; Randles et al., 2010). However, nesprins have been demonstrated to depend on SUN proteins for their localization, which show redundant function in anchoring nesprins at the ONM (Crisp et al., 2006; Ketema et al., 2007; Roux et al., 2009).

Although disruption of SUN protein interactions with lamin A, emerin and nesprins is not a consistent feature of the mutants that I tested, other mutations have been shown to disrupt different sets of interactions. For example, Wheeler et al. have observed decreased interaction between nesprin-1α and p183T emerin EDMD mutant and, increased interaction between nesprin-2β and p183T emerin EDMD mutant (Wheeler et al., 2007). Since these mutations rarely cause dramatic effects on NE localization of other components of the LINC complex, their effect may be to cause a more subtle weakening of nucleo-cytoskeletal connections that is only of significance in muscle tissues and lead to gradual accumulation of damage over time. A more widespread and dramatic effect is observed with knock out of the components of LINC complex, for example nesprin-1 knock-out mice have decreased survival rate (Zhang et al., 2010).

7.4.2 Disruption of SUN proteins interaction in HGPS

Recently progeria has become a major subject of interest for researchers in the laminopathy field. Several mutations in lamin A/C cause progeria (section 1.4.4). In this project, both SUN1 and SUN2 interaction with two progeria lamin A mutants, G608G and T623S, was found to be disrupted. G608G and T623S cause 50 and 35 residue deletions from the CTD of lamin A and are responsible for HGPS and mild progeria, respectively (Eriksson et al., 2003; De Sandre-Giovannoli et al., 2003; Fukuchi et al., 2004; Shalev et al., 2007). It is likely, from other experiments presented in this thesis that the SUN1 binding region on lamin A lies at the extreme C-terminus. It is therefore possible that these deletions are interfering with SUN protein interaction with lamin A.

Interestingly, localization studies with progeria patient fibroblasts demonstrated variable localization of SUN1 to the NE. This is apparently contradictory to the finding that SUN1 displays reduced binding to G608G and T623S mutants. However, I have already discussed the fact that SUN1 binds preferentially to prelamin A and prelamin A is accumulated at the NE in HGPS cells, by an unknown mechanism (Goldman et al., 2004). Thus prelamin A might preferentially recruit SUN1 to the NE, but not SUN2. Indeed, this was found in a follow-up experiment in the lab, where HGPS cells showed a strong correlation between prelamin A and SUN1 expression, but not SUN2 (Haque et al., 2010). Therefore, although SUN1 and SUN2 interact less strongly with progeria lamin A mutants, SUN1 is still recruited to the NE by the increased prelamin A pool. This could explain the increased mechanical stiffness of HGPS nuclei observed by Verstraeten et al., as it would seem logical to predict that increased expression of SUN proteins would over-strengthen the LINC complex (Verstraeten et al., 2008). This could in turn explain the reduced ability of HGPS cells to migrate in wound healing assay (Verstraeten et al., 2008). Together, these studies show that SUN proteins might have a role in HGPS pathogenesis.

7.5 CONCLUSION

Taken together, the findings in this thesis and those of other groups have significantly advanced our understanding of SUN proteins. Like SUN2, SUN1 is a typical INM protein, with a nucleoplasmic N-terminus and lumenal C-terminus. SUN proteins are predicted to form a stable platform at the INM for association of various macromolecules. At the nucleoplasmic interface, SUN1 interacts with lamin A, emerin, nesprin-2, histone 2B, hALP and is also associated with telomeres and NPCs (Fig. 7.2). SUN1 and SUN2 bind promiscuously to all types of nesprins, thus linking the nucleus to all three cytoskeletal networks of the cell. Therefore, SUN proteins are components of LINC complex and are important for nuclear positioning in muscle cells and for nuclear migration in neurons. SUN proteins also have a role in gametogenesis and, during meiosis, SUN1 and SUN2 tether telomeres at the NE.

SUN proteins may also play a role in EDMD and progeria disease processes, demonstrated by disruption of SUN protein interaction with EDMD and progeria lamin A mutants. Since SUN proteins are part of the LINC complex, disrupting SUN protein connection with either lamin A or nesprins would disrupt the link that is continuous from the cell surface to the inside of nucleus. Consequently, nucleo-cytoskeletal communication will be disrupted, which is required for extracellular stimuli, such as mechanical stimuli in muscles, to be translated. Also, if the LINC complex is disrupted it is likely to alter the rigidity of the NE. Thus, decrease in SUN1 interaction with lamin A/nesprins/emerin might reduce the stiffness of the NE and increase the fragility of the NE, that would affect tissues vulnerable to force, such as muscle. On the other hand, increased interaction of SUN1 with lamin/emerin/nesprin might stiffen the NE, which has been demonstrated as a phenotype in HGPS cells. Therefore optimal association of SUN protein with the LINC complex is important for maintaining the homeostasis of the NE and its connection to the cytoskeleton, alteration of which could lead to laminopathies, as discussed.

7.6 FUTURE DIRECTIONS

Considering the findings in this thesis, study on SUN proteins could advance in various directions. The mechanism of stable anchoring of SUN proteins at the NE is still a mystery and an important future objective should be to identify the protein(s) responsible for SUN1 retention at the INM. Likely candidates are chromatin-associated proteins. However, it is possible that other INM proteins could play a role in anchoring SUN1 at the INM. SUN1 interaction with nesprins and emerin can be further analysed to determine whether their interactions are competitive or co-operative. Also, it should be clarified whether these interactions are direct or indirect. Affinity interaction assays can be performed between the deletion fragments of SUN proteins and lamin A, emerin and nesprins to test whether they interact with similar binding affinity as to the FL SUN proteins. Moreover, SUN protein interaction with BAF or other transcription factors or heterochromatin proteins can be tested to shed light if they are involved in gene expression or organizing chromatin structure.

Since SUN protein interactions are disrupted in EDMD and progeria, SUN proteins involvement in laminopathies should be the subject of future investigation. It would be logical to test SUN protein localization in L530P and R527P EDMD lamin A mutant patients fibroblasts. Additional binding assay can be performed between SUN proteins and lamin A EDMD mutants occurring in the coiled-coil region. As 60 % of EDMD patients do not have mutations in lamin A or emerin, an important aim should be to screen these patients for mutations in SUN1 and SUN2. If SUN protein mutations are found in EDMD patients, then these can be analysed to test their role along with other LINC complex proteins in the EDMD disease process. For example, nuclear envelope rigidity experiments can be performed on the EDMD patients muscle nuclei, by inducing strain on the nuclei to observe their deformity as demonstrated by Lee et al. (Lee et al., 2007). Additionally, the mobility of mutant SUN proteins by FRAP can be investigated. Also, SUN protein role in cell migration should be assessed by RNAi of SUN1 and SUN2.

Another question that remains to be solved is, how SUN1 is recruited more at the NE even though its interaction is interrupted with progeria lamin A mutants, and why SUN2 is behaving differently in this regard. By FRAP analysis of SUN1 or other LINC

complex components in HGPS fibroblasts, SUN mobility in these cells could be assessed and this would shed more light in our understanding of the mechanism.

Since SUN1 knock-out mice are sterile and both SUN1 and SUN2 are required for tethering telomeres to the NE, the role of SUN proteins in meiosis should be further studied. It would be interesting to investigate whether SUN1 is actually mutated in infertile patients, by screening processes. Also, as SUN proteins are now proved to be related to nuclear migrations and neurogenesis, SUN proteins involvement in brain disease, such as lissencephaly, should also be investigated, where there is smoothness in brain with neuronal migration defects (Burke and Stewart, 2002). In conclusion, SUN proteins might have various conserved functions in cells which are only now becoming evident and further research into these different aspects would advance our present knowledge on its function and related laminopathies.

CHAPTER 8

BIBLIOGRAPHY

Aaronson, R.P. & Blobel, G. 1975, "Isolation of nuclear pore complexes in association with a lamina.", *Proc Natl Acad Sci U S A.,* vol. 72, no. 3, pp. 1007-1011.

Adam, S.A., Marr, R.S. & Gerace, L. 1990, "Nuclear protein import in permeabilized mammalian cells requires soluble cytoplasmic factors.", *The Journal of cell biology,* vol. 111, no. 3, pp. 807-816.

Aebi, U., Cohn, J., Buhle, L. & Gerace, L. 1986, "The nuclear lamina is a meshwork of intermediate-type filaments", *Nature,* vol. 323, no. 6088, pp. 560-4.

Agarwal, A.K., Fryns, J.P., Auchus, R.J. & Garg, A. 2003, "Zinc metalloproteinase, ZMPSTE24, is mutated in mandibuloacral dysplasia", *Hum Mol Genet,* vol. 12, no. 16, pp. 1995-2001.

Alberts, B., Bray, D., Lewis, J., Raff, M., Roberts, K. & Watson, J.D. 1994, *Molecular biology of the cell, .*

Alberts, B., Johnson, A., Lewis, J., Raff, M., Roberts, K. & Watson, J.D. 2007, *Molecular Biology of the Cell.*

Antoniacci, L.M., Kenna, M.A. & Skibbens, R.V. 2007, "The nuclear envelope and spindle pole body-associated Mps3 protein bind telomere regulators and function in telomere clustering", *Cell Cycle,* vol. 6, no. 1, pp. 75-9.

Apel, E.D., Lewis, R.M., Grady, R.M. & Sanes, J.R. 2000, "Syne-1, a dystrophin- and Klarsicht-related protein associated with synaptic nuclei at the neuromuscular junction", *J. Biol. Chem.,* vol. 275, no. 41, pp. 31986-95.

Arimura, T., Helbling-Leclerc, A., Massart, C., Varnous, S., Niel, F., Lacene, E., Fromes, Y., Toussaint, M., Mura, A., Keller, D.I., Amthor, H., Isnard, R., Malissen, M., Schwartz, K. & Bonne, G. 2005, "Mouse model carrying H222P-Lmna mutation develops muscular dystrophy and dilated cardiomyopathy similar to human striated muscle laminopathies", *Human molecular genetics,* vol. 14, no. 1, pp. 155-169.

Bakay, M., Wang, Z., Melcon, G., Schiltz, L., Xuan, J., Zhao, P., Sartorelli, V., Seo, J., Pegoraro, E., Angelini, C., Shneiderman, B., Escolar, D., Chen, Y.W., Winokur, S.T., Pachman, L.M., Fan, C., Mandler, R., Nevo, Y., Gordon, E., Zhu, Y., Dong, Y., Wang, Y. & Hoffman, E.P. 2006, "Nuclear envelope dystrophies show a transcriptional fingerprint suggesting disruption of Rb-MyoD pathways in muscle regeneration", *Brain.,* vol. 129, no. Pt 4, pp. 996-1013.

Barrowman, J., Hamblet, C., George, C.M. & Michaelis, S. 2008, "Analysis of Prelamin A Biogenesis Reveals the Nucleus to be a CaaX Processing Compartment", Molecular biology of the cell, vol. 19, no. 12, pp. 5398-5408.

Beaudouin, J., Gerlich, D., Daigle, N., Eils, R. & Ellenberg, J. 2002, "Nuclear envelope breakdown proceeds by microtubule-induced tearing of the lamina", *Cell,* vol. 108, no. 1, pp. 83-96.

Benavente, R., Krohne, G. & Franke, W.W. 1985, "Cell type-specific expression of nuclear lamina proteins during development of Xenopus laevis", *Cell,* vol. 41, no. 1, pp. 177-190.

Bengtsson, L. & Wilson, K.L. 2004, "Multiple and surprising new functions for emerin, a nuclear membrane protein", *Current opinion in cell biology,* vol. 16, no. 1, pp. 73-79.

Berger, R., Theodor, L., Shoham, J., Gokkel, E., Brok-Simoni, F., Avraham, K.B., Copeland, N.G., Jenkins, N.A., Rechavi, G. & Simon, A.J. 1996, "The characterization and localization of the mouse thymopoietin/lamina-associated polypeptide 2 gene and its alternatively spliced products.", *Genome research,* vol. 6, no. 5, pp. 361-370.

Bergo, M.O., Gavino, B., Ross, J., Schmidt, W.K., Hong, C., Kendall, L.V., Mohr, A., Meta, M., Genant, H., Jiang, Y., Wisner, E.R., Van Bruggen, N., Carano, R.A., Michaelis, S., Griffey, S.M. & Young, S.G. 2002, "Zmpste24 deficiency in mice causes spontaneous bone fractures, muscle weakness, and a prelamin A processing defect", *Proc Natl Acad Sci U S A,* vol. 99, no. 20, pp. 13049-54.

Bettinger, B.T., Gilbert, D.M. & Amberg, D.C. 2004, "Actin up in the nucleus", vol. 5, no. 5, pp. 415.

Bione, S., Maestrini, E., Rivella, S., Mancini, M., Regis, S., Romeo, G. & Toniolo, D. 1994, "Identification of a novel X-linked gene responsible for Emery-Dreifuss muscular dystrophy", *Nat Genet,* vol. 8, no. 4, pp. 323-7.

Bloom, K. 2001, " Nuclear migration: cortical anchors for cytoplasmic dynein. .", *Curr. Biol.,* vol. 11, pp. R326-R329.

Bonne, G., DiBarletta, M.R., Varnous, S., Becane, H.M., Hammouda, E.H., Merlini, L., Muntoni, F., Greenberg, C.R., Gary, F., Urtizberea, J.A., Duboc, D., Fardeau, M., Toniolo, D. & Schwartz, K. 1999, "Mutations in the gene encoding lamin A/C cause autosomal dominant Emery-Dreifuss muscular dystrophy", *Nature Genetics,* vol. 21, no. 3, pp. 285-288.

Bonne, G., Mercuri, E., Muchir, A., Urtizberea, A., Bécane, H.M., Recan, D., Merlini, L., Wehnert, M., Boor, R., Reuner, U., Vorgerd, M., Wicklein, E.M., Eymard, B., Duboc, D., Penisson-Besnier, I., Cuisset, J.M., Ferrer, X., Desguerre, I., Lacombe, D., Bushby, K., Pollitt, C., Toniolo, D., Fardeau, M., Schwartz, K. & Muntoni, F. 2000, "Clinical and molecular genetic spectrum of autosomal dominant Emery-Dreifuss muscular dystrophy due to mutations of the lamin A/C gene.", *Ann Neurol,* vol. 48, no. 2, pp. 170-180.

Boyle, S., Gilchrist, S., Bridger, J.M., Mahy, N.L., Ellis, J.A. & Bickmore, W.A. 2001, "The spatial organization of human chromosomes within the nuclei of normal and emerin-mutant cells", *Human molecular genetics,* vol. 10, no. 3, pp. 211-219.

Bridger, J., Kill, I., O'Farrell, M. & Hutchison, C. 1993, "Internal lamin structures within G1 nuclei of human dermal fibroblasts", *Journal of cell science,* vol. 104, no. 2, pp. 297-306.

Brodsky, G.L., Muntoni, F., Miocic, S., Sinagra, G., Sewry, C. & Mestroni, L. 2000, "Lamin A/C Gene Mutation Associated With Dilated Cardiomyopathy With Variable Skeletal Muscle Involvement", *Circulation,* vol. 101, no. 5, pp. 473-476.

Broers, J.L., Machiels, B.M., Kuijpers, H.J., Smedts, F., van den Kieboom, R., Raymond, Y. & Ramaekers, F.C. 1997, "A- and B-type lamins are differentially expressed in normal human tissues", *Histochem Cell Biol,* vol. 107, no. 6, pp. 505-517.

Broers, J., Machiels, B., van Eys, G., Kuijpers, H., Manders, E., van Driel, R. & Ramaekers, F. 1999, "Dynamics of the nuclear lamina as monitored by GFP-tagged A-type lamins", *Journal of cell science,* vol. 112, no. 20, pp. 3463-3475.

Broers, J.L., Peeters, E.A., Kuijpers, H.J., Endert, J., Bouten, C.V., Oomens, C.W., Baaijens, F.P. & Ramaekers, F.C. 2004, "Decreased mechanical stiffness in LMNA-/- cells is caused by defective nucleo-cytoskeletal integrity: implications for the development of laminopathies", *Hum Mol Genet,* vol. 13, no. 21, pp. 2567-80.

Broers, J.L.V., Ramaekers, F.C.S., Bonne, G., Yaou, R.B. & Hutchison, C.J. 2006, "Nuclear Lamins: Laminopathies and Their Role in Premature Ageing", *Physiological Reviews,* vol. 86, no. 3, pp. 967-1008.

Buendia, B. & Courvalin, J. 1997, "Domain-Specific Disassembly and Reassembly of Nuclear Membranes during Mitosis", *Experimental cell research,* vol. 230, no. 1, pp. 133-144.

Bupp, J.M., Martin, A.E., Stensrud, E.S. & Jaspersen, S.L. 2007, "Telomere anchoring at the nuclear periphery requires the budding yeast Sad1-UNC-84 domain protein Mps3", *The Journal of cell biology,* vol. 179, no. 5, pp. 845-854.

Burke, B. & Gerace, L. 1986, "A cell free system to study reassembly of the nuclear envelope at the end of mitosis", *Cell,* vol. 44, no. 4, pp. 639-652.

Burke, B. & Stewart, C. 2002, "Life at the edge: the nuclear envelope and human disease", *Nat. Rev. Mol. Cell Biol.,* vol. 3, pp. 575-585.

Burke, B. & Stewart, C.L. 2006, "The laminopathies: the functional architecture of the nucleus and its contribution to disease", *Annu Rev Genomics Hum Genet.,* vol. 7, pp. 369-405.

Cao, H. & Hegele, R.A. 2000, "Nuclear lamin A/C R482Q mutation in Canadian kindreds with Dunnigan- type familial partial lipodystrophy", *Human Molecular Genetics,* vol. 9, no. 1, pp. 109-112.

Cao, K., Capell, B.C., Erdos, M.R., Djabali, K. & Collins, F.S. 2007, "A lamin A protein isoform overexpressed in Hutchinson-Gilford progeria syndrome interferes with mitosis in progeria and normal cells", *Proc Natl Acad Sci U S A,* vol. 104, no. 12, pp. 4949-54.

Capanni, C., Cenni, V., Mattioli, E., Sabatelli, P., Ognibene, A., Columbaro, M., Parnaik, V.K., Wehnert, M., Maraldi, N.M., Squarzoni, S. & Lattanzi, G. 2003, "Failure of lamin A/C to functionally assemble in R482L mutated familial partial lipodystrophy fibroblasts: altered intermolecular interaction with emerin and implications for gene transcription", *Experimental cell research,* vol. 291, no. 1, pp. 122-134.

Capanni, C., Mattioli, E., Columbaro, M., Lucarelli, E., Parnaik, V.K., Novelli, G., Wehnert, M., Cenni, V., Maraldi, N.M., Squarzoni, S. & Lattanzi, G. 2005, "Altered pre-lamin A processing is a common mechanism leading to lipodystrophy", *Human molecular genetics,* vol. 14, no. 11, pp. 1489-1502.

Capell, B.C., Erdos, M.R., Madigan, J.P., Fiordalisi, J.J., Varga, R., Conneely, K.N., Gordon, L.B., Der, C.J., Cox, A.D. & Collins, F.S. 2005, "Inhibiting farnesylation of progerin prevents the characteristic nuclear blebbing of Hutchinson-Gilford progeria syndrome", *Proc Natl Acad Sci U S A,* vol. 102, no. 36, pp. 12879-84.

Capell, B.C. & Collins, F.S. 2006, "Human laminopathies: nuclei gone genetically awry", *Nat Rev Genet,* vol. 7, no. 12, pp. 940-52.

Cartegni, L., di Barletta, M.R., Barresi, R., Squarzoni, S., Sabatelli, P., Maraldi, N., Mora, M., Di Blasi, C., Cornelio, F., Merlini, L., Villa, A., Cobianchi, F. & Toniolo, D. 1997, "Heart-specific localization of emerin: new insights into Emery-Dreifuss muscular dystrophy", *Hum Mol Genet,* vol. 6, no. 13, pp. 2257-64.

Chaouch, M., Allal, Y., De Sandre-Giovannoli, A., Vallat, J.M., Amer-el-Khedoud, A., Kassouri, N., Chaouch, A., Sindou, P., Hammadouche, T., Tazir, M., Lévy, N. & Grid, D. 2003, "The phenotypic manifestations of autosomal recessive axonalCharcot–Marie–Tooth due to a mutation in Lamin A/C gene", *Neuromuscular Disorders,* vol. 13, no. 1, pp. 60-67.

Chaudhary, N. & Courvalin, J. 1993, "Stepwise reassembly of the nuclear envelope at the end of mitosis", *The Journal of cell biology,* vol. 122, no. 2, pp. 295-306.

Chen, L., Lee, L., Kudlow, B.A., Dos Santos, H.G., Sletvold, O., Shafeghati, Y., Botha, E.G., Garg, A., Hanson, N.B., Martin, G.M., Mian, I.S., Kennedy, B.K. & Oshima, J. 2003, "LMNA mutations in atypical Werner's syndrome", *Lancet,* vol. 362, no. 9382, pp. 440-5.

Chi, Y., Cheng, L.I., Myers, T., Ward, J.M., Williams, E., Su, Q., Faucette, L., Wang, J. & Jeang, K. 2009, "Requirement for Sun1 in the expression of meiotic reproductive genes and piRNA", *Development,* vol. 136, no. 6, pp. 965-973.

Chikashige, Y., Ding, D., Funabiki, H., Haraguchi, T., Mashiko, S., Yanagida, M. & Hiraoka, Y. 1994, "Telomere-led premeiotic chromosome movement in fission yeast", *Science,* vol. 264, no. 5156, pp. 270-273.

Chikashige, Y., Tsutsumi, C., Yamane, M., Okamasa, K., Haraguchi, T. & Hiraoka, Y. 2006, "Meiotic proteins bqt1 and bqt2 tether telomeres to form the bouquet arrangement of chromosomes", *Cell,* vol. 125, no. 1, pp. 59-69.

Chytilova, E., Macas, J., Sliwinska, E., Rafelski, S.M., Lambert, G.M. & Galbraith, D.W. 2000, "Nuclear Dynamics in Arabidopsis thaliana", *Molecular biology of the cell,* vol. 11, no. 8, pp. 2733-2741.

Cohen, M., Lee, K.K., Wilson, K.L. & Gruenbaum, Y. 2001, "Transcriptional repression, apoptosis, human disease and the functional evolution of the nuclear lamina", *Trends Biochem Sci,* vol. 26, no. 1, pp. 41-7.

Cohen, T.V., Kosti, O. & Stewart, C.L. 2007, "The nuclear envelope protein MAN1 regulates TGFβ signaling and vasculogenesis in the embryonic yolk sac", *Development,* vol. 134, no. 7, pp. 1385-1395.

Cohen, T.V., Hernandez, L. & Stewart, C.L. 2008, "Functions of the nuclear envelope and lamina in development and disease", *Biochem Soc Trans.,* vol. 36, no. Pt 6, pp. 1329-34.

Conrad, M.N., Lee, C., Wilkerson, J.L. & Dresser, M.E. 2007, "MPS3 mediates meiotic bouquet formation in Saccharomyces cerevisiae", *Proceedings of the National Academy of Sciences,* vol. 104, no. 21, pp. 8863-8868.

Cooper, G., M. 2000, *The Cell - A Molecular Approach.*

Corrigan, D.P., Kuszczak, D., Rusinol, A.E., Thewke, D.P., Hrycyna, C.A., Michaelis, S. & Sinensky, M.S. 2005, "Prelamin A endoproteolytic processing in vitro by recombinant Zmpste24", *Biochem J,* vol. 387, no. Pt 1, pp. 129-38.

Courvalin, J.C., Segil, N., Blobel, G. & Worman, H.J. 1992, "The Lamin-B Receptor of the Inner Nuclear-Membrane Undergoes Mitosis- Specific Phosphorylation and Is a Substrate For P34cdc2-Type Protein- Kinase", *Journal of Biological Chemistry,* vol. 267, no. 27, pp. 19035-19038.

Crisp, M., Liu, Q., Roux, K., Rattner, J.B., Shanahan, C., Burke, B., Stahl, P.D. & Hodzic, D. 2006, "Coupling of the nucleus and cytoplasm", *The Journal of cell biology,* vol. 172, no. 1, pp. 41-53.

Croft, J.A., Bridger, J.M., Boyle, S., Perry, P., Teague, P. & Bickmore, W.A. 1999, "Differences in the Localization and Morphology of Chromosomes in the Human Nucleus", *The Journal of cell biology,* vol. 145, no. 6, pp. 1119-1131.

Csoka, A.B., Cao, H., Sammak, P.J., Constantinescu, D., Schatten, G.P. & Hegele, R.A. 2004, "Novel lamin A/C gene (LMNA) mutations in atypical progeroid syndromes", *J Med Genet,* vol. 41, no. 4, pp. 304-8.

D'Angelo, M.A. & Hetzer, M.W. 2008, "Structure, dynamics and function of nuclear pore complexes", *Trends in cell biology,* vol. 18, no. 10, pp. 456-466.

Dahl, K.N., Ribeiro, A.J.S. & Lammerding, J. 2008, "Nuclear Shape, Mechanics, and Mechanotransduction", *Circulation research,* vol. 102, no. 11, pp. 1307-1318.

Dahl, K.N., Scaffidi, P., Islam, M.F., Yodh, A.G., Wilson, K.L. & Misteli, T. 2006, "Distinct structural and mechanical properties of the nuclear lamina in Hutchinson–Gilford progeria syndrome", *Proceedings of the National Academy of Sciences,* vol. 103, no. 27, pp. 10271-10276.

Davies, B.S.J., Fong, L.G., Yang, S.H., Coffinier, C. & Young, S.G. 2009, "The Posttranslational Processing of Prelamin A and Disease", Annual Review of Genomics and Human Genetics, vol. 10, no. 1, pp. 153-174.

De Sandre-Giovannoli, A., Chaouch, M., Kozlov, S., Vallat, J.M., Tazir, M., Kassouri, N., Szepetowski, P., Hammadouche, T., Vandenberghe, A., Stewart, C.L., Grid, D. & Levy, N. 2002, "Homozygous defects in LMNA, encoding lamin A/C nuclear-envelope proteins, cause autosomal recessive axonal neuropathy in human (Charcot-Marie-Tooth disorder type 2) and mouse", *Am J Hum Genet,* vol. 70, no. 3, pp. 726-36.

De Sandre-Giovannoli, A., Bernard, R., Cau, P., Navarro, C., Amiel, J., Boccaccio, I., Lyonnet, S., Stewart, C.L., Munnich, A., Le Merrer, M. & Levy, N. 2003, "Lamin A truncation in Hutchinson-Gilford progeria", *Science,* vol. 300, no. 5628, pp. 2055.

Dechat, T., Vlcek, S. & Foisner, R. 2000, "Review: lamina-associated polypeptide 2 isoforms and related proteins in cell cycle-dependent nuclear structure dynamics", *J Struct Biol,* vol. 129, no. 2-3, pp. 335-45.

Dechat, T., Gajewski, A., Korbei, B., Gerlich, D., Daigle, N., Haraguchi, T., Furukawa, K., Ellenberg, J. & Foisner, R. 2004, "LAP2{alpha} and BAF transiently localize to telomeres and specific regions on chromatin during nuclear assembly", *Journal of cell science,* vol. 117, no. 25, pp. 6117-6128.

Dechat, T., Shimi, T., Adam, S.A., Rusinol, A.E., Andres, D.A., Spielmann, H.P., Sinensky, M.S. & Goldman, R.D. 2007, "Alterations in mitosis and cell cycle progression caused by a mutant lamin A known to accelerate human aging", *Proc Natl Acad Sci U S A,* vol. 104, no. 12, pp. 4955-60.

Dechat, T., Pfleghaar, K., Sengupta, K., Shimi, T., Shumaker, D.K., Solimando, L. & Goldman, R.D. 2008, "Nuclear lamins: major factors in the structural organization and function of the nucleus and chromatin", *Genes Dev,* vol. 22, no. 7, pp. 832-53.

Dechat, T., Adam, S.A., Taimen, P., Shimi, T. & Goldman, R.D. 2010, "Nuclear Lamins", Cold Spring Harbor Perspectives in Biology, vol. 2, no. 11.

Dhe-Paganon, S., Werner, E.D., Chi, Y.I. & Shoelson, S.E. 2002, "Structure of the globular tail of nuclear lamin", *J Biol Chem,* vol. 277, no. 20, pp. 17381-4.

Ding, D., Chikashige, Y., Haraguchi, T. & Hiraoka, Y. 1998, "Oscillatory nuclear movement in fission yeast meiotic prophase is driven by astral microtubules, as revealed by continuous observation of chromosomes and microtubules in living cells", *Journal of cell science,* vol. 111, no. 6, pp. 701-712.

Ding, R., West, R., Morphew, D., Oakley, B. & McIntosh, J. 1997, "The spindle pole body of Schizosaccharomyces pombe enters and leaves the nuclear envelope as the cell cycle proceeds", *Molecular biology of the cell,* vol. 8, no. 8, pp. 1461-1479.

Ding, X., Xu, R., Yu, J., Xu, T., Zhuang, Y. & Han, M. 2007, "SUN1 is required for telomere attachment to nuclear envelope and gametogenesis in mice", *Dev Cell,* vol. 12, no. 6, pp. 863-72.

Döring, V. & Stick, R. 1990, "Gene structure of nuclear lamin LIII of Xenopus laevis; a model for the evolution of IF proteins from a lamin-like ancestor.", *EMBO J.,* vol. 9, no. 12, pp. 4073-81.

Dorner, D., Vlcek, S., Foeger, N., Gajewski, A., Makolm, C., Gotzmann, J., Hutchison, C.J. & Foisner, R. 2006, "Lamina-associated polypeptide 2α regulates cell cycle progression and differentiation via the retinoblastoma–E2F pathway", *The Journal of cell biology,* vol. 173, no. 1, pp. 83-93.

Dreger, M., Bengtsson, L., Schoneberg, T., Otto, H. & Hucho, F. 2001, "Nuclear envelope proteomics: novel integral membrane proteins of the inner nuclear membrane", *Proc. Natl. Acad. Sci. USA,* vol. 98, no. 21, pp. 11943-8.

Dreuillet, C., Tillit, J., Kress, M. & Ernoult-Lange, M. 2002, "In vivo and in vitro interaction between human transcription factor MOK2 and nuclear lamin A/C", *Nucleic acids research,* vol. 30, no. 21, pp. 4634-4642.

Dunnigan, M.G., Cochrane, M.A., Kelly, A. & Scott, J.W. 1974, "Familial lipoatrophic diabetes with dominant transmission. A new syndrome", *Q J Med,* vol. 43, no. 169, pp. 33-48.

Ellenberg, J., Siggia, E.D., Moreira, J.E., Smith, C.L., Presley, J.F., Worman, H.J. & Lippincott-Schwartz, J. 1997, "Nuclear membrane dynamics and reassembly in living cells: targeting of an inner membrane protein in interphase and mitosis", *J. Cell Biol.,* vol. 138, pp. 1193-1206.

Ellis, D., Jenkins, H., Whitfield, W. & Hutchison, C. 1997, "GST-lamin fusion proteins act as dominant negative mutants in Xenopus egg extract and reveal the function of the lamina in DNA replication", *Journal of cell science,* vol. 110, no. 20, pp. 2507-2518.

Ellis, J.A., Craxton, M., Yates, J.R. & Kendrick-Jones, J. 1998, "Aberrant intracellular targeting and cell cycle-dependent phosphorylation of emerin contribute to the Emery-Dreifuss muscular dystrophy phenotype", *J Cell Sci,* vol. 111 (Pt 6), pp. 781-92.

Ellis, J.A., Yates, J.R.W., Kendrick-Jones, J. & Brown, C.B. 1999, "Changes at P183 of emerin weaken its protein-proteininteractions resulting in X-linked EDMD. ", *Hum. Genet.,* vol. 104, pp. 262-268.

Ellis, J.A. 2006, "Emery-Dreifuss muscular dystrophy at the nuclear envelope: 10 years on.", *Cell Mol Life Sci.,* vol. 63, no. 23, pp. 2702-9.

Emery, A.E. 1989, "Emery-Dreifuss syndrome", *J Med Genet,* vol. 26, no. 10, pp. 637-41.

Emery, A.E.H. 2000, "Emery–Dreifuss muscular dystrophy – a 40 year retrospective", Neuromuscular Disorders, vol. 10, no. 4-5, pp. 228-232.

Eriksson, M., Brown, W.T., Gordon, L.B., Glynn, M.W., Singer, J., Scott, L., Erdos, M.R., Robbins, C.M., Moses, T.Y., Berglund, P., Dutra, A., Pak, E., Durkin, S., Csoka, A.B., Boehnke, M., Glover, T.W. & Collins, F.S. 2003, "Recurrent de novo point mutations in lamin A cause Hutchinson-Gilford progeria syndrome", *Nature,* vol. 423, no. 6937, pp. 293-8.

Fairley, E.A., Kendrick-Jones, J. & Ellis, J.A. 1999, "The Emery-Dreifuss muscular dystrophy phenotype arises from aberrant targeting and binding of emerin at the inner nuclear membrane", *J Cell Sci,* vol. 112 (Pt 15), pp. 2571-82.

Farnsworth, C.C., Wolda, S.L., Gelb, M.H. & Glomset, J.A. 1989, "Human lamin B contains a farnesylated cysteine residue.", *Journal of Biological Chemistry,* vol. 264, no. 34, pp. 20422-20429.

Fatkin, D., MacRae, C., Sasaki, T., Wolff, M.R., Porcu, M., Frenneaux, M., Atherton, J., Vidaillet, H.J., Spudich, S., DeGirolami, U., Seidman, J.G., Seidman, C.E., Muntoni, F., Muehle, G., Johnson, W. & McDonough, B. 1999, "Missense mutations in the rod domain of the lamin A/C gene as causes of dilated cardiomyopathy and conduction-system disease", *New England Journal of Medicine,* vol. 341, no. 23, pp. 1715-1724.

Fawcett, D.W. 1966, "On the occurrence of a fibrous lamina on the inner aspect of the nuclear envelope in certain cells of vertebrates.", *Am J Anat.,* vol. 119, no. 1, pp. 129-45.

Filesi, I., Gullotta, F., Lattanzi, G., D'Apice, M.R., Capanni, C., Nardone, A.M., Columbaro, M., Scarano, G., Mattioli, E., Sabatelli, P., Maraldi, N.M., Biocca, S. & Novelli, G. 2005, "Alterations of nuclear envelope and chromatin organization in mandibuloacral dysplasia, a rare form of laminopathy", *Physiological Genomics,* vol. 23, no. 2, pp. 150-158.

Fischer, J.A., Acosta, S., Kenny, A., Cater, C., Robinson, C. & Hook, J. 2004, "Drosophila Klarsicht Has Distinct Subcellular Localization Domains for Nuclear Envelope and Microtubule Localization in the Eye", *Genetics,* vol. 168, no. 3, pp. 1385-1393.

Fischer-Vize, J.A. & Mosley, K.L. 1994, "Marbles mutants: uncoupling cell determination and nuclear migration in the developing Drosophila eye", *Development,* vol. 120, no. 9, pp. 2609-2618.

Fisher, D.Z., Chaudhary, N. & Blobel, G. 1986, "cDNA sequencing of nuclear lamin-A and lamin-C reveals primary and secondary structural homology to intermediate filament proteins", *Proc. Natl. Acad. Sci. USA,* vol. 83, no. 17, pp. 6450-6454.

Foisner, R. & Gerace, L. 1993, "Integral Membrane-Proteins of the Nuclear-Envelope Interact With Lamins and Chromosomes, and Binding Is Modulated By Mitotic Phosphorylation", *Cell,* vol. 73, no. 7, pp. 1267-1279.

Fong, L.G., Ng, J.K., Meta, M., Coté, N., Yang, S.H., Stewart, C.L., Sullivan, T., Burghardt, A., Majumdar, S., Reue, K., Bergo, M.O. & Young, S.G. 2004, "Heterozygosity for Lmna deficiency eliminates the progeria-like phenotypes in Zmpste24-deficient mice", *Proceedings of the National Academy of Sciences of the United States of America,* vol. 101, no. 52, pp. 18111-18116.

Fong, L.G., Frost, D., Meta, M., Qiao, X., Yang, S.H., Coffinier, C. & Young, S.G. 2006, "A protein farnesyltransferase inhibitor ameliorates disease in a mouse model of progeria", *Science,* vol. 311, no. 5767, pp. 1621-3.

Fridkin, A., Mills, E., Margalit, A., Neufeld, E., Lee, K.K., Feinstein, N., Cohen, M., Wilson, K.L. & Gruenbaum, Y. 2004, "Matefin, a Caenorhabditis elegans germ line-specific SUN-domain nuclear membrane protein, is essential for early embryonic and germ cell development", *Proc Natl Acad Sci U S A,* vol. 101, no. 18, pp. 6987-92.

Fukuchi, K., Katsuya, T., Sugimoto, K., Kuremura, M., Kim, H.D., Li, L. & Ogihara, T. 2004, "LMNA mutation in a 45 year old Japanese subject with Hutchinson-Gilford progeria syndrome", *J Med Genet,* vol. 41, no. 5, pp. e67.

Furukawa, K. & Hotta, Y. 1993, "cDNA cloning of a germ cell specific lamin B3 from mouse spermatocytes and analysis of its function by ectopic expression in somatic cells.", *EMBO J.,* vol. 12, no. 1, pp. 97-106.

Furukawa, K., Inagaki, H. & Hotta, Y. 1994, "Identification and Cloning of an mRNA Coding for a Germ Cell-Specific A-Type Lamin in Mice", *Experimental cell research,* vol. 212, no. 2, pp. 426-430.

Furukawa, K., Glass, C. & Kondo, T. 1997, "Characterization of the Chromatin Binding Activity of Lamina-Associated Polypeptide (LAP) 2", *Biochemical and biophysical research communications,* vol. 238, no. 1, pp. 240-246.

Furukawa, K. & Kondo, T. 1998, "Identification of the lamina-associated-polypeptide-2-binding domain of B-type lamin.", *Eur J Biochem,* vol. 251, pp. 729-733.

Furukawa, K., Pante, N., Aebi, U. & Gerace, L. 1995, "Cloning of a Cdna For Lamina-Associated Polypeptide-2 (Lap2) and Identification of Regions That Specify Targeting to the Nuclear- Envelope", *Embo Journal,* vol. 14, no. 8, pp. 1626-1636.

Furukawa, K. 1999, "LAP2 binding protein 1 (L2BP1/BAF) is a candidate mediator of LAP2-chromatin interaction", *Journal of cell science,* vol. 112, no. 15, pp. 2485-2492.

Gant, T.M., Harris, C.A. & Wilson, K.L. 1999, "Roles of LAP2 Proteins in Nuclear Assembly and DNA Replication: Truncated LAP2β Proteins Alter Lamina Assembly, Envelope Formation, Nuclear Size, and DNA Replication Efficiency in Xenopus laevis Extracts", *The Journal of cell biology,* vol. 144, no. 6, pp. 1083-1096.

Gerace, L., Blum, A. & Blobel, G. 1978, "Immunocytochemical localization of the major polypeptides of the nuclear pore complex-lamina fraction. Interphase and mitotic distribution.", *The Journal of cell biology,* vol. 79, no. 2, pp. 546-566.

Gerace, L. & Blobel, G. 1980, "The nuclear envelope lamina is reversibly depolymerized during mitosis", *Cell,* vol. 19, no. 1, pp. 277-287.

Gilford, H. & Shepherd, R.C. 1904, "Ateleiosis and progeria: continuous youth and premature old age", *Brit. Med. J.,* vol. 2 (5157), no. 914, pp. 8.

Goldman, A.E., Maul, G., Steinert, P.M., Yang, H.Y. & Goldman, R.D. 1986, "Keratin-like proteins that coisolate with intermediate filaments of BHK-21 cells are nuclear lamins", *Proceedings of the National Academy of Sciences of the United States of America,* vol. 83, no. 11, pp. 3839-3843.

Goldman, A.E., Moir, R.D., Montag-Lowy, M., Stewart, M. & Goldman, R.D. 1992, "Pathway of incorporation of microinjected lamin A into the nuclear envelope.", *The Journal of cell biology,* vol. 119, no. 4, pp. 725-735.

Goldman, R.D., Gruenbaum, Y., Moir, R.D., Shumaker, D.K. & Spann, T.P. 2002, "Nuclear lamins: building blocks of nuclear architecture", *Genes Dev,* vol. 16, no. 5, pp. 533-47.

Goldman, R.D., Shumaker, D.K., Erdos, M.R., Eriksson, M., Goldman, A.E., Gordon, L.B., Gruenbaum, Y., Khuon, S., Mendez, M., Varga, R. & Collins, F.S. 2004, "Accumulation of mutant lamin A causes progressive changes in nuclear architecture in Hutchinson-Gilford progeria syndrome", *Proc Natl Acad Sci U S A,* vol. 101, no. 24, pp. 8963-8.

Grady, R.M., Starr, D.A., Ackerman, G.L., Sanes, J.R. & Han, M. 2005, "Syne proteins anchor muscle nuclei at the neuromuscular junction", *Proceedings of the National Academy of Sciences of the United States of America,* vol. 102, no. 12, pp. 4359-4364.

Gros-Louis, F., Dupre, N., Dion, P., Fox, M.A., Laurent, S., Verreault, S., Sanes, J.R., Bouchard, J.P. & Rouleau, G.A. 2007, "Mutations in SYNE1 lead to a newly discovered form of autosomal recessive cerebellar ataxia", *Nat Genet,* vol. 39, no. 1, pp. 80-5.

Gruenbaum, Y., Margalit, A., Goldman, R.D., Shumaker, D.K. & Wilson, K.L. 2005, "The nuclear lamina comes of age", *Nat Rev Mol Cell Biol,* vol. 6, no. 1, pp. 21-31.

Guo, Y., Jangi, S. & Welte, M.A. 2005, "Organelle-specific Control of Intracellular Transport: Distinctly Targeted Isoforms of the Regulator Klar", *Molecular biology of the cell,* vol. 16, no. 3, pp. 1406-1416.

Hagan, I. & Yanagida, M. 1995, "The product of the spindle formation gene *sad1+* associates with the fission yeast spindle pole body and is essential for viability", *J. Cell Biol.,* vol. 129, no. 4, pp. 1033-47.

Hamaguchi, M.S. & Hiramoto, Y. 1986, "Analysis of the role of astral rays in pronuclear migration by the colcemid-UV method.", *Dev. Growth Differ.,* vol. 28, pp. 143-156.

Haque, F., Lloyd, D., Smallwood, D., Dent, C., Shanahan, C., Fry, A.M., Trembath, R.C. & Shackleton, S. 2006, "SUN1 interacts with nuclear lamin A and cytoplasmic nesprins to provide a physical connection between the nuclear lamina and the cytoskeleton", *Mol Cell Biol,* vol. 26, pp. 3738-3751.

Haque, F., Mazzeo, D., Patel, J.T., Smallwood, D.T., Ellis, J.A., Shanahan, C.M. & Shackleton, S. 2010, "Mammalian SUN Protein Interaction Networks at the Inner Nuclear Membrane and Their Role in Laminopathy Disease Processes", *Journal of Biological Chemistry,* vol. 285, no. 5, pp. 3487-3498.

Haraguchi, T., Koujin, T., Hayakawa, T., Kaneda, T., Tsutsumi, C., Imamoto, N., Akazawa, C., Sukegawa, J., Yoneda, Y. & Hiraoka, Y. 2000, "Live fluorescence imaging reveals early recruitment of emerin, LBR, RanBP2, and Nup153 to reforming functional nuclear envelopes", *Journal of cell science,* vol. 113, no. 5, pp. 779-794.

Haraguchi, T., Koujin, T., Segura-Totten, M., Lee, K.K., Matsuoka, Y., Yoneda, Y., Wilson, K.L. & Hiraoka, Y. 2001, "BAF is required for emerin assembly into the reforming nuclear envelope", *Journal of cell science,* vol. 114, no. 24, pp. 4575-4585.

Haraguchi, T., Holaska, J.M., Yamane, M., Koujin, T., Hashiguchi, N., Mori, C., Wilson, K.L. & Hiraoka, Y. 2004, "Emerin binding to Btf, a death-promoting transcriptional repressor, is disrupted by a missense mutation that causes Emery-Dreifuss muscular dystrophy", *Eur J Biochem,* vol. 271, no. 5, pp. 1035-45.

Harris, C.A., Andryuk, P.J., Cline, S.W., Mathew, S., Siekierka, J.J. & Goldstein, G. 1995, "Structure and Mapping of the Human Thymopoietin (TMPO) Gene and Relationship of Human TMPO β to Rat Lamin-Associated Polypeptide 2", *Genomics,* vol. 28, no. 2, pp. 198-205.

Hasan, S., Güttinger, S., Mühlhäusser, P., Anderegg, F., Bürgler, S. & Kutay, U. 2006, "Nuclear envelope localization of human UNC84A does not require nuclear lamins", *FEBS letters,* vol. 580, no. 5, pp. 1263-1268.

Hasty, P., Campisi, J., Hoeijmakers, J., van Steeg, H. & Vijg, J. 2003, "Aging and genome maintenance: lessons from the mouse?", *Science,* vol. 299, no. 5611, pp. 1355-9.

Heald, R. & McKeon, F. 1990, "Mutations of phosphorylation sites in lamin A that prevent nuclear lamina disassembly in mitosis", *Cell,* vol. 61, no. 4, pp. 579-589.

Hedgecock, E.M. & Thomson, J.N. 1982, "A gene required for nuclear and mitochondrial attachment in the nematode *Caenorhabditis elegans*", *Cell,* vol. 30, no. 1, pp. 321-30.

Hegele, R.A. 2001, "Premature Atherosclerosis Associated With Monogenic Insulin Resistance", *Circulation,* vol. 103, no. 18, pp. 2225-2229.

Helbling-Leclerc, A., Bonne, G. & Schwartz, K. 2002, "Emery-Dreifuss muscular dystrophy", European Journal of Human Genetics, vol. 10, no. 3, pp. 157--161.

Hellemans, J., Preobrazhenska, O., Willaert, A., Debeer, P., Verdonk, P.C.M., Costa, T., Janssens, K., Menten, B., Roy, N.V., Vermeulen, S.J.T., Savarirayan, R., Hul, W.V., Vanhoenacker, F., Huylebroeck, D., Paepe, A.D., Naeyaert, J., Vandesompele, J., Speleman, F., Verschueren, K., Coucke, P.J. & Mortier, G.R. 2004, "Loss-of-function mutations in LEMD3 result in osteopoikilosis, Buschke-Ollendorff syndrome and melorheostosis", vol. 36, no. 11, pp. 1218.

Hennekes, H. & Nigg, E. 1994, "The role of isoprenylation in membrane attachment of nuclear lamins. A single point mutation prevents proteolytic cleavage of the lamin A precursor and confers membrane binding properties", Journal of cell science, vol. 107, no. 4, pp. 1019-1029.

Hodzic, D.M., Yeater, D.B., Bengtsson, L., Otto, H. & Stahl, P.D. 2004, "Sun2 is a novel mammalian inner nuclear membrane protein", *J Biol Chem,* vol. 279, pp. 25805-25812.

Hofemeister, H. & O'Hare, P. 2005, "Analysis of the localization and topology of nurim, a polytopic protein tightly associated with the inner nuclear membrane", *J Biol Chem,* vol. 280, no. 4, pp. 2512-21.

Hoffmann, K., Dreger, C.K., Olins, A.L., Olins, D.E., Shultz, L.D., Lucke, B., Karl, H., Kaps, R., Muller, D., Vaya, A., Aznar, J., Ware, R.E., Cruz, N.S., Lindner, T.H., Herrmann, H., Reis, A. & Sperling, K. 2002, "Mutations in the gene encoding the lamin B receptor produce an altered nuclear morphology in granulocytes (Pelger-Huet anomaly)", vol. 31, no. 4, pp. 414.

Hoffmann, K., Sperling, K., Olins, A.L. & Olins, D.E. 2007, "The granulocyte nucleus and lamin B receptor: avoiding the ovoid.", *Chromosoma,* vol. 116, no. 3, pp. 227-35.

Höger, T.H., Krohne, G. & Franke, W.W. 1988, "Amino acid sequence and molecular characterization of murine lamin B as deduced from cDNA clones.", *Eur J Cell Biol.,* vol. 47, no. 2, pp. 283-90.

Höger, T.H., Zatloukal, K., Waizenegger, I. & Krohne, G. 1990, "Characterization of a second highly conserved B-type lamin present in cells previously thought to contain only a single B-type lamin.", *Chromosoma.,* vol. 99, no. 6, pp. 379-90.

Holaska, J.M., Lee, K.K., Kowalski, A.K. & Wilson, K.L. 2003, "Transcriptional repressor germ cell-less (GCL) and barrier to autointegration factor (BAF) compete for binding to emerin in vitro", *J Biol Chem,* vol. 278, no. 9, pp. 6969-75.

Holaska, J.M., Kowalski, A.K. & Wilson, K.L. 2004, "Emerin caps the pointed end of actin filaments: evidence for an actin cortical network at the nuclear inner membrane", *PLoS Biol,* vol. 2, no. 9, pp. E231.

Holaska, J.M. & Wilson, K.L. 2006, "Multiple roles for emerin: implications for Emery-Dreifuss muscular dystrophy.", *Anat Rec A Discov Mol Cell Evol Biol,* vol. 288, no. 7, pp. 676-80.

Holaska, J.M. 2008, "Emerin and the Nuclear Lamina in Muscle and Cardiac Disease", *Circulation research,* vol. 103, no. 1, pp. 16-23.

Holmer, L., Pezhman, A. & Worman, H.J. 1998, "The Human Lamin B Receptor/Sterol Reductase Multigene Family", *Genomics,* vol. 54, no. 3, pp. 469-476.

Holmer, L. & Worman, H.J. 2001, "Inner nuclear membrane proteins: functions and targeting", *Cell Mol Life Sci,* vol. 58, no. 12-13, pp. 1741-7.

Holt, I., Ostlund, C., Stewart, C.L., Man, N., Worman, H.J. & Morris, G.E. 2003, "Effect of pathogenic mis-sense mutations in lamin A on its interaction with emerin in vivo", *J Cell Sci,* vol. 116, no. Pt 14, pp. 3027-35.

Holt, I., Man, N.t., Wehnert, M. & Morris, G.E. 2006, "Lamin A/C assembly defects in Emery–Dreifuss muscular dystrophy can be regulated by culture medium composition", *Neuromuscular Disorders,* vol. 16, no. 6, pp. 368-373.

Holtz, D., Tanaka, R.A., Hartwig, J. & McKeon, F. 1989, "The CaaX motif of lamin A functions in conjunction with the nuclear localization signal to target assembly to the nuclear envelope", *Cell,* vol. 59, no. 6, pp. 969-977.

Horvitz, H.R. & Sulston, J.E. 1980, "Isolation and genetic characterization of cell-lineage mutants of the nematode *Caenorhabditis Elegans*", *Genetics,* vol. 96, no. 2, pp. 435-454.

Houben, F., Ramaekers, F.C., Snoeckx, L.H. & Broers, J.L. 2007, "Role of nuclear lamina-cytoskeleton interactions in the maintenance of cellular strength", *Biochim Biophys Acta,* vol. 1773, no. 5, pp. 675-86.

Huang, S., Risques, R.A., Martin, G.M., Rabinovitch, P.S. & Oshima, J. 2008, "Accelerated telomere shortening and replicative senescence in human fibroblasts overexpressing mutant and wild-type lamin A", *Exp Cell Res,* vol. 314, no. 1, pp. 82-91.

Hutchinson, J. 1886, "A case of congenital absence of hair with atrophic condition of the skin and its appendages. ", *Lancet, Londn,* vol. 1, pp. 923.

Hutchison, C.J. & Worman, H.J. 2004, "A-type lamins: Guardians of the soma?", vol. 6, no. 11, pp. 1067.

Imai, S., Nishibayashi, S., Takao, K., Tomifuji, M., Fujino, T., Hasegawa, M. & Takano, T. 1997, "Dissociation of Oct-1 from the nuclear peripheral structure induces the cellular aging-associated collagenase gene expression", *Mol Biol Cell,* vol. 8, no. 12, pp. 2407-19.

Ishimura, A., Ng, J.K., Taira, M., Young, S.G. & Osada, S. 2006, "Man1, an inner nuclear membrane protein, regulates vascular remodeling by modulating transforming growth factor β signaling", *Development,* vol. 133, no. 19, pp. 3919-3928.

Jagatheesan, G., Thanumalayan, S., Muralikrishna, B., Rangaraj, N., Karande, A.A. & Parnaik, V.K. 1999, "Colocalization of intranuclear lamin foci with RNA splicing factors", *J Cell Sci,* vol. 112, no. Pt 24, pp. 4651-61.

Jaspersen, S.L., Martin, A.E., Glazko, G., Giddings, T.H., Morgan, G., Mushegian, A. & Winey, M. 2006, "The Sad1-UNC-84 homology domain in Mps3 interacts with Mps2 to connect the spindle pole body with the nuclear envelope", *The Journal of cell biology,* vol. 174, no. 5, pp. 665-675.

Jin, H., Tan, S., Hermanowski, J., Böhm, S., Pacheco, S., McCauley, J.M., Greener, M.J., Hinits, Y., Hughes, S.M., Sharpe, P.T. & Roberts, R.G. 2007, "The dystrotelin, dystrophin and dystrobrevin superfamiliy: newparalogues and old isoforms.", BMC Genomics, vol. 8, no. 19.

Kandert, S., Luke, Y., Kleinhenz, T., Neumann, S., Lu, W., Jaeger, V.M., Munck, M., Wehnert, M., Muller, C.R., Zhou, Z., Noegel, A.A., Dabauvalle, M. & Karakesisoglou, I. 2007, "Nesprin-2 giant safeguards nuclear envelope architecture in LMNA S143F progeria cells", *Human molecular genetics,* vol. 16, no. 23, pp. 2944-2959.

Kay, R.R. & Johnston, R.I. 1973, "The nuclear envelope: current problems of structure and of function", *Sub-Cell. Biochem.,* vol. 2, pp. 127-166.

Kennedy, B.K., Barbie, D.A., Classon, M., Dyson, N. & Harlow, E. 2000, "Nuclear organization of DNA replication in primary mammalian cells", *Genes Dev,* vol. 14, no. 22, pp. 2855-68.

Ketema, M., Wilhelmsen, K., Kuikman, I., Janssen, H., Hodzic, D. & Sonnenberg, A. 2007, "Requirements for the localization of nesprin-3 at the nuclear envelope and its interaction with plectin", *Journal of cell science,* vol. 120, no. 19, pp. 3384-3394.

Kieran, M.W., Gordon, L. & Kleinman, M. 2007, "New approaches to progeria", *Pediatrics,* vol. 120, no. 4, pp. 834-41.

Kilic, F., Dalton, M.B., Burrell, S.K., Mayer, J.P., Patterson, S.D. & Sinensky, M. 1997, "In Vitro Assay and Characterization of the Farnesylation-dependent Prelamin A Endoprotease", Journal of Biological Chemistry, vol. 272, no. 8, pp. 5298-5304.

King, M.C., Lusk, C. & Blobel, G. 2006, "Karyopherin-mediated import of integral inner nuclear membrane proteins", vol. 442, no. 7106, pp. 1007.

Kirschner, J., Brune, T., Wehnert, M., Denecke, J., Wasner, C., Feuer, A., Marquardt, T., Ketelsen, U.-., Wieacker, P., Bönnemann, C.G. & Korinthenberg, R. 2005, "p.S143F mutation in lamin A/C: A new phenotype combining myopathy and progeria", *Annals of Neurology,* vol. 57, no. 1, pp. 148-151.

Kitten, G.T. & Nigg, E.A. 1991, "The CaaX motif is required for isoprenylation, carboxyl methylation, and nuclear membrane association of lamin B2.", *The Journal of cell biology,* vol. 113, no. 1, pp. 13-23.

Kracklauer, M.P., Banks, S.M., Xie, X., Wu, Y. & Fischer, J.A. 2007, "Drosophila klaroid encodes a SUN domain protein required for Klarsicht localization to the nuclear envelope and nuclear migration in the eye.", *Fly (Austin),* vol. 1, no. 2, pp. 75-85.

Krimm, I., Ostlund, C., Gilquin, B., Couprie, J., Hossenlopp, P., Mornon, J.P., Bonne, G., Courvalin, J.C., Worman, H.J. & Zinn-Justin, S. 2002, "The Ig-like structure of the C-terminal domain of lamin A/C, mutated in muscular dystrophies, cardiomyopathy, and partial lipodystrophy", *Structure,* vol. 10, no. 6, pp. 811-23.

Krohne, G., Waizenegger, I. & Höger, T.H. 1989, "The conserved carboxy-terminal cysteine of nuclear lamins is essential for lamin association with the nuclear envelope.", *The Journal of cell biology,* vol. 109, no. 5, pp. 2003-2011.

Kutay, U. & Muhlhausser, P. 2006, "Cell biology: Taking a turn into the nucleus", vol. 442, no. 7106, pp. 992.

Lammerding, J., Schulze, P.C., Takahashi, T., Kozlov, S., Sullivan, T., Kamm, R.D., Stewart, C.L. & Lee, R.T. 2004, "Lamin A/C deficiency causes defective nuclear mechanics and mechanotransduction", *J Clin Invest,* vol. 113, no. 3, pp. 370-8.

Lammerding, J., Hsiao, J., Schulze, P.C., Kozlov, S., Stewart, C.L. & Lee, R.T. 2005, "Abnormal nuclear shape and impaired mechanotransduction in emerin-deficient cells", *J Cell Biol,* vol. 170, no. 5, pp. 781-91.

Lange, A., Mills, R.E., Lange, C.J., Stewart, M., Devine, S.E. & Corbett, A.H. 2007, "Classical Nuclear Localization Signals: Definition, Function, and Interaction with Importin α", *Journal of Biological Chemistry,* vol. 282, no. 8, pp. 5101-5105.

Lattanzi, G., Cenni, V., Marmiroli, S., Capanni, C., Mattioli, E., Merlini, L., Squarzoni, S. & Mario Maraldi, N. 2003, "Association of emerin with nuclear and cytoplasmic actin is regulated in differentiating myoblasts", *Biochemical and biophysical research communications,* vol. 303, no. 3, pp. 764-770.

Lazebnik, Y.A., Cole, S., Cooke, C.A., Nelson, W.G. & Earnshaw, W.C. 1993, "Nuclear events of apoptosis in vitro in cell-free mitotic extracts: a model system for analysis of the active phase of apoptosis.", *The Journal of cell biology,* vol. 123, no. 1, pp. 7-22.

Lazebnik, Y.A., Takahashi, A., Moir, R.D., Goldman, R.D., Poirier, G.G., Kaufmann, S.H. & Earnshaw, W.C. 1995, "Studies of the lamin proteinase reveal multiple parallel biochemical pathways during apoptotic execution", *Proceedings of the National Academy of Sciences of the United States of America,* vol. 92, no. 20, pp. 9042-9046.

Lee, J.S., Hale, C.M., Panorchan, P., Khatau, S.B., George, J.P., Tseng, Y., Stewart, C.L., Hodzic, D. & Wirtz, D. 2007, "Nuclear lamin A/C deficiency induces defects in cell mechanics, polarization, and migration.", *Biophys J.,* vol. 93, no. 7, pp. 2542-52.

Lee, K.K., Haraguchi, T., Lee, R.S., Koujin, T., Hiraoka, Y. & Wilson, K.L. 2001, "Distinct functional domains in emerin bind lamin A and DNA-bridging protein BAF", *J Cell Sci,* vol. 114, no. Pt 24, pp. 4567-73.

Lee, K.K., Starr, D., Cohen, M., Liu, J., Han, M., Wilson, K.L. & Gruenbaum, Y. 2002, "Lamin-dependent localization of UNC-84, a protein required for nuclear migration in *Caenorhabditis elegans*", *Mol. Biol. Cell,* vol. 13, no. 3, pp. 892-901.

Lee, K.K. & Wilson, K.L. 2004, "All in the family: Evidence for four new LEM-domain proteins Lem2 (NET-25), Lem3, Lem4 and Lem5 in the human genome", *Symp.Soc.Exp.Biol.,* , pp. 239-329.

Lehner, C.F., Fürstenberger, G., Eppenberger, H.M. & Nigg, E.A. 1986, "Biogenesis of the nuclear lamina: in vivo synthesis and processing of nuclear protein precursors", Proceedings of the National Academy of Sciences of the United States of America, vol. 83, no. 7, pp. 2096-2099.

Lei, K., Zhang, X., Ding, X., Guo, X., Chen, M., Zhu, B., Xu, T., Zhuang, Y., Xu, R. & Han, M. 2009, "SUN1 and SUN2 play critical but partially redundant roles in anchoring nuclei in skeletal muscle cells in mice", *Proceedings of the National Academy of Sciences,* vol. 106, no. 25, pp. 10207-10212.

Lenz-Böhme, B., Wismar, J., Fuchs, S., Reifegerste, R., Buchner, E., Betz, H. & Schmitt, B. 1997, "Insertional Mutation of the Drosophila Nuclear Lamin Dm0 Gene Results in Defective Nuclear Envelopes, Clustering of Nuclear Pore Complexes, and Accumulation of Annulate Lamellae", *The Journal of cell biology,* vol. 137, no. 5, pp. 1001-1016.

Leung, G.K., Schmidt, W.K., Bergo, M.O., Gavino, B., Wong, D.H., Tam, A., Ashby, M.N., Michaelis, S. & Young, S.G. 2001, "Biochemical Studies of Zmpste24-deficient Mice", *Journal of Biological Chemistry,* vol. 276, no. 31, pp. 29051-29058.

Libotte, T., Zaim, H., Abraham, S., Padmakumar, V.C., Schneider, M., Lu, W., Munck, M., Hutchison, C., Wehnert, M., Fahrenkrog, B., Sauder, U., Aebi, U., Noegel, A.A. & Karakesisoglou, I. 2005, "Lamin A/C-dependent localization of Nesprin-2, a giant scaffolder at the nuclear envelope", *Mol Biol Cell,* vol. 16, no. 7, pp. 3411-24.

Lin, F. & Worman, H.J. 1993, "Structural Organization of the Human Gene Encoding Nuclear Lamin-a and Nuclear Lamin-C", *Journal of Biological Chemistry,* vol. 268, no. 22, pp. 16321-16326.

Lin, F. & Worman, H.J. 1995, "Structural Organization of the Human Gene (LMNB1) Encoding Nuclear Lamin B1", *Genomics,* vol. 27, no. 2, pp. 230-236.

Lin, F., Blake, D.L., Callebaut, I., Skerjanc, I.S., Holmer, L., McBurney, M.W., Paulin-Levasseur, M. & Worman, H.J. 2000, "MAN1, an Inner Nuclear Membrane Protein That Shares the LEM Domain with Lamina-associated Polypeptide 2 and Emerin", *Journal of Biological Chemistry,* vol. 275, no. 7, pp. 4840-4847.

Lin, F., Morrison, J.M., Wu, W. & Worman, H.J. 2005, "MAN1, an integral protein of the inner nuclear membrane, binds Smad2 and Smad3 and antagonizes transforming growth factor-{beta} signaling", *Human molecular genetics,* vol. 14, no. 3, pp. 437-445.

264

Liu, B., Wang, J., Chan, K.M., Tjia, W.M., Deng, W., Guan, X., Huang, J.D., Li, K.M., Chau, P.Y., Chen, D.J., Pei, D., Pendas, A.M., Cadinanos, J., Lopez-Otin, C., Tse, H.F., Hutchison, C., Chen, J., Cao, Y., Cheah, K.S., Tryggvason, K. & Zhou, Z. 2005, "Genomic instability in laminopathy-based premature aging", *Nat Med,* vol. 11, no. 7, pp. 780-5.

Liu, J., Ben-Shahar, T.R., Riemer, D., Treinin, M., Spann, P., Weber, K., Fire, A. & Gruenbaum, Y. 2000, "Essential roles for Caenorhabditis elegans lamin gene in nuclear organization, cell cycle progression, and spatial organization of nuclear pore complexes", *Mol Biol Cell,* vol. 11, no. 11, pp. 3937-47.

Liu, J., Lee, K.K., Segura-Totten, M., Neufeld, E., Wilson, K.L. & Gruenbaum, Y. 2003, "MAN1 and emerin have overlapping function(s) essential for chromosome segregation and cell division in Caenorhabditis elegans", *Proceedings of the National Academy of Sciences of the United States of America,* vol. 100, no. 8, pp. 4598-4603.

Liu, Q., Pante, N., Misteli, T., Elsagga, M., Crisp, M., Hodzic, D., Burke, B. & Roux, K.J. 2007, "Functional association of Sun1 with nuclear pore complexes", *The Journal of cell biology,* vol. 178, no. 5, pp. 785-798.

Liu, Y., Rusinol, A., Sinensky, M., Wang, Y. & Zou, Y. 2006, "DNA damage responses in progeroid syndromes arise from defective maturation of prelamin A", *J Cell Sci,* vol. 119, no. Pt 22, pp. 4644-9.

Lloyd, D., Trembath, R.C. & Shackleton, S. 2002, "A novel interaction between lamin A and SREBP1: implications for partial lipodystrophy and other laminopathies", *Hum. Mol. Genet.,* vol. 11, pp. 769-777.

Lodish, H., Berk, A., Zipursky, S.L., Matsudaira, P., Baltimore, D. & Darnell, J. 2000, *Molecular Cell Biology,* .

Loewinger, L. & McKeon, F. 1988, "Mutations in the Nuclear Lamin Proteins Resulting in Their Aberrant Assembly in the Cytoplasm", *Embo Journal,* vol. 7, no. 8, pp. 2301-2309.

Lopez-Soler, R.I., Moir, R.D., Spann, T.P., Stick, R. & Goldman, R.D. 2001, "A role for nuclear lamins in nuclear envelope assembly", *The Journal of cell biology,* vol. 154, no. 1, pp. 61-70.

Lourim, D. & Krohne, G. 1993, "Membrane-associated lamins in Xenopus egg extracts: identification of two vesicle populations.", *The Journal of cell biology,* vol. 123, no. 3, pp. 501-512.

Lu, W., Gotzmann, J., Sironi, L., Jaeger, V., Schneider, M., Lüke, Y., Uhlén, M., Szigyarto, C.A., Brachner, A., Ellenberg, J., Foisner, R., Noegel, A.A. & Karakesisoglou, I. 2008, "Sun1 forms immobile macromolecular assemblies at the nuclear envelope", *Biochimica et Biophysica Acta (BBA) - Molecular Cell Research,* vol. 1783, no. 12, pp. 2415-2426.

Lusk, C.P., Blobel, G. & King, M.C. 2007, "Highway to the inner nuclear membrane: rules for the road", *Nature Reviews: Molecular Cell Biology,* vol. 8, no. 5, pp. 420.

Lutz, R.J., Trujillo, M.A., Denham, K.S., Wenger, L. & Sinensky, M. 1992, "Nucleoplasmic localization of prelamin A: implications for prenylation-dependent lamin A assembly into the nuclear lamina", Proceedings of the National Academy of Sciences of the United States of America, vol. 89, no. 7, pp. 3000-3004.

Machiels, B.M., Zorenc, A.H.G., Endert, J.M., Kuijpers, H.J.H., van Eys, G.J.J.M., Ramaekers, F.C.S. & Broers, J.L.V. 1996, "An Alternative Splicing Product of the Lamin A/C Gene Lacks Exon 10", *Journal of Biological Chemistry,* vol. 271, no. 16, pp. 9249-9253.

Malone, C.J., Fixsen, W.D., Horvitz, H.R. & Han, M. 1999, "UNC-84 localizes to the nuclear envelope and is required for nuclear migration and anchoring during *C. elegans* development", *Development,* vol. 126, no. 14, pp. 3171-81.

Malone, C.J., Misner, L., Le Bot, N., Tsai, M.C., Campbell, J.M., Ahringer, J. & White, J.G. 2003, "The *C. elegans* hook protein, ZYG-12, mediates the essential attachment between the centrosome and nucleus", *Cell,* vol. 115, no. 7, pp. 825-36.

Mancini, M.A., Shan, B., Nickerson, J.A., Penman, S. & Lee, W.H. 1994, "The retinoblastoma gene product is a cell cycle-dependent, nuclear matrix-associated protein", *Proc Natl Acad Sci U S A,* vol. 91, no. 1, pp. 418-22.

Manilal, S., Nguyen, T.M., Sewry, C.A. & Morris, G.E. 1996, " The Emery-Dreifuss muscular dystrophy protein, emerin, is a nuclear membrane protein.", *Hum Mol Genet,* vol. 5, pp. 801-808.

Maniotis, A.J., Chen, C.S. & Ingber, D.E. 1997, "Demonstration of mechanical connections between integrins, cytoskeletal filaments, and nucleoplasm that stabilize nuclear structure", *Proc Natl Acad Sci U S A,* vol. 94, no. 3, pp. 849-54.

Mansharamani, M. & Wilson, K.L. 2005, "Direct Binding of Nuclear Membrane Protein MAN1 to Emerin in Vitro and Two Modes of Binding to Barrier-to-Autointegration Factor", *Journal of Biological Chemistry,* vol. 280, no. 14, pp. 13863-13870.

Margalit, A., Vlcek, S., Gruenbaum, Y. & Foisner, R. 2005, "Breaking and making of the nuclear envelope", *J Cell Biochem,* vol. 95, no. 3, pp. 454-65.

Markiewicz, E., Tilgner, K., Barker, N., van de Wetering, M., Clevers, H., Dorobek, M., Hausmanowa-Petrusewicz, I., Ramaekers, F.C., Broers, J.L., Blankesteijn, W.M., Salpingidou, G., Wilson, R.G., Ellis, J.A. & Hutchison, C.J. 2006, "The inner nuclear membrane protein emerin regulates beta-catenin activity by restricting its accumulation in the nucleus", *Embo J,* vol. 25, no. 14, pp. 3275-85.

Martin, L., Crimaudo, C. & Gerace, L. 1995, "cDNA Cloning and Characterization of Lamina-associated Polypeptide 1C (LAP1C), an Integral Protein of the Inner Nuclear Membrane", *Journal of Biological Chemistry,* vol. 270, no. 15, pp. 8822-8828.

Mattout, A., Dechat, T., Adam, S.A., Goldman, R.D. & Gruenbaum, Y. 2006, "Nuclear lamins, diseases and aging", *Current opinion in cell biology,* vol. 18, no. 3, pp. 335-341.

McKeon, F.D., Kirschner, M.W. & Caput, D. 1986, "Homologies in both primary and secondary structure between nuclear envelope and intermediate filament proteins", *Nature,* vol. 319, pp. 463-468.

McNally, E.M. 2007, "New Approaches in the Therapy of Cardiomyopathy in Muscular Dystrophy", Annual Review of Medicine, vol. 58, no. 1, pp. 75-88.

Meier, I. 2001, "The plant nuclear envelope.", *Cell Mol Life Sci.,* vol. 58, no. 12-13, pp. 1774-80.

Meier, J., Campbell, K., Ford, C., Stick, R. & Hutchison, C. 1991, "The role of lamin LIII in nuclear assembly and DNA replication, in cell-free extracts of Xenopus eggs", *Journal of cell science,* vol. 98, no. 3, pp. 271-279.

Melcer, S., Gruenbaum, Y. & Krohne, G. 2007, "Invertebrate lamins", *Experimental cell research,* vol. 313, no. 10, pp. 2157-2166.

Melcon, G., Kozlov, S., Cutler, D.A., Sullivan, T., Hernandez, L., Zhao, P., Mitchell, S., Nader, G., Bakay, M., Rottman, J.N., Hoffman, E.P. & Stewart, C.L. 2006, "Loss of emerin at

the nuclear envelope disrupts the Rb1/E2F and MyoD pathways during muscle regeneration", *Human molecular genetics,* vol. 15, no. 4, pp. 637-651.

Meune, C., Van Berlo, J.H., Anselme, F., Bonne, G., Pinto, Y.M. & Duboc, D. 2006, "Primary Prevention of Sudden Death in Patients with Lamin A/C Gene Mutations", New England Journal of Medicine, vol. 354, no. 2, pp. 209-210.

Meyerzon, M., Fridolfsson, H.N., Ly, N., McNally, F.J. & Starr, D.A. 2009, "UNC-83 is a nuclear-specific cargo adaptor for kinesin-1-mediated nuclear migration", *Development,* vol. 136, no. 16, pp. 2725-2733.

Mislow, J.M., Kim, M.S., Davis, D.B. & McNally, E.M. 2002a, "Myne-1, a spectrin repeat transmembrane protein of the myocyte inner nuclear membrane, interacts with lamin A/C", *J. Cell Sci.,* vol. 115, no. Pt 1, pp. 61-70.

Mislow, J.M., Holaska, J.M., Kim, M.S., Lee, K.K., Segura-Totten, M., Wilson, K.L. & McNally, E.M. 2002b, "Nesprin-1alpha self-associates and binds directly to emerin and lamin A in vitro", *FEBS Lett,* vol. 525, no. 1-3, pp. 135-40.

Moir, R.D., Montag-Lowy, M. & Goldman, R.D. 1994, "Dynamic properties of nuclear lamins: lamin B is associated with sites of DNA replication.", *The Journal of cell biology,* vol. 125, no. 6, pp. 1201-1212.

Moir, R.D., Spann, T.P. & Goldman, R.D. 1995, "The dynamic properties and possible functions of nuclear lamins", *Int. Rev. Cytol.,* vol. 162B, pp. 141-82.

Moir, R.D., Spann, T.P., Lopez-Soler, R.I., Yoon, M., Goldman, A.E., Khuon, S. & Goldman, R.D. 2000a, "Review: The Dynamics of the Nuclear Lamins during the Cell Cycle— Relationship between Structure and Function", *Journal of structural biology,* vol. 129, no. 2-3, pp. 324-334.

Moir, R.D., Spann, T.P., Herrmann, H. & Goldman, R.D. 2000b, "Disruption of nuclear lamin organization blocks the elongation phase of DNA replication", *J Cell Biol,* vol. 149, no. 6, pp. 1179-92.

Moir, R.D., Yoon, M., Khuon, S. & Goldman, R.D. 2000c, "Nuclear Lamins a and B1: different pathways of assembly during nuclear envelope formation in living cells", *The Journal of cell biology,* vol. 151, no. 6, pp. 1155-1168.

Morris, G.E. 2001, "The role of the nuclear envelope in Emery–Dreifuss muscular dystrophy", *Trends in molecular medicine,* vol. 7, no. 12, pp. 572-577.

Morris, N.R. 2003, "Nuclear positioning: the means is at the ends", *Current opinion in cell biology,* vol. 15, no. 1, pp. 54-59.

Morris, G.E.,. & Randles, K.N. 2010, "Nesprin isoforms: are they inside or outside the nucleus?", Biochem Soc Trans., vol. 38, pp. 278-80.

Moulson, C.L., Go, G., Gardner, J.M., van der Wal, A.C., Smitt, J.H., van Hagen, J.M. & Miner, J.H. 2005, "Homozygous and compound heterozygous mutations in ZMPSTE24 cause the laminopathy restrictive dermopathy", *J Invest Dermatol,* vol. 125, no. 5, pp. 913-9.

Moulson, C.L., Fong, L.G., Gardner, J.M., Farber, E.A., Go, G., Passariello, A., Grange, D.K., Young, S.G. & Miner, J.H. 2007, "Increased progerin expression associated with unusual LMNA mutations causes severe progeroid syndromes", *Human mutation,* vol. 28, no. 9, pp. 882-889.

Mounkes, L., Kozlov, S., Burke, B. & Stewart, C.L. 2003, "The laminopathies: nuclear structure meets disease", *Curr. Opin. Genet. Dev.,* vol. 13, no. 3, pp. 223-30.

Muchir, A., Bonne, G., van der Kooi, A.J., van Meegen, M., Baas, F., Bolhuis, P.A., de Visser, M. & Schwartz, K. 2000, "Identification of mutations in the gene encoding lamins A/C in autosomal dominant limb girdle muscular dystrophy with atrioventricular conduction disturbances (LGMD1B)", *Hum. Mol. Genet.,* vol. 9, pp. 1453-1459.

Naetar, N., Korbei, B., Kozlov, S., Kerenyi, M.A., Dorner, D., Kral, R., Gotic, I., Fuchs, P., Cohen, T.V., Bittner, R., Stewart, C.L. & Foisner, R. 2008, "Loss of nucleoplasmic LAP2[alpha]-lamin A complexes causes erythroid and epidermal progenitor hyperproliferation", vol. 10, no. 11, pp. 1348.

Navarro, C.L., De Sandre-Giovannoli, A., Bernard, R., Boccaccio, I., Boyer, A., Genevieve, D., Hadj-Rabia, S., Gaudy-Marqueste, C., Smitt, H.S., Vabres, P., Faivre, L., Verloes, A., Van Essen, T., Flori, E., Hennekam, R., Beemer, F.A., Laurent, N., Le Merrer, M., Cau, P. & Levy, N. 2004, "Lamin A and ZMPSTE24 (FACE-1) defects cause nuclear disorganization and identify restrictive dermopathy as a lethal neonatal laminopathy", *Hum Mol Genet,* vol. 13, no. 20, pp. 2493-503.

Navarro, C.L., Cadinanos, J., De Sandre-Giovannoli, A., Bernard, R., Courrier, S., Boccaccio, I., Boyer, A., Kleijer, W.J., Wagner, A., Giuliano, F., Beemer, F.A., Freije, J.M., Cau, P., Hennekam, R.C., Lopez-Otin, C., Badens, C. & Levy, N. 2005, "Loss of ZMPSTE24 (FACE-1) causes autosomal recessive restrictive dermopathy and accumulation of Lamin A precursors", *Hum Mol Genet,* vol. 14, no. 11, pp. 1503-13.

Newport, J.W., Wilson, K.L. & Dunphy, W.G. 1990, "A lamin-independent pathway for nuclear envelope assembly.", *The Journal of cell biology,* vol. 111, no. 6, pp. 2247-2259.

Nili, E., Cojocaru, G.S., Kalma, Y., Ginsberg, D., Copeland, N.G., Gilbert, D.J., Jenkins, N.A., Berger, R., Shaklai, S., Amariglio, N., Brok-Simoni, F., Simon, A.J. & Rechavi, G. 2001, "Nuclear membrane protein LAP2beta mediates transcriptional repression alone and together with its binding partner GCL (germ-cell-less)", *J Cell Sci,* vol. 114, no. Pt 18, pp. 3297-307.

Novelli, G., Muchir, A., Sangiuolo, F., Helbling-Leclerc, A., D'Apice, M.R., Massart, C., Capon, F., Sbraccia, P., Federici, M., Lauro, R., Tudisco, C., Pallotta, R., Scarano, G., Dallapiccola, B., Merlini, L. & Bonne, G. 2002, "Mandibuloacral dysplasia is caused by a mutation in LMNA-encoding lamin A/C", *Am J Hum Genet,* vol. 71, no. 2, pp. 426-31.

Ohba, T., Schirmer, E.C., Nishimoto, T. & Gerace, L. 2004, "Energy- and temperature-dependent transport of integral proteins to the inner nuclear membrane via the nuclear pore", *The Journal of cell biology,* vol. 167, no. 6, pp. 1051-1062.

Osada, S., Ohmori, S. & Taira, M. 2003, "XMAN1, an inner nuclear membrane protein, antagonizes BMP signaling by interacting with Smad1 in Xenopus embryos", *Development,* vol. 130, no. 9, pp. 1783-1794.

Osman, M., Paz, M., Landesman, Y., Fainsod, A. & Gruenbaum, Y. 1990, "Molecular analysis of the Drosophila nuclear lamin gene", *Genomics,* vol. 8, no. 2, pp. 217-224.

Ostlund, C., Ellenberg, J., Hallberg, E., Lippincott-Schwartz, J. & Worman, H.J. 1999, "Intracellular trafficking of emerin, the Emery-Dreifuss muscular dystrophy protein", *J. Cell Sci.,* vol. 112, pp. 1709-19.

Ostlund, C., Bonne, G., Schwartz, K. & Worman, H.J. 2001, "Properties of lamin A mutants found in Emery-Dreifuss muscular dystrophy, cardiomyopathy and Dunnigan-type partial lipodystrophy", *J Cell Sci,* vol. 114, pp. 4435-4445.

Ostlund, C., Folker, E.S., Choi, J.C., Gomes, E.R., Gundersen, G.G. & Worman, H.J. 2009, "Dynamics and molecular interactions of linker of nucleoskeleton and cytoskeleton (LINC) complex proteins", *Journal of cell science,* vol. 122, no. 22, pp. 4099-4108.

Ozaki, T., Saijo, M., Murakami, K., Enomoto, H., Taya, Y. & Sakiyama, S. 1994, "Complex formation between lamin A and the retinoblastoma gene product: identification of the domain on lamin A required for its interaction", *Oncogene,* vol. 9, no. 9, pp. 2649-53.

Ozawa, R., Hayashi, Y.K., Ogawa, M., Kurokawa, R., Matsumoto, H., Noguchi, S., Nonaka, I. & Nishino, I. 2006, "Emerin-Lacking Mice Show Minimal Motor and Cardiac Dysfunctions with Nuclear-Associated Vacuoles", *American Journal of Pathology,* vol. 168, no. 3, pp. 907-917.

Padmakumar, V.C., Abraham, S., Braune, S., Noegel, A.A., Tunggal, B., Karakesisoglou, I. & Korenbaum, E. 2004, "Enaptin, a giant actin-binding protein, is an element of the nuclear membrane and the actin cytoskeleton", *Exp Cell Res,* vol. 295, no. 2, pp. 330-9.

Padmakumar, V.C., Libotte, T., Lu, W., Zaim, H., Abraham, S., Noegel, A.A., Gotzmann, J., Foisner, R. & Karakesisoglou, I. 2005, "The inner nuclear membrane protein Sun1 mediates the anchorage of Nesprin-2 to the nuclear envelope", *J Cell Sci,* vol. 118, no. Pt 15, pp. 3419-30.

Palmer, R.E., Sullivan, D.S., Huffaker, T. & Koshland, D. 1992, "Role of astral microtubules and actin in spindle orientation and migration in the budding yeast, Saccharomyces cerevisiae.", *The Journal of cell biology,* vol. 119, no. 3, pp. 583-593.

Pan, D., Estévez-Salmerón, L.D., Stroschein, S.L., Zhu, X., He, J., Zhou, S. & Luo, K. 2005, "The Integral Inner Nuclear Membrane Protein MAN1 Physically Interacts with the R-Smad Proteins to Repress Signaling by the Transforming Growth Factor-β Superfamily of Cytokines", *Journal of Biological Chemistry,* vol. 280, no. 16, pp. 15992-16001.

Patterson, K., Molofsky, A.B., Robinson, C., Acosta, S., Cater, C. & Fischer, J.A. 2004, "The Functions of Klarsicht and Nuclear Lamin in Developmentally Regulated Nuclear Migrations of Photoreceptor Cells in the Drosophila Eye", *Molecular biology of the cell,* vol. 15, no. 2, pp. 600-610.

Paulin-Levasseur, M., Blake, D.L., Julien, M. & Rouleau, L. 1996, "The MAN antigens are non-lamin constituents of the nuclear lamina in vertebrate cells.", *Chromosoma,* vol. 104, pp. 367-379.

Pendas, A.M., Zhou, Z., Cadinanos, J., Freije, J.M., Wang, J., Hultenby, K., Astudillo, A., Wernerson, A., Rodriguez, F., Tryggvason, K. & Lopez-Otin, C. 2002, "Defective prelamin A processing and muscular and adipocyte alterations in Zmpste24 metalloproteinase-deficient mice", *Nat Genet,* vol. 31, no. 1, pp. 94-9.

Peter, M., Kitten, G.T., Lehner, C.F., Vorburger, K., Bailer, S.M., Maridor, G. & Nigg, E.A. 1989, "Cloning and sequencing of cDNA clones encoding chicken lamins A and B1 and comparison of the primary structures of vertebrate A- and B-type lamins", *Journal of Molecular Biology,* vol. 208, no. 3, pp. 393-404.

Peter, M., Nakagawa, J., Dorée, M., Labbé, J.C. & Nigg, E.A. 1990, "In vitro disassembly of the nuclear lamina and M phase-specific phosphorylation of lamins by cdc2 kinase", *Cell,* vol. 61, no. 4, pp. 591-602.

Plasilova, M., Chattopadhyay, C., Pal, P., Schaub, N.A., Buechner, S.A., Mueller, H., Miny, P., Ghosh, A. & Heinimann, K. 2004, "Homozygous missense mutation in the lamin A/C gene causes autosomal recessive Hutchinson-Gilford progeria syndrome", *J Med Genet,* vol. 41, no. 8, pp. 609-14.

Puckelwartz, M.J., Kessler, E., Zhang, Y., Hodzic, D., Randles, K.N., Morris, G., Earley, J.U., Hadhazy, M., Holaska, J.M., Mewborn, S.K., Pytel, P. & McNally, E.M. 2009, "Disruption of nesprin-1 produces an Emery Dreifuss muscular dystrophy-like phenotype in mice", *Human molecular genetics,* vol. 18, no. 4, pp. 607-620.

Puckelwartz, M.J., Kessler, E.J., Kim, G., DeWitt, M.M., Zhang, Y., Earley, J.U., Depreux, F.F.S., Holaska, J., Mewborn, S.K., Pytel, P. & McNally, E.M. 2010, "Nesprin-1 mutations in human and murine cardiomyopathy", Journal of Molecular and Cellular Cardiology, vol. 48, no. 4, pp. 600-608.

Qumsiyeh, M.B. 1999, "Structure and function of the nucleus: anatomy and physiology of chromatin.", *Cell Mol Life Sci.,* vol. 55, no. 8-9, pp. 1129-40.

Raff, J.W. 1999, "The missing (L) UNC?", *Curr. Biol.,* vol. 9, no. 18, pp. R708-10.

Raffaele Di Barletta, M., Ricci, E., Galluzzi, G., Tonali, P., Mora, M., Morandi, L., Romorini, A., Voit, T., Orstavik, K.H., Merlini, L., Trevisan, C., Biancalana, V., Housmanowa-Petrusewicz, I., Bione, S., Ricotti, R., Schwartz, K., Bonne, G. & Toniolo, D. 2000, "Different mutations in the LMNA gene cause autosomal dominant and autosomal recessive Emery-Dreifuss muscular dystrophy.", *Am J Hum Genet.,* vol. 66, no. 4, pp. 1407-12.

Raharjo, W.H., Enarson, P., Sullivan, T., Stewart, C. & Burke, B. 2001, "Nuclear envelope defects associated with *LMNA* mutations cause dilated cardiomyopathy and Emery-Dreifuss muscular dystrophy", *J Cell Sci,* vol. 114, pp. 4447-4457.

Randles, K.N., Lam, L.T., Sewry, C.A., Puckelwartz, M., Furling, D., Wehnert, M., McNally, E.M. & Morris, G.E. 2010, "Nesprins, but not sun proteins, switch isoforms at the nuclear envelope during muscle development," *Developmental Dynamics* Vol. 239. Wiley-Liss, Inc.

Rao, L., Perez, D. & White, E. 1996, "Lamin proteolysis facilitates nuclear events during apoptosis.", *The Journal of cell biology,* vol. 135, no. 6, pp. 1441-1455.

Razafsky, D. & Hodzic, D. 2009, "Bringing KASH under the SUN: the many faces of nucleo-cytoskeletal connections", *The Journal of cell biology,* vol. 186, no. 4, pp. 461-472.

Reichart, B., Klafke, R., Dreger, C., Krüger, E., Motsch, I., Ewald, A., Schäfer, J., Reichmann, H., Müller, C.R. & Dabauvalle, M.C. 2004, "Expression and localization of nuclear proteins in autosomal-dominant Emery-Dreifuss muscular dystrophy with LMNA R377H mutation", *BMC Cell Biol.,* vol. 30, no. 5, pp. 12.

Reinsch, S. & Gonczy, P. 1998, "Mechanisms of nuclear positioning", *J. Cell Sci.,* vol. 111, pp. 2283-95.

Rober, R.A., Weber, K. & Osborn, M. 1989, "Differential timing of nuclear lamin A/C expression in the various organs of the mouse embryo and the young animal: a developmental study", *Development,* vol. 105, no. 2, pp. 365-78.

Rober, R., Sauter, H., Weber, K. & Osborn, M. 1990, "Cells of the cellular immune and hemopoietic system of the mouse lack lamins A/C: distinction versus other somatic cells", *Journal of cell science,* vol. 95, no. 4, pp. 587-598.

Robinson, D.N. & Cooley, L. 1997, "Genetic analysis of the actin cytoskeleton in the Drosophila ovary", *Annual Review of Cell and Developmental Biology,* vol. 13, no. 1, pp. 147-170.

Rosenberg-Hasson, Y., Renert-Pasca, M. & Volk, T. 1996, "A Drosophila Dystrophin-related protein, MSP-300, is required for embryonic muscle morphogenesis", *Mechanisms of development,* vol. 60, no. 1, pp. 83-94.

Roux, K.J., Crisp, M.L., Liu, Q., Kim, D., Kozlov, S., Stewart, C.L. & Burke, B. 2009, "Nesprin 4 is an outer nuclear membrane protein that can induce kinesin-mediated cell polarization", *Proceedings of the National Academy of Sciences,* vol. 106, no. 7, pp. 2194-2199.

Rusinol, A.E. & Sinensky, M.S. 2006, "Farnesylated lamins, progeroid syndromes and farnesyl transferase inhibitors", *Journal of cell science,* vol. 119, no. 16, pp. 3265-3272.

Salina, D., Bodoor, K., Enarson, P., Raharjo, W.H. & Burke, B. 2001, " Nuclear envelope dynamics. ", *Biochem Cell Biol.,* vol. 79, no. 5, pp. 533-42.

Salpingidou, G., Smertenko, A., Hausmanowa-Petrucewicz, I., Hussey, P.J. & Hutchison, C.J. 2007, "A novel role for the nuclear membrane protein emerin in association of the centrosome to the outer nuclear membrane", The Journal of cell biology, vol. 178, no. 6, pp. 897-904.

Simpson, J.G. & Roberts, R.G. 2008, "Patterns of evolutionary conservation in the nesprin genes highlight probable functionally important protein domains and isoforms", Biochemical Society Transactions, vol. 036, no. 6, pp. 1359-1367.

Sarkar, P.K. & Shinton, R.A. 2001, "Hutchinson-Guilford progeria syndrome", *Postgraduate medical journal,* vol. 77, no. 907, pp. 312-317.

Scaffidi, P. & Misteli, T. 2005, "Reversal of the cellular phenotype in the premature aging disease Hutchinson-Gilford progeria syndrome", vol. 11, no. 43, pp. 445.

Schirmer, E.C., Florens, L., Guan, T., Yates, J.R.,3rd & Gerace, L. 2003, "Nuclear membrane proteins with potential disease links found by subtractive proteomics", *Science,* vol. 301, no. 5638, pp. 1380-2.

Schirmer, E.C. & Gerace, L. 2005, "The nuclear membrane proteome: extending the envelope", *Trends in biochemical sciences,* vol. 30, no. 10, pp. 551-558.

Schmitt, J., Benavente, R., Hodzic, D., Höög, C., Stewart, C.L. & Alsheimer, M. 2007, "Transmembrane protein Sun2 is involved in tethering mammalian meiotic telomeres to the nuclear envelope", *Proceedings of the National Academy of Sciences,* vol. 104, no. 18, pp. 7426-7431.

Schneider, M., Noegel, A.A. & Karakesisoglou, I. 2008, "KASH-domain proteins and the cytoskeletal landscapes of the nuclear envelope.", *Biochem Soc Trans.,* vol. 36, no. Pt 6, pp. 1368-72.

Segura-Totten, M. & Wilson, K.L. 2004, "BAF: roles in chromatin, nuclear structure and retrovirus integration. ", vol. 14, no. 5, pp. 261-266.

Shackleton, S., Lloyd, D.J., Jackson, S.N.J., Evans, R., Niermeijer, M.F., Singh, B.M., Schmidt, H., Brabant, G., Kumar, S., Durrington, P.N., Gregory, S., O'Rahilly, S. & Trembath, R.C. 2000, "*LMNA*, encoding lamin A/C, is mutated in partial lipodystrophy", *Nat. Genet.,* vol. 24, pp. 153-156.

Shackleton, S., Smallwood, D.T., Clayton, P., Wilson, L.C., Agarwal, A.K., Garg, A. & Trembath, R.C. 2005, "Compound heterozygous ZMPSTE24 mutations reduce prelamin A processing and result in a severe progeroid phenotype", *J Med Genet,* vol. 42, no. 6, pp. e36.

Shalev, S.A., De Sandre-Giovannoli, A., Shani, A.A. & Levy, N. 2007, "An association of Hutchinson-Gilford progeria and malignancy", *Am J Med Genet A,* vol. 143A, no. 16, pp. 1821-6.

Shaw, S.L., Yeh, E., Maddox, P., Salmon, E.D. & Bloom, K. 1997, "Astral Microtubule Dynamics in Yeast: A Microtubule-based Searching Mechanism for Spindle Orientation and Nuclear Migration into the Bud", *The Journal of cell biology,* vol. 139, no. 4, pp. 985-994.

Shumaker, D.K., Lee, K.K., Tanhehco, Y.C., Craigie, R. & Wilson, K.L. 2001, "LAP2 binds to BAF[middot]DNA complexes: requirement for the LEM domain and modulation by variable regions", vol. 20, no. 7, pp. 1764.

Siderakis, M. & Tarsounas, M. 2007, "Telomere regulation and function during meiosis.", *Chromosome Res.,* vol. 15, no. 5, pp. 667-79.

Simha, V., Agarwal, A.K., Oral, E.A., Fryns, J. & Garg, A. 2003, "Genetic and Phenotypic Heterogeneity in Patients with Mandibuloacral Dysplasia-Associated Lipodystrophy", *Journal of Clinical Endocrinology Metabolism,* vol. 88, no. 6, pp. 2821-2824.

Smallwood, D.T. & Shackleton, S. 2010, "Lamin A-linked progerias: is farnesylation the be all and end all? ", *Biochem Soc Trans.,* vol. 38, no. Pt 1, pp. 281-6.

Smith, S. & Blobel, G. 1993, "The first membrane spanning region of the lamin B receptor is sufficient for sorting to the inner nuclear membrane.", *The Journal of cell biology,* vol. 120, no. 3, pp. 631-637.

Smythe, C., Jenkins, H.E. & Hutchison, C.J. 2000, "Incorporation of the nuclear pore basket protein nup153 into nuclear pore structures is dependent upon lamina assembly: evidence from cell- free extracts of Xenopus eggs", *Embo J,* vol. 19, no. 15, pp. 3918-31.

Soullam, B. & Worman, H.J. 1993, "The Amino-Terminal Domain of the Lamin-B Receptor Is a Nuclear- Envelope Targeting Signal", *Journal of Cell Biology,* vol. 120, no. 5, pp. 1093-1100.

Soullam, B. & Worman, H.J. 1995, "Signals and structural features involved in integral membrane-protein targeting to the inner nuclear-membrane", *J. Cell Biol.,* vol. 130, no. 1, pp. 15-27.

Spann, T.P., Moir, R.D., Goldman, A.E., Stick, R. & Goldman, R.D. 1997, "Disruption of nuclear lamin organization alters the distribution of replication factors and inhibits DNA synthesis", *Journal of Cell Biology,* vol. 136, no. 6, pp. 1201-1212.

Spann, T.P., Goldman, A.E., Wang, C., Huang, S. & Goldman, R.D. 2002, "Alteration of nuclear lamin organization inhibits RNA polymerase II-dependent transcription", *J Cell Biol,* vol. 156, no. 4, pp. 603-8.

Starr, D.A., Hermann, G.J., Malone, C.J., Fixsen, W., Priess, J.R., Horvitz, H.R. & Han, M. 2001, "*unc-83* encodes a novel component of the nuclear envelope and is essential for proper nuclear migration", *Development,* vol. 128, no. 24, pp. 5039-50. Starr, D.A. & Han, M. 2002, "Role of ANC-1 in tethering nuclei to the actin cytoskeleton", *Science,* vol. 298, no. 5592, pp. 406-9.

Starr, D.A. & Han, M. 2003, "ANChors away: an actin based mechanism of nuclear positioning", *J. Cell Sci.,* vol. 116, no. Pt 2, pp. 211-6.

Starr, D.A. & Han, M. 2005, "A genetic approach to study the role of nuclear envelope components in nuclear positioning.", *Novartis Found Symp.,* vol. 264, pp. 208-19.

Stearns, T. 1997, "Motoring to the Finish: Kinesin and Dynein Work Together to Orient the Yeast Mitotic Spindle", *The Journal of cell biology,* vol. 138, no. 5, pp. 957-960.

Steen, R.L. & Collas, P. 2001, "Mistargeting of B-Type Lamins at the End of Mitosis", *The Journal of cell biology,* vol. 153, no. 3, pp. 621-626.

Stewart, C. & Burke, B. 1987, "Teratocarcinoma stem cells and early mouse embryos contain only a single major lamin polypeptide closely resembling lamin B", *Cell,* vol. 51, no. 3, pp. 383-392.

Stewart-Hutchinson, P.J., Hale, C.M., Wirtz, D. & Hodzic, D. 2008, "Structural requirements for the assembly of LINC complexes and their function in cellular mechanical stiffness", *Experimental cell research,* vol. 314, no. 8, pp. 1892-1905.

Stick, R. & Hausen, P. 1985, "Changes in the nuclear lamina composition during early development of Xenopus laevis", *Cell,* vol. 41, no. 1, pp. 191-200.

Stick, R., Angres, B., Lehner, C.F. & Nigg, E.A. 1988, "The fates of chicken nuclear lamin proteins during mitosis: evidence for a reversible redistribution of lamin B2 between inner nuclear membrane and elements of the endoplasmic reticulum.", *The Journal of cell biology,* vol. 107, no. 2, pp. 397-406.

Stierlé, V., Couprie, J., Ostlund, C., Krimm, I., Zinn-Justin, S., Hossenlopp, P., Worman, H.J., Courvalin, J.C. & Duband-Goulet, I. 2003, "The carboxyl-terminal region common to lamins A and C contains a DNA binding domain.", *Biochemistry,* vol. 42, no. 17, pp. 4819-4828.

Stuurman, N., Heins, S. & Aebi, U. 1998, "Nuclear lamins: their structure, assembly, and interactions", *J Struct Biol,* vol. 122, no. 1-2, pp. 42-66.

Sullivan, T., Escalante-Alcalde, D., Bhatt, H., Anver, M., Bhat, N., Nagashima, K., Stewart, C.L. & Burke, B. 1999, "Loss of A-type lamin expression compromises nuclear envelope integrity leading to muscular dystrophy", *J. Cell Biol.,* vol. 147, pp. 913-919.

Sulston, J.E. & Horvitz, H.R. 1981, "Abnormal cell lineages in mutants of the nematode Caenorhabditis elegans", *Developmental biology,* vol. 82, no. 1, pp. 41-55.

Takahashi, A., Alnemri, E.S., Lazebnik, Y.A., Fernandes-Alnemri, T., Litwack, G., Moir, R.D., Goldman, R.D., Poirier, G.G., Kaufmann, S.H. & Earnshaw, W.C. 1996, "Cleavage of lamin A by Mch2 alpha but not CPP32: multiple interleukin 1 beta-converting enzyme-related proteases with distinct substrate recognition properties are active in apoptosis", *Proceedings of the National Academy of Sciences of the United States of America,* vol. 93, no. 16, pp. 8395-8400.

Talkop, U.A., Talvik, I., Sonajalg, M., Sibul, H., Kolk, A., Piirsoo, A., Warzok, R., Wulff, K., Wehnert, M.S. & Talvik, T. 2002, "Early onset of cardiomyopathy in two brothers with X-linked Emery-Dreifuss muscular dystrophy", *Neuromuscul Disord,* vol. 12, no. 9, pp. 878-81.

Taniura, H., Glass, C. & Gerace, L. 1995, "A Chromatin Binding-Site in the Tail Domain of Nuclear Lamins That Interacts With Core Histones", *Journal of Cell Biology,* vol. 131, no. 1, pp. 33-44.

Taylor, M.R., Slavov, D., Gajewski, A., Vlcek, S., Ku, L., Fain, P.R., Carniel, E., Di Lenarda, A., Sinagra, G., Boucek, M.M., Cavanaugh, J., Graw, S.L., Ruegg, P., Feiger, J., Zhu, X., Ferguson, D.A., Bristow, M.R., Gotzmann, J., Foisner, R. & Mestroni, L. 2005, "Thymopoietin (lamina-associated polypeptide 2) gene mutation associated with dilated cardiomyopathy", *Human mutation,* vol. 26, no. 6, pp. 566-574.

Thompson, E.B. 1998, "Special topic: apoptosis.", *Annu Rev Physiol.,* vol. 60, pp. 525-32.

Tomita, K. & Cooper, J.P. 2006, "The Meiotic Chromosomal Bouquet: SUN Collects Flowers", *Cell,* vol. 125, no. 1, pp. 19-21.

273

Toth, J.I., Yang, S.H., Qiao, X., Beigneux, A.P., Gelb, M.H., Moulson, C.L., Miner, J.H., Young, S.G. & Fong, L.G. 2005, "Blocking protein farnesyltransferase improves nuclear shape in fibroblasts from humans with progeroid syndromes", *Proc Natl Acad Sci U S A,* vol. 102, no. 36, pp. 12873-8.

Ulitzur, N., Harel, A., Feinstein, N. & Gruenbaum, Y. 1992, "Lamin activity is essential for nuclear envelope assembly in a Drosophila embryo cell-free extract.", *The Journal of cell biology,* vol. 119, no. 1, pp. 17-25.

Vaughan, A., Alvarez-Reyes, M., Bridger, J.M., Broers, J.L., Ramaekers, F.C., Wehnert, M., Morris, G.E., Whitfield, W.G.F. & Hutchison, C.J. 2001, "Both emerin and lamin C depend on lamin A for localization at the nuclear envelope", *J Cell Sci,* vol. 114, no. Pt 14, pp. 2577-90.

Vergnes, L., Péterfy, M., Bergo, M.O., Young, S.G. & Reue, K. 2004, "Lamin B1 is required for mouse development and nuclear integrity", *Proceedings of the National Academy of Sciences of the United States of America,* vol. 101, no. 28, pp. 10428-10433.

Verstraeten, V.L., Broers, J.L., van Steensel, M.A., Zinn-Justin, S., Ramaekers, F.C., Steijlen, P.M., Kamps, M., Kuijpers, H.J., Merckx, D., Smeets, H.J., Hennekam, R.C., Marcelis, C.L. & van den Wijngaard, A. 2006, "Compound heterozygosity for mutations in LMNA causes a progeria syndrome without prelamin A accumulation", *Hum Mol Genet,* vol. 15, no. 16, pp. 2509-22.

Verstraeten, V.L.R.M., Ji, J.Y., Cummings, K.S., Lee, R.T. & Lammerding, J. 2008, "Increased mechanosensitivity and nuclear stiffness in Hutchinson?Gilford progeria cells: effects of farnesyltransferase inhibitors", *Aging Cell,* vol. 7, no. 3, pp. 383-393.

Voeltz, G.K., Rolls, M.M.& Rapoport, T.A. 2002, "Structural organization of the endoplasmic reticulum", *EMBO Rep,* vol. 3, no. 10, pp. 944-50.

Volk, T. 1992, "A new member of the spectrin superfamily may participate in the formation of embryonic muscle attachments in Drosophila", *Development,* vol. 116, no. 3, pp. 721-730.

von Dassow, G. & Schubiger, G. 1994, "How an actin network might cause fountain streaming and nuclear migration in the syncytial Drosophila embryo.", *The Journal of cell biology,* vol. 127, no. 6, pp. 1637-1653.

Vorburger, K., Kitten, G.T. & Nigg, E.A. 1989, "Modification of nuclear lamin proteins by a mevalonic acid derivative occurs in reticulocyte lysates and requires the cysteine residue of the C-terminal CXXM motif.", *EMBO J.,* vol. 8, no. 13, pp. 4007-4013.

Walter, J., Sun, L. & Newport, J. 1998, "Regulated chromosomal DNA replication in the absence of a nucleus.", *Mol Cell.,* vol. 1, no. 4, pp. 519-29.

Wang, Q., Du, X., Cai, Z. & Greene, M.I. 2006, "Characterization of the Structures Involved in Localization of the SUN Proteins to the Nuclear Envelope and the Centrosome", *DNA and cell biology,* vol. 25, no. 10, pp. 554-562.

Warren, D.T., Zhang, Q., Weissberg, P.L. & Shanahan, C.M. 2005, "Nesprins: intracellular scaffolds that maintain cell architecture and coordinate cell function?", Expert Reviews in Molecular Medicine, vol. 7, no. 11, pp. 1.

Waterham, H.R., Koster, J., Mooyer, P., Noort Gv, G., Kelley, R.I., Wilcox, W.R., Wanders, R.J., Hennekam, R.C. & Oosterwijk, J.C. 2003, "Autosomal recessive HEM/Greenberg skeletal dysplasia is caused by 3 beta-hydroxysterol delta 14-reductase deficiency due to mutations in the lamin B receptor gene", *Am J Hum Genet,* vol. 72, no. 4, pp. 1013-7.

Weber, K., Plessmann, U. & Traub, P. 1989, "Maturation of nuclear lamin A involves a specific carboxy-terminal trimming, which removes the polyisoprenylation site from the precursor; implications for the structure of the nuclear lamina", *FEBS letters,* vol. 257, no. 2, pp. 411-414.

Wehnert, M. & Muntoni, F. 1999, "60th ENMC International Workshop: Non X-linked Emery–Dreifuss Muscular Dystrophy, 5–7 June 1998, Naarden, The Netherlands", Neuromuscular Disorders, vol. 9, no. 2, pp. 115-121.

Wheeler, M.A., Davies, J.D., Zhang, Q., Emerson, L.J., Hunt, J., Shanahan, C.M. & Ellis, J.A. 2007, "Distinct functional domains in nesprin-1alpha and nesprin-2beta bind directly to emerin and both interactions are disrupted in X-linked Emery-Dreifuss muscular dystrophy", *Exp Cell Res,* .

Wilhelmsen, K., Litjens, S.H., Kuikman, I., Tshimbalanga, N., Janssen, H., van den Bout, I., Raymond, K. & Sonnenberg, A. 2005, "Nesprin-3, a novel outer nuclear membrane protein, associates with the cytoskeletal linker protein plectin", *J Cell Biol,* vol. 171, no. 5, pp. 799-810.

Wilhelmsen, K., Ketema, M., Truong, H. & Sonnenberg, A. 2006, "KASH-domain proteins in nuclear migration, anchorage and other processes", *Journal of cell science,* vol. 119, no. 24, pp. 5021-5029.

Wilkinson, F.L., Holaska, J.M., Zhang, Z., Sharma, A., Manilal, S., Holt, I., Stamm, S., Wilson, K.L. & Morris, G.E. 2003, "Emerin interacts in vitro with the splicing-associated factor, YT521-B", *Eur J Biochem,* vol. 270, no. 11, pp. 2459-66.

Wilson, E.B. 1928, "The Cell in Development and Heredity.", *MacMillan Publishing Co.,* , pp. 377.

Wilson, K.L., Zastrow, M.S. & Lee, K.K. 2001, "Lamins and disease: insights into nuclear infrastructure", *Cell,* vol. 104, no. 5, pp. 647-50.

Wilson, K.L. & Foisner, R. 2010, "Lamin-binding Proteins", *Cold Spring Harbor Perspectives in Biology,* vol. 2, no. 4.

Winter-Vann, A.M. & Casey, P.J. 2005, "Post-prenylation-processing enzymes as new targets in oncogenesis", vol. 5, no. 5, pp. 412.

Wolff, N., Gilquin, B., Courchay, K., Callebaut, I., Worman, H.J. & Zinn-Justin, S. 2001, "Structural analysis of emerin, an inner nuclear membrane protein mutated in X-linked Emery–Dreifuss muscular dystrophy", *FEBS letters,* vol. 501, no. 2-3, pp. 171-176.

Worman, H.J., Evans, C.D. & Blobel, G. 1990, "The lamin B receptor of the nuclear envelope inner membrane: a polytopic protein with eight potential transmembrane domains", *J Cell Biol,* vol. 111, no. 4, pp. 1535-42.

Worman, H.J. & Bonne, G. 2007, ""Laminopathies": a wide spectrum of human diseases", *Exp Cell Res,* vol. 313, no. 10, pp. 2121-33.

Worman, H.J., Fong, L.G., Muchir, A. & Young, S.G. 2009, "Laminopathies and the long strange trip from basic cell biology to therapy.", *J Clin Invest,* vol. 119, no. 7, pp. 1825-36.

Worman, H.J., Ostlund, C. & Wang, Y. 2010, "Diseases of the nuclear envelope", *Cold Spring Harb Perspect Biol.,* vol. 2, no. 2, pp. a000760.

Worman, H.J., Yuan, J., Blobel, G. & Georgatos, S.D. 1988, "A lamin B receptor in the nuclear envelope", *Proc Natl Acad Sci U S A,* vol. 85, no. 22, pp. 8531-4.

Wu, W., Lin, F. & Worman, H.J. 2002, "Intracellular trafficking of MAN1, an integral protein of the nuclear envelope inner membrane", *J. Cell Sci.,* vol. 115, no. Pt 7, pp. 1361-71.

Yang, S.H., Bergo, M.O., Toth, J.I., Qiao, X., Hu, Y., Sandoval, S., Meta, M., Bendale, P., Gelb, M.H., Young, S.G. & Fong, L.G. 2005, "Blocking protein farnesyltransferase improves nuclear blebbing in mouse fibroblasts with a targeted Hutchinson–Gilford progeria syndrome mutation", *Proceedings of the National Academy of Sciences of the United States of America,* vol. 102, no. 29, pp. 10291-10296.

Yang, S.H., Meta, M., Qiao, X., Frost, D., Bauch, J., Coffinier, C., Majumdar, S., Bergo, M.O., Young, S.G. & Fong, L.G. 2006, "A farnesyltransferase inhibitor improves disease phenotypes in mice with a Hutchinson-Gilford progeria syndrome mutation", *J Clin Invest,* vol. 116, no. 8, pp. 2115-21.

Yang, S.H., Andres, D.A., Spielmann, H.P., Young, S.G. & Fong, L.G. 2008, "Progerin elicits disease phenotypes of progeria in mice whether or not it is farnesylated", *J Clin Invest,* vol. 118, no. 10, pp. 3291-300.

Yao, K.T.S. & Ellingson, D.J. 1969, "Observations on nuclear rotation and oscillation in chinese hamster germinal cells in vitro", *Experimental cell research,* vol. 55, no. 1, pp. 39-42.

Yates, J.R.W., Bagshaw, J., Aksmanovic, V.M.A., Coomber, E., McMahon, R., Whittaker, J.L., Morrison, P.J., Kendrick-Jones, J. & Ellis, J.A. 1999, "Genotype-phenotype analysis in X-linked Emery–Dreifuss muscular dystrophy and identification of a missense mutation associated with a milder phenotype", *Neuromuscular Disorders,* vol. 9, no. 3, pp. 159-165.

Ye, Q. & Worman, H.J. 1994, "Primary structure-analysis and lamin-B and DNA-binding of human LBR, an integral protein of the nuclear-envelope inner membrane", *J. Biol. Chem.,* vol. 269, no. 15, pp. 11306-11311.

Ye, Q. & Worman, H.J. 1996, "Interaction between an integral protein of the nuclear envelope inner membrane and human chromodomain proteins homologous to Drosophila HP1", *Journal of Biological Chemistry,* vol. 271, no. 25, pp. 14653-14656.

Ye, Q.A., Callebaut, I., Pezhman, A., Courvalin, J.C. & Worman, H.J. 1997, "Domain-specific interactions of human HP1-type chromodomain proteins and inner nuclear membrane protein LBR", *Journal of Biological Chemistry,* vol. 272, no. 23, pp. 14983-14989.

Yeh, E., Skibbens, R.V., Cheng, J.W., Salmon, E.D. & Bloom, K. 1995, "Spindle dynamics and cell cycle regulation of dynein in the budding yeast, Saccharomyces cerevisiae.", *The Journal of cell biology,* vol. 130, no. 3, pp. 687-700.

Young, S.G., Fong, L.G. & Michaelis, S. 2005, "Thematic Review Series: Lipid Posttranslational Modifications. Prelamin A, Zmpste24, misshapen cell nuclei, and progeria--new evidence suggesting that protein farnesylation could be important for disease pathogenesis", *Journal of lipid research,* vol. 46, no. 12, pp. 2531-2558.

Yu, J., Starr, D.A., Wu, X., Parkhurst, S.M., Zhuang, Y., Xu, T., Xu, R. & Han, M. 2006, "The KASH domain protein MSP-300 plays an essential role in nuclear anchoring during Drosophila oogenesis", *Developmental biology,* vol. 289, no. 2, pp. 336-345.

Zastrow, M.S., Vlcek, S. & Wilson, K.L. 2004, "Proteins that bind A-type lamins: integrating isolated clues", *J Cell Sci,* vol. 117, no. Pt 7, pp. 979-87.

Zewe, M., Höger, T.H., Fink, T., Lichter, P., Krohne, G. & Franke, W.W. 1991, "Gene structure and chromosomal localization of the murine lamin B2 gene.", *Eur J Cell Biol.,* vol. 56, no. 2, pp. 342-50.

Zhang, F.L. & Casey, P.J. 1996, "Protein prenylation: molecular mechanisms and functional consequences.", *Annu Rev Biochem,* vol. 65, pp. 241-69.

Zhang, J., Felder, A., Liu, Y., Guo, L.T., Lange, S., Dalton, N.D., Gu, Y., Peterson, K.L., Mizisin, A.P., Shelton, G.D., Lieber, R.L. & Chen, J. 2010, "Nesprin 1 is critical for nuclear positioning and anchorage", *Human molecular genetics,* vol. 19, no. 2, pp. 329-341.

Zhang, Q., Skepper, J.N., Yang, F., Davies, J.D., Hegyi, L., Roberts, R.G., Weissberg, P.L., Ellis, J.A. & Shanahan, C.M. 2001, "Nesprins: a novel family of spectrin-repeat-containing proteins that localize to the nuclear membrane in multiple tissues", *J. Cell Sci.,* vol. 114, no. Pt 24, pp. 4485-98.

Zhang, Q., Ragnauth, C., Greener, M.J., Shanahan, C.M. & Roberts, R.G. 2002, "The nesprins are giant actin-binding proteins, orthologous to Drosophila melanogaster muscle protein MSP-300", *Genomics,* vol. 80, no. 5, pp. 473-81.

Zhang, Q., Ragnauth, C.D., Skepper, J.N., Worth, N.F., Warren, D.T., Roberts, R.G., Weissberg, P.L., Ellis, J.A. & Shanahan, C.M. 2005, "Nesprin-2 is a multi-isomeric protein that binds lamin and emerin at the nuclear envelope and forms a subcellular network in skeletal muscle", *J Cell Sci,* vol. 118, no. Pt 4, pp. 673-87.

Zhang, Q., Bethmann, C., Worth, N.F., Davies, J.D., Wasner, C., Feuer, A., Ragnauth, C.D., Yi, Q., Mellad, J.A., Warren, D.T., Wheeler, M.A., Ellis, J.A., Skepper, J.N., Vorgerd, M., Schlotter-Weigel, B., Weissberg, P.L., Roberts, R.G., Wehnert, M. & Shanahan, C.M. 2007b, "Nesprin-1 and -2 are involved in the pathogenesis of Emery Dreifuss muscular dystrophy and are critical for nuclear envelope integrity", *Hum Mol Genet,* vol. 16, no. 23, pp. 2816-33.

Zhang, X., Xu, R., Zhu, B., Yang, X., Ding, X., Duan, S., Xu, T., Zhuang, Y. & Han, M. 2007a, "Syne-1 and Syne-2 play crucial roles in myonuclear anchorage and motor neuron innervation", *Development,* vol. 134, no. 5, pp. 901-8.

Zhang, X., Lei, K., Yuan, X., Wu, X., Zhuang, Y., Xu, T., Xu, R. & Han, M. 2009, "SUN1/2 and Syne/Nesprin-1/2 complexes connect centrosome to the nucleus during neurogenesis and neuronal migration in mice. ", *Neuron,* vol. 64, no. 2, pp. 173-187.

Zhen, Y.Y., Libotte, T., Munck, M., Noegel, A.A. & Korenbaum, E. 2002, "NUANCE, a giant protein connecting the nucleus and actin cytoskeleton", *J. Cell Sci.,* vol. 115, no. Pt 15,

Zhou, K., Rolls, M.M., Hall, D.H., Malone, C.J. & Hanna-Rose, W. 2009, "A ZYG-12–dynein interaction at the nuclear envelope defines cytoskeletal architecture in the C. elegans gonad", *The Journal of cell biology,* vol. 186, no. 2, pp. 229-241.

APPENDIX

Construct name	Obtained from
pCI-mycSUN1	Generated in the lab
pCI-mycSUN1(1-355)	Generated in the lab
pCI-mycSUN1(450-913)	Generated in the lab
pCI-SUN1(1-355)	Generated in the lab
pCMV-SUN1(1-432)	Generated by myself
pCMV-SUN1(355-913)	Generated by myself
pCMV-SUN1(1-229)	Generated by myself
pCMV-SUN1(223-355)	Generated by myself
pCMV-SUN1(229-913)	Generated by myself
pCI-SUN1myc	Generated in the lab
pCI-SUN1-355myc	Generated in the lab
pCI-SUN1-456myc	Generated in the lab
pCI-HAmSUN1	Generated in the lab
pMAL-hSUN1(1-217)	Generated by myself
pMAL-hSUN1(352-812)	Generated by myself
pCMV-hSUN1(1-217)	Generated by myself
pCMV-hSUN1(352-812)	Generated by myself

Table. A.1 SUN protein constructs (Continued)

Construct name	Obtained from
pMAL-SUN1(1-355)	Generated in the lab
pMAL-SUN1(450-913)	Generated in the lab
pMAL-SUN1(1-229)	Generated in the lab
pMAL-SUN1(223-355)	Generated in the lab
pGEX-SUN1(1-355)	Generated in the lab
pGEX-SUN1(1-229)	Generated by myself
pGEX-SUN1(223-355)	Generated by myself
pGEX-SUN1(1-208)	Generated in the lab
pGEX-SUN1(209-355)	Generated in the lab
pGEX-SUN1(1-170)	Generated in the lab
pGEX-SUN1(1-138))	Generated by myself
pGEX-SUN1(50-208)	Generated in the lab
pGEX-SUN1(50-170)	Generated in the lab
pGEX-SUN2(1-224)	Generated in the lab
pGEX-SUN2(1-129)	Generated by myself
pGEX-SUN2(1-83)	Generated by myself
pCDNA3.1TOPO-V5/His-hSUN2	Kind gift from D. Hodzic

Table. A.1 SUN protein constructs

Construct name	Obtained from
pCI-LMNA	Generated in the lab
pCI-LMNB1	Generated in the lab
pBS-LMNB2	Gift from E. Schirmer
pCI-LMNC	Generated by myself
pET-laminA(1-664)	Generated in the lab
pET-laminA(1-389)	Generated in the lab
pET-laminA(389-664)	Generated in the lab
pET-laminA(389-647X)	Generated in the lab
pET-laminA(389-510)	Generated by myself
pET-laminA(450-664)	Generated by myself
pGEX-laminA(389-664)	Generated in the lab
pGEX-laminA(389-510)	Generated in the lab
pGEX-laminA(450-664)	Generated in the lab
pGEX-laminA(450-510)	Generated in the lab
pGEX-laminA(510-664)	Generated in the lab

Table. A.2 Lamin constructs (continued)

Construct name	Obtained from
pCI-mycLMNA	Generated in the lab
pCI-mycLMNAR482W	Generated in the lab
pCI-mycLMNAE203G	Generated in the lab
pCI-mycLMNAL530P	Generated in the lab
pCI-mycLMNAR60G	Generated in the lab
pCI-mycLMNAR453W	Generated in the lab
pCI-mycLMNAR298C	Generated in the lab
pCI-mycLMNAR527H	Generated in the lab
pCI-mycLMNAG608G	Generated in the lab
pCI-mycLMNAE358K	Generated in the lab
pCI-mycLMNAW520S	Generated in the lab
pCI-mycLMNAR527P	Generated in the lab
pCI-mycLMNAR541C	Generated in the lab
pCI-mycLMNAT528M	Generated in the lab
pCI-mycLMNAK542N	Generated in the lab
pCI-mycLMNAT623S	Generated in the lab
pCI-mycLMNAL647R	Generated in the lab
pCI-mycLMNAL647X	Generated in the lab

Table. A.2 Lamin constructs

Construct name	Obtained from
pCDNA3.1-hemerin	Kind gift from J. Ellis
pCI-hemerin-myc	Generated in the lab
pGEX-emerin(1-221)	Kind gift from J. Ellis
pGEX-emerin(1-120)	Generated in the lab
pGEX-emerin(120-221)	Generated in the lab
pGEX-emerin(140-221)	Generated in the lab
pGEX-emerin(140-176)	Generated in the lab
pGEX-emerin(170-220)	Kind gift from J. Ellis
pCDNA3-emerinP183H	Kind gift from J. Ellis
pCDNA3-emerinP183T	Kind gift from J. Ellis
pCDNA3-emerin-del(95-99)	Kind gift from J. Ellis
pCDNA3-emerinQ133H	Kind gift from J. Ellis
pCDNA3-emerinS54F	Kind gift from J. Ellis
pCDNA3.1-emerin(1-169)208	Kind gift from J. Ellis
pCDNA3.1-emerin-del(236-241)	Kind gift from J. Ellis

Table. A.3 Emerin constructs

Construct name	Obtained from
pCDNA3-nesprin2α	Kind gift from J. Ellis
pCDNA3-nesprin2β	Kind gift from J. Ellis
pEGFP-nesprin2α	Kind gift from C. Shanahan
pEGFP-nesprin2αΔTM	Kind gift from C. Shanahan
pEGFP-nesprin2αKASH	Kind gift from C. Shanahan
pTNT-nesprin-2βΔTM	Kind gift from C. Shanahan
pTNT-nesprin1αΔTM	Kind gift from C. Shanahan
pEGFP-nesprin1αΔTM	Kind gift from C. Shanahan
pEGFP-nesprin1αKASH	Kind gift from C. Shanahan

Table. A.4 Nesprin constructs

pCMV-Tag 3B Multiple Cloning Site Region
(sequence shown 620–847)

T3 promoter
AA TTA ACC CTC ACT AAA GGG AAC AAA AGC TGG AGC TCC ACC GCG GTG GCG GCC GCC ATG... **M**
  KOZAK

myc tag
E   Q   K   L   I   S   E   Srf I   BamH I   Pst I   EcoR I
...GAG CAG AAA CTC ATC TCT GAA AGC CCG GGC GGA TCC CCC GGG CTG CAG GAA TTC...

EcoR V   Hind III   Acc I/Sal I   Xho I   Apa I
...GAT ATC AAG CTT ATC GAT ACC GTC GAC CTC GAG GGG GGG CCC GGT ACC T...

T7 promoter
...TAATTAATTAAGGTACCAGGTAAGTGTACCCAATTCGCCCTATAGTGAGTCGTATTA
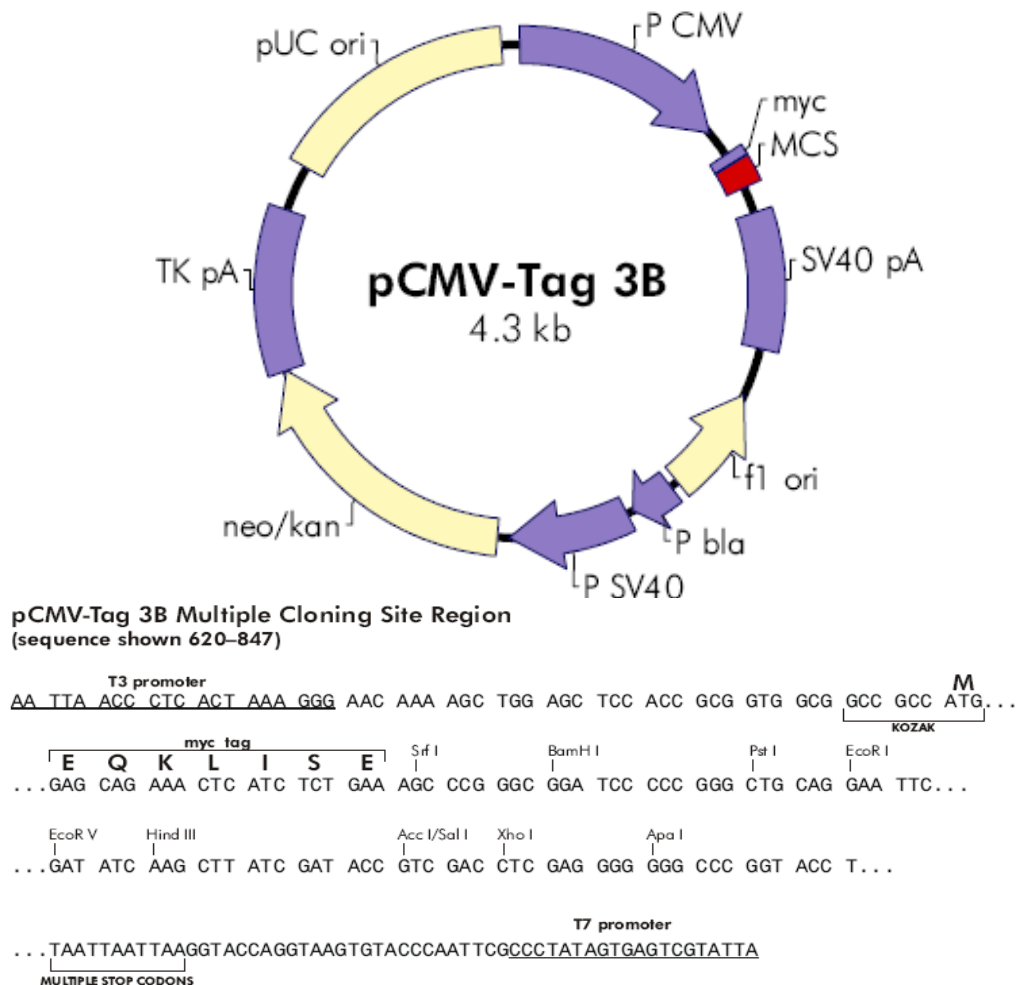MULTIPLE STOP CODONS

Fig. A.1. pCMV-Tag 3B plasmid map and constructs. The constructs generated using this vector are as follows:

pCMV-SUN1(1-432): generated by PCR amplification of relevant region of mouse SUN1 cDNA, using pCI-mSUN1 as template and then cloned into *Bam*HI and *Sal*I sites of pCMV-Tag3B.

pCMV-SUN1(355-913): generated by PCR amplification of relevant region of mouse SUN1 cDNA, using pCI-mSUN1 as template and then cloned into *Bam*HI and *Sal*I siteS of pCMV-Tag3B.

pCMV-SUN1(1-229): generated by PCR amplification of relevant region of mouse SUN1 cDNA, using pCI-mSUN1 as template and then cloned into *Bam*HI and *Sal*I sites of pCMV-Tag3B.

pCMV-SUN1(223-355): generated by PCR amplification of relevant region of mouse SUN1 cDNA, using pCI-mSUN1 as template and then cloned into *Bam*HI and *Sal*I sites of pCMV-Tag3B.

pCMV-SUN1(229-913): generated by PCR amplification of relevant region of mouse SUN1 cDNA, using pCI-mSUN1 as template and then cloned into *Bam*HI and *Sal*I sites of pCMV-Tag3B.

pCMV-hSUN1(1-217): generated by excising human SUN1(1-217) fragment from pMAL-hSUN1(1-217), at *Eco*RI and *Sal*I siteSUN1 cDNA and then cloned into this sites of pCMV-Tag3B .

pCMV-hSUN1(352-812): generated by PCR amplification of relevant region of human SUN1 cDNA, using pBS-hSUN1 as template at *Eco*RI and *Sal*I siteSUN1 cDNA and then cloned into this sites of pCMV –Tag3B.
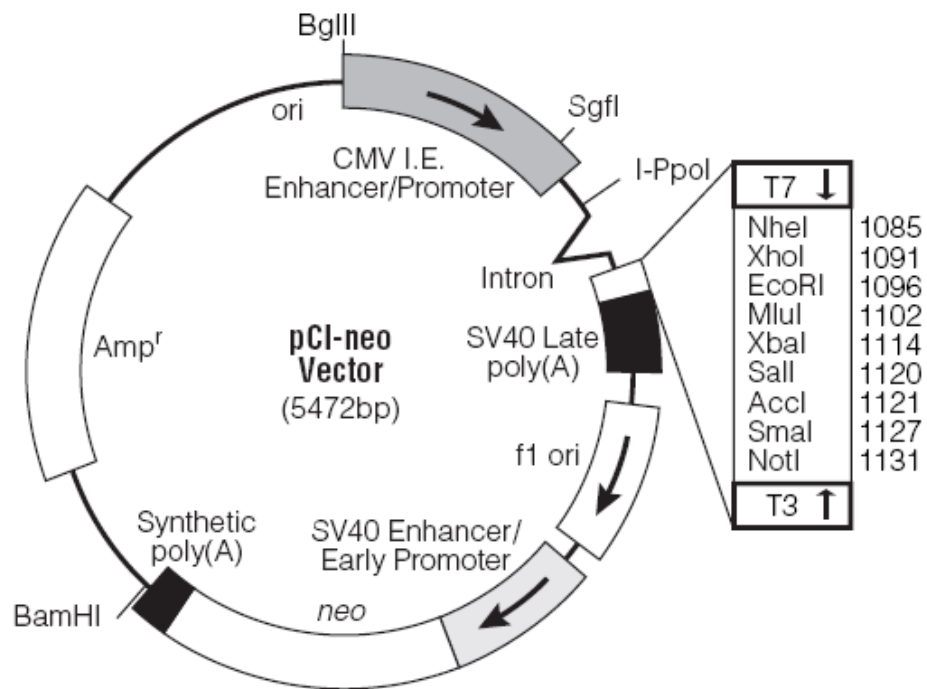
Fig. A.2. pCI-neo plasmid map and construct. The construct generated using this vector is as follows:

pCI-LMNC: generated by subcloning, excising lamin C fragment from pCI-mycLMNC at *Apa*I and *Not*I site, *Apa*I site is present within the laminA/C cDNA and *Not*I site at the end of laminC fragment in pCI-mycLMNC. Then this fragment was inserted into pCI-LMNA, replacing equivalent sequences.
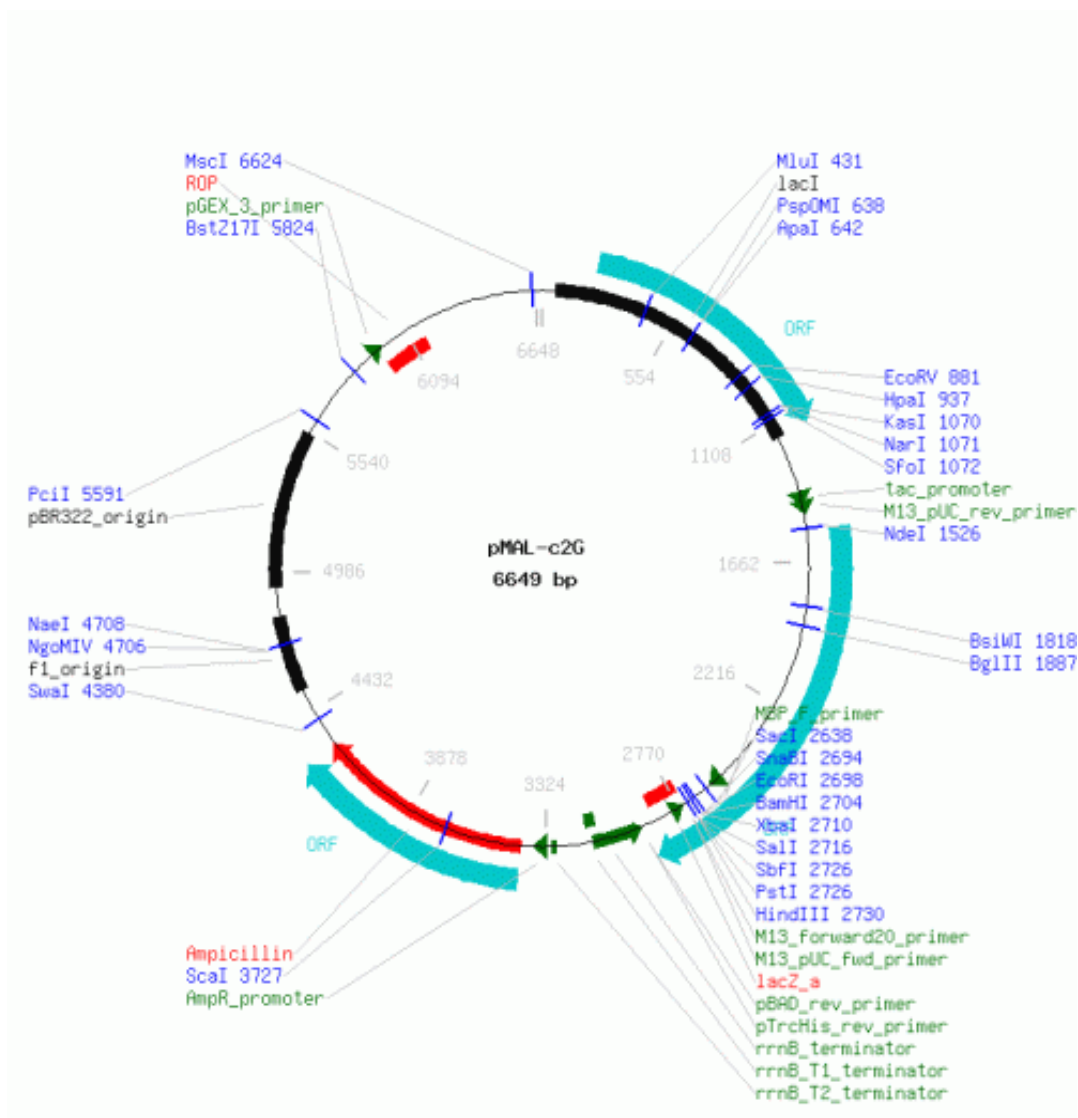
Fig. A.3. pMAL-c2G plasmid map and constructs. The constructs generated using this vector are as follows:

pMAL-hSUN1(1-217): generated PCR amplification of relavent region of human SUN1 cDNA, using pBS-hSUN1 as a template and then cloned into at *Eco*RI and *Sal*I sites of pMAL-c2G vector.

pMAL-hSUN1(352-812): generated PCR amplification of relavent region of human SUN1 cDNA, using pBS-hSUN1 as a template and then cloned into at *Eco*RI and *Sal*I sites of pMAL-c2G vector.
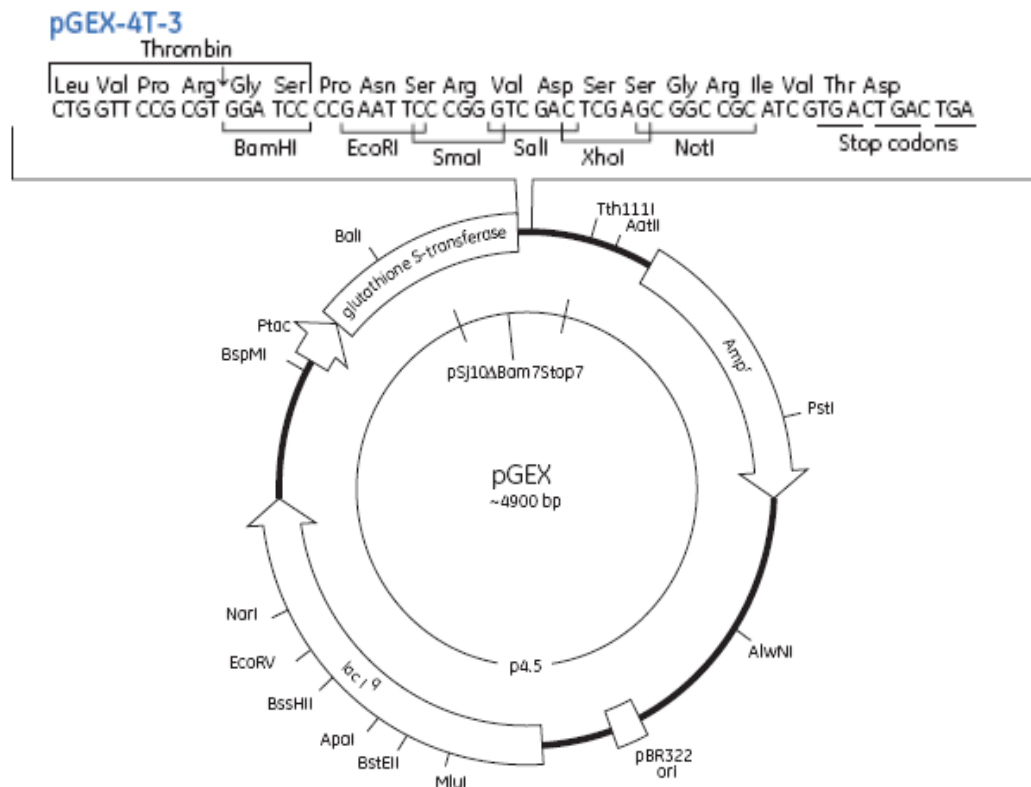
pGEX-4T-3

Thrombin

Leu Val Pro Arg↓Gly Ser Pro Asn Ser Arg Val Asp Ser Ser Gly Arg Ile Val Thr Asp
CTG GTT CCG CGT GGA TCC CCG AAT TCC CGG GTC GAC TCG AGC GGC CGC ATC GTG ACT GAC TGA

BamHI   EcoRI SmaI SalI XhoI NotI   Stop codons

Ball
glutathione S-transferase
Tth111I
AatII

Ptac
BspMI

Amp^r

pSJ10ΔBam7Stop7

pGEX
~4900 bp

PstI

NarI
EcoRV
BssHII
lac I q
ApaI
BstEII
MluI

p4.5

AlwNI

pBR322 ori

Fig. A.4. pGEX-4T3 plasmid map and constructs. The constructs generated using this vector are as follows:

pGEX-SUN1(1-229): generated by excising mouse SUN1(1-229) form pCMV-SUN1(1-229) at *Bam*HI and *Sal*I sites, and then cloned into these sites of pGEX-4T3 vector.

pGEX-SUN1(223-355): generated by excising mouse SUN1(223-355) form pCMV-SUN1(223-355) at *Bam*HI and *Sal*I sites, and then cloned into these sites of pGEX-4T3 vector.

pGEX-SUN1(1-138): generated PCR amplification of relavent region on mouse SUN1 cDNA, using pCI-mSUN1 as template and then cloned into at *Eco*RI and *Sal*I sites of pGEX -4T3 vector.

pGEX-SUN2(1-129): generated PCR amplification of relavent region on mouse SUN2 cDNA, using IMAGE clone 6827666 as template and then cloned into at *Eco*RI and *Sal*I sites of pGEX -4T3 vector.

pGEX-SUN2(1-83): generated PCR amplification of relavent region on mouse SUN2 cDNA, using IMAGE clone 6827666 as template and then cloned into at *Eco*RI and *Sal*I sites of pGEX -4T3 vector.
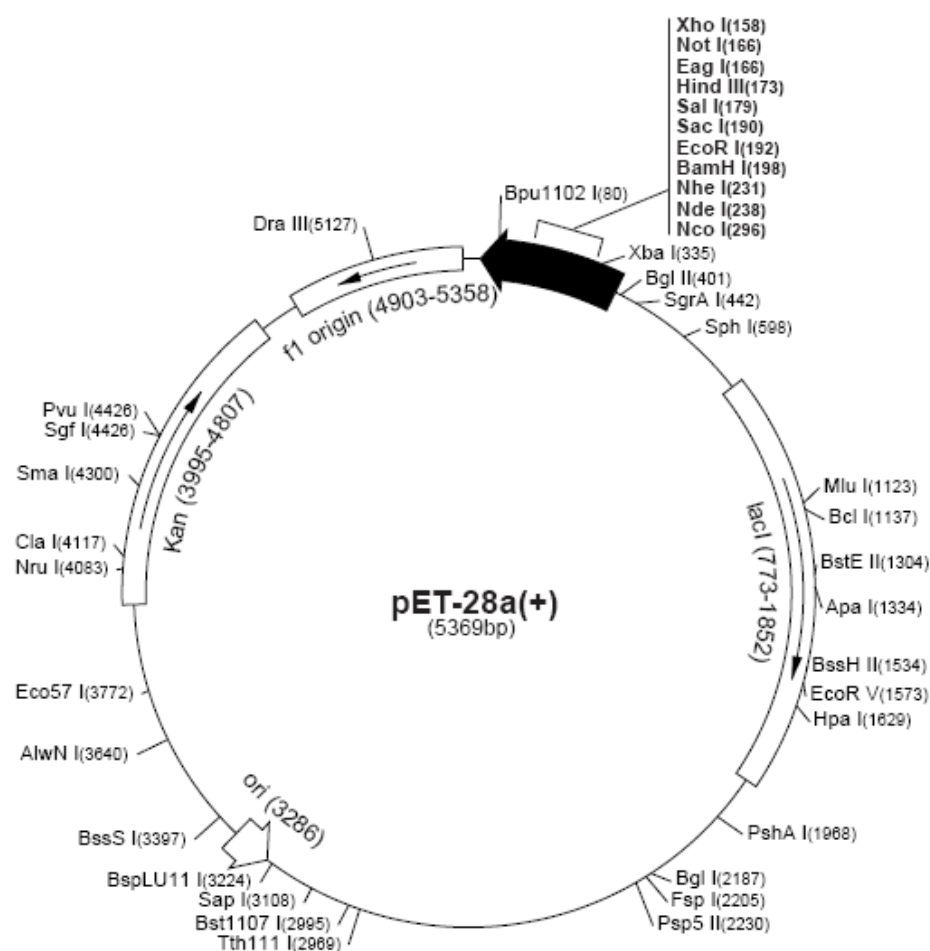
Fig. A.5. pET-28a plasmid map and constructs. The constructs generated using this vector are as follows:

pET-laminA(389-510): generated by excising laminA(389-510) form pGBDU-LMNA(389-510) at *Eco*RI and *Sal*I sites, and then cloned into these sites of pET-28a vector.

pET-laminA(450-664): generated by excising laminA(450-664) form pGBDU-LMNA(450-664) at *Eco*RI and *Sal*I sites, and then cloned into these sites of pET-28a vector.